New FMS Calibration

Chong Kim
UC Riverside
chongk@ucr.edu

Abstract

A new offline calibration framework is developed for the STAR FMS (Forward Meson Spectrometer) based on the STAR analysis framework. The new framework performs cell by cell calibration by using reconstructed π^0 peak which is obtained by STAR Scheduler and μDSTs. The framework is developed by using the real data acquired in the RUN15pp200trans period with 2 days' ($\sim$80 runs) statistics. After the framework is fully developed, its performance was tested by using 9 independent samples from the RUN15pp200trans period: the final convergence ratio of each sample was 85 $\pm$ 3 % with the masked out cells' ratio of 4.5 $\pm$ 0.5 %. The remaining unconverged cells are mostly the ones located at the outer edge of the FMS or the problematic ones near the beam pipe. Each sample's reconstructed mass matches well to the true π^0 in the range of 20 $<$ reconstructed π^0 energy (GeV) $<$ 40 and shows consistent behavior for various conditions.

Contents

1 Introduction **1**

1.1 Motivation 1

1.2 Nomenclature 2

1.3 Location of codes and macros 4

1.4 Quick instructions for user 5

2 Analysis **8**

2.1 Overview 8

2.2 Calibration 12

2.2.1 Requirements for data 12

2.2.2 Maker and Scripts 13

2.2.3 Assign a π^0 to a cell 16

2.2.4 Fit on π^0 mass distribution 22

2.2.5 Update gainCorr 25

2.3 Challenges and Crosschecks 29

2.3.1 Bad/Dead/Hot channels 29

2.3.2 Skewed mass problem 35

2.3.3 Effect of applied cuts 40

2.3.4 Finalize a group's calibration 53

2.3.5 Degradation study 55

3 Results **59**

3.1 RUN15 pptrans 59

A Additional QA plots for RUN15pptrans **78**

A.1 Bad/Dead/Hot channels QA 78

A.2 Mass vs. pairE, mass vs. Zgg, and Points' XY 90

Chapter 1

Introduction

1.1 Motivation

Throughout its entire operations until it decommissioned in 2018, the FMS had bimodal frameworks for its data analysis: the PSU (Penn State University) framework and the STAR framework, respectively. Many parts of the STAR framework are ported from the PSU framework thus two frameworks share many features, however, after 2014 a few notable modifications are implemented to the STAR framework. Unfortunately, until very recently (October 2019) there are no stringent crosschecks between the two frameworks thus the actual difference between them is not known clearly.

In its entire operations, the FMS solely relied on its calibration to the PSU framework, in both online and offline calibrations. However, besides to the unknown differences previously mentioned, the PSU framework uses the trigger files as its input: it's an advantage when fast feedback is required like the online calibration, however, at the stage of offline calibration and the analysis followed by, it can cause inconsistency, especially since the STAR framework uses μDSTs as its input.

The goal of this analysis is the development of an offline calibration framework based on the STAR framework. Also, various crosschecks and sanity tests are performed on each step of the framework, to empower the reliability and to estimate the limit of the framework itself. Finally, although it won't be mentioned in this note, during the development various comparisons with the calibration results by conventional framework were made. The detailed test results can be found here. [1]

1.2 Nomenclature

This section explains terms used in this analysis.

Nomenclature (alphabetical order)

- **An iteration and A full iteration** *An iteration* means one complete calibration composed of the following steps: Scheduler running, Merge, Cell by Cell fit on π^0 mass, gainCorr update, and Convergence test, respectively. *A full iteration* means a certain number of iterations performed in series: the script for iteration control stops itself after a certain number of iterations. Usually 9 iterations in succession is regarded as a full iteration, but the number only decided by convenience and can be changed by necessity.
- **Calibration factor**: in FMS, conversion of a cell's ADC to energy is defined as follows.

$$\text{Hit (cell) energy} = \text{ADC} \times \text{gain} \times \text{gainCorr} \tag{1.1}$$

  The *gain* is theoretically calculated value by considering a cell's η position. Its value differ cell by cell but in general varies within the range of [0.045, 0.140]. The *gainCorr* is the value obtained by offline calibration and target of this analysis. Its value can vary in a wide range. Finally, by necessity the value *gain* $\times$ *gainCorr* also used with the term *total gain*.
- **Cell and Channel**: two terms used in exactly the same meaning.
- **Cell status**: there are four status to judge a cell's state when iteration is underway. Note that the integer in parenthesis indicates actual enumeration index used in calibration.
  a. GOOD (0): the cell is not bad nor dead, but gainCorr is not converged yet.
  b. BAD (1): the cell is bad and will be ignored.
  c. DEAD (2): the cell is dead and will be ignored.
  d. CONVERGED (9): the cell's gainCorr is converged.
  * Only gainCorr of cells with status GOOD will be updated while the others are fixed. In addition, bad cell' gainCorr set to 0 to make them ignored in reconstruction.
- **Hit, Cluster, Point, and Pair**: a hit means meaningful response of a cell after pedestal subtraction. After converting each hit's ADC to energy by using predefined gain and gainCorr, cluster finding algorithm reconstructs clusters in an event. As a next step, the point reconstruction algorithm performs fit on each cluster and reconstructs points (photon candidates). Note that by circumstance a cluster can have more than one point. Finally, pairing performed by using reconstructed points in an event. For instance, by paring 4 points total 3! pairs will be obtained. In this analysis, a pair usually regarded as a π^0 candidate.
- $mass_{fit}$: peak position of the π^0 mass, obtained by fit on reconstructed mass distribution.
- $mass_{\pi^0}$: true mass of π^0 (134.9766 $\pm$ 0.0006 (MeV)). [2]

- **Online calibration**: during the data taking, each cell's PMT HV (high voltage) was adjusted by necessity for optimization. Therefore it is possible multiple HV settings exist for a period of interest.
- **Zgg**: energy asymmetry between two points ($\text{Zgg} = \frac{|e_1 - e_2|}{e_1 + e_2}$). Zgg = 0 means each point has an equal amount of energy.

1.3 Location of codes and macros

This section provides a list of files compose new calibration framework.

Home directory
/star/u/ckimstar/work/fms_calib
(StRoot/StSpinPool/StFmsCalibMaker)

Maker and Scripts for STAR Scheduler / iteration
- StRoot/StFmsCalibMaker/StFmsCalibMaker.h
- StRoot/StFmsCalibMaker/StFmsCalibMaker.cxx
- StRoot/StFmsCalibMaker/StFmsCalibMakerQa.h
- StRoot/StFmsCalibMaker/StFmsCalibMakerQa.cxx
- runMudst.C
- iterFmsCalib.pl (iteration control script)

Macros for gainCorr update / plot generation
- calibFmsTools.C (definitions and essential functions)
- calibFmsShow.C (functions for plot generation, requires calibFmsTools.C)
- calibFms.C (update/print gainCorr and generates in-situ QA plots, requires calibFmsShow.C)
- TestShow.C (shows example of each plot generation function and its usage)

In addition to the above items following input files are required for proper running.

Input files for calibration process
- FmsGainCorr.txt (list of gainCorr for each FMS cell)
- FmsCellStat.txt (list of cell status for each FMS cell)
- FmsMapBase.txt (position information and gain for each FMS cell)
- FmsMapBitShift.txt (bit shift of each FMS cell, not essentially required for running)
- BBC slewing correction (written by Oleg Eyser, required for vertex correction)

1.4 Quick instructions for user

This section provides quick instructions for actual analyzers.

1. Prerequisite conditions

   a. Bit shift (BS) QA: each cell's BS QA must be done beforehand thus precise BS values already stored in DB. As BS directly affects a cell's hit energy, calibration results without proper BS QA cannot be trusted.
   b. Production status: μDSTs must be available for STAR Scheduler. This framework uses Physics stream (st_physics) for QA and FMS stream (st_fms) for actual calibration.
   c. Data selection:
   - Online calibration: selected runs must share the same online calibration condition (i.e. HV setting). Check references [3][4] for notable events in RUN15 and RUN17.
   - Statistics: the framework was developed with statistics of 2 days in RUN15pp200trans period (day 80-81, ~70 runs). If given statistics is too small it is likely a cell won't have enough π^0 invariant mass yields per cell, therefore ends up with poor calibration results.

2. Bad/Dead cells QA by ADC

   a. Check selected runs in the RunLog browser [5] to acquire a MinBias trigger. The trigger should be independent of any FMS trigger in addition to have large enough statistics (small prescale applied). Also, it is recommended to check if the trigger's bit stays the same throughout the selected runs.
   b. Use the function "StFmsCalibMaker→GetQaHistAdc(*MB_trigger_bit*)" on physics stream μDSTs to get FMS trigger independent ADC distributions. Once the Scheduler run is finished merge the output in run by run basis.
   c. Perform ADC QA to pick out bad/dead cells and mark them as follows. Detailed discussions about bad/dead cells decision can be found in section 2.3.1.
   - Cell status (FmsCellStat.txt): 1 for bad, 2 for dead
   - gainCorr (FmsGainCorr.txt): 0.000 for both bad and dead

3. Preparing iterations

   a. Following 4 files are required as input:
   - FmsCellStat.txt (status of each cell. All starting indices should be 0 except for bad/dead)
   - FmsGainCorr.txt (starting gainCorr. Bad cells' gainCorr should be 0.000)
   - FmsMapBase.txt
   - FmsMapBitShift.txt
   b. To generate map files (FmsMapBase.txt and FmsMapBistShift.txt), prepare a sample μDST and use the function "StFmsCalibMaker→GetMap()". The function reads relevant values from DB via StFmsDbMaker and prints them out in text file. Be careful that the values read from DB determined by given sample μDST's run number.

c. Activate following flags in macro for μDSTs running (runMudst.C).
- StFmsDbMaker→readGainCorrFromText(*true*)
- Do NOT use SetReadMuDst() in either FmsHitMaker or FmsPointMaker
- StFmsCalibMaker→ReadCellStat(*"FmsCellStat.txt"*)
- StFmsCalibMaker→ReadBbcSlewing(*"SlewingCorrFileByOleg"*)

4. Executing iterations

a. Prepare a working folder for multiple iterations and make sure enough disk space is available. Typically maximum instantaneous disk usage does not exceed 1 GB for an iteration with ∼70 runs in RUN15pp200trans, but it can vary depends on the dataset.

b. Copy following 4 + 3 files into the working folder.
- All input files in 3-a.
- calibFms.C
- calibFmsShow.C
- calibFmsTools.C

c. Once all requirements are prepared the iteration can be launched as follows. Recording the log is an option but strongly recommended to keep it.
./iterFmsCalib.pl run_list.txt > log.txt

d. The iteration script (iterFmsCalib.pl) works as follows:
Submit Scheduler job → Merge → Perform calibration (calibFms.C) → Print new cell status and gainCorr → Submit Scheduler job...

e. The iteration script continually checks the Condor status and starts the next process when the number of running / idle Condor jobs are 0. Therefore when the iteration is underway it's not recommended to run another analysis relies on Condor in the same rcas machine.

5. Monitoring

a. When an iteration is finished (ex. iteration 0 of 8) the script generates multiple in-situ QA maps such as Fig. 1.1. The analyzer needs to check these QA maps as frequently as possible and judge if user-defined correction is required for problematic cells. Currently, 4 types of QA map is prepared in addition to 2 gainCorr maps.
- MapQABadF: fit quality is poor
- MapQACold: too small π^0 invariant mass yields
- MapQALoHi: gainCorr is too low or too high
- MapQaSkew: these cells judged "skewed". Only applies to small cells.

b. By necessity the analyzer can enforce certain gainCorr during iterations are underway. To enforce such user-defined gainCorr, prepare a file with the following name: FmsGainCorrManual_<*ongoing_iteration_index*>.txt (ex. FmsGainCorrManual_5.txt). The contents of the file should be as follows: detId channel gainCorr (ex. 8 75 1.500). Lastly, this file must be located in the same work folder at 4-a. Note that this user enforced gainCorr will be applied in the next iteration.

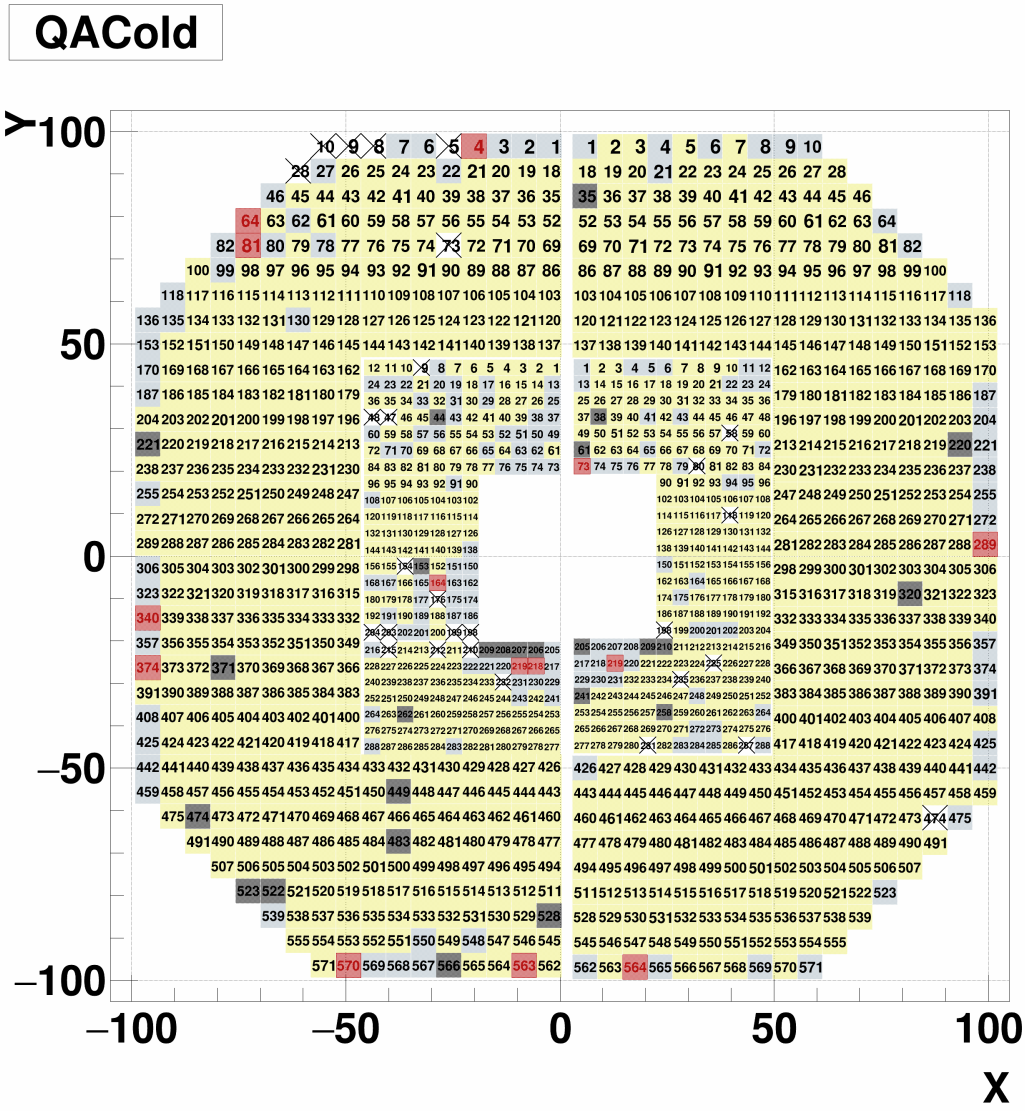

Figure 1.1: An example of an in-situ QA map. The red-colored cells indicate they're cold. The other colors' meanings are as follows: bad (black), dead (white with crossing), calibration is underway (blue), and calibration is finished (yellow).

Chapter 2

Analysis

2.1 Overview

This section provides general information about the new calibration framework.

Withdrawing the two-step calibration

Originally the new calibration framework was planned to be composed of two independent steps: **1st calibration by using MIP** (minimum ionizing particles) in FMS and **2nd calibration by using** π^0, respectively. As the conventional calibration framework by PSU (Penn State University) group only utilizes π^0, the 1st calibration by MIP was expected to provide another degree of precision, especially thanks to its characteristic which MIP does not require reconstruction process like π^0.

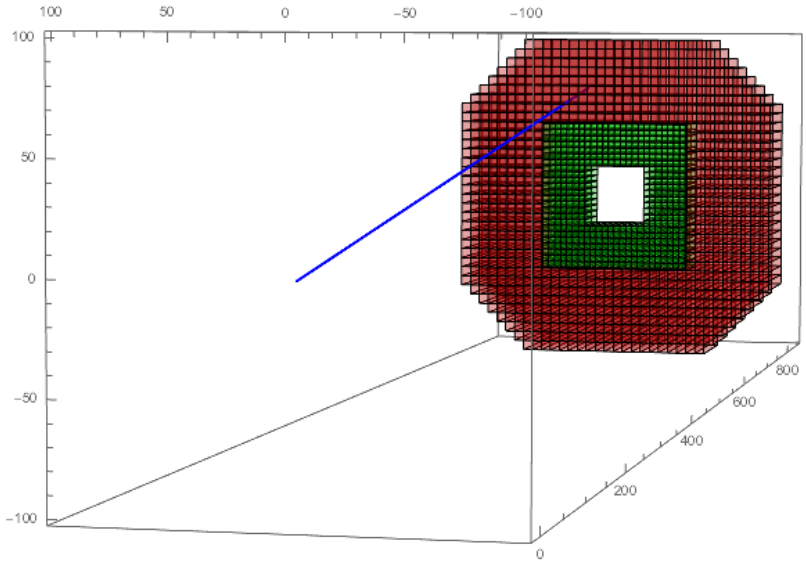

Figure 2.1: Incidence of a particle into FMS. Plot generated by David Kapukchyan

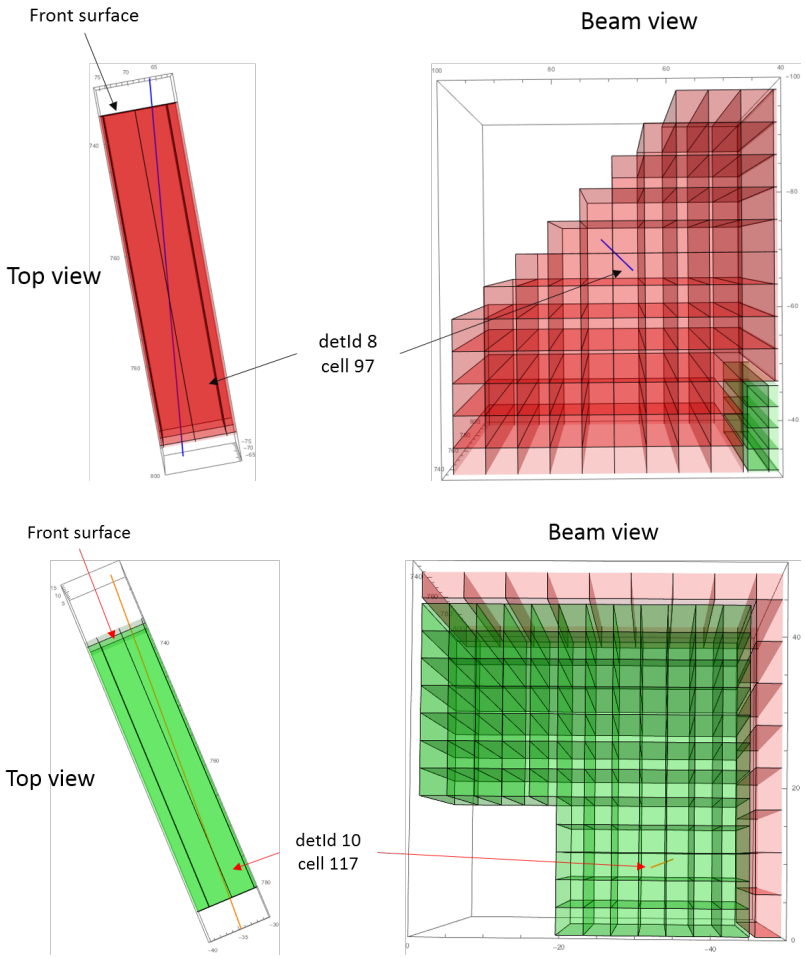

Figure 2.2: Passage of a particle into a typical large cell (top, red) and a typical small cell (bottom, green). In small cells, the majority of passage length contained in a cell. Plots generated by David Kapukchyan.

For this purpose, the MIP was intensively studied by using ADC distributions from the physics stream. However, after a thorough study by David Kapukchyan it was concluded that the MIP cannot be used for calibration due to the following problems.

First, to find a MIP in FMS one must depend on algorithms to isolate it from pedestals and EM shower backgrounds. Second, the FMS cells are not projectively arranged to the primary vertex (Fig. 2.1). This causes a particle passes through multiple cells even if there's no scattering. Besides, this phenomenon affected seriously by the η (pseudorapidity) of the cell: a cell located far from the beam pipe (smaller η) takes a larger effect. Since the calibration requires 1-to-1 correspondence between deposited energy and a cell, such a phenomenon induces additional ambiguity even if one succeeds to isolate a MIP. Third and finally, the energy deposited by a MIP is only a few hundred MeV: when converted to the ADC, this amount of energy sits only a few ticks above the pedestal, thus works as a harsh limit on the development of MIP isolation algorithm.

Because of the second problem, the MIP cannot be used for large cells' calibration. Also, due to the third problem combined with small cells' severe bit shift condition in RUN15 [6] the isolation of MIP is practically not feasible. As a result, it is concluded that the new framework also utilizes only the reconstructed π^0 for the calibration.

Comparison to the conventional framework

	New	Conventional
Base analysis framework	STAR	PSU
Compatible data format	μDSTs	Trigger files
MergeSmallToLarge [a]	Yes	No
Update on π^0 reco. algorithm (2018)	Yes	No
Consider event by event zVtx	Yes	No
Bad channels exclusion	Before reco	After reco

Table 2.1: Notable differences between new and conventional framework

Although both conventional and new frameworks use reconstructed π^0 for the calibration, there are a few notable differences as summarized in Table 2.1.
First of all, the new calibration framework is based on STAR libraries and μDSTs, while the conventional framework is based on an independent framework developed by PSU group and the Trigger files. Although the FMS libraries in STAR CVS were more or less the same to PSU until 2014, however, some important updates were made to codes in STAR in the last few years (2015-2019). One such update is the consideration for a cluster formed across small-large cell boundary by Akio Ogawa [7]. Without this update the cluster finding process performed independently for each detId, thus one cannot retrieve such cluster formed across the boundary. Another important update is the improvement of the π^0 reconstruction algorithm studied by Zhanwen Zhu in 2018. To enhance the precision of the algorithm, especially for a π^0 decay photons' energy and opening angle, following items were studied and applied to FMS library in STAR: inclusive zVtx consideration, anchor point based energy correction, incident angle effect in shower development, and set lower limit of the opening angle, respectively [8]. Also, some minor differences exist as well: by default, the new framework applies BBC slewing corrected zVtx [9] event by event and exclude bad channels before reconstruction thus completely negate them from the calibration, while conventional framework doesn't.

[a] StFmsPointMaker→setMergeSamllToLarge(*true*). This flag enables consideration for a cluster formed across small-large cells boundary.

Summary of overall calibration process

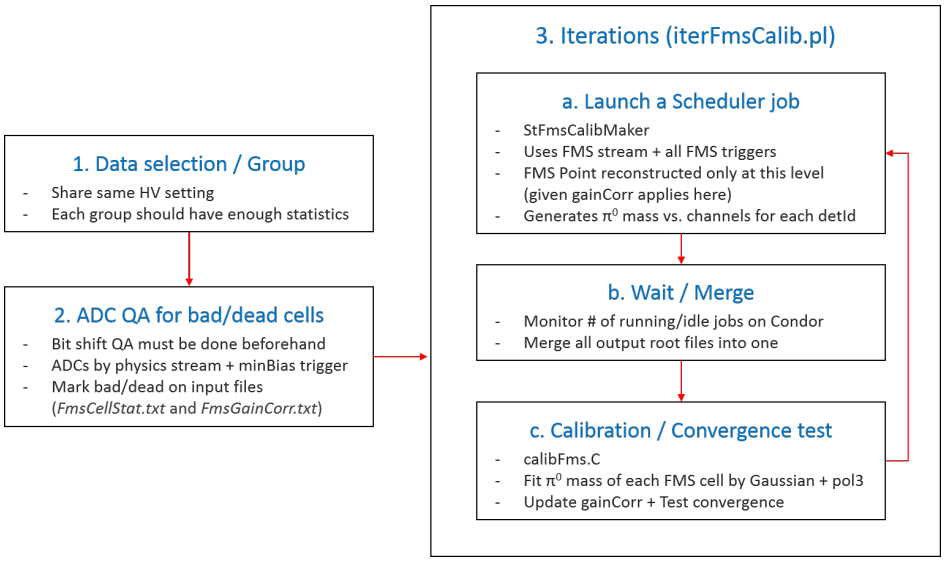

Figure 2.3: Summary of the overall calibration process

The overall process of new calibration can be described as follows.

1. Separate a whole period of interest (ex. RUN15pp200trans) into proper subgroups. Each subgroup should have enough statistics and should share the same online calibration status (HV setting).
2. Perform bad/dead cells QA (* details about QA procedures can be found in section 2.3.1). To avoid any bias from FMS itself, use the Physics stream and a minimum bias trigger for collecting ADC. Once the QA is finished, modify *FmsCellStat.txt* and *FmsGainCorr.txt* accordingly to exclude them from reconstruction.
3. Launch the iterations by using prepared Maker and Script.
    a. If all requirements are satisfied the script submits Scheduler jobs for runs in the list and wait until they're finished. Note that π^0 reconstruction performed only at this stage for each iteration.
    b. After Scheduler (Condor) jobs are finished (# of running + idle jobs are 0), the script merges all output root files into one. This one final root file used as input in the next step.
    c. Perform fit to retrieve each cell's π^0 peak position and update gainCorr accordingly. If enough # of iterations done already, convergence test routine checks previous iterations' results retrospectively and judge if the cell's gainCorr is converged. Finally, new *FmsCellStat.txt* and *FmsGainCorr.txt* are printed out and return to step a. and launch the next iteration.

2.2 Calibration

This section visits each process of calibration in detail.

2.2.1 Requirements for data

Before any other calibration process, **all FMS cells' BS (bit shift) value must be cross-checked** [6] if the BS in the DB matches the applied one. Since the BS directly affects a cell's ADC distribution and its energy [a], a cell with wrong BS value in the DB can affect not only the calibration status of the cell itself but also multiple cells in the vicinity, as multiple cells contribute for the reconstruction of a π^0 event.

Purpose	Stream	Trigger
Calibration	st_fms	All FMS triggers except FMS_LED
Bad/Dead/Hot QA	st_physics	MinBias

Table 2.2: Data stream and Trigger condition by purpose

By purpose, two types of data streams are used in the calibration (Table 2.2). Physics stream (st_physics) is used for QA, especially for the ADC QA for the bad/dead cell exclusion. To avoid any possible bias from FMS only the events triggered by a specific MinBias trigger [b] are used. FMS stream (st_fms) is used for the actual calibration [c]. To obtain as many as statistics all FMS triggers except FMS_LED are used.

For the amount of data to be used in calibration two conditions should be considered: **statistics and online calibration status**, respectively. As calibrating the whole period of interest at once is practically impossible, a period needs to be separated into a few subgroups, which have enough statistics and share the same online calibration status. There's no specific upper limit in the size of a subgroup, however, the CPU time required for an iteration gets longer as data size increases. Note that during the development new framework used a couple of days' (RUN15pp200trans, day 80-81) statistics. Finally, an example of subgroup determination can be found in section 3.1.

[a] Hit (cell) energy = ADC × gain × gainCorr

[b] Any MinBias trigger is ok but it's recommended to select a trigger (to enable normalization by number of trigger) with small prescale (to obtain more statistics) throughout the period of interest (ex. RUN15pp200trans). During the framework development, *BHT1*VPDMB-30* was used for RUN15pp200trans data.

[c] st_physics is also considered but discarded eventually as statistics is too scarce

2.2.2 Maker and Scripts

Analysis Maker (StFmsCalibMaker)

A dedicated analysis maker is prepared for the calibration. Its composition is as follows:

StFmsCalibMaker

- StFmsCalibMaker.h
- StFmsCalibMaker.cxx
- StFmsCalibMakerQa.h
- StFmsCalibMakerQa.cxx

Primarily the maker runs on STAR μDSTs and returns π^0 invariant mass distribution for each FMS cell. Note that the total invariant mass yields by this process is **NOT** equivalent to the π^0 cross section. The conditions applied to obtain the mass distribution will be discussed in the next section (section 2.2.3).

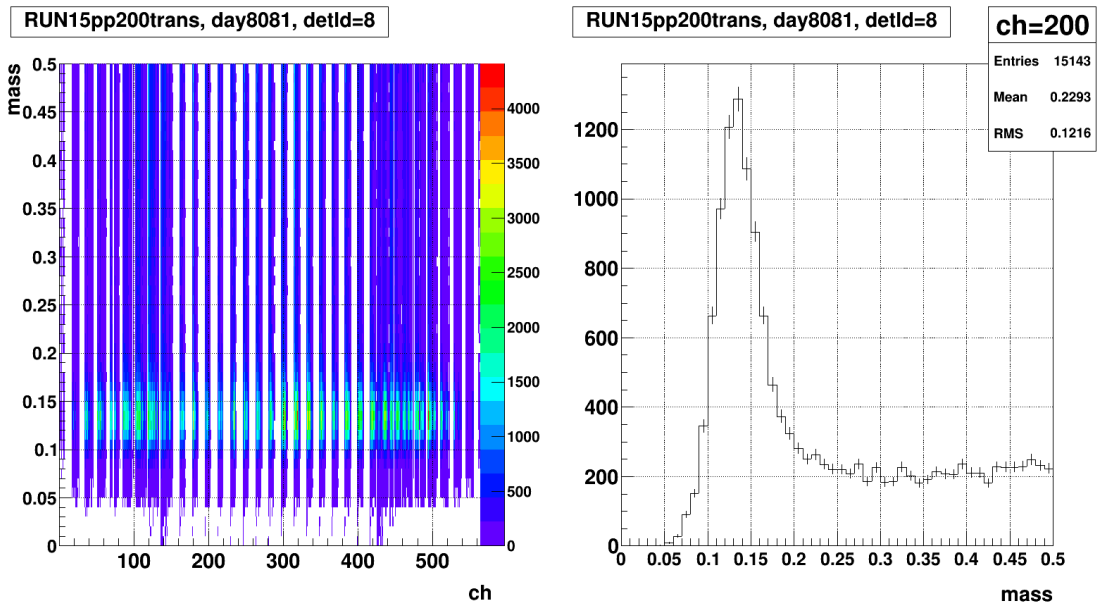

Figure 2.4: A sample of mass vs. channels histogram by StFmsCalibMaker (left) and a channel's mass distribution obtained by projecting an x bin (right).

In addition to its main purpose, multiple member functions exist. Most of them can be enabled or disabled: to disable a function, simply comment it out at the macro for μDST running. Some functions should be applied as a default condition but some functions are optional. The list of functions is as follows. Note that functions highlighted in red indicate they should be enabled as default.

StFmsCalibMaker, member functions (alphabetical order)

8	1	0.060	1	34	-2.50	96.55	8	1	0
8	2	0.059	2	34	-8.36	96.55	8	2	0
8	3	0.059	3	34	-14.22	96.55	8	3	0
8	4	0.058	4	34	-20.08	96.55	8	4	0
8	5	0.058	5	34	-25.94	96.55	8	5	0
8	6	0.057	6	34	-31.80	96.55	8	6	0
8	7	0.055	7	34	-37.66	96.55	8	7	0
8	8	0.054	8	34	-43.52	96.55	8	8	0
8	9	0.053	9	34	-49.38	96.55	8	9	0
8	10	0.052	10	34	-55.24	96.55	8	10	0
8	18	0.063	1	33	-2.50	90.70	8	18	0
8	19	0.063	2	33	-8.36	90.70	8	19	0
8	20	0.063	3	33	-14.22	90.70	8	20	0
8	21	0.062	4	33	-20.08	90.70	8	21	0
8	22	0.061	5	33	-25.94	90.70	8	22	0
8	23	0.060	6	33	-31.80	90.70	8	23	0
8	24	0.059	7	33	-37.66	90.70	8	24	0
8	25	0.057	8	33	-43.52	90.70	8	25	0
8	26	0.056	9	33	-49.38	90.70	8	26	0

Figure 2.5: Display of FmsMapBase.txt (left) and FmsMapBitShift.txt (right) obtained by function *GetMap*. From left each value means: detId, channel, gain, column, row, x, y, detId, channel, and bit shift, respectively.

1. *GetMap()*: prints out following text files. Note that the values are read from *StFmsDbMaker* and depend on given μDST's run number.
   - FmsMapBase.txt: detId, channel, gain, column, row, x, and y
   - FmsMapBitShift.txt: detId, channel, and bit shift
2. *GetQaHist()*: add following QA histograms to output root file.
   - mass vs. channels, extended mass range (0.5 (GeV) $\rightarrow$ 1.0)
   - mass vs. pair energy, separated by Zgg (point energy asymmetry) in the stepwidth of 0.1
   - mass vs. opening angle, separated by Zgg in the stepwidth of 0.1
   - mass vs. Zgg, separated by pair energy in the stepwidth of 10 (GeV)
   - Reco. points' η vs. ϕ, separated by detId
   - Reco. points' XY distribution, separated by large/small cells
3. *GetQaHistAdc(triggerId)*: add QA purpose ADC histograms to output root file. This function requires a MinBias trigger's offline trigger id as an argument. Note that any other process including π^0 mass collection will be skipped if this function is enabled. Lastly when this function is used it's recommended to use st_physics.
   - ADC vs. channel, $0 <$ ADC < 250, requires ADC > 3 to cut out pedestal tail
   - ADC vs. channel, $0 <$ ADC < 5000
4. *GetQaTree()*: add QA purpose ROOT tree to output file.

5. *ReadBbcSlewing*: apply slewing corrected zVtx (BBC_z) to π^0 mass. Require a BBC slewing correction file written by Oleg Eyser [9]. Once enabled add following QA histograms to output root file.

   - Slewing corrected zVtx distribution
   - ΔMass (reco. mass wo/ applying zVtx (z=0) - reco. mass w/ applying zVtx)
   - ΔOpening_angle

6. *ReadCellStat(FmsCellStat.txt)*: reads FMS cells' status file and checks bad marked cells' gainCorr. Stops the entire process if any bad marked cell's gainCorr isn't 0.

Analysis macro (runMudst.C)

A couple of caveats exist for μDSTs running macro.
First, make sure to call *StFmsDbMaker* before and use function *readGainCorrFromText(true)*. By doing this external gainCorr values defined in file StFmsGainCorr.txt will be applied in reconstruction, instead of values in DB.
Second, make sure to call both *StFmsHitMaker* and *StFmsPointMaker* before and do **NOT** use *SetReadMuDst()* for both of them. If the *SetReadMuDst()* is used neither cluster finding nor point reconstruction won't be performed.

Iteration script (iterFmsCalib.pl)

In addition to a run list the iteration script requires the following files to starts.

- FmsCellStat.txt (cell status file)
- FmsGainCorr.txt (gainCorr values to be applied in reconstruction)
- FmsMapBase.txt
- FmsMapBitShift.txt (BS values in this file are not used: only exists to show them in plot)
- calibFmsTools.C (includes definitions and essential functions for calibration)
- calibFmsShow.C (defines functions for plot generation, requires calibFmsTools.C)
- calibFms.C (macro for fit and gainCorr update, requires calibFmsShow.C)

Once successfully started, the script submits Scheduler job for each run in the list and waits until all jobs are finished. To judge if the jobs are finished or not it continually checks Condor status by using *condor_q* and determines all jobs are finished if the number of running or idle jobs are 0. [a] Once all jobs are finished, the script merges all output files into one, and then executes calibration macro (calibFms.C) to perform fit and gainCorr update. If all previous processes are finished successfully new FmsCellStat.txt and FmsGainCorr.txt are printed out and the next iteration is started by using those new inputs.

[a] In RCF frequently serious delay happens by a few jobs which take too long for unknown reason. Therefore if number of remaining jobs is smaller than 10 the script starts counting and kills remaining jobs after an hour.

2.2.3 Assign a π^0 to a cell

A π^0 decay into two daughter photons and each photon starts EM shower as they enter the FMS. Since an EM shower spreads over in both azimuthal and longitudinal direction as it passes through the FMS, inevitably multiple cells fire during a shower's development, even without considering incident angle. To put it the other way around, having strict one-to-one correspondence between a π^0 event and a cell is impossible. Rather, only a relatively weak relation with intrinsic uncertainty can be established. Therefore the following two conditions are important for the good calibration: collecting clean π^0 samples and set reliable standards for the better $\pi^0 \leftrightarrow$ cell relation, respectively.

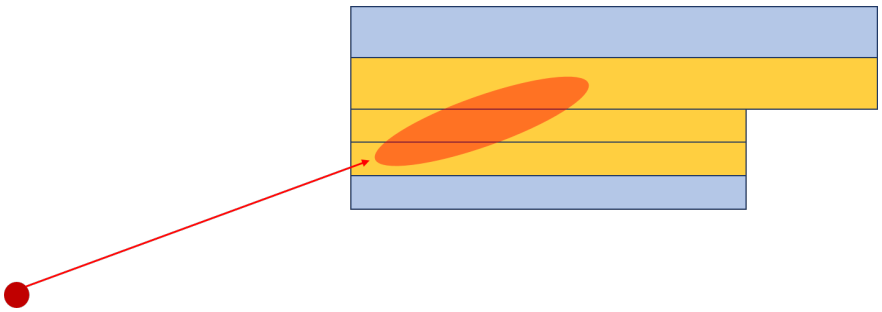

Figure 2.6: A diagram shows the development of an EM shower across small and large cells (side view). Yellow-colored cells indicate they're fired by the shower.

Summary of cuts

The following lists show cuts to obtain clean π^0 samples and to assign a π^0 mass to certain cells.

List of cuts for each event

1. Skip events in abort gap ($30 \leq$ crossingId < 40 or $110 \leq$ crossingId < 120)
2. Skip events if FMS_LED is fired [a]
3. Skip events if no BBC zVtx is available while zVtx flag is on (on is default)

List of cuts for each pair in an event

1. Use only clusters with single reconstructed point (single point cluster, SPC)
2. $20 <$ pair energy (GeV) < 40
3. Mass < 0.5 (GeV)
4. Zgg < 0.7
5. Satisfy *Cluster quality cut* (* section 2.3.2), applied only to small cells

A cut for $\pi^0 \leftrightarrow$ cell relation, applies to each hit in a pair

- Hit (cell) energy / Pair energy > 0.3

Details of each cut will be discussed in following paragraphs.

[a] 12 triggers exist for FMS: sm-bs1, sm-bs2, sm-bs3, lg-bs1, lg-bs2, lg-bs3, DiBS, JP2, JP1, JP0, DiJP, and LED.

Cuts for each pair (π^0 candidate)

Due to the FMS' forward position ($2.5 < \eta < 4.0$), under certain condition showers from a π^0 decay photons are merged into a cell. Such merged showers induce a large shift in the reconstructed mass since both energy and opening angle of such event are largely deviate from truth. As the π^0 is more energetic, as the π^0 decay photons' energy is more symmetric (Zgg $\rightarrow$ 0), and as the π^0's η is larger (closer to beam pipe) it is more likely they're merged, and then after certain threshold two showers cannot be distinguished at all.

Applying an η cut or a minimum Zgg cut to obtain clean π^0 can be dangerous since they can work as bias for the samples being collected. The same logic applies to the energy as well, however, unlike the other two the cut on energy is necessary for the following reasons. First, one cannot use whole energy for the calibration since the attenuation in a cell can vary seriously by the energy. Second, as energy gets lower it is likely more backgrounds are introduced in collected π^0 samples. Third and finally, due to the showers' merging previously discussed, after certain threshold two showers cannot be distinguished at all. Thus an upper energy limit is required, either.

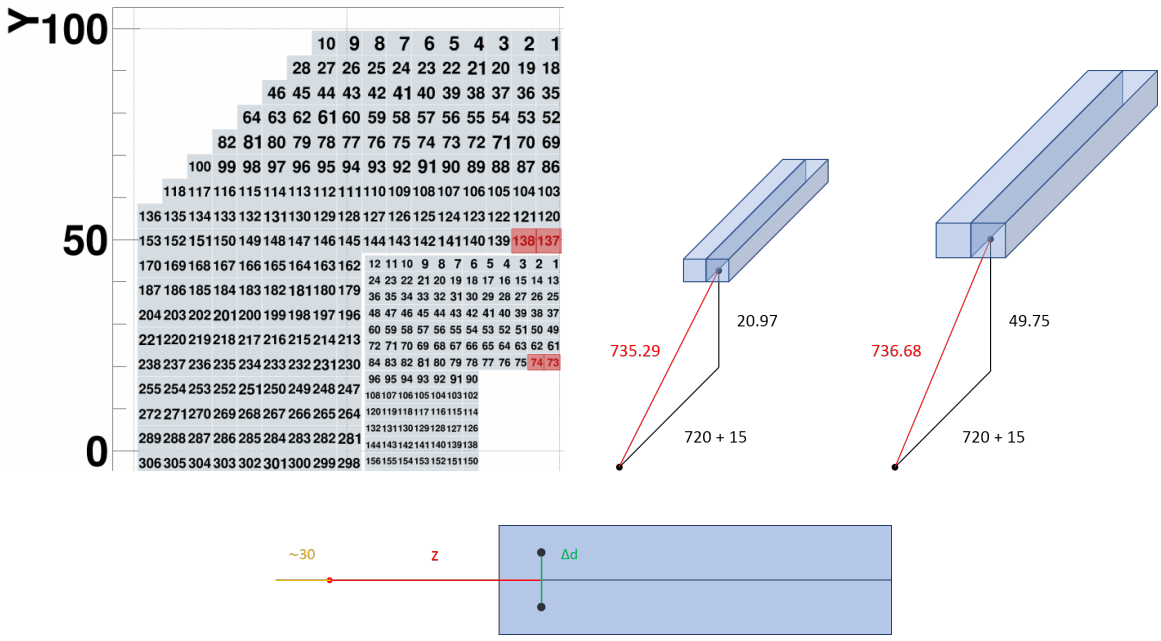

Figure 2.7: One quadrant (top half of detId 8 and 10) of FMS (top left), red-marked cells' y/z position and distance to the vertex (top right), and schematic diagram of a pair of red marked cells in top view (bottom). A pair of red marked cells indicate closest cells from the beam pipe by its type (large or small) [a], which expected to suffer merging effect most seriously. In the bottom plot, ~30 (cm) indicates a typical zVtx shift in RUN15, z indicates the distance between the vertex to shower max (15 cm from cell surface), and Δd indicates the distance between two showers which can be distinguished by reconstruction algorithm, respectively.

[a] A cell's dimention is as follows: 3.8 (cm) $\times$ 3.8 $\times$ 45 (small) and 5.8 $\times$ 5.8 $\times$ 60 (large), respectively.

For the lower energy cut, **20 GeV** was chosen based on background study in RUN11 data analysis. On the other hand, for the upper energy cut the value which showers start merging was studied by introducing two extreme conditions: select a pair of cells with the largest η and set the daughter photons' energy perfectly symmetric ($E_1 = E_2$, Zgg = 0), respectively. Top plots in Fig. 2.7 shows position information of cells selected for this study. Starting with the equation for invariant mass, by counting in two previous conditions the shower merging energy can be estimated as follows.

$$M_{inv}^2 = 2E_1E_2\,(1 - cos\theta) \tag{2.1}$$

$$E^2 = \frac{0.135^2}{2\,(1 - cos\theta)} \tag{2.2}$$

The opening angle θ is determined by distance from vertex to shower max position z [10] and minimum distinguishable distance (Δd). The bottom plot of Fig. 2.7 depicts each item. Then the equation for θ calculation is as follows.

$$\theta = tan^{-1}\,(\frac{\Delta d}{z}) \tag{2.3}$$

The Δd is not a strictly determined value. It can be changed by various conditions such as zVtx, calibration status, cell status, etc. Therefore two cases are considered in this calculation: Δd is equivalent to a cell's width (5.8 cm for large, 3.8 cm for small) or half cell width, respectively. In addition, the effect of typical zVtx shift ($\sim$30 cm) also considered. The results are summarized in Table 2.3.

Cell Type	Δd (cm)	ΔzVtx (cm)	θ (rad)	Energy (GeV)
Large	5.8	0	0.00787300	17.1473
		30	0.00756494	17.8455
	2.9	0	0.00393656	34.2939
		30	0.00378252	35.6905
Small	3.8	0	0.00516798	26.1224
		30	0.00496540	27.1882
	1.9	0	0.00258401	52.2444
		30	0.00248271	54.3760

Table 2.3: Calculation of shower merging start π^0 energy

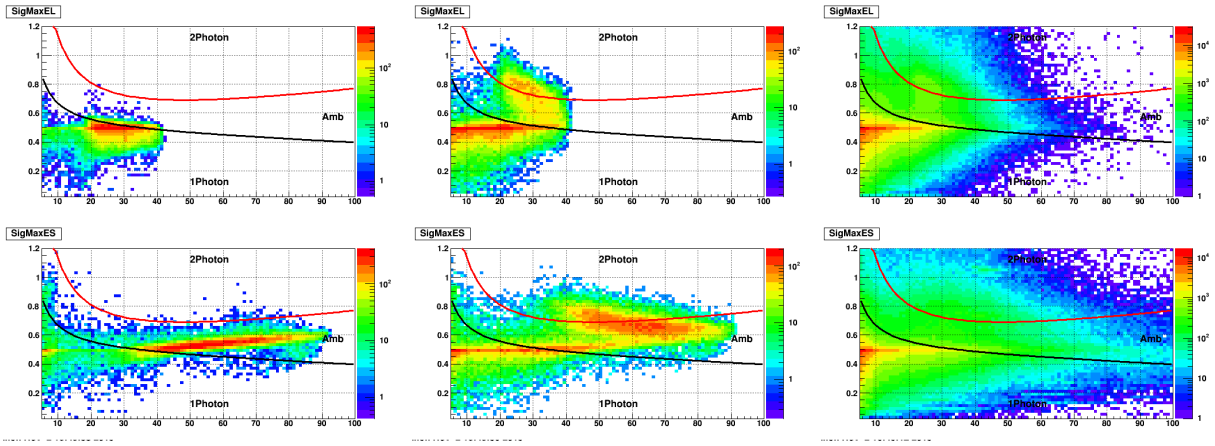

Figure 2.8: FMS cluster categorization by σ_{max}. Each plot indicates σ_{max} vs. energy. Each row indicates large (Top) or small (Bottom) cells. Each column indicates different types of samples: single photon MC (left), π^0 MC (middle), and RUN15 data (right), respectively. Each line (either red or black) on top of each plot indicates σ_{max} cut determines the number of photons in this cluster. Finally, the area marked as "Amb" between red and black lines indicates ambiguous. The study and plot generation was done by Akio Ogawa. [11]

Although the energy can be estimated to some extent, however, these values change fast by the Δd. In actual reconstruction, a parameter (σ_{max}) and a chain of algorithms are used to judge if the cluster originated from a shower or multiple showers (or how many points a cluster got) [a]. Fig. 2.8 shows the distribution of σ_{max} vs. π^0 energy for various samples [11]. According to the single photon MC and π^0 MC study by Akio Ogawa, especially for small cells, the judgment starting to be ambiguous from 30 GeV (Fig. 2.8, bottom left) and then becomes almost indistinguishable around 60 GeV (Fig. 2.8, bottom middle). In conclusion, to prevent having merged showers in the collected π^0 samples, the upper limit of a pair's energy was set conservatively as **40 GeV**, in addition to using only the **clusters with the single reconstructed point**.

For the rest of the cuts applied to a point pair are as follows. The maximum range of mass distribution was restricted to **0.5 GeV** to avoid any possible peak from η meson. Next, the maximum Zgg set to **0.7**. as fake photons largely contribute to the high Zgg events. Also, this 0.7 cut is well known in the FMS analysis, proven by various studies. Finally, there is a set of cut defined by cluster related parameters named **Cluster quality cut**, which applies only to small cells to suppress a specific problem. The problem and The cut will be discussed in section 2.3.2.

[a] StRoot/ StFmsUtil/StFmsTowerCluster

A cut for pair (π^0 candidate) $\leftrightarrow$ cell relation

At the early stage, to establish $\pi^0 \leftrightarrow$ cell relation a pair's mass was assigned to the cell with leading hit [a], assuming it has strong correlation to the pair. If there's a cell with particularly large energy portion it'd be a reasonable guess, however, if there are multiple cells with more or less same energy this argument no longer holds (Fig. 2.9).

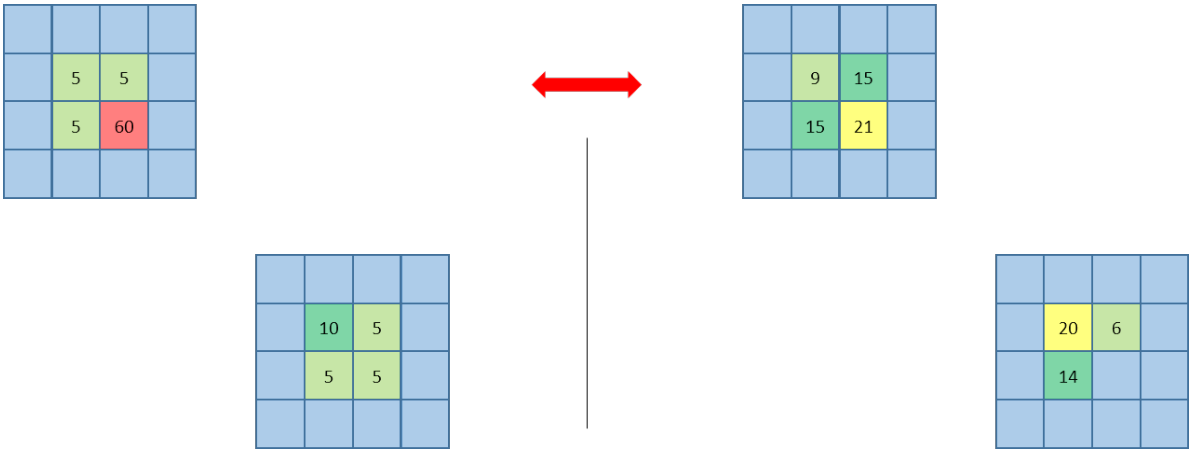

Figure 2.9: A π^0 event with one distinct leading energy cell (left) or A π^0 event with its energy distributed over multiple cells (right). The value inside a cell denotes the ratio of the cell's energy to the π^0's energy.

In addition, the leading hit's energy is not always undoubtedly large. For instance, if a cell has 60 % of the pair's energy it'd be safe enough to treat this cell represents the pair. However, if it has only 15 % of the energy it wouldn't. Fig. 2.10 shows the distribution of leading hit's energy portion to the pair's energy. As it shows the leading hit's energy portion goes down to almost 0, which is likely from fakes.

As a result, instead of using leading energy hit, the minimum hit energy ratio cut was applied for pair (π^0) $\leftrightarrow$ cell relation. If a cell has more than **30** % of the pair's energy, the pair's mass will be assigned to the cell under the assumption of it represents the pair. Note that the 30 % cut was chosen to obtain as much statistics as possible: because of this slightly loose cut, it is possible that a pair's mass can be assigned to more than one cell (i.e. two cells exist with 30 % energy of a pair), although such cases are very rare. Practically this condition is almost equivalent to using leading energy hit with minimum energy ratio cut.

[a] A cell with highest energy in two clusters

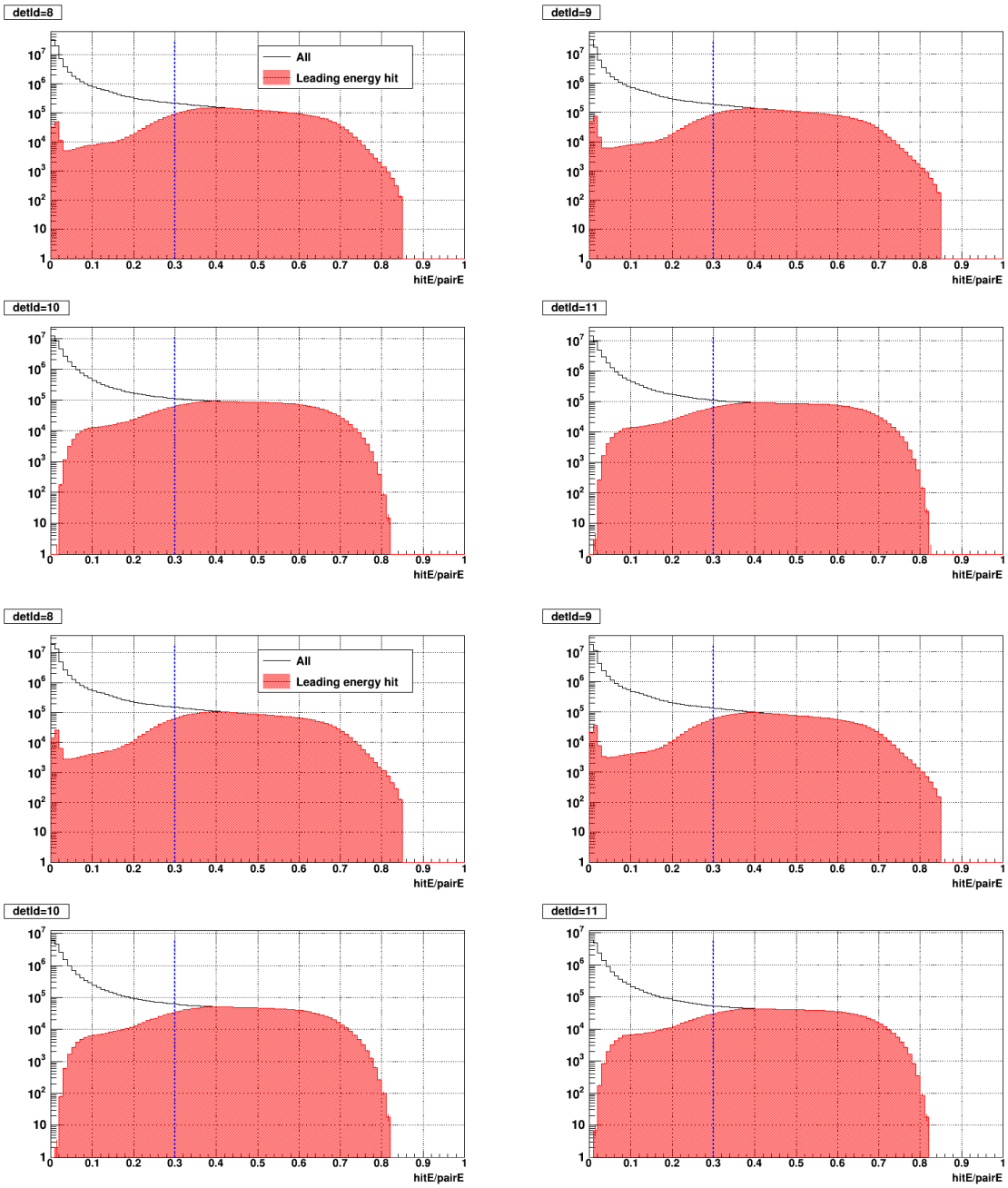

Figure 2.10: Ratio (percentage) of each hit's energy to the pair (π^0 candidate) energy separated by detId. Black line indicates all hit and Red filled histogram indicates leading energy hit. The blue vertical line on top of each histogram indicates the final cut (30 %). Top four distributions were obtained from day 82-84 and Bottom for distributions were obtained from day 89-90 in RUN15pptrans. As two different periods show the ratio distribution does not vary over time.

2.2.4 Fit on π^0 mass distribution

This section provides detailed information about fit procedures for gainCorr update in the next section.

Fit functions

To check a cell's calibration status the π^0 peak's position on reconstructed mass distribution is used as the parameter. If a cell is well calibrated its π^0 peak must be very close to its true value (0.135 GeV) with reasonably narrow width. The peak position is retrieved by the fit, and the function for the fit process is defined by the combination of a Gaussian and a modified 3rd-degree polynomial. The definition can be found in the following equations 2.4 - 2.6. Also Fig. 2.11 shows an example of typical mass distribution and fit on it for each cell type (large or small).

$$f(x) = f_{sig}(x) + f_{bg}(x) \tag{2.4}$$

$$f_{sig}(x)\ ^{a} = p_0 \times exp\left(-\frac{(x-p_1)^2}{2p^2}\right) \tag{2.5}$$

$$f_{bg}(x) = (x - p_0'\ ^{b}) \times (p_1' + p_2'\,x + p_3'\,x^2) \tag{2.6}$$

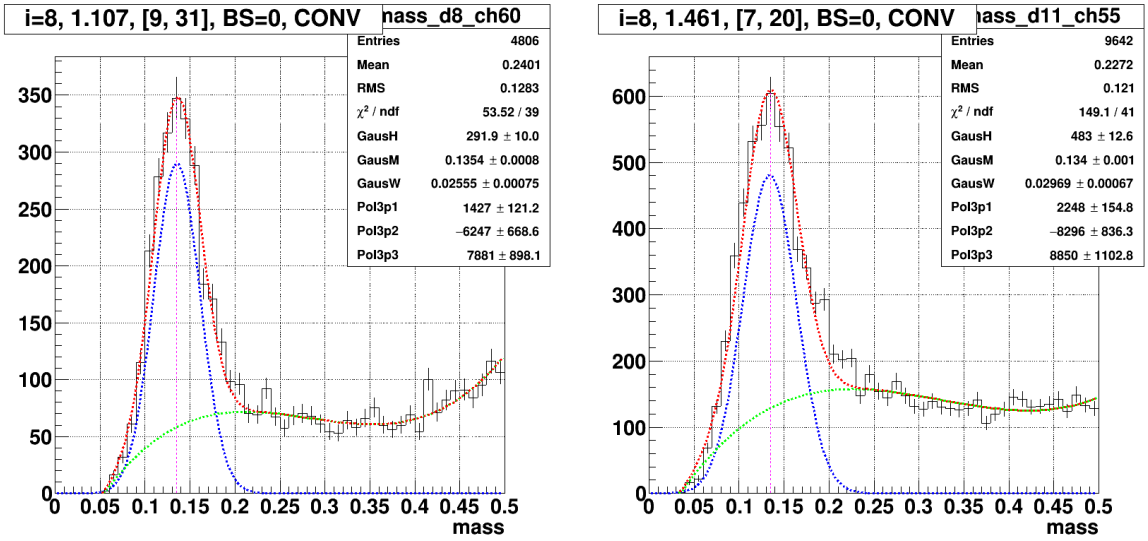

Figure 2.11: Example of fit on reconstructed mass distribution for a large cell (left) or a small cell (right). Dashed lines on top of mass distribution indicates combined fit (red), combined fit's signal part (blue), combined fit's background part (green), and true π^0 mass (magenta) respectively.

[a] $p_0 \times$ TMath::Gaus$(x,\ p_1,\ p_2)$

[b] Fixed parameter in the fit, by using the value of first nonzero bin in the mass distribution

Fit process

To retrieve the π^0 peak's position following fit process is performed for each cell.

Fit process for each cell

1. Get a cell's mass distribution. If statistics is too small ($<$ **100**) [a] skip remaining steps.
2. Set range of signal and background region. Default signal range is **0.135** $\pm$ **0.06** (GeV). [b] [c]
3. Make two temporary copies of original distribution and leave only signal or BG part.
4. Perform preliminary fit on each part (signal or BG)
5. Perform final fit on original distribution by using preliminary fits' results as seed parameters.
6. Check fit quality and retry fit if necessary (details will be given in the next paragraph).

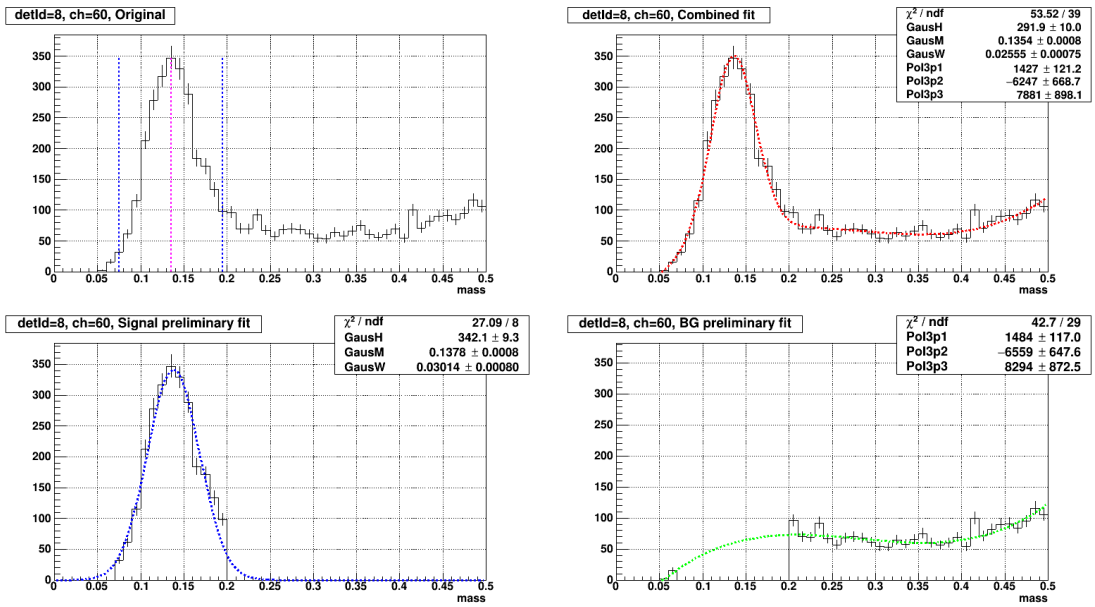

Figure 2.12: Flow of overall fit process for a cell including a preliminary fit. Starting from top left and in the counterclockwise direction, each plot indicates: raw reconstructed mass distribution (top left), signal part with preliminary fit (bottom left), BG part with preliminary fit (bottom right), and raw distribution with final combined fit (top right), respectively. In top-left plot, magenta line indicates true π^0 mass (0.135 GeV) and blue lines indicate the range of signal part defined by 0.135 $\pm$ 0.06.

[a] Empirically a reconstructed mass distribution requires at least a few hundreds of entries to have clear peak/BG structure. Although the value 100 is determined very loosely, it still works as tight cut for the large cells located at outer edge of the FMS.

[b] For a typical, clean distribution, the width 0.06 roughly corresponds to 3 σ (2 σ) for large (small) cell. The BG range is defined as entire mass distribution coverage except the signal range.

[c] If the peak (highest bin in the mass distribution) is located outside of 0.135 $\pm$ 0.06, extend the signal range to the peak's direction as follows: [0, 0.135 + 0.06] or [0.135 - 0.06, 0.35], respectively.

Safeguards for random fit failure

Although the fit function (eq. 2.4) works reliably in most cases, there also exist the cases fit quality is very poor or even completely fails. Mostly such failure happens when the mass distribution is messy: too small statistics, too large backgrounds, largely shifted peak position, etc. Since the gainCorr update solely rely on the mass_{fit} (retrieved peak position by fit), such failure can lead the cell's gainCorr to the value not trustworthy.

To ensure the quality of the fit a couple of parameters are used: **deviation of mass_{fit} from mass_{π^0}** and **χ^2/NDF of the combined fit**. Note that the χ^2/NDF can vary largely: even if it's value is substantially large or small compared to 1.0, it doesn't guarantee the fit is poor. However, if there are large deviation in both mass and χ^2/NDF simultaneously, it is unlikely the fit's quality is trustable. Therefore if any of the following conditions are satisfied the fit is regarded as **suspicious**, and then retry process is executed.

Fit quality criteria

- $|\ \text{mass}_{\pi^0} - \text{mass}_{fit}\ | > 0.03$ and $\chi^2/\text{NDF} < 0.5$
- $|\ \text{mass}_{\pi^0} - \text{mass}_{fit}\ | > 0.03$ and $\chi^2/\text{NDF} > 3.0$

Retry

1. Set all fit parameters (eq. 2.4) anew as follows.
   a. p_0 (Gaussian height): a random number between [half max, max] of the original mass peak
   b. p_1 (Gaussian mean): a random number within the range of 0.135 ± 0.06
   c. p_2 (Gaussian width): a random number between [0.01, 0.3]
   d. p_3 (p_0', Pol3p0): fixed as 1st nonzero bin's position
   e. p_4 - p_6 (p_1' - p_3'): 1
2. Perform combined fit and check fit quality criteria.
3. Break the loop if new fit is no longer suspicious, otherwise return to step 1. [a]

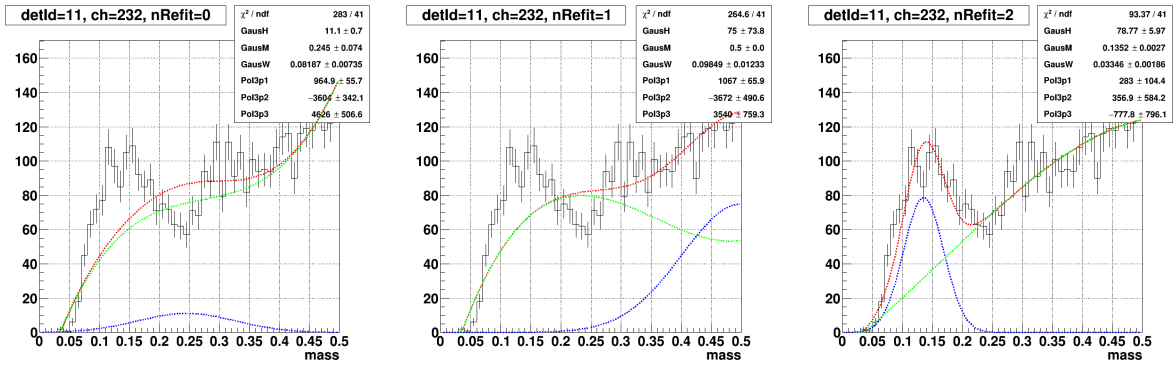

Figure 2.13: Example of suspicious case caught by fit quality criteria and retry attempts followed by. The fit succeeded in 2nd attempt and escaped the loop.

[a] Default maximum number of retry is 10.

2.2.5 Update gainCorr

This section provides detailed information about gainCorr update procedures.

Update gainCorr

Once the fit process on the cell is finished and mass $_{fit}$ is retrieved, the gainCorr of the cell will be updated by using the following equation.

$$\text{gainCorr}_{next} = \frac{mass_{\pi^0}}{mass_{fit}} \times \text{gainCorr}_{current} \tag{2.7}$$

The gainCorr $_{current}$ means the very gainCorr value applied to obtain the current reconstructed mass distribution used for fit (mass $_{fit}$), and gainCorr $_{next}$ means the value will be applied in upcoming reconstruction (iteration). Note that a couple of safeguards exist to reduce the error before gainCorr $_{next}$ is confirmed: the gainCorr $_{next}$ not always follow the eq. 2.7 exactly.

Skip update (use gainCorr $_{current}$)

- The cell's status is not GOOD (either BAD, DEAD, or CONVERGED)
- The cell has too small statistics (fit was not performed at all)
- The cell was judged as **skewed** (section 2.3.2)

Suspicious: limit maximum allowed gainCorr change to 20 % [a]

- | mass $_{\pi^0}$ - mass $_{fit}$ | > 0.03
- The fit's χ^2/NDF < 0.5 or χ^2/NDF > 25
- Number of fit retry hit the maximum

As one may noticed already, the conditions for 2nd safeguard (limit maximum gainCorr change) is more or less the same to the suspicious fit criteria explained in the previous section. Note that the maximum χ^2/NDF is much loosened and each condition is checked independently. The cut value for χ^2/NDF was determined by collecting feedback from multiple independent full iterations: Fig. 2.14 shows an example of such feedback.

[a] For instance, if gainCorr $_{current} = 1.000$ gainCorr $_{next}$ will be limited to 1.000 ± 0.200.

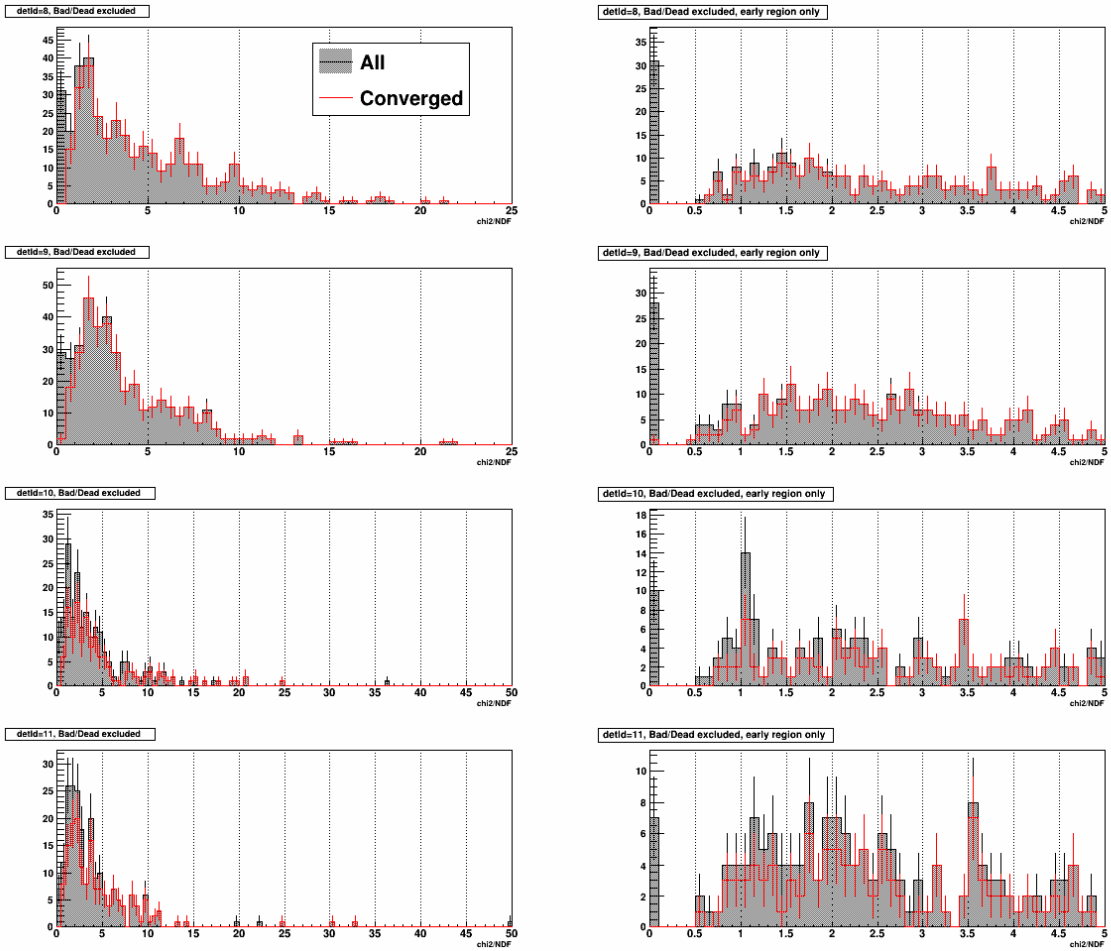

Figure 2.14: FMS cells' fit χ^2/NDF distribution after a full iteration. Each row shows the results of each detId and each column shows a different range ([0, 25] for left and [0, 5] for right). For each plot, black filled histograms indicate all cells and red line histograms indicate converged cells. The large spike at $\chi^2/\text{NDF} = 0$ in right column indicates cells with too small statistics (fit process returns 0 if the fit is not performed at all). Note that bad or dead cells are excluded beforehand. Finally, this distribution is obtained from day 91-93 in RUN15pptrans.

Convergence test

Assuming the overall process (mass reconstruction, fit, and gainCorr update) went well, as iterations go on a cell's gainCorr will gradually approach to certain value and will be converged eventually. Such converged value is the final gainCorr factor for the cell. Therefore certain standards required to judge a cell's gainCorr convergence status. For the judgment following two parameters are used: **deviation of mass $_{fit}$ from mass $_{\pi^0}$** and **Ratio of the cell's gainCorr change (R $_{gcc}$)**, respectively.

$$R_{gcc} = \frac{|\, gainCorr_{new} - gainCorr_{old} \,|}{gainCorr_{old}} \tag{2.8}$$

The convergence test performed retrospectively: to check previous parameters' stability over iterations the test routine requires at least 4 samples. Thus, in general, the test starts from 4th iteration (iteration index i=3). Detailed criteria are as follows.

Convergence criteria

1. | mass $_{\pi^0}$ - mass $_{fit}$ | < **0.005**
2. R $_{gcc}$ < **0.035**
3. Check both conditions independently over 4 iterations' results:
   a. Between each iteration index (ex. at iteration i=3, check 0-1, 1-2, and 2-3)
   b. Between 1st and final index (ex. at iteration i=3, check 0-3)

Note that the R $_{gcc}$ < 0.035 is calculated value based on mass deviation tolerance (0.005). For instance, if a cell's gainCorr is 1.000 or 2.000, possible R $_{gcc}$ is as follows.

- $0.135/(0.135 \pm 0.005) \times 1.000 = 1.000\,^{-0.0357}_{+0.0385} \rightarrow \mathrm{R}_{gcc} = 0.0357/1.000 = 0.0357$
- $0.135/(0.135 \pm 0.005) \times 2.000 = 2.000\,^{-0.0714}_{+0.0769} \rightarrow \mathrm{R}_{gcc} = 0.0769/2.000 = 0.0385$

Although it heavily depends on by the dataset, in RUN15pptrans the ratio of convergence (# of converged cells/All cells) is above 80 % after a full iteration (9 successive iterations) in general. Also, the cells judged converged showed reasonable mass distribution precisely centered around the mass $_{\pi^0}$.

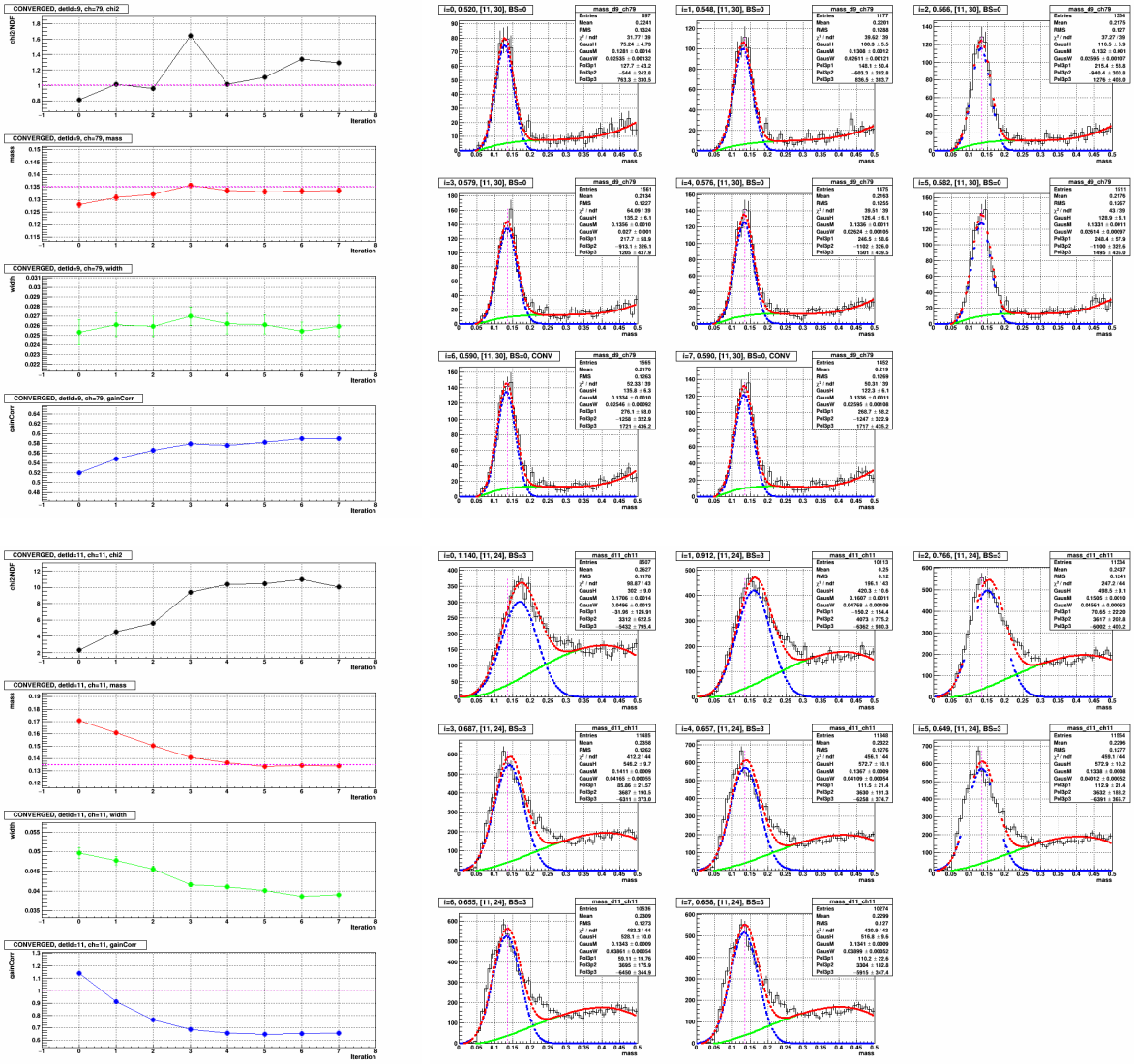

Figure 2.15: A couple of examples for convergence over iterations. For the left column, from top to bottom each row indicates: fit $\chi 2^2$/NDF, mass $_{fit}$, width of the mass, and gainCorr, respectively. Each mass distribution in the right column corresponds to each iteration index in the left plot. Both examples show mass $_{fit}$ and gainCorr gradually approach to certain value as iteration goes on.

2.3 Challenges and Crosschecks

This section visits challenges during the development and crosschecks for each of them.

2.3.1 Bad/Dead/Hot channels

Zgg bump: necessity of excluding problematic channels

As explained in section 1.2, the variable Zgg means asymmetry between two reconstructed points' energy. Typical Zgg distribution behaves as follows: lowest at 0 (equal energy), slightly increases with its value until 0.7, and then rapidly rises afterward. The rapid rising after 0.7 is a well-known issue due to the fake points originated from backgrounds.

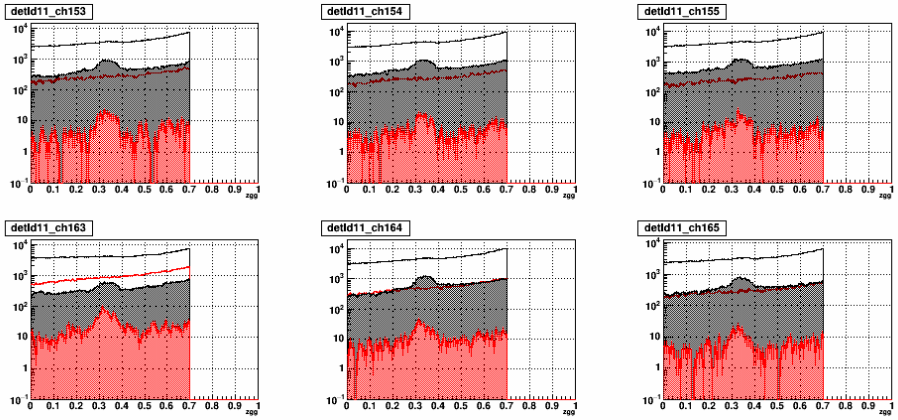

Figure 2.16: Zgg distribution of a few channels in detId 11. Black (Red) distribution indicates FMS (Physics) stream, and Line (Filled) distribution indicates its point pair energy requirements is 20 < E (GeV) < 40 (35 < E < 40).

However, at the early stage of the framework development, a strange bump-like structure was observed in Zgg distributions as shown in Fig. 2.16. The applied conditions were as follows.

Conditions for Zgg distribution

1. RUN15pp200trans, day 80 - 90
2. No bad/dead/hot channels QA applied
3. gainCorr from database (conventional calibration by PSU)
4. Tested data streams: Physics (st_physics) and FMS (st_FMS)
5. Cut on point pair energy (GeV): 20 < E < 40 or 35 < E < 40

A few additional characteristics were found by studies followed by: first, strong correlation exists between the bump structure and the pair's energy; second, although the bump can be seen almost all region but it's more distinct in small cells and Southside; third and finally, the bump strongly affected by invariant mass. It getting weakened with a tighter mass cut and completely disappears with mass < 0.3 (GeV), respectively.

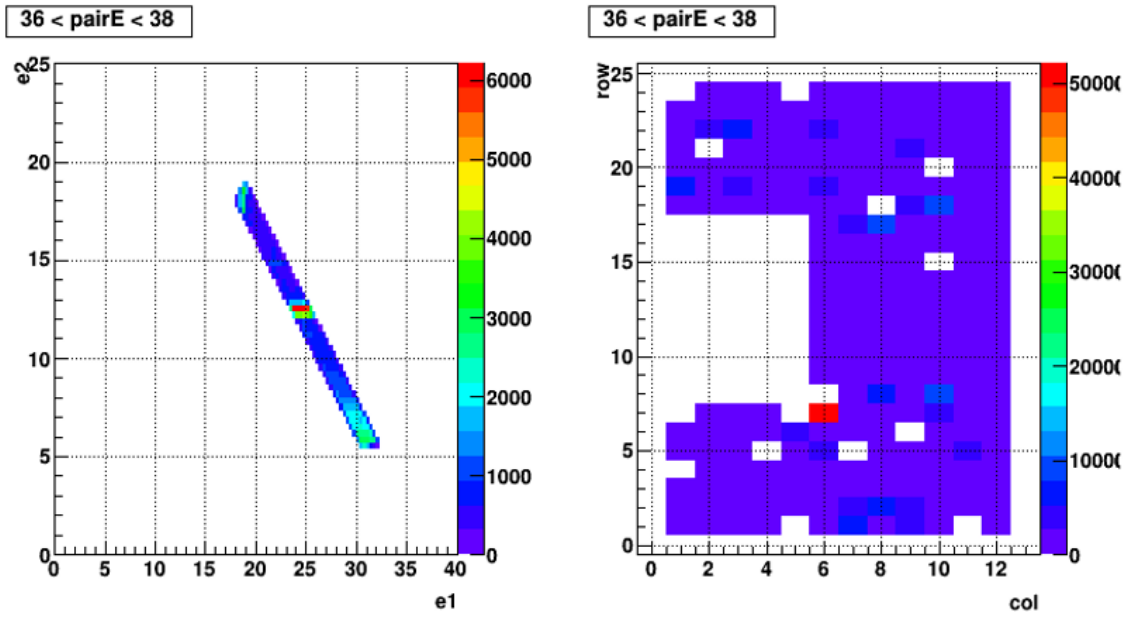

Figure 2.17: Concentration in point energy (left) and a hot channel responsible to (right)

Consequently, it turns out this phenomenon was caused by a problematic cell combined with poor calibration. The cell (detId 11, channel 210) was located at the inner edge of the small cells and had a few problems: first, the cell was largely bit shifted (+4) thus the cell's ADC starts from 32 [a]; second, the cell was hot thus it generated large amount of hit; third and finally, strangely large and artificial-looking gainCorr value (4.000) [b] was assigned to this cell, respectively. If one converts the ADC to energy the value is as follows.

$$32\ (\text{ADC}) \times 0.095\ (\text{gain}) \times 4.000\ (\text{gainCorr}) = 12.16\ (\text{GeV})$$

In the FMS framework, the point reconstruction routine searches X and Y position with the highest energy in a cluster to reconstruct a point. Considering the substantial size of the energy, it's likely the cell was chosen very frequently and eventually hindered proper reconstruction across a wide region. Fig. 2.17 shows the concentration at 12 GeV in the reconstructed point energy, which is originated from the problematic cell.

In conclusion, this study proved even single problematic channel can be devastating: therefore **all problematic cells must be masked out** via thorough QA before any calibration attempt. Finally, a more detailed report on the Zgg bump study can be found here. [12]

[a] No ADC = 16 (2^{0+4}) exists due to the pedestal subtraction
[b] The upper limit of gainCorr in the PSU calibration

QA criteria and procedures

The problematic channels categorized into 3 types: dead, bad, and hot [a], respectively. All these problematic cells' gainCorr set as **0.000** to mask them out in the reconstruction.

The dead/bad/hot channels QA utilizes cell by cell ADC distribution obtained from STAR official μDSTs. To obtain the ADC, the events from Physics stream and single minBias trigger are used: by using Physics stream and minBias trigger any possible bias from FMS triggers will be ruled out, and by using only one trigger [b] precise normalization is available.

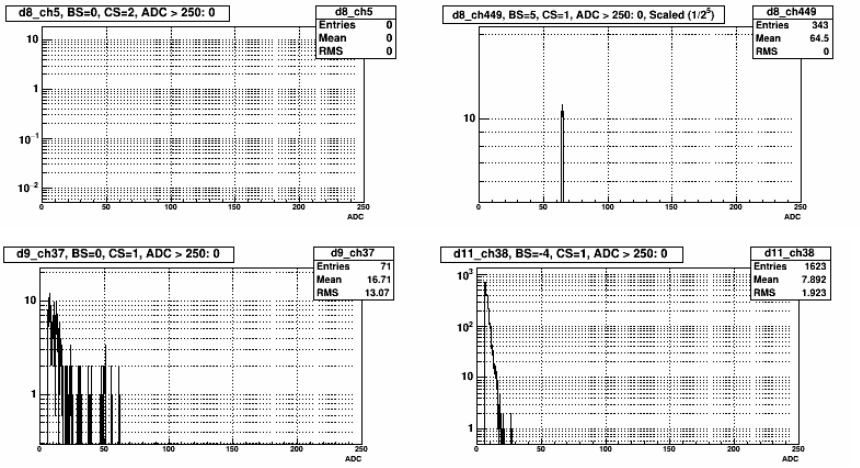

Figure 2.18: Examples of a dead cell (top left) and three bad cells (top right and bottom).

For the dead cells judgment, **only the cells with exactly 0 entries** are marked as dead. In principle, the cells with extremely small entries also should be marked as dead, however, to reduce the confusion during the QA such cells were marked as bad.

The cells marked as bad can be sorted out into 3 groups: first, **cells with noticeably bad ADC distribution**; second, **cells with extremely small entries**; third and finally, **cells with ADC distribution falling too fast**; respectively. A more detailed explanation for the 3rd type is as follows: typically an FMS cell's ADC starts from 2 [c] after pedestal subtraction and its yields gradually decrease with the ADC [d]. However, the 3rd type of bad cells' yields decay very quickly [e]. The slope of such cells' fall varies cell by cell and some cells can be salvaged with proper calibration [f], however, if the slope is too stiff calibration itself cannot be tried as it requires minimum statistics. In short, if a cell's ADC distribution decays very fast and **its tail ends before 50**, the cell will be marked as bad.

[a] In the manner of cell status (section 1.2) hot channels also categorized as bad
[b] Any minBias trigger independent of FMS is ok, but one with small prescale is recommended for more statistics
[c] 1 for cells with negative bit shift
[d] Soft upper limit of ADC is around 250 for most of cells
[e] It's a reflection of too low HV applied during the online calibration
[f] Usually such cells require very large gainCorr value

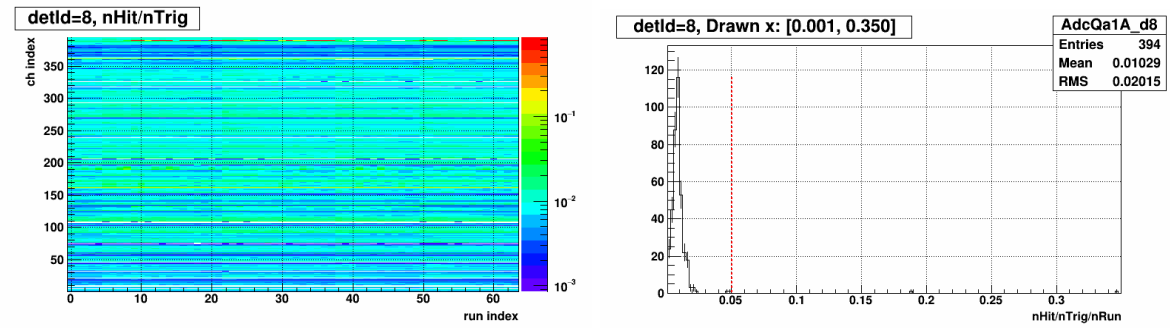

Figure 2.19: Cell vs. run for detId 8 (left) and its Y projection with normalization by # of runs (right). For the left plot, each bin content corresponds to a cell's # of entries normalized by # of triggers. Also note that both axes are indices, instead of actual cell or run number to remove dummy numbers. For the right plot red vertical line indicates a rough hot channel threshold defined by its own mean and RMS. Lastly, these plots were obtained from Day 80-81 in RUN15pp200trans.

Unlike the case of dead or bad channels, determination of hot channels is more complicated. As a first step of hot channels QA, each cell's number of entries were checked as shown in the right plot of Fig. 2.19. For better judgment, each cell's entry was normalized by the number of triggers and the number of runs, and then the following rough hot channel threshold was defined by using its own mean and RMS.

$$\text{Hot channel threshold} = \text{Mean} + 3 \times \text{RMS} \tag{2.9}$$

Note that a cell does not automatically judged as hot, even if it was got caught by this threshold: first, due to the uncertainty of thepedestal subtraction process, sometimes **a large fraction of pedestal tail** remains in the ADC distribution; second, due to the **high HV applied during the online calibration**, some cells have intrinsically large number of entries, respectively. The common feature of these two cases is a large portion of their entries are concentrated in rather small ADCs ($< \sim$50), which affect relatively small in the point reconstruction. Therefore if a cell got caught by the threshold in Eq. 2.9, the cell will be flagged as 'potential' hot channel. In later processes, these potential hot channels will be drawn in red color to pay extra attention.

After acquiring potential hot channels list, all cells' ADC distributions are printed out and checked one by one. In principle, if their online calibration status is the same [a], the ADC response of the cells in the vicinity should be similar [b], too. Therefore, in the QA, multiple cells' ADC in the vicinity are compared with each other, especially the **Y scale at the ADC = 50, 100, 150, and 200** are intensively checked as main checkpoints. Fig. 2.20 shows an example of ADC distributions used for the QA.

[a] In reality, it is unlikely they would be same. Therefore another crosscheck by using hit energy (ADC × gain × gainCorr) is performed after the calibration is finished.

[b] Same logic holds for cells in similar pseudorapidity

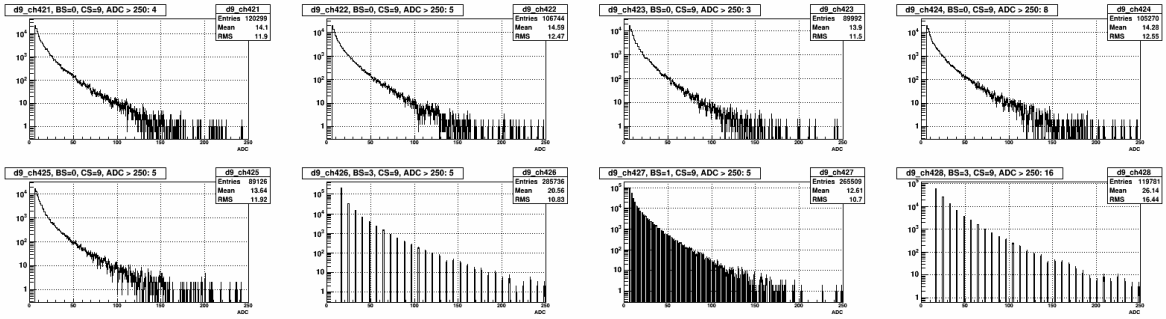

Figure 2.20: ADC distributions of detId 11, channels 421-428. No corrections were applied.

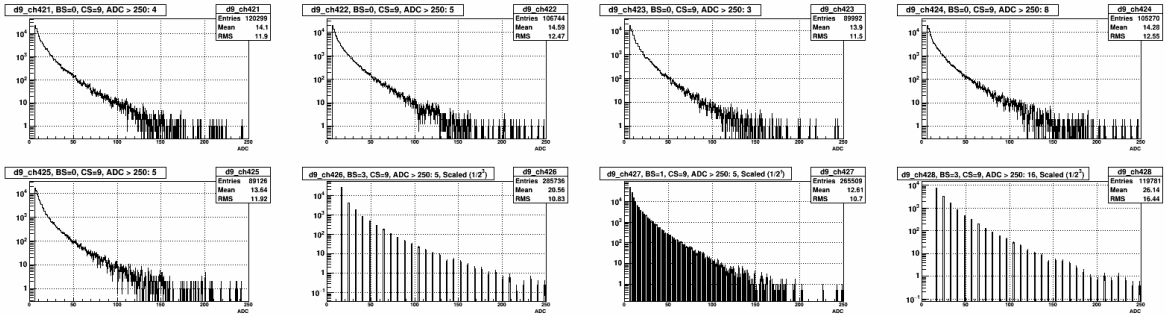

Figure 2.21: ADC distributions of detId 11, channels 421-428. Channels with positive bit shift (426 and 428) were normalized by $1/2^{\mathrm{BS}}$ for proper comparison.

Before the QA performed, one final correction is required to the **cells with a positive bit shift**. Typically, compared to the cells in the vicinity, the cells with a positive bit shift (BS > 0) tend to have a noticeably larger number of entries at the checkpoints (ex. ADC $= 100$). Since this is an artificial effect originated from applied bit shift, such cells need to be normalized by applied bit shift itself ($\times\ 1/2^{\mathrm{BS}}$) for proper comparison. The necessity of the normalization is obvious by comparing Fig. 2.20 and Fig. 2.21. After the correction, if a cell's entries at the checkpoints are noticeably high by at least a factor of 3 or 4, mark the channel as hot.

As one may noticed already, the overall QA procedures for bad/dead/hot channels, especially for the hot channels are rather conservative than aggressive. Although it wasn't mentioned so far, the very first premise of overall prerequisite QA is **the cells being masked out should be as least as possible**. Therefore it is possible that a few or even more problematic cells can slip out the QA criteria, especially the hot ones. Such remaining problematic cells should be ruled out by additional QA for a specific topic.

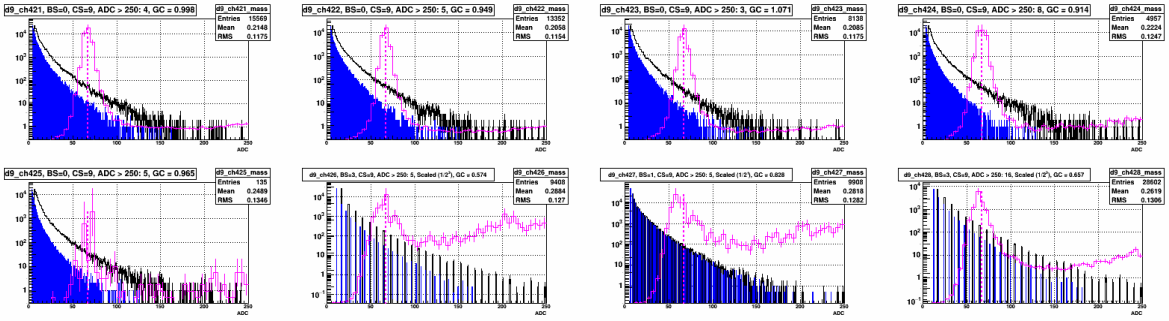

Figure 2.22: ADC distributions, Hit energy distributions (Blue), and Reconstructed mass distributions (Magenta) of detId 11, channels 421-428. Note that arbitrary value (10) was multiplied for each hit energy to draw it on top of the ADC distribution. Also Mass distribution's x is independent of drawn x-axis: its range is always [0, 0.5 (GeV)] and the vertical dashed line indicates position of the π^0 mass (0.135 GeV).

The overall procedures for bad/dead/hot channels QA can be summarized as follows.

Summary of prerequisite QA for bad/dead/hot channels (set gainCorr to 0.000)

1. Bad:
   - A cell has noticeably bad ADC distribution
   - A cell has too small number of entries
   - A cell's ADC distribution falls too fast, especially its tail ends before ADC = 50
2. Dead: a cell has exactly 0 entry
3. Hot:
   a. Check each cell's number of entries, which normalized by number of triggers and runs
   b. Obtain cell by cell ADC distribution, which normalized by its bit shift if BS > 0
   c. Compare the scale of ADC at 50, 100, 150, and 200 with cells in the vicinity
   d. Mark a cell hot if it has noticeably larger number of entries, at least by a factor of 3 or 4

Finally, although it is not a prerequisite QA, after the calibration is finished its quality can be checked by using hit energy distribution drawn together with the ADC. Fig. 2.22 shows an example of such post-calibration crosscheck.

2.3.2 Skewed mass problem

A particular problem caused quite a trouble in this analysis: for some cells, the position of the **mass peak is almost fixed** independent of gainCorr changes. Also, the location of the peak is always smaller than the π^0. Hereafter this problem will be denoted as **skewed** case. If a cell is skewed, the gainCorr update process continually tries to push the peak to the higher value by applying higher gainCorr, but as explained already and as shown in Fig. 2.23, the peak position doesn't move even if higher gainCorr is applied. Consequently, the gainCorr applied to the channel continually grows with iterations and screws up the calibration status over a wide region.

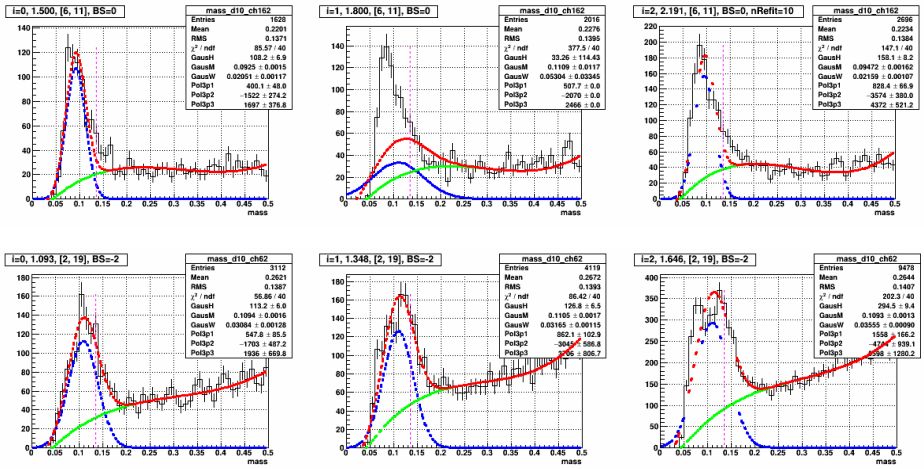

Figure 2.23: Examples of typical skewed mass for two different channels in different periods. The top plot was obtained from day 77-79 and The bottom plot was obtained from day 69-73.

At first glance, these skewed cells look behaving well except its position is a little shifted. Especially they're hard to be distinguished with decent cells which simply require larger gainCorr. Clear distinction between the two only can be done after multiple iterations, by checking the mass peak change, the applied gainCorr, and the obtained yields for each iteration index. [a]

There are a few characteristics of this problem. First, this problem **only happens in the small cells**: throughout entire RUN15pp200trans period, not even single skewed cell was observed in the large cells. Second, the fixed **mass position is always smaller than the** π^0 mass. Again, no counterexample was observed. Thrid and Finally, clearly skewed cells were chosen and their gainCorr change over iterations were checked (ex. Fig. 2.15). Not all skewed cells show the same behavior, however, in many cases a threshold like gainCorr exists: the skewed behavior starts after such threshold.

[a] In general strong positive correlation exists between the applied gainCorr and the obtained yields.

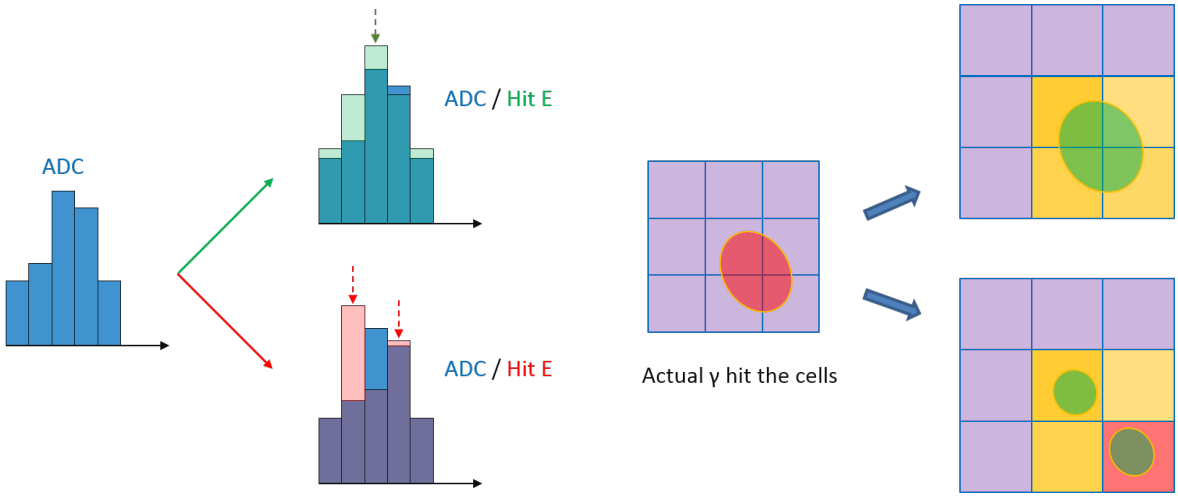

Figure 2.24: Hypothesis for how the skewed mass distribution happens. Left 3 diagrams show how the skewed cell being formed in 1D: middle shows the raw ADC, top shows the successful reconstruction by proper calibration (light green bars on top of the ADC means hit energy and an arrow means reconstructed point), and bottom shows the cluster split into two by poor calibration which ends up as skewed cell, respectively. Right 3 diagrams' format is similar to the left 3, but it shows the explanation in 2D.

Considering the previous characteristics and the additional studies followed by, a hypothesis was proposed to explain how this problem happens. In FMS framework, a point is reconstructed by performing fit on the clusters found in the event. For the cluster finding mainly a couple of factors are considered: **the connectivity among the cells** and **each cell's hit energy**, respectively. If a chunk of cells are well connected and their hit energy are smoothly distributed (highest at the center and then smoothly decay with increasing radius) the chunk will be regarded as a cluster. However, the cluster finder must consider **the case of two or more particles incident very closely to each other** as well: therefore among the connected cells, if a cell's hit energy is higher than certain threshold [a], the clsuter finder regards the cell as an independent cluster. Therefore, if a cell's hit energy is either too high or too low compared to the cells in the vicinity, a cluster in truth can be splitted into two. Fig. 2.24 visually shows the hypothesis.

If this hypothesis is true all previous characteristics can be explained: first, considering the cell size and its location (smaller incident angle), the small cells must be much more susceptible to this problem than the large cells; second, two reconstructed points in the skewed case are one in truth. Thus each of their energy and opening angle between them must be much smaller than the true π^0 decay photons, eventually the reconstructed mass will always be smaller than the π^0; third and finally, the existence of threshold-like gainCorr can be easily explained by the hit energy threshold in cluster finder; respectively.

[a] 1.6: a cell's energy is 60 % higher than the adjacent cells

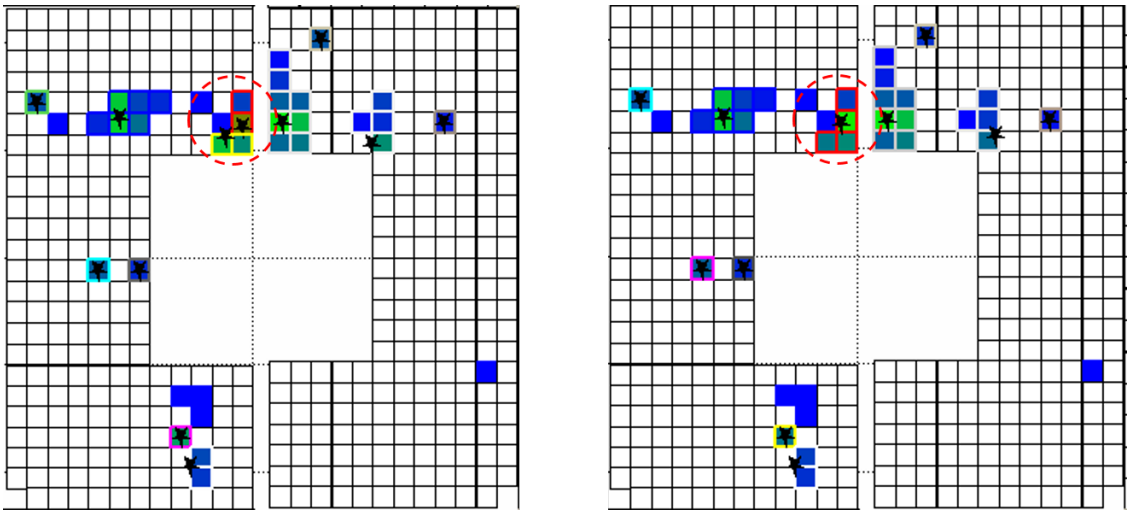

Figure 2.25: A crosscheck performed for the hypothesis. By choosing one skewed cell and one specific event, two different gainCorr was tested: in one case the cell was skewed (left) and in the other case it wasn't (right), respectively. Then the event's hit (each colored cell), clusters (colored boundary around connected cells), and reconstructed points (star) are checked. A single point in the right plot (in red dashed circle) splits into two in the left plot.

To check the hypothesis following test was performed. A cell looks decent at starting iteration but skewed at later iterations was selected, and then its event display [a] for a few tenth of events were printed out to check the relevant reconstruction status around the cell. The only difference between the two control groups is the applied gainCorr. If the skewed behavior indeed happens by the splitting cluster caused by poor calibration, for the same event, in one case number of clusters and points will be one while in the other they will not. Fig. 2.25 shows exactly such behavior.

If all cells are perfectly calibrated this problem won't happen. However, to calibrate cells precisely one needs good quality clusters, which is affected by the hit energy. But as explained multiple times, the hit energy of a cell is calculated by the applied gainCorr. In short, this is the chicken or the egg problem.

Although it's impossible to remove this problem completely, one can try to place a cut which suppresses the skewed cases being included in the invariant mass distribution. Therefore following items were considered to prepare countermeasures. First, **the distance and the opening angle between the points are likely small**. Second, since a cluster was split into two or more, **the number of cells in a cluster and the cluster's size also will be relatively small**. Third and Finally, there's **a strong correlation between the applied gainCorr and the position of the reconstructed mass**, respectively. Among the items, the first was discarded as it can induce serious bias, however, the second and the third were utilized for the *cluster quality cut* and an additional safeguard in the gainCorr update process.

[a] StFmsEventDisplay, written by Akio Ogawa

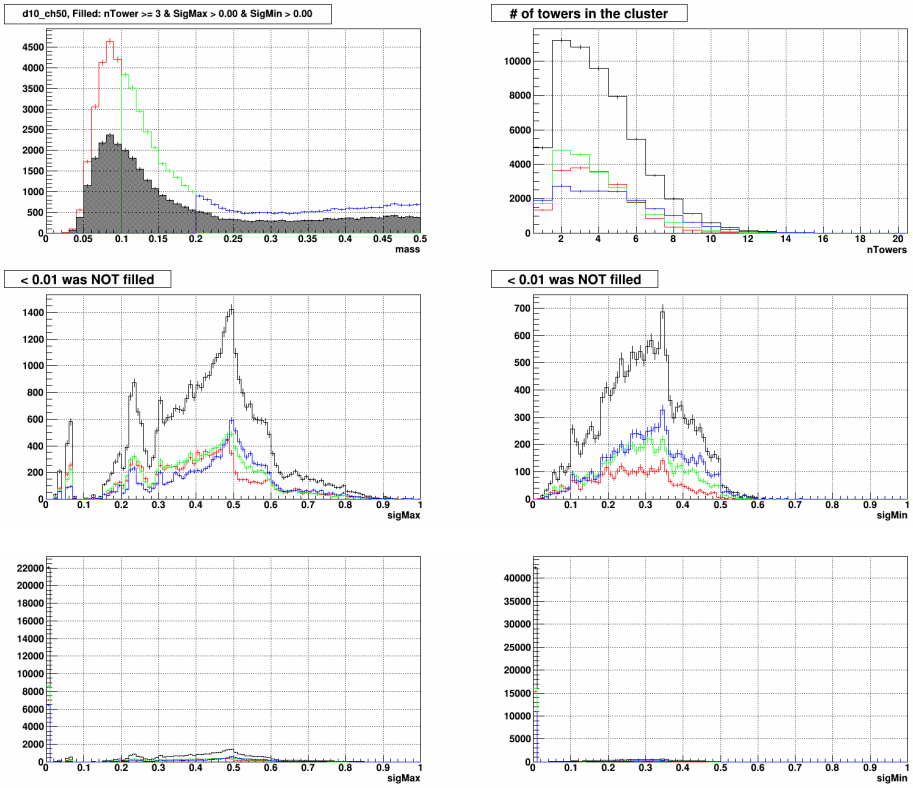

Figure 2.26: An example of cluster quality study on a typical skewed cell. Each color in all plots are corresponds to the mass separation in top left plot (mass < 0.1, $0.1 <$ mass < 0.2, and mass > 0.2). The top left plot shows mass distribution before and after the cut in its title. The top right plot shows the number of participating cells per cluster [a]. 2nd and 3rd rows show σ_{max} (left column) and σ_{min} (right column) of a cluster, but the values smaller than 0.01 are not included in the 2nd row.

The following variables are cluster related parameters in the FMS analysis framework: **number of participating cells**, σ_{max}, and σ_{min} [b], respectively. The conclusions drawn by studying these parameters are as follows: first, the number of cells per cluster in skewed cases are in general small, and mostly distributed around n $= 2 \sim 4$ with relatively small dispersion, while normal case's peak is located at n $\gg 4$, with wider distribution; second, in both σ_{max} and σ_{min}, huge entries are focused near 0 for skewed case; third and finally, in general, a normal cell's σ_{max} is distributed around 0.5 and its early tail ends near 0.2; respectively. A detailed report can be found here [13]. By using these conclusions *Cluster quality cut* is defined as follows. Note that this cut **only applied in small cells** during the calibration.

Cluster quality cut: # of cells per cluster ≥ 3 & $\sigma_{max} > 0.1$ & $\sigma_{min} > 0.01$

[a] In this plot, the black distribution is the sum of all the other colors.

[b] The σ value indicates a cell's distance from the cluster's center, weighted by the cell's energy (0.5 GeV minimum threshold exists). For the determination of σ_{max} and σ_{min}, additional moment analysis is performed to determine major and minor axes (imagine an almond shape cluster) of the cluster.

Finally, the *Cluster quality cut* was determined rather conservatively to reduce possible bias it induces. Therefore, although the cut helps suppressing the skewed events, it cannot completely get rid of all of them. In short, the skewed cells still appear during the iterations even if this cut is applied. Therefore additional safeguard was placed in the gainCorr update process: the purpose of this safeguard is not an optimization of the gainCorr, rather preventing the cell causes a further problem. The detailed information is as follows.

Safeguard for skewed cell's gainCorr update

1. Go to step 2 if the following conditions are satisfied:
   a. At least one iteration was done (iteration index > 0)
   b. The cell is NOT converged
   c. The cell is located in the small cells
   d. The cell's estimated mass is smaller than 0.12 (GeV)
2. Check the difference in the applied gainCorr (ΔgainCorr) [a] and estimated mass (Δmass), increase count if $\Delta\text{gainCorr} \geq 0$ & $\Delta\text{mass} < 0$.
3. If the count reaches 3, reset the cell's gainCorr to 0.750.

[a] $\Delta\text{gainCorr} = \text{gainCorr}_{\,i}$ - $\text{gainCorr}_{\,i-1}$

2.3.3 Effect of applied cuts

As explained in section 2.2.3, multiple cuts are applied on both event-wise and pair-wise to obtain clean π^0 samples. For the quality calibration, it is inevitable to use such cuts, however, one need to make sure the cuts applied does not cause a serious bias on reconstruction results. If a cut applied in the calibration makes such bias, but cannot be tolerated in physics analysis, the calibration results cannot be used at all. Therefore following cuts are selected and tested among the cuts in section 2.2.3.

Cuts tested for the bias check

1. For each event: BBC zVtx
2. For each point pair:
   - 20 < pair energy (GeV) < 40
   - Single point cluster
   - *Cluster quality cut* (* applied to all detId in this time)

For the comparison, all relevant conditions are set the same to the calibration except the cuts being tested. Also, each point pair was sorted out by detId and top/bottom [a], by using the pair's leading cell location. The tested items are as follows.

QA details

1. Type of plots
   - Mass vs. pair energy (GeV), with pair energy > 20 GeV
   - Mass vs. Zgg, with pair energy > 20 GeV
   - Mass distributions, separated by pair energy in the stepwidth of 10 GeV
2. Type of QA
   - QA0. Zgg < 0.7
   - QA1. Zgg < 0.7 + zVtx
   - QA2. Zgg < 0.7 + zVtx + Single point cluster
   - QA3. Zgg < 0.7 + zVtx + Two points from same cluster
   - QA4. Zgg < 0.7 + zVtx + Else condition of QA2 and QA3
   - QA5. Zgg < 0.7 + zVtx + *Cluster quality cut*
   - QA6. Zgg < 0.7 + zVtx + Single point cluster + *Cluster quality cut*

Note that the plots being tested only check pairs with energy larger than 20 GeV: if the lower energy part included, due to the overwhelming backgrounds the distribution in higher energy part can't be distinguished at all. [14] Among the QA items QA3 and QA4 are the ones which intentionally excluded in the calibration [b]. The QA6 is the closest condition to the calibration. The surviving statistics for each QA items can be checked in Fig. 2.27. Finally, the plots will be shown in following paragraphs are mainly obtained from day 80-81, but the other days are not very different.

[a] Top half or Bottom half of FMS

[b] Conditions QA2 - QA4 are exclusive to each other

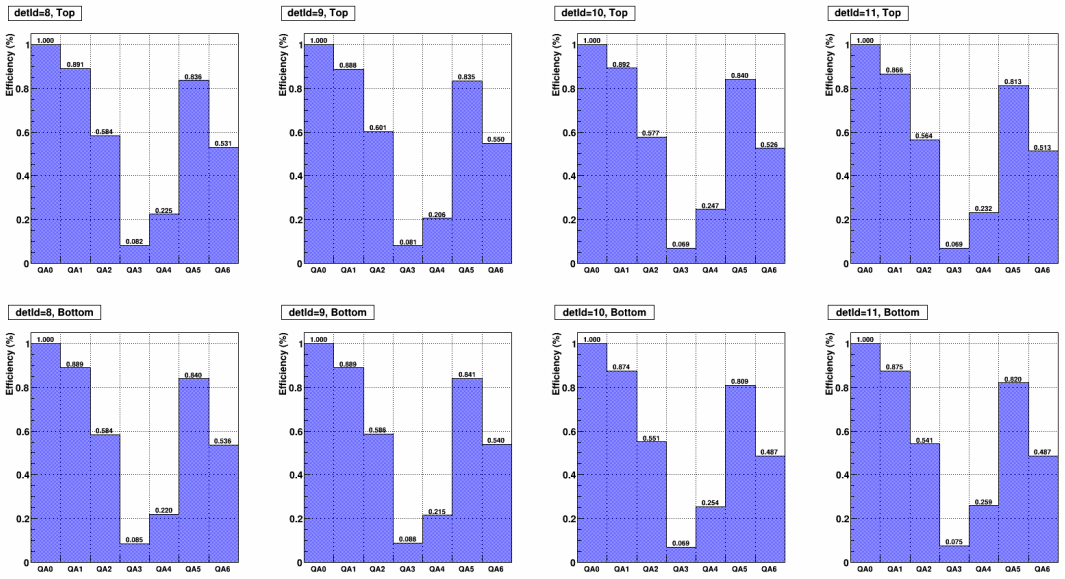

Figure 2.27: Surviving statistics for each QA item. Each bin was normalized by 1st bin's entries. Each column corresponds to each detId and Each row corresponds to the top half and bottom half of FMS.

BBC zVtx

As shown in Fig. 2.28, in RUN15pp200trans the position of the zVtx is shifted about **-30 cm** (IP located between the FMS and zVtx) with substantial dispersion (RMS $\sim$ 80 cm) throughout the period. Judging from the difference between the 1st bin and 2nd bin in Fig. 2.27, the vertex finding efficiency of the BBC is about **90 %**.

As illustrated in the left plot of Fig. 2.29, the shift in the zVtx directly affect the opening angle, thus the reconstructed π^0 mass followed by (Eq. 2.2). Judging from the substantial shift in one direction, it's not difficult to expect that applying zVtx will cause a shift in the reconstructed mass: therefore new calibration framework applies the zVtx corrected opening angle (and mass) as a default condition.

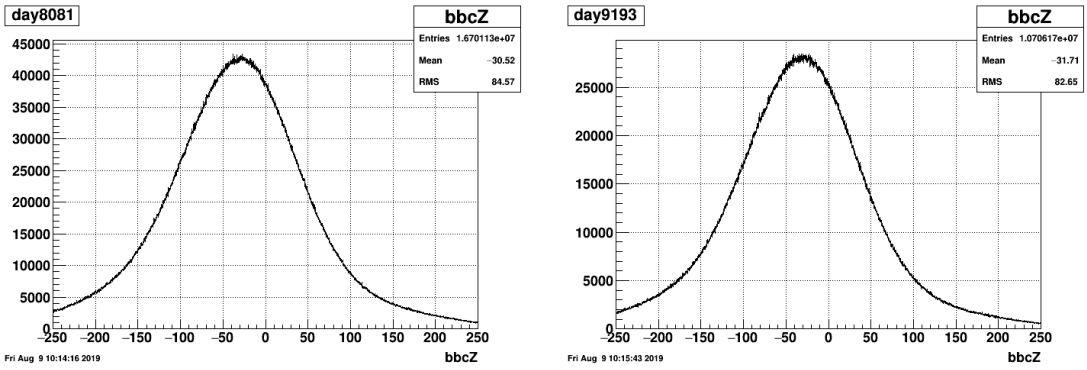

Figure 2.28: Slewing corrected BBC zVtx [9] distribution for day 80-81 (leff) and day 91-93 (right).

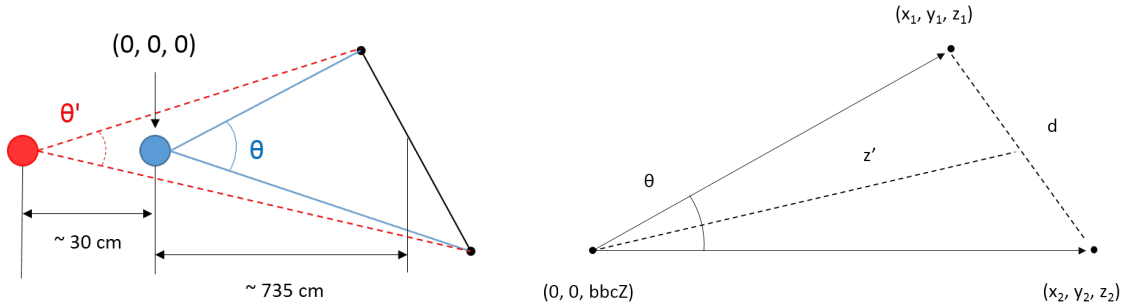

Figure 2.29: Schematic diagrams of effect of zVtx shift to the π^0 opening angle (left) and components for opening angle correction (right). 735 cm is a typical distance between zero point and the shower maximum position in the FMS cell.

In FMS framework, the opening angle calculation is independent of the cluster finding (and the point reconstruction). Therefore, to reflect the zVtx, simple mathematical correction was applied to the already reconstructed point pair's opening angle. The correction is described in the right plot of Fig. 2.29 and following equations. Note that the (x, y, z) in the equation corresponds to a point's position.

$$d = \sqrt{(x_1 - x_2)^2 + (y_1 - y_2)^2} \tag{2.10}$$

$$z' = \frac{(z'_1 + z'_2)}{2}, \text{ where } z'_1 = z_1 - \text{zVtx} \tag{2.11}$$

$$\theta = 2 \cdot \tan^{-1}\left(\frac{d}{2z'}\right) \tag{2.12}$$

The effect of the correction can be seen in Fig. 2.30. Since the zVtx is shifted to the farther direction than the IP, both corrected angle and corrected mass are in general smaller than the original values. Finally, as a crosscheck for the correction itself, both the angle and the mass were calculated by set zVtx = 0 and then compared to the values before correction: the results match within the order of 10^{-4}. Figure 2.31 shows the effect of zVtx on reconstructed π^0 mass.

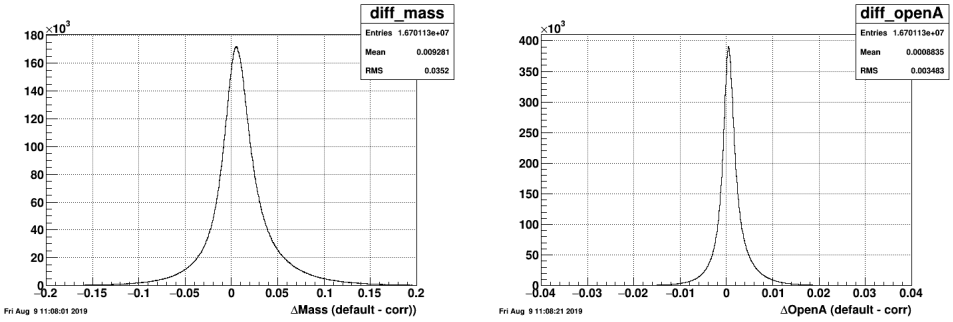

Figure 2.30: Difference between the values before and after the zVtx correction, for reconstructed mass (left) and for opening angle (right)

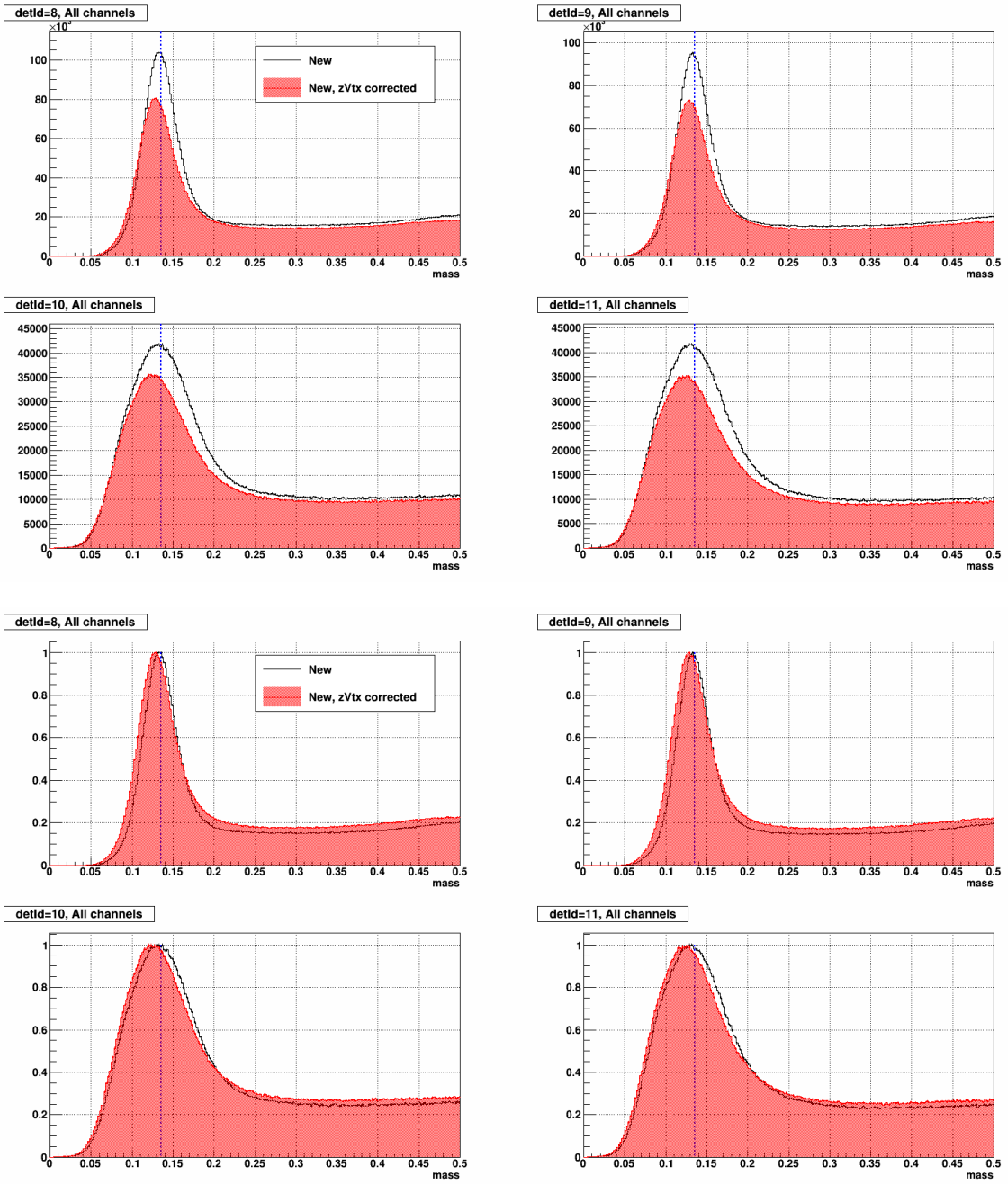

Figure 2.31: Effect of zVtx application on the π^0 mass, obtained from day 80-81. Each plot corresponds to each detId. Black (Red) lines indicate the mass without (with) zVtx correction. The bottom four plots are exactly the same plots to the top four but normalized by its own maximum to check the shift more clearly. Note that the calibration applied in these plots are the one before zVtx correction is officially introduced: thus the calibration is optimized to the case without zVtx correction (black lines). Lastly, the conditions applied for these plots are not exactly the same as the QA items explained earlier in this section. The closest item is the QA6.

Pair energy dependence

As explained earlier this section and in section 2.2.3, only the point pairs in a specific energy window (20 < pairE (GeV) < 40) were used for the calibration. Following Fig. 2.32 shows the mass distributions for the pair energy above 20 GeV, to check the obtained gainCorr's validity in different energy ranges. Although a notable shift can be observed in the small cells with increasing energy, however, the tendency of the shift is consistent for all the regions of small cells.

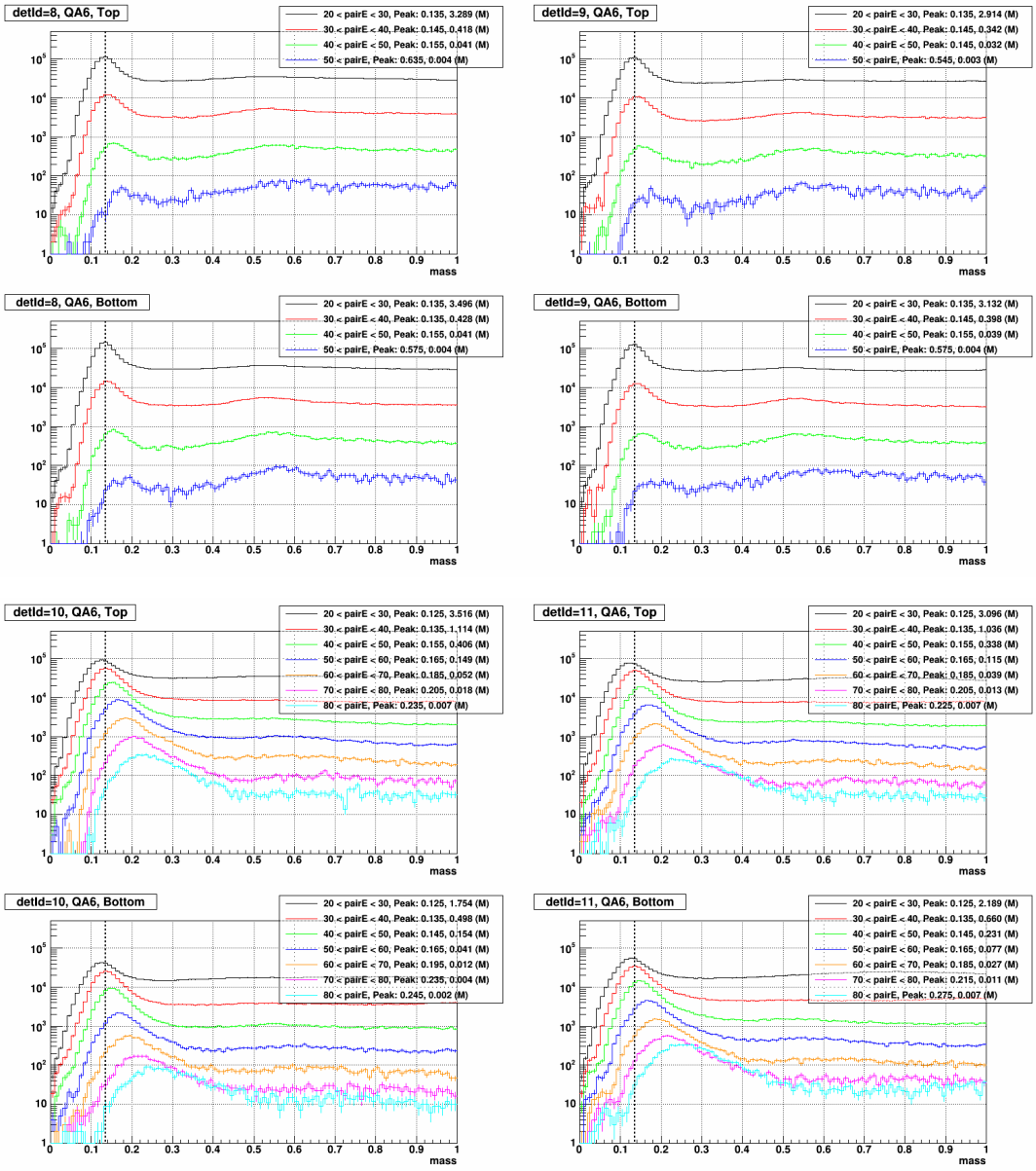

Figure 2.32: Mass distributions for QA6 (Zgg < 0.7 + zVtx + Single point cluster + *Cluster quality cut*), separated by pair energy in the stepwidth of 10 GeV. Each plot corresponds to a detId's top half or bottom half.

Single point cluster

Along with the cut on pair energy, the cut on the number of points per cluster also strongly affects the π^0 samples being collected. Repeatedly, new calibration only uses the clusters which has only one reconstructed point (single point cluster) and exclude all the other cases. Among the QA items defined earlier in this section, the relevant ones are QA2 - QA4. Each item's detailed explanation and its portion to the entire sample are as follows: note that the portions were calculated by using each bin's statistics in Fig. 2.27, by using entries in QA1 as a denominator.

Type of clusters and its portion, related to the defined QA items

- QA2: a pair from two clusters, each cluster has only one point
  0.662 (large), 0.639 (small)
- QA3: a pair from one cluster, the cluster has at least two points
  0.094 (large), 0.080 (small)
- QA4: a pair from two clusters, at least a cluster has more than two points (neither QA2 nor QA3)
  0.244 (large), 0.281 (small)

Mass vs. pair energy and Mass vs. Zgg distributions are presented in the following figures from 2.33 to 2.37. First of all, QA2 is the closest condition to the actual calibration among QA1 - QA4: in both mass vs. pairE and mass vs. Zgg, the reconstructed mass sitting well on the π^0 position with reasonable background distribution. In the case of QA4, judging from its definition it's likely many fakes would be included, thus the large backgrounds and suppressed mass peak in the distribution is not very surprising. On the contrary, the **QA3** shows some disturbing patterns: in mass vs. pairE, it shows a dramatic change in its mass peak position with increasing energy, besides to seriously small reconstructed mass in pairE < 35 GeV; in mass vs. Zgg, it shows similar small reconstructed mass with serious Zgg dependence, especially for small cells; respectively.

However, there's a suspicion if these collected pairs in QA3 are truly the π^0s. If the majority of them are truly the π^0s, which very closely located to each other thus recognized as one cluster, the following two features can be expected. First, due to their relatively small opening angle, their Zgg also likely distributed in rather smaller value (close to the 0). Second, judging from the MC study shown in Fig. 2.8, such two-photon merged clusters starting to arise from rather higher energy, at least 20 GeV for large cells (40 GeV for small cells). But Fig. 2.35 shows exactly opposite behavior. The Zgg distribution is distributed in a wide range, even looks concentrated at Zgg > 0.5 for small cell. Also, the entries in mass vs. pairE are concentrated at rather smaller energy for both large and small cells. In conclusion, it's doubtful that the majority of pairs in QA3 are true π^0. Thus the validity of new calibration can't be judged by this case.

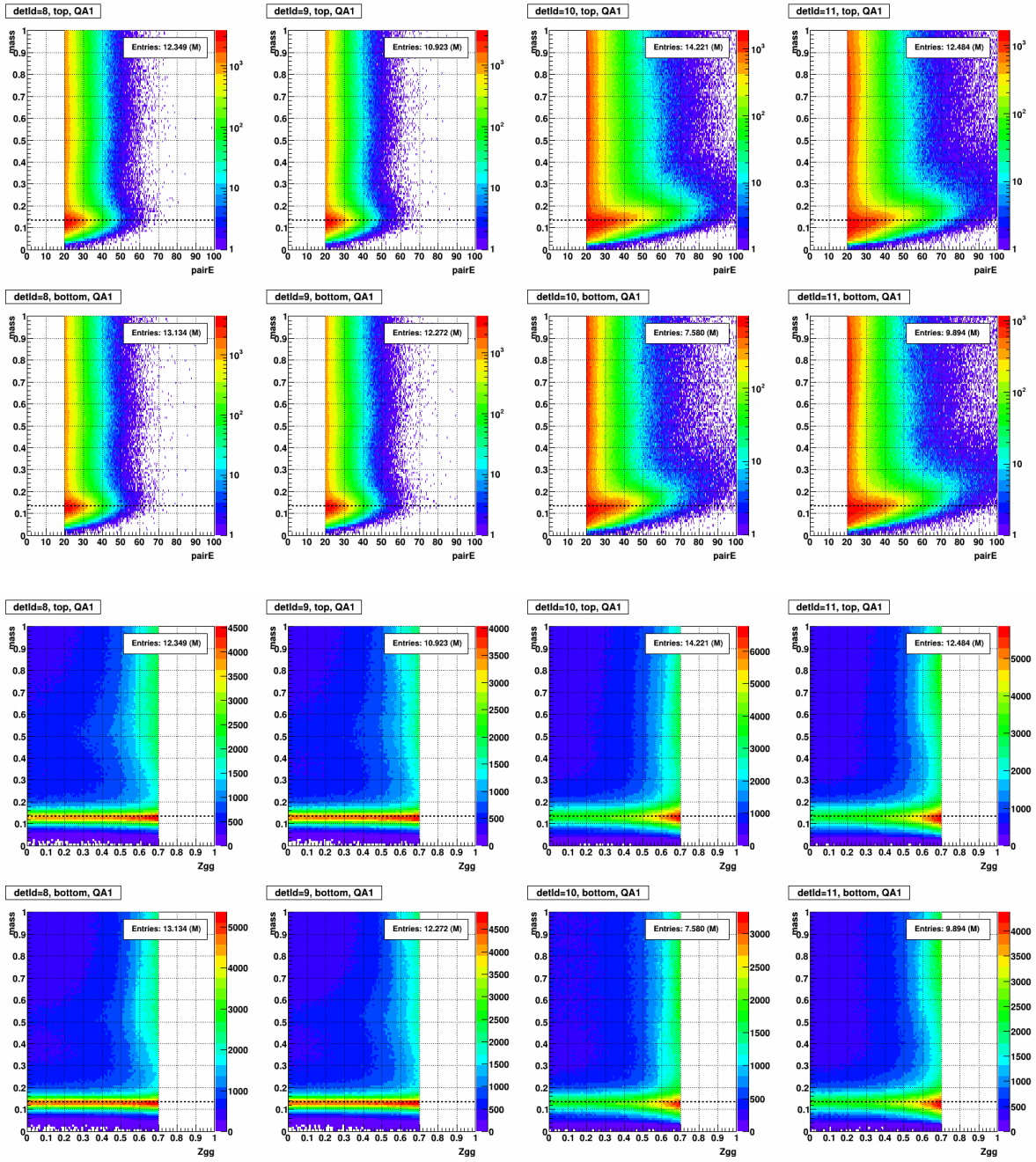

Figure 2.33: Mass vs. pair energy (top 8 plots) and Mass vs. Zgg (bottom 8 plots) in the condition of QA1 (Zgg $< 0.7 +$ zVtx). Each column corresponds to each detId and Each row corresponds to either the top half or bottom half of the FMS.

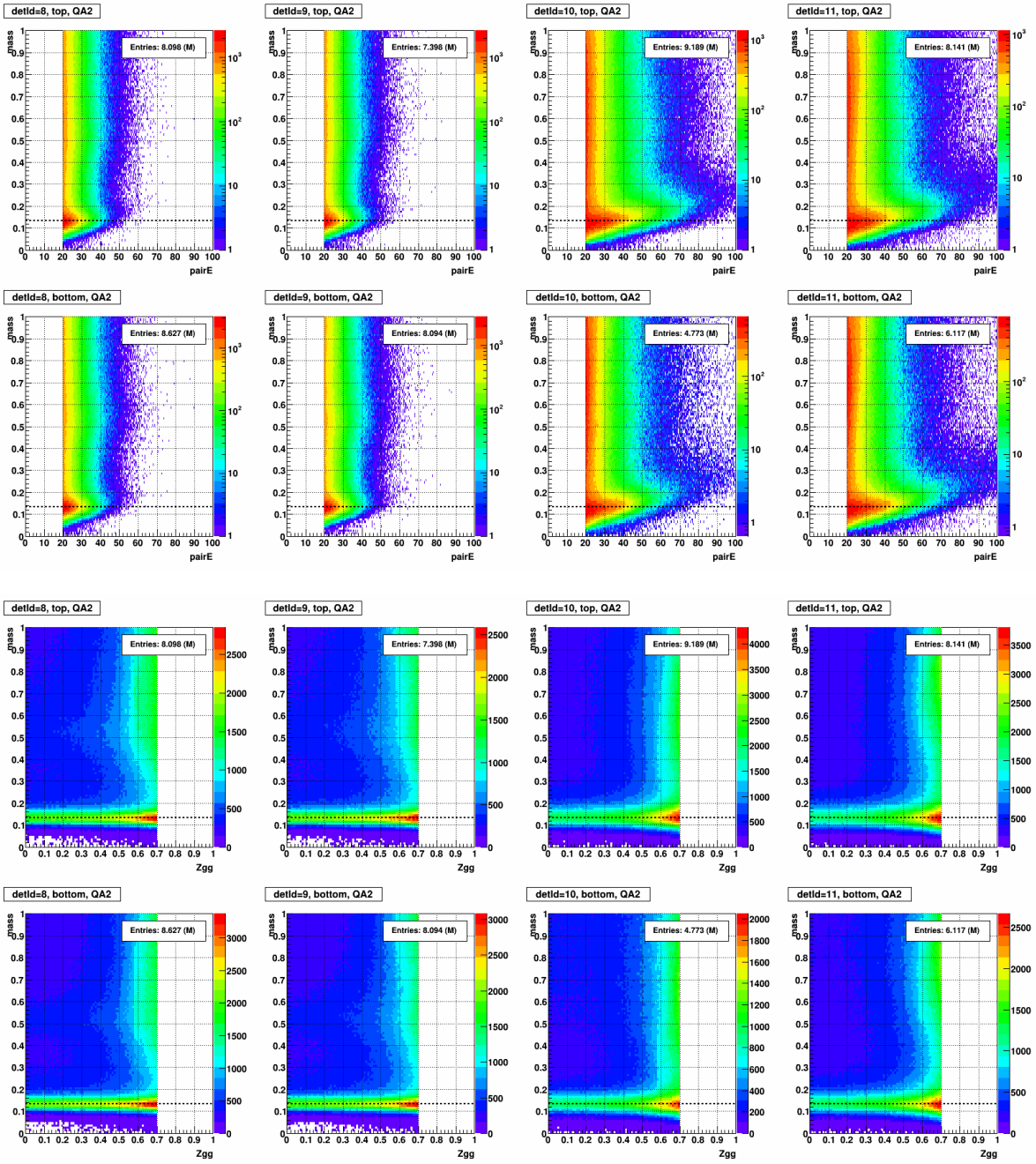

Figure 2.34: Mass vs. pair energy and Mass vs. Zgg for QA2 (Zgg < 0.7 + zVtx + Single point cluster).

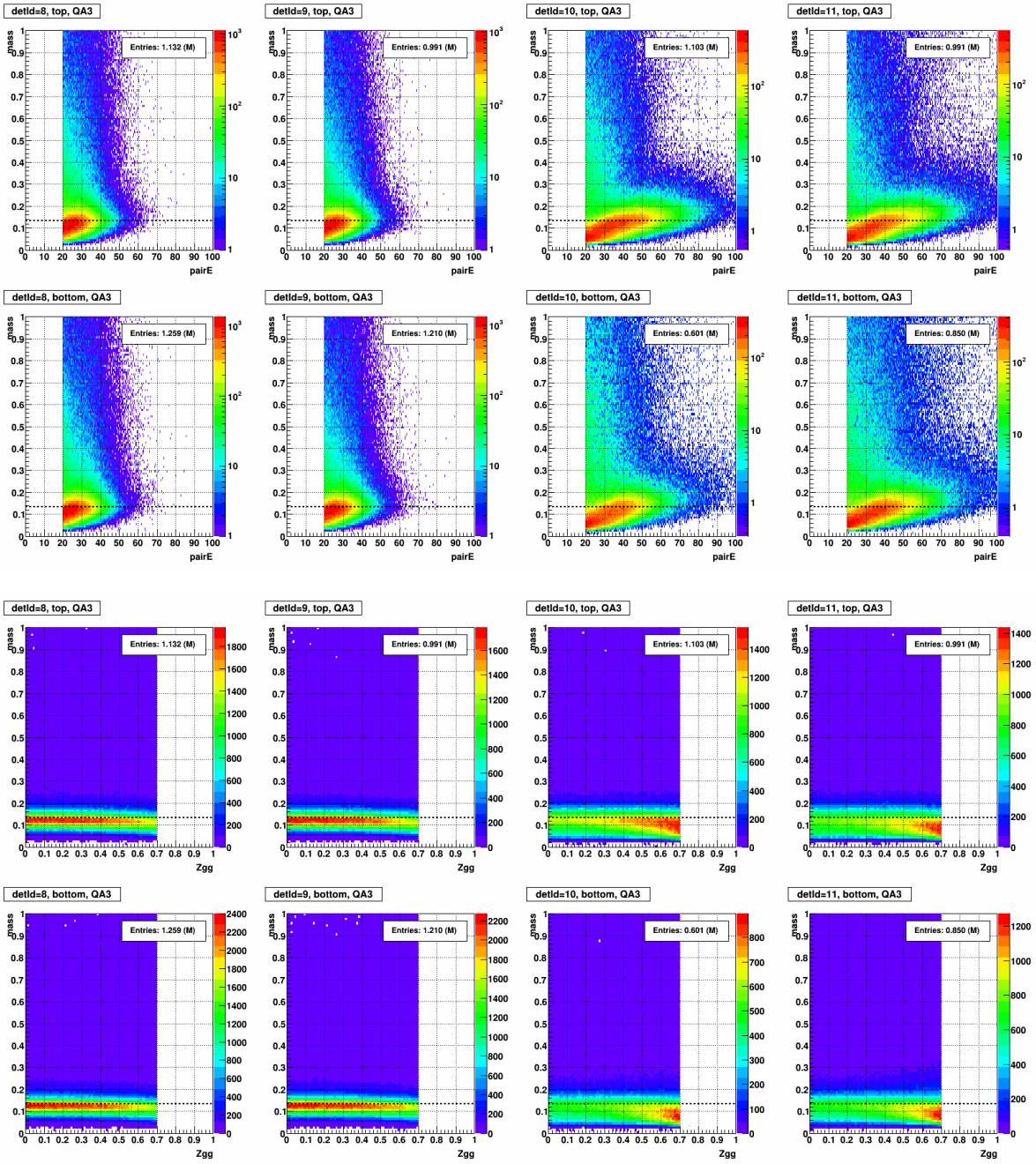

Figure 2.35: Mass vs. pair energy and Mass vs. Zgg for QA3 (Zgg < 0.7 + zVtx + Two points from same cluster).

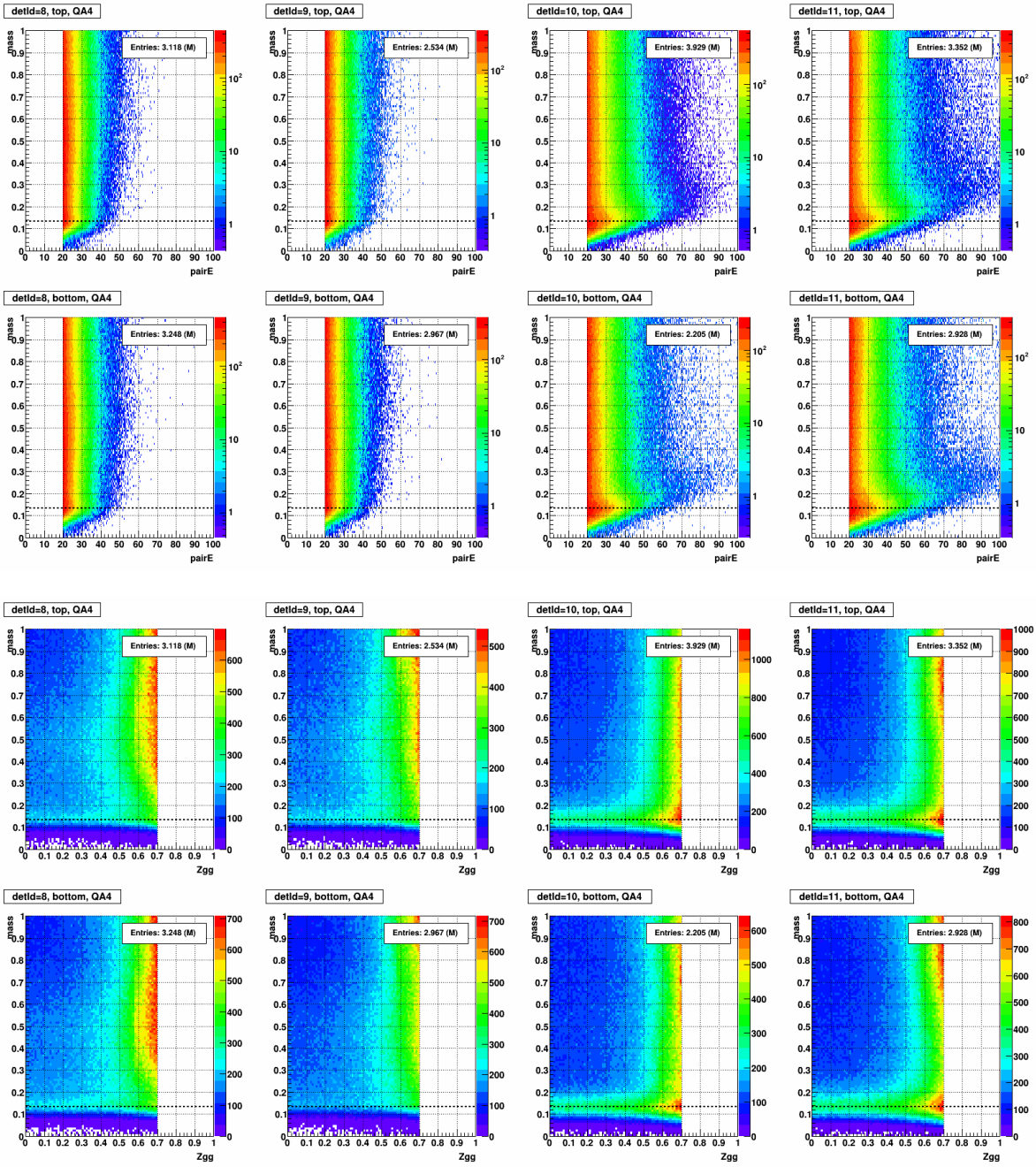

Figure 2.36: Mass vs. pair energy and Mass vs. Zgg for QA4 (Zgg < 0.7 + zVtx + Else condition of QA2 and QA3).

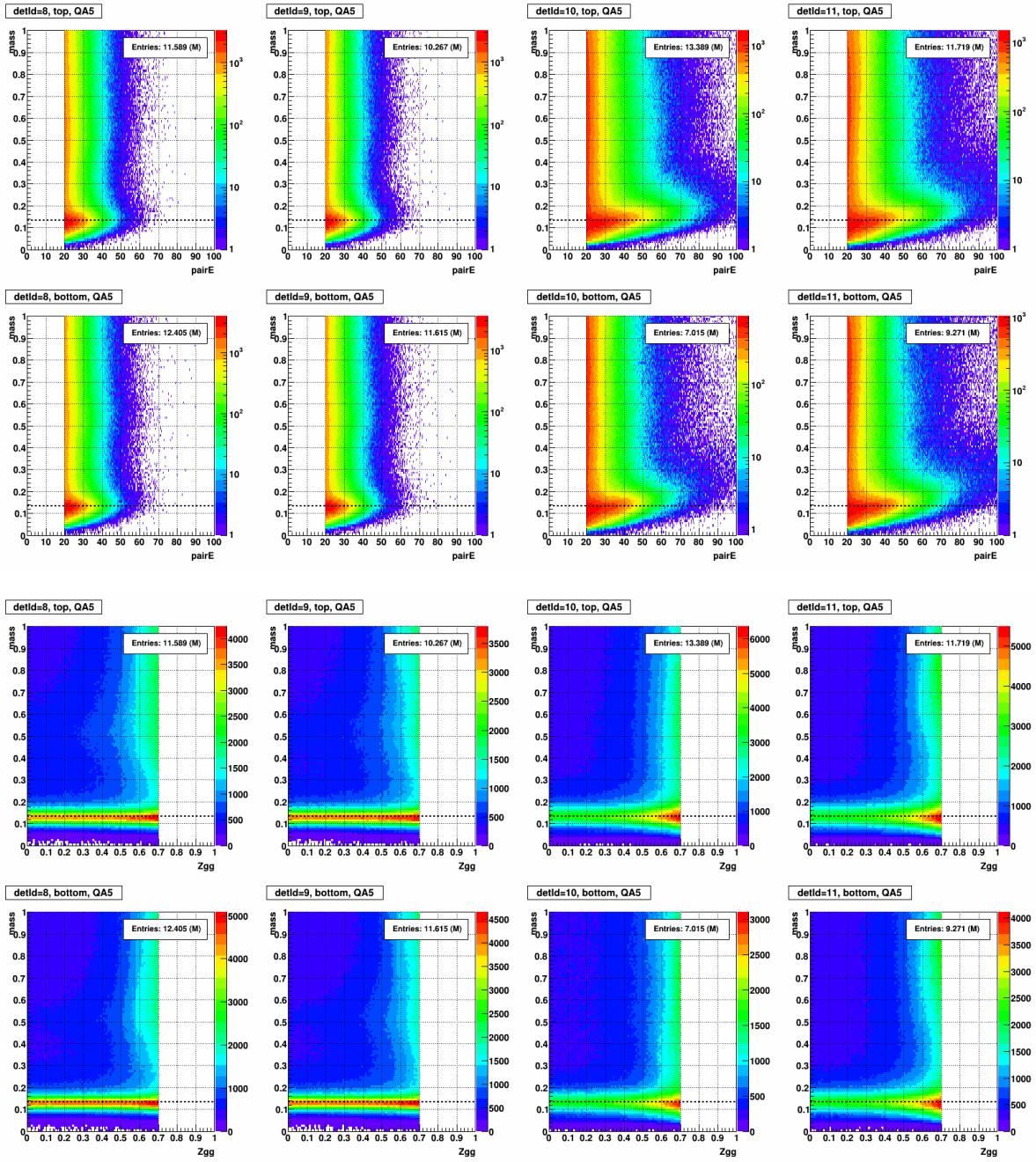

Figure 2.37: Mass vs. pair energy and Mass vs. Zgg for QA5 (Zgg < 0.7 + zVtx + *Cluster quality cut*).

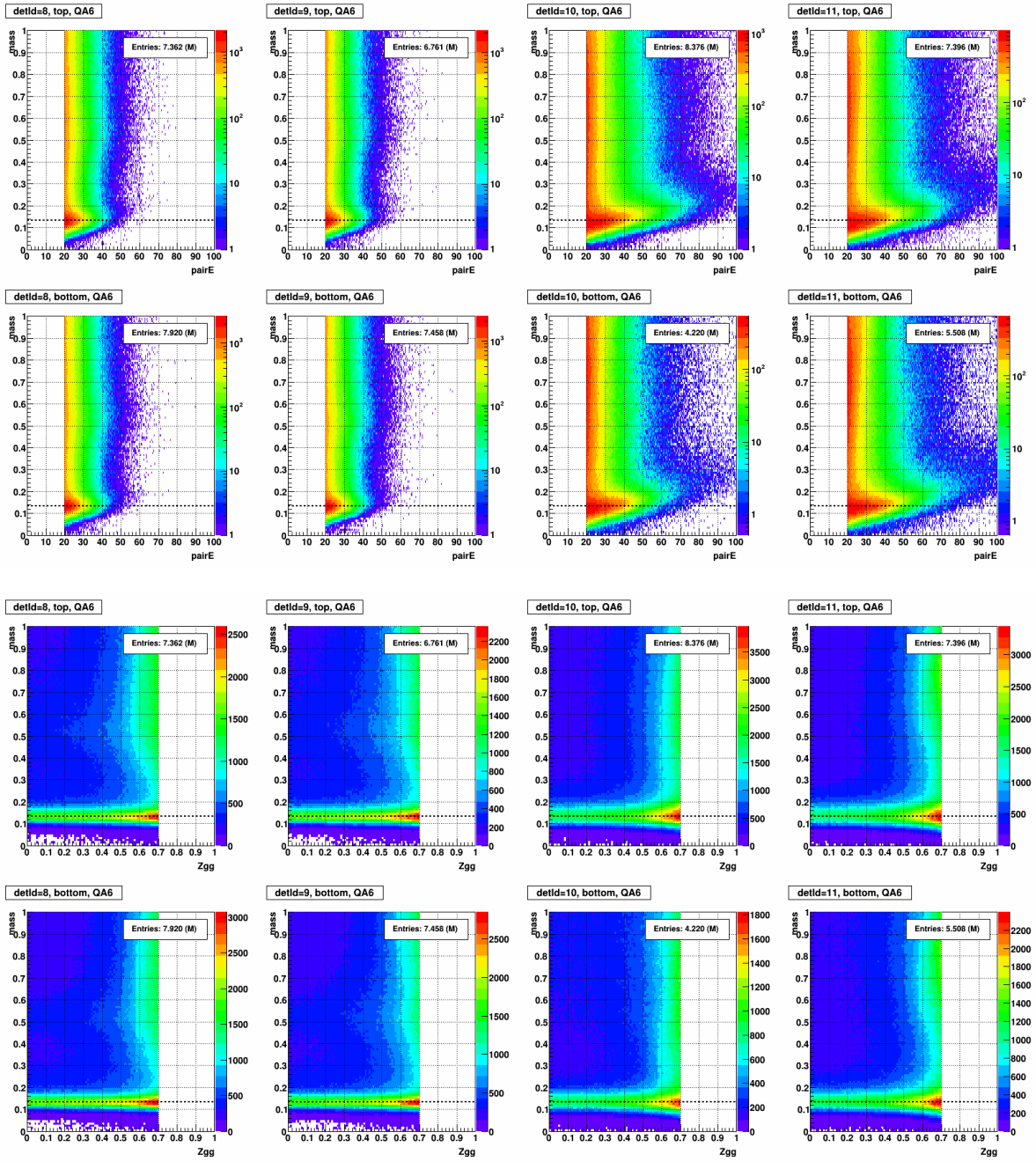

Figure 2.38: Mass vs. pair energy and Mass vs. Zgg for QA6 (Zgg < 0.7 + zVtx + Single point cluster + *Cluster quality cut*). This is the closest condition to the calibration.

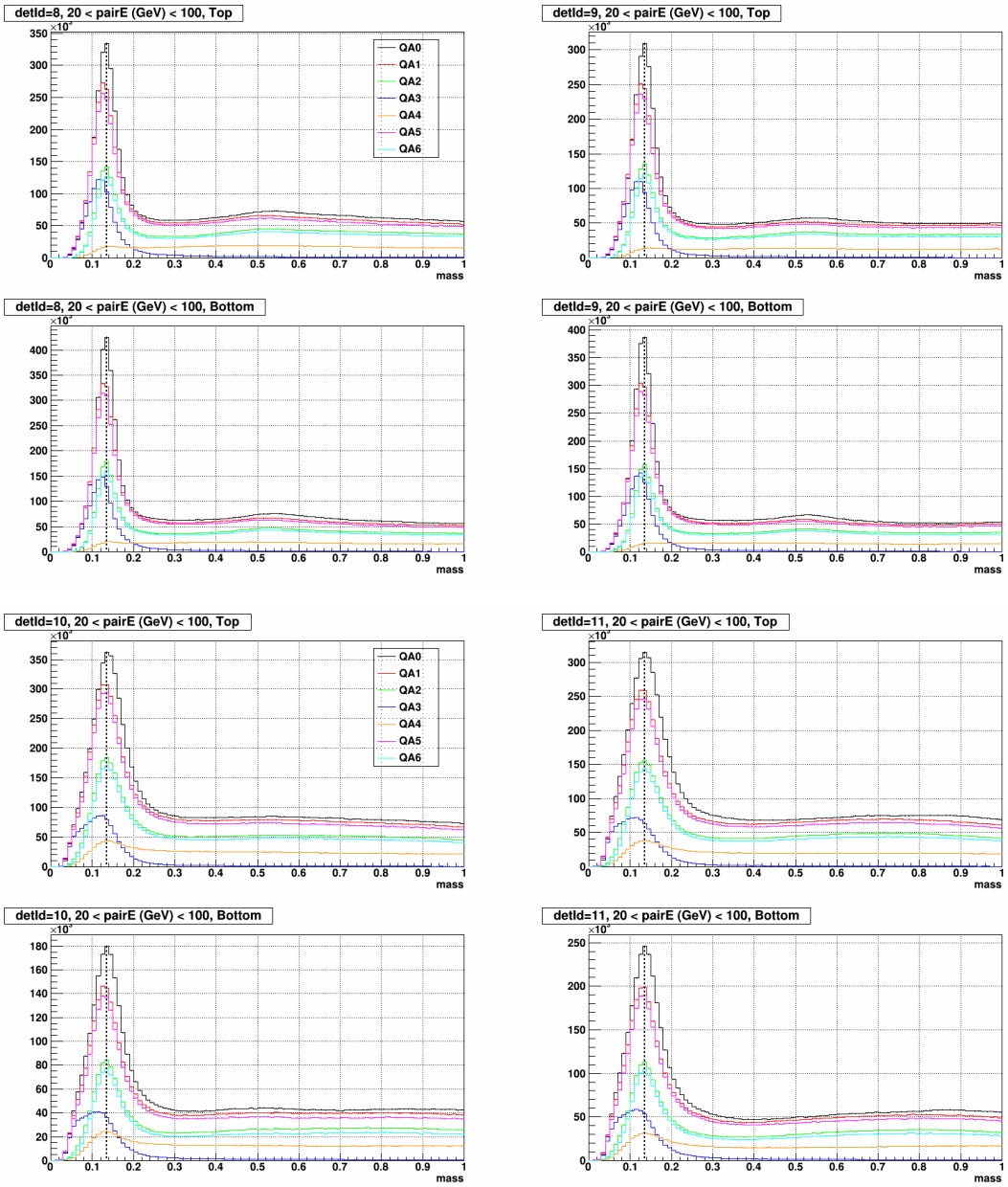

Figure 2.39: 1D mass distribution for each QA items. The top four plots are large cells and Bottom four plots are small cells. Each row corresponds to either the top half or bottom half of the FMS.

Cluster quality cut

The effect of the *Cluster quality cut* (section 2.3.2) can be checked by comparing previous Fig. 2.33 and Fig. 2.37. The QA1 and QA5 distributions in Fig. 2.39 also will be helpful. Note that, however, all these QA items were obtained with final calibration results: all skewed cells were thoroughly checked and corrected with finalization procedures in section 2.3.4. Therefore the effect of *Cluster quality cut* looks very weak or even negligible in all of previous figures.

2.3.4 Finalize a group's calibration

After the framework developed successfully, the entire RUN15pp200trans period was separated into 9 subgroups and calibrated independently (section 3.1). Although some fluctuations exist, the general calibration performance is as follows.

Calibration performance (RUN15pp200trans, by ratio to the entire (1,264) cells

- Converged: 85 ± 3 (%)
- Masked out (dead/bad/hot): 4.5 ± 0.5 (%)
- Others (NOT converged nor dead/bad/hot): 10 ± 5 (%)

The remaining cells in category 'Others' were thoroughly investigated why they don't converge, and then sorted out into four categories.

Categorization of the cells which not converging nor masked out

a. Good: just failed to satisfy the convergence criteria
b. Poor statistics: mostly located at the outer edge of FMS, 50 - 70 cells (4 - 5.5 %)
c. Dirty distribution: mass distribution itself is dirty and heavily fluctuating
d. Skewed mass distribution
   * Sum of c + d: 20 - 45 cells (1.5 - 3.5 %)

The case *b* and *c* can be checked in Fig. 2.40. More detailed discussion for each type is as follows: first, the cells in case *a* are not a problem at all. All they require is a few more iterations; second, cells in case *b* are mostly located at the very outer edge of the FMS. As explain in section 2.2.4, to perform the fit process and gainCorr update followed by minimum statistics (100) is required. However, due to their location and the framework's characteristic, such a small amount of statistics is not easily gathered for those cells; third, the cells belong to case *c* are mostly concentrated near the beam pipe, especially its below and left ($x < 0$). It's a known issue that the cells in this location suffered heavy damage in RUN15. fourth and finally, the skewed cells (section 2.3.2) are sorted as case *d*; respectively. Finally, cases *c* and *d* are mostly located in small cells.

For the finalization of a group's calibration, no specific correction is required for the case *a* and *b*. However, the case *c* and *d* must not be left untouched. The following summary shows treatment on each type to obtain final gainCorr values.

Finalization

a, b. No further action required (last iteration index's gainCorr will be assigned)
c, d. Check the cell's gainCorr change retrospectively and Select a gainCorr when the distribution looks best. If the judgment is not available at all, assign default gainCorr (1.000)

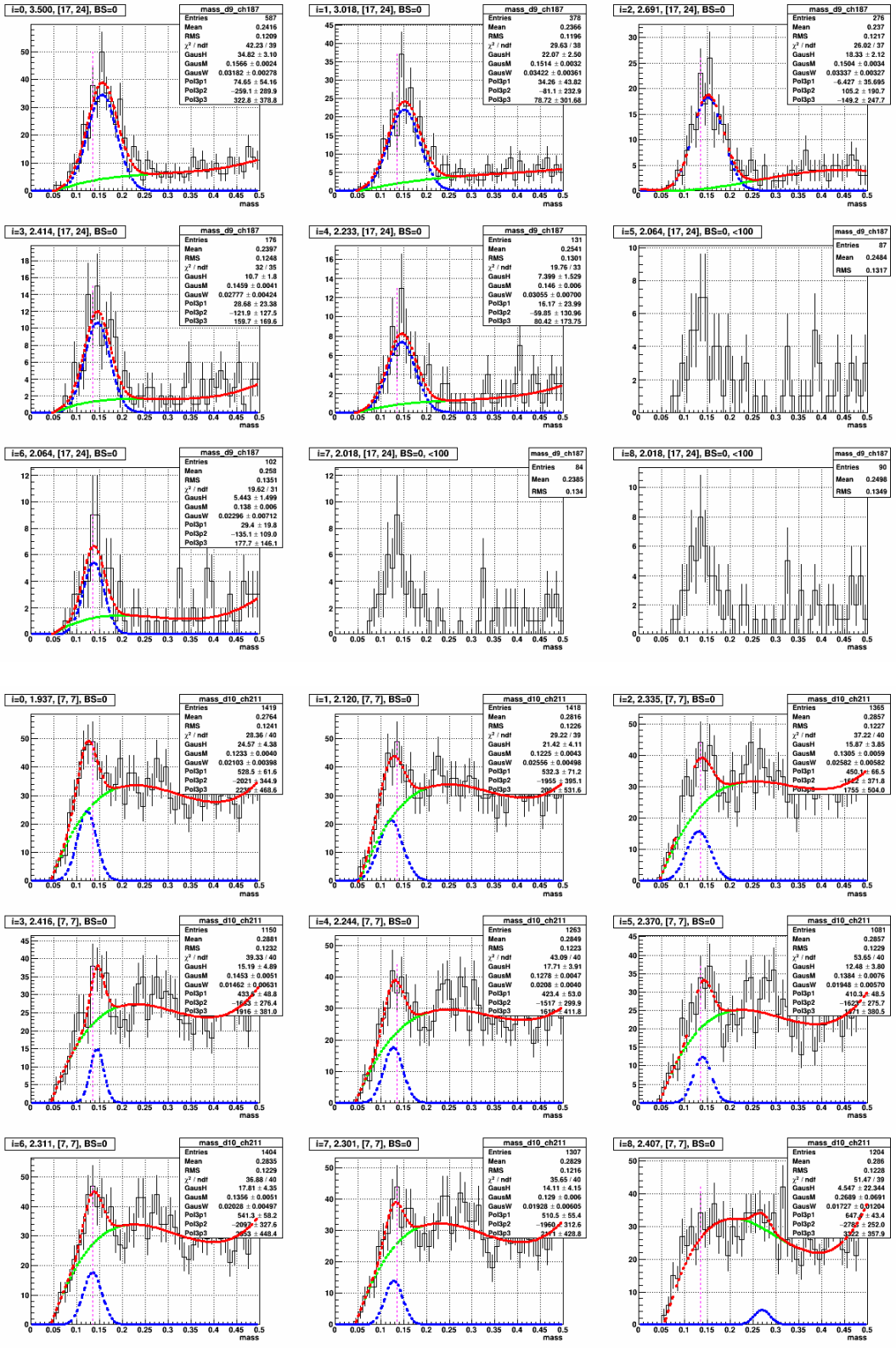

Figure 2.40: Examples of poor statistics case (top 9) and dirty distribution case (bottom 9).

2.3.5 Degradation study

It is a well-known issue that FMS cells' response degrades over time by accumulating radiation damage. To restore the accumulated radiation damage from the commissioning of the FMS, before RUN15 all FMS cells were disassembled and exposed to the natural UV light and commissioned again. However, after RUN15, it turned out even a year's damage isn't negligible. Fig. 2.41 shows the results of radiation damage study by using FMS LEDs. [15] To address this problem, in RUN17 an in-situ recovery system based on UV LEDs were installed. [16]

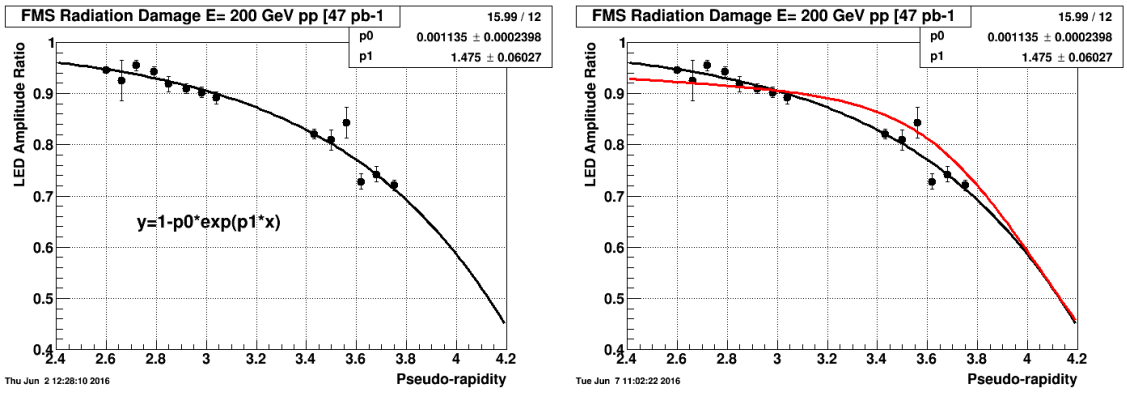

Figure 2.41: Results of radiation damage study by using FMS LED, by Stephen Trentalange (2016).

The dataset used for this analysis is RUN15pp200trans. Unlike the RUN17 no UV recovery system exists thus each cell's response would simply get worse over time. Related to the damage accumulating over time a few following characteristics can be expected:

Expected behaviors by radiation damage

1. Extend of the radiation damage by condition
   a. The cells closer to the beam pipe (larger η) would experience more damage
   b. The damage accumulating over time, thus data taken in later days would experience more damage
2. Each cell's gainCorr (assuming the calibration is precisely done)
   a. As time goes on, larger gainCorr will be required to the same cell to compensate the damage
   b. The change in the gainCorr will be more distinct in the small cells
2. Each cell's invariant mass yields
   a. The damage directly affects the raw ADC by making a PbGl cell opaque
   b. The lowered ADC likely to be connected to the reconstruction, thus the obtained mass yields

If new calibration results succeed to reflect all these expectations, it'd be a solid proof of the performance of the framework. In addition, the measure of degradation also can be estimated quantitatively. Therefore previous expectations were tested by using final calibration's gainCorr and the obtained mass yields.

By gainCorr

Again, the measure of degradation effect will be different by the cell's location (η) the radiation exposed time. Therefore all FMS cells and RUN15pp200trans periods were separated as follows. Note that Each group by location was adjusted to have a similar number of cells (250 ± 30). Also, the earliest days in RUN15pp200trans (day 66-73) were not used due to HV change at day 77. For detailed information check the section 3.1.

Degradation effect test group

- By location
  1. Large cells only, $\eta < 2.75$
  2. Large cells only, $2.75 < \eta < 2.95$
  3. Large cells only, $2.95 < \eta$
  4. Small cells only, $3.58 < \eta$
  5. Small cells only, $\eta < 3.58$
- By periods
  1. day 77-79 (base period)
  2. day 80-81
  3. day 82-84
  4. day 85-86
  5. day 87-88
  6. day 89-90
  7. day 91-93

For the test, a specific cell's gainCorr difference between two periods (ex. ΔgainCorr of detId 8, ch1, between day 77-79 and day 80-81). The results can be checked in Fig. 2.42 and Fig. 2.43: as expected, the slope gets stiffer with increasing η and with time. There are two caveats for the results in Fig. 2.43: first, the slope in small cells change sensitively by selection of η. Thus the fluctuating tendency in small cells likely originated from this matter; second, to increase the statistics all cells were used instead of only the converged cells. The largely deviating entries in a plot (ex. entries at y > 0.1 in first x bin in Fig. 2.43) is likely originated from those cells which were not converged in both compared periods.

By mass yields

The invariant mass yields of each period are shown in Fig. 2.44. Clear degradation effect can be seen in small cells while the effect is very weak or almost negligible in large cells, which is consistent with the results observed in the study by gainCorr.

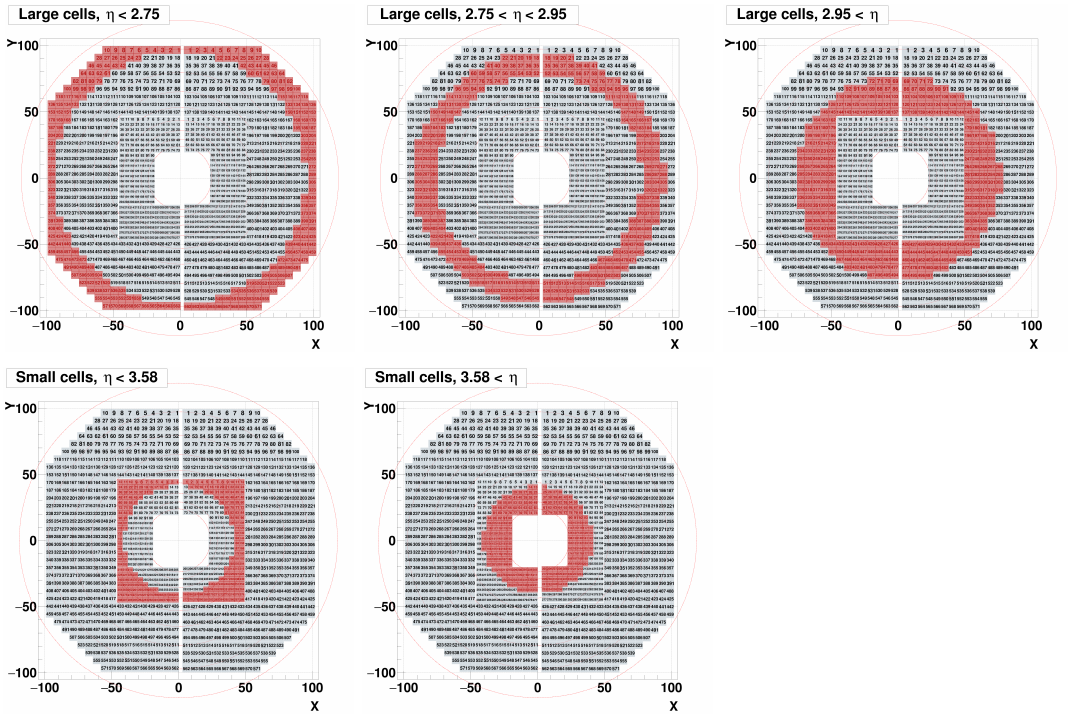

Figure 2.42: The groups separated by cell type (large or small) and the cell's η. Each group was determined to have a similar number of cells (250 ± 30). The red dashed rings indicate η in the range of $2.5 < \eta < 4.1$ with stepwidth of 0.2

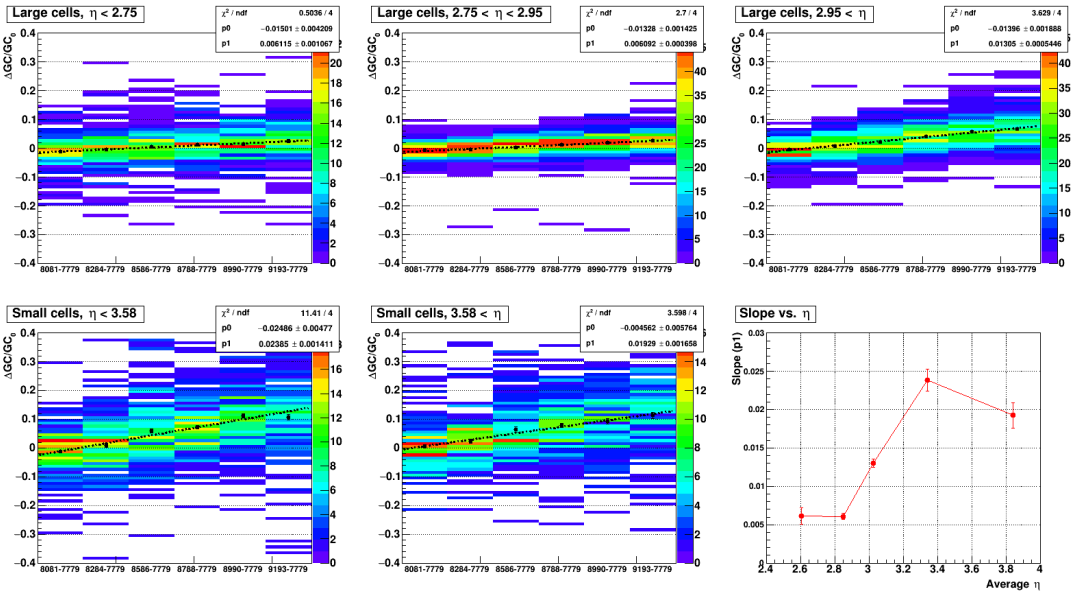

Figure 2.43: Results of degradation study by final gainCorr values in day 77-93. Each plot corresponds to the group in Fig. 2.42. Each x bin indicates the difference between the later period and the earliest period (ex. day 8081 - day7779). Y-axis indicates gainCorr difference of the same cell in two different periods (ΔGC), normalized by the earliest period's gainCorr (GC_0)

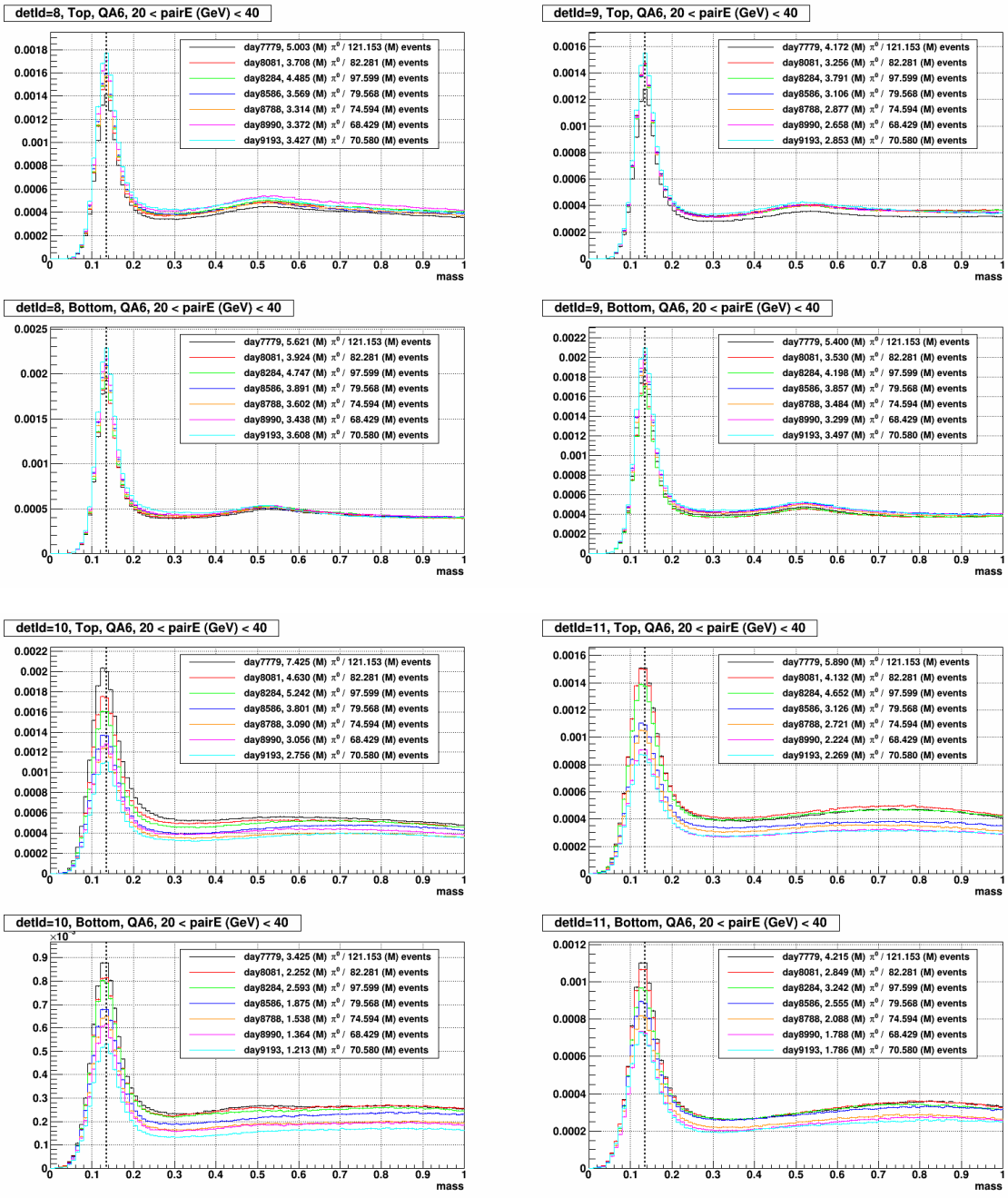

Figure 2.44: Invariant mass for multiple periods in day 77 - 93, obtained with similar condition to the calibration (QA6 in section 2.3.3). Each distribution was normalized by the number of events. Each column corresponds to the different detId and Each row corresponds to the top half or bottom half of the FMS. The clear degradation effect can be seen in small cells.

Chapter 3

Results

3.1 RUN15 pptrans

RUN15 ppttrans FMS Operations

A couple of summary logs exist for FMS operations in RUN15 [3][4]. By using these logs' information cross-checked with STAR shift log a few checkpoint runs were selected as follows.

RUN15pp200trans - checkpoints

- 16066033: FMS triggers elevated to physics
- 16069039: prescale factors change
- 16073022: new HV settings (i7) applied but lasted for only a few runs
- 16073050: power dip after this run (* Chris' log says it's 16073026 - it looks typo or error)
- 16076032: new HV settings (i8) applied
- 16077019: first physics run after power dip
- 16093019: last pptrans run

As explained in section 2.2.1, the new calibration framework was developed by using 2 days' data in pptrans period. Therefore it will be a proper choice that separating the whole target period into several subgroups, which has similar data size in addition to considering previous checkpoints. As a result, the entire pptrans period separated into 9 subgroups as follows.

RUN15pp200trans - subgroups

1. day 66-69, run 16066033 - 16069038 (74 runs)
2. day 69-73, run 16069039 - 16073021 (102 runs)
   (* i7 online calibration was applied for runs 16073030 - 16073040: should be treated independently)
3. day 77-79, run 16077021 - 16079063 (90 runs)
4. day 80-81, run 16080002 - 16081061 (69 runs) (* runs used for framework development)
5. day 82-84, run 16082001 - 16084015 (79 runs)
6. day 85-86, run 16085005 - 16086054 (72 runs)
7. day 87-88, run 16087001 - 16088050 (71 runs)
8. day 89-90, run 16089001 - 16090054 (73 runs)
9. day 91-93, run 16091003 - 16093019 (72 runs)

Day 66-69

Final results for day 66-69

- Dead + Bad: 10 + 40 (0.039)
- Total converged cells: 1074/1264 (0.8497)

  detId 8: 349/394 (0.8858)

  detId 9: 356/394 (0.9036)

  detId 10: 169/238 (0.7101)

  detId 11: 200/238 (0.8403)

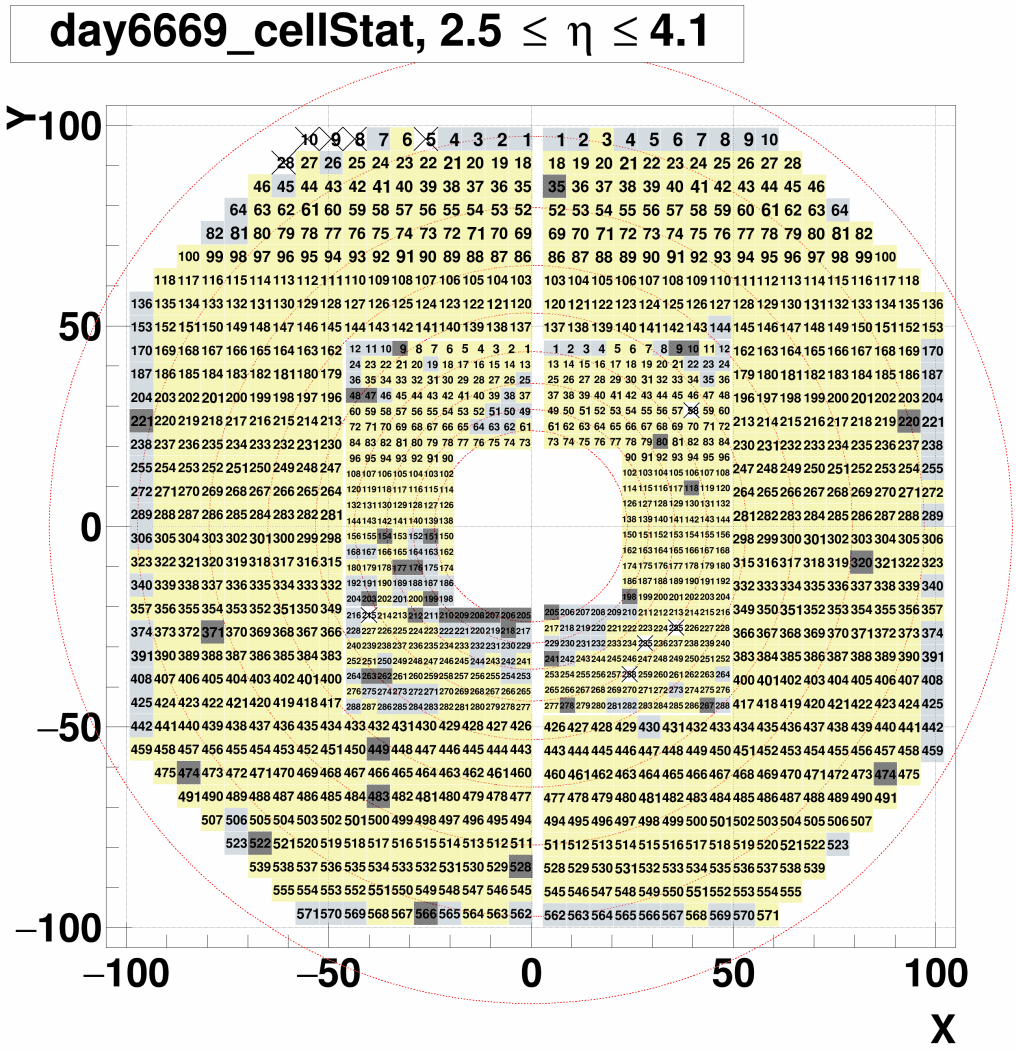

Figure 3.1: Final map of cell status for day 66-69. Each color corresponds to: good but not converged yet (light blue), bad (black), dead (white with crossing), and converged (yellow), respectively.

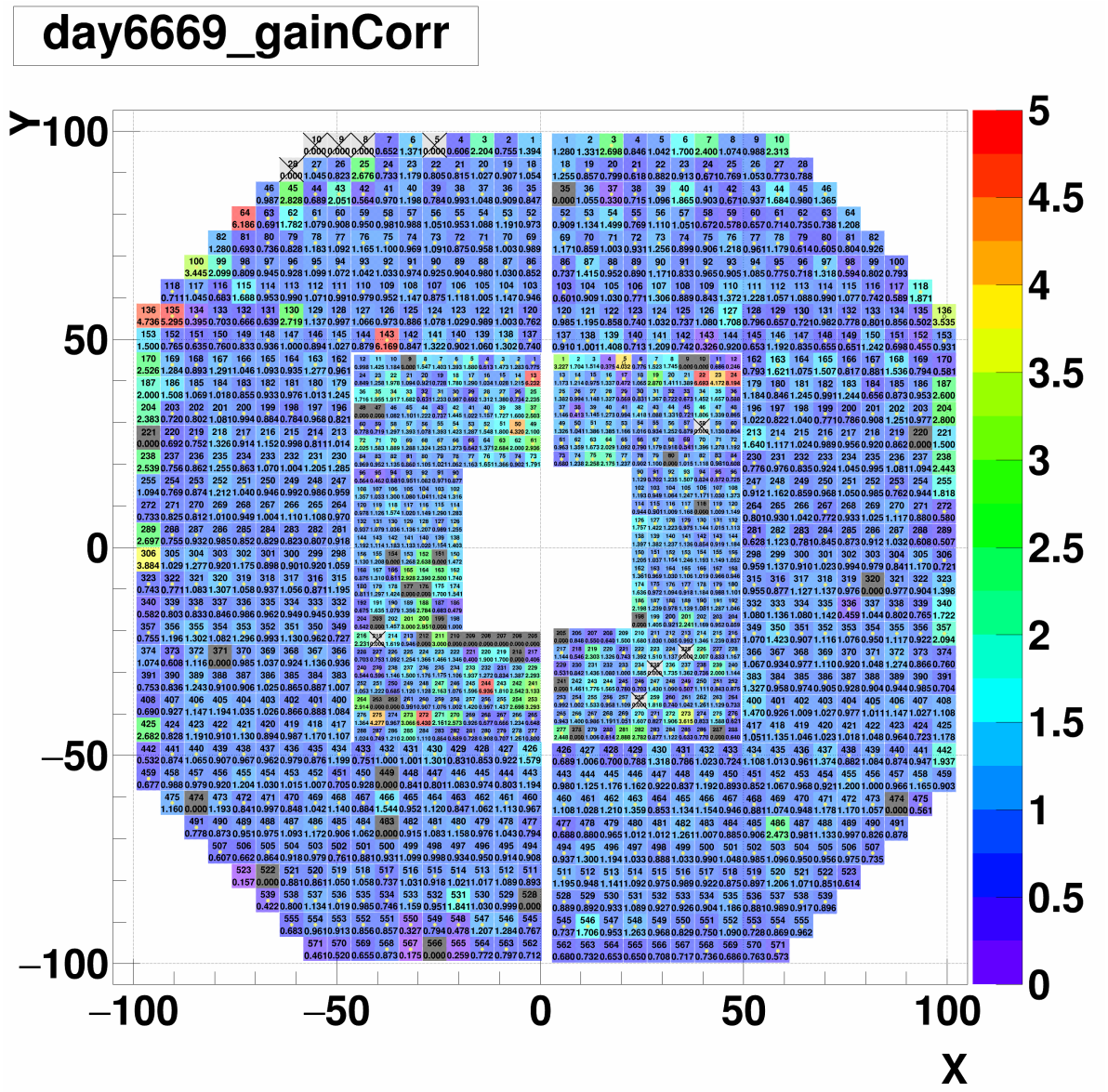

Figure 3.2: Final map of gainCorr for day 66-69. The numbers in a cell are cell number and the assigned gainCorr. The yellow filled circle (black open circle for yellow-colored cells) means the cell is converged.

Day 69-73

Final results for day 69-73

- Dead + Bad: 11 + 46 (0.045)
- Total converged cells: 1092/1264 (0.8639)

detId 8: 362/394 (0.9188)

detId 9: 367/394 (0.9315)

detId 10: 172/238 (0.7227)

detId 11: 191/238 (0.8025)

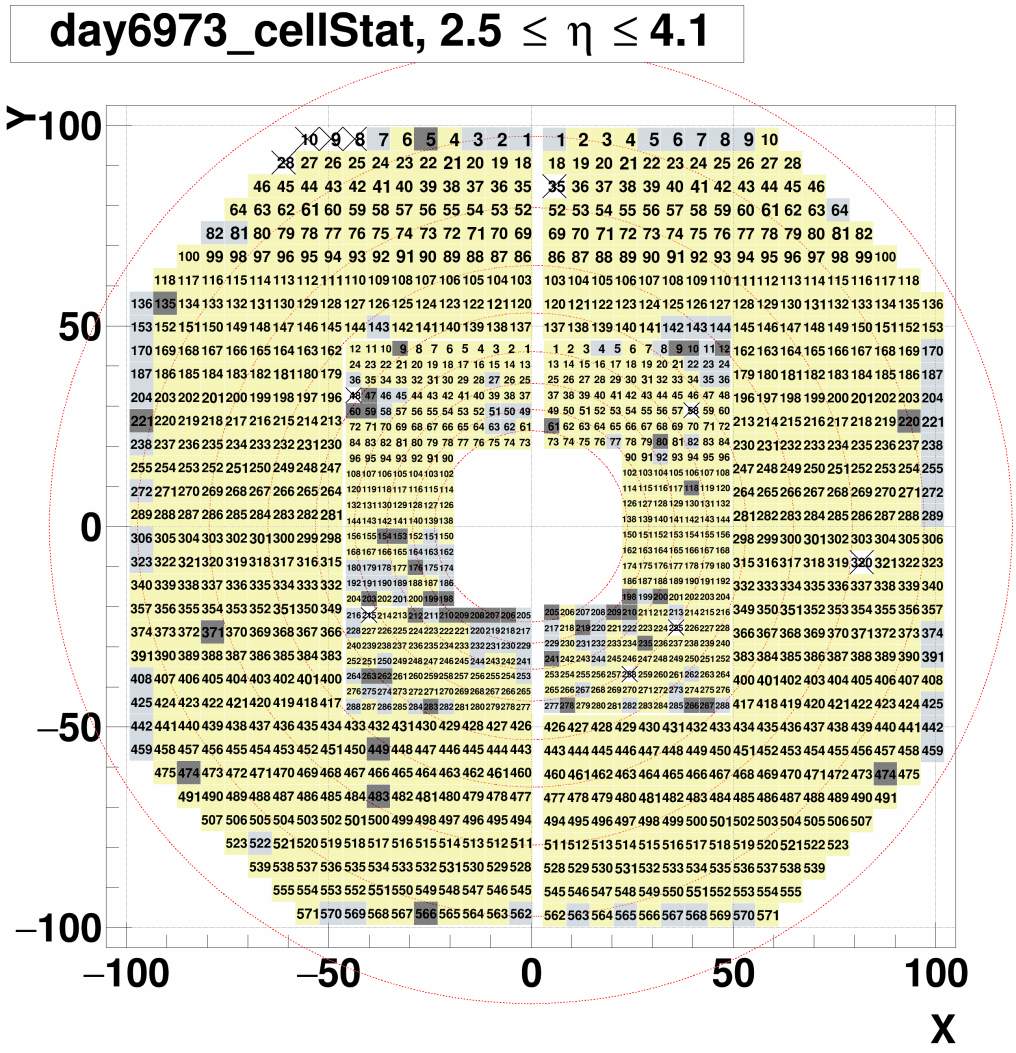

Figure 3.3: Final map of cell status for day 69-73. Each color corresponds to: good but not converged yet (light blue), bad (black), dead (white with crossing), and converged (yellow), respectively.

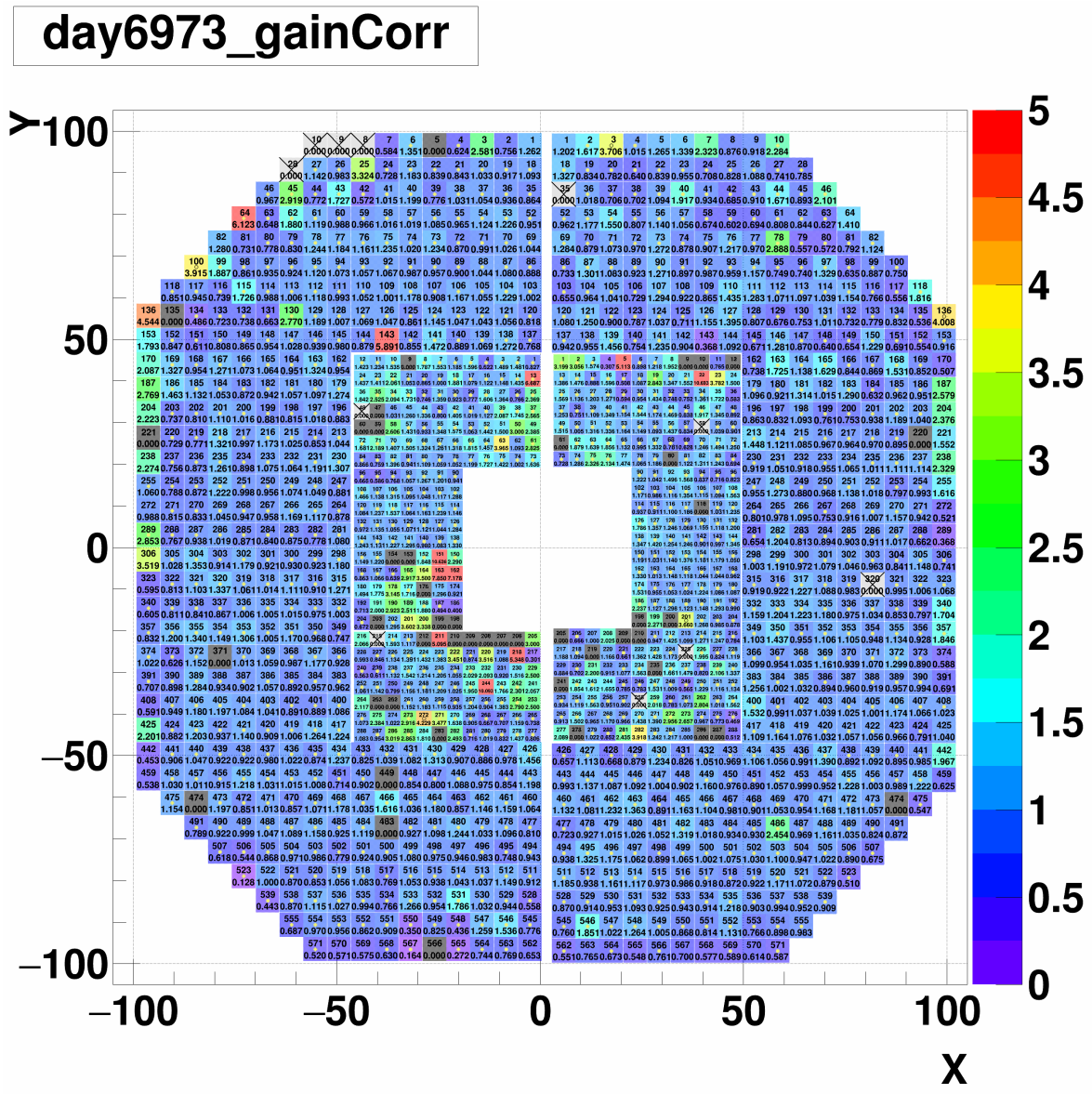

Figure 3.4: Final map of gainCorr for day 69-73. The numbers in a cell are cell number and the assigned gainCorr. The yellow filled circle (black open circle for yellow-colored cells) means the cell is converged.

Day 77-79

Final results for day 77-79

- Dead + Bad: 28 + 26 (0.042)
- Total converged cells: 1089/1264 (0.8616)

detId 8: 343/394 (0.8706)

detId 9: 360/394 (0.9137)

detId 10: 183/238 (0.7689)

detId 11: 203/238 (0.8529)

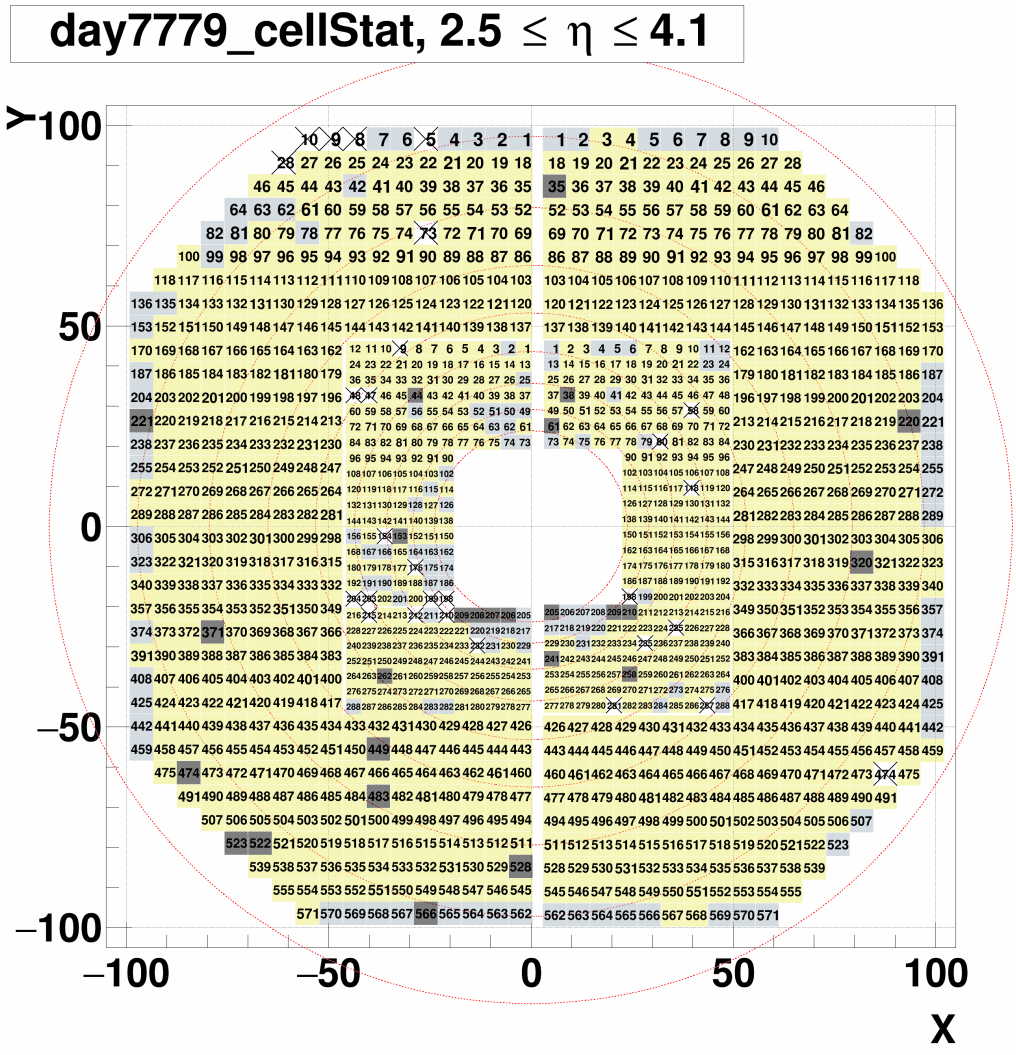

Figure 3.5: Final map of cell status for day 77-79. Each color corresponds to: good but not converged yet (light blue), bad (black), dead (white with crossing), and converged (yellow), respectively.

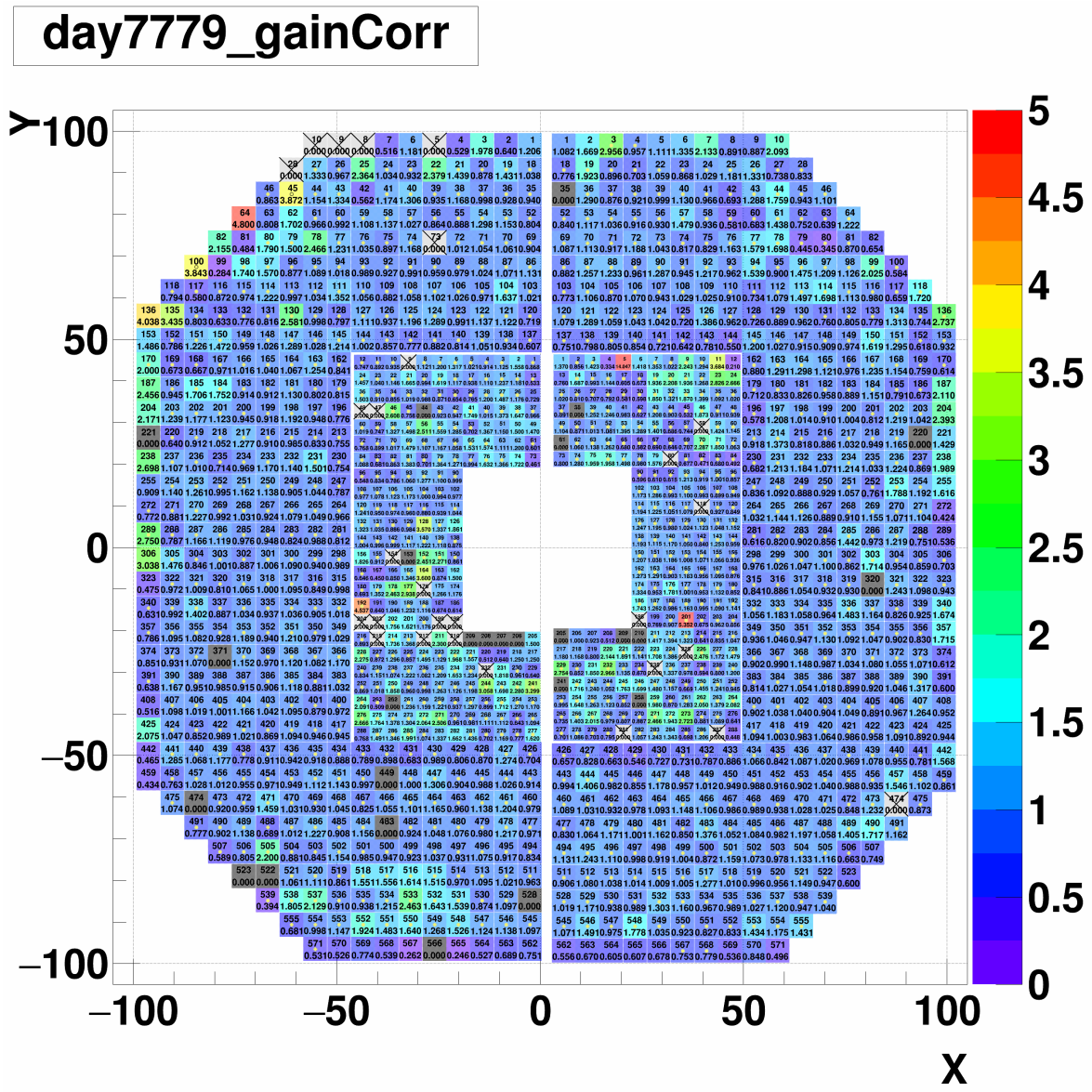

Figure 3.6: Final map of gainCorr for day 77-79. The numbers in a cell are cell number and the assigned gainCorr. The yellow filled circle (black open circle for yellow-colored cells) means the cell is converged.

Day 80-81

Final results for day 80-81

- Dead + Bad: 30 + 21 (0.040)
- Total converged cells: 1099/1264 (0.8695)

  detId 8: 348/394 (0.8832)

  detId 9: 364/394 (0.9239)

  detId 10: 183/238 (0.7689)

  detId 11: 204/238 (0.8571)

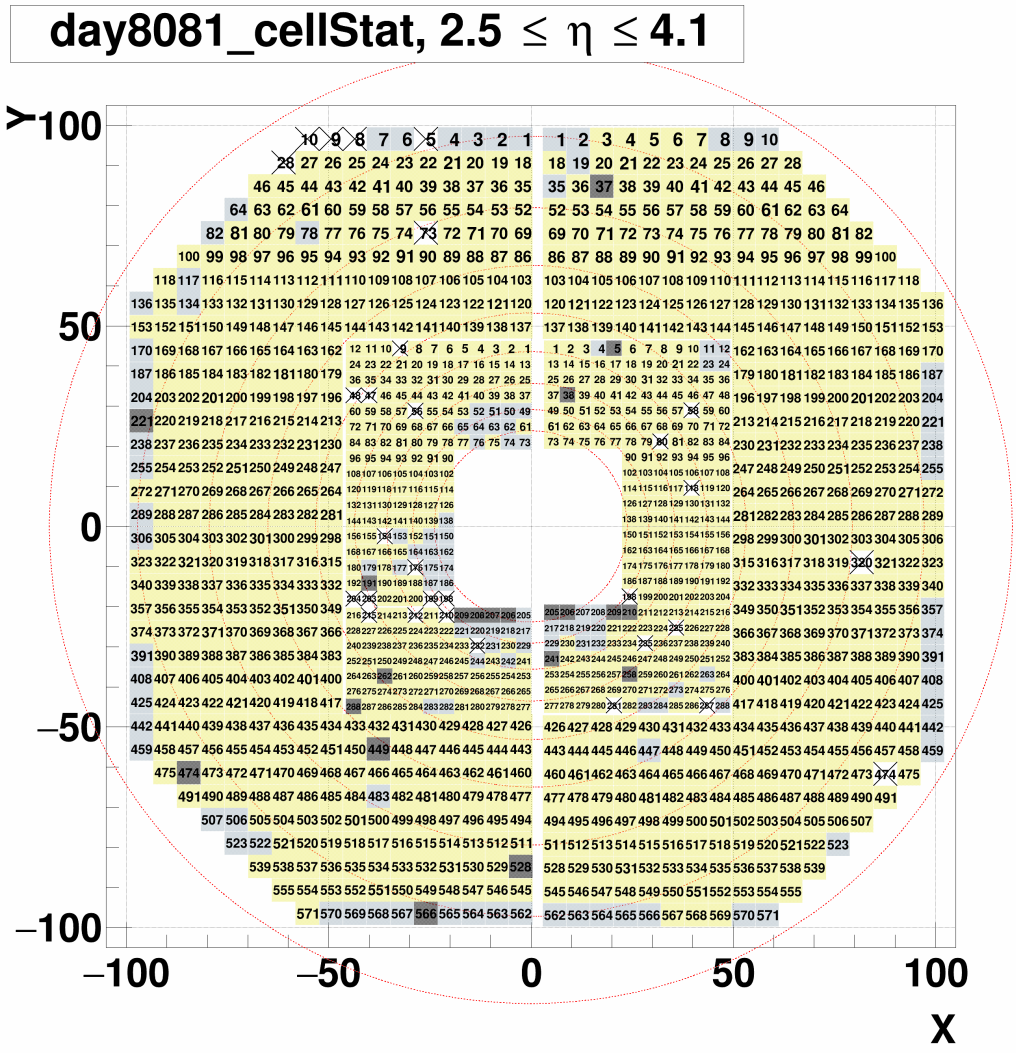

Figure 3.7: Final map of cell status for day 80-81. Each color corresponds to: good but not converged yet (light blue), bad (black), dead (white with crossing), and converged (yellow), respectively.

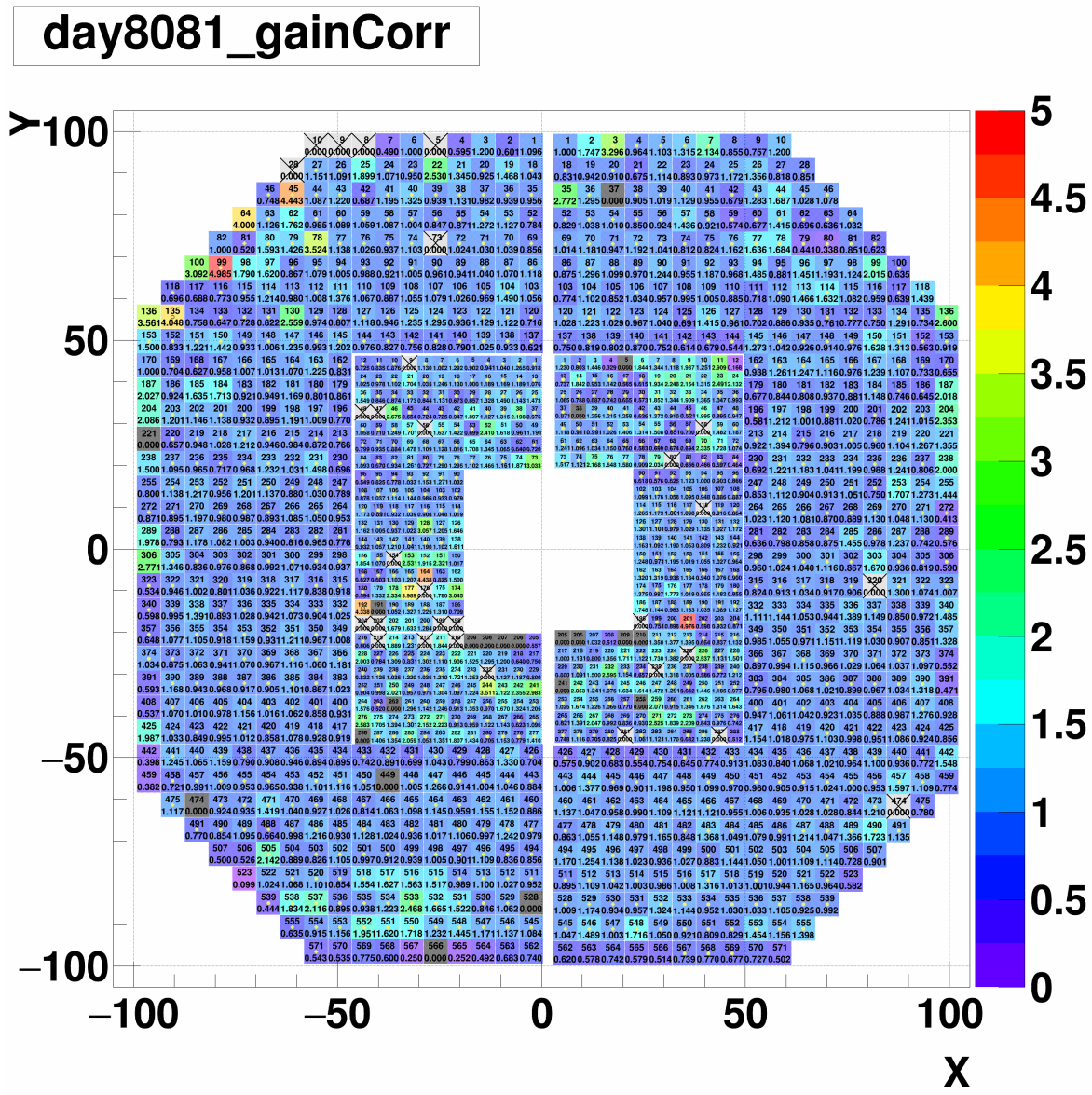

Figure 3.8: Final map of gainCorr for day 80-81. The numbers in a cell are cell number and the assigned gainCorr. The yellow filled circle (black open circle for yellow-colored cells) means the cell is converged.

Day 82-84

Final results for day 82-84

- Dead + Bad: 30 + 25 (0.044)
- Total converged cells: 1100/1264 (0.8703)
  detId 8: 351/394 (0.8909)
  detId 9: 372/394 (0.9442)
  detId 10: 176/238 (0.7395)
  detId 11: 201/238 (0.8445)

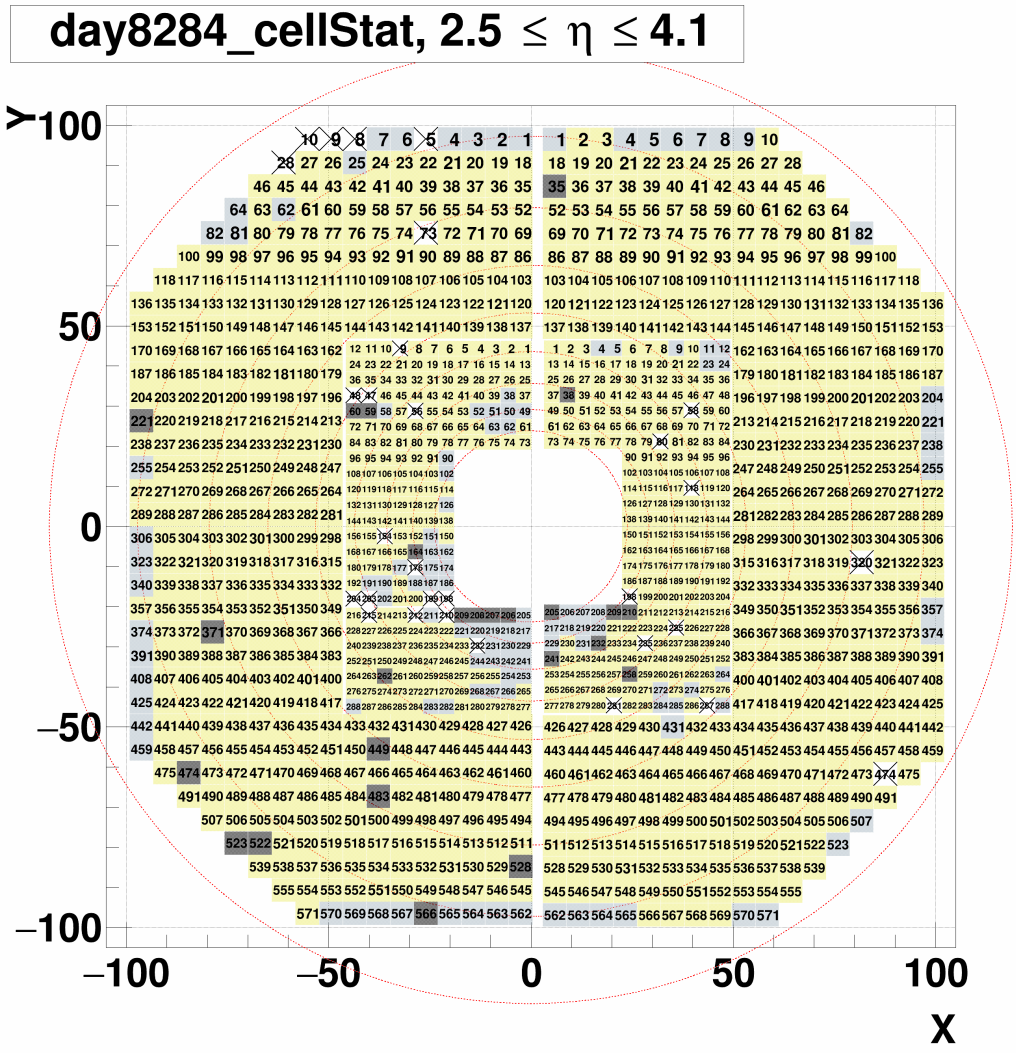

Figure 3.9: Final map of cell status for day 82-84. Each color corresponds to: good but not converged yet (light blue), bad (black), dead (white with crossing), and converged (yellow), respectively.

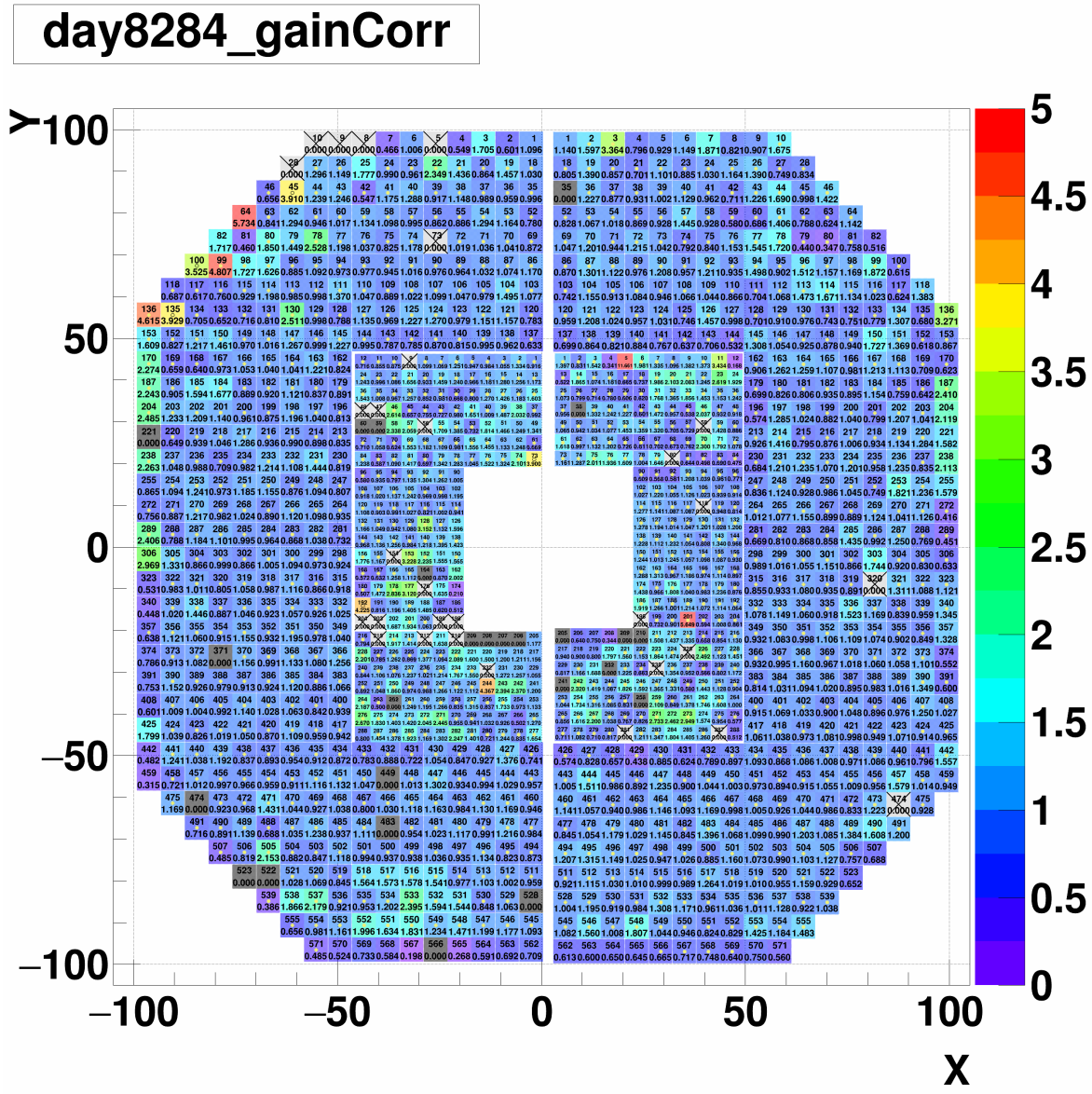

Figure 3.10: Final map of gainCorr for day 82-84. The numbers in a cell are cell number and the assigned gainCorr. The yellow filled circle (black open circle for yellow-colored cells) means the cell is converged.

Day 85-86

Final results for day 85-86

- Dead + Bad: 29 + 31 (0.047)
- Total converged cells: 1087/1264 (0.8600)
  detId 8: 350/394 (0.8883)
  detId 9: 367/394 (0.9315)
  detId 10: 176/238 (0.7395)
  detId 11: 194/238 (0.8151)

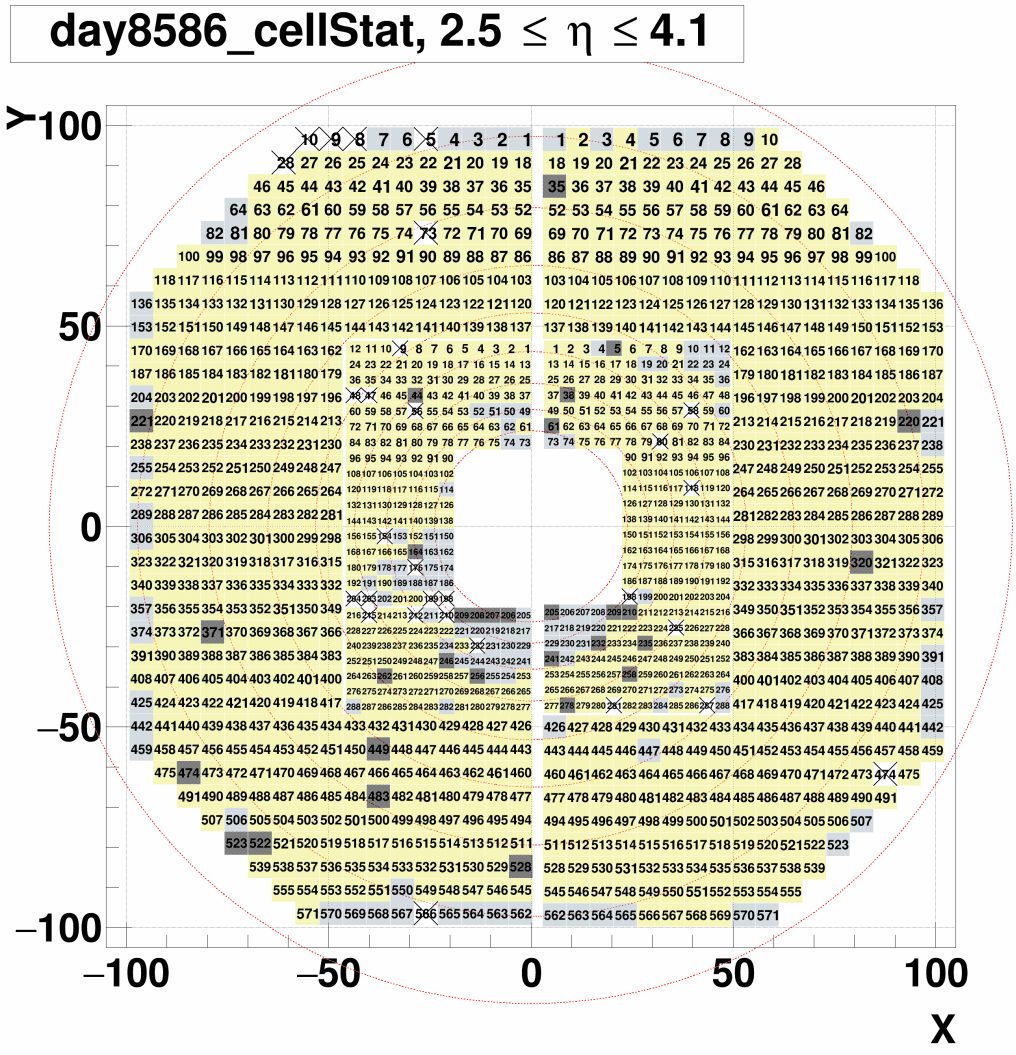

Figure 3.11: Final map of cell status for day 85-86. Each color corresponds to: good but not converged yet (light blue), bad (black), dead (white with crossing), and converged (yellow), respectively.

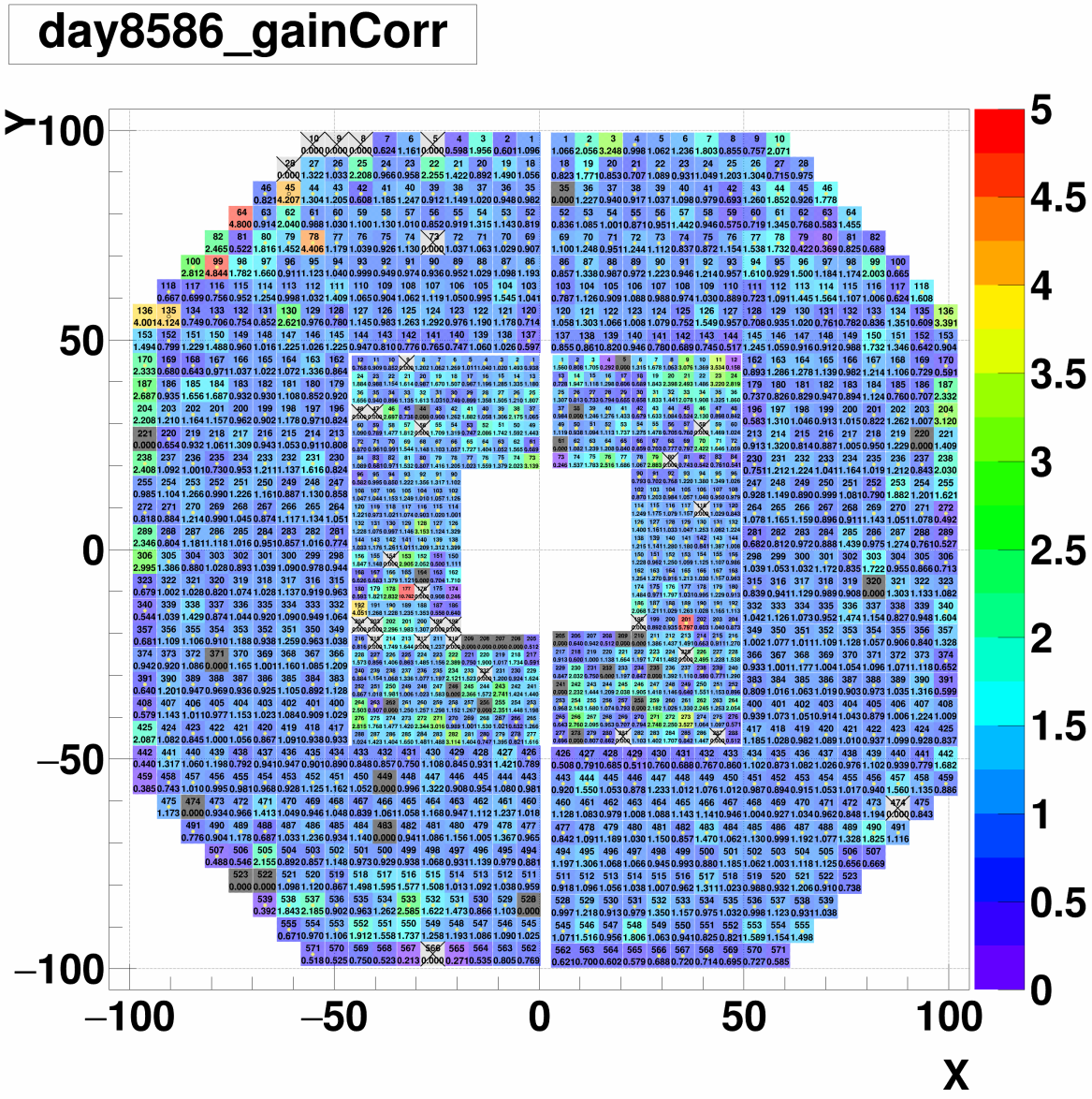

Figure 3.12: Final map of gainCorr for day 85-86. The numbers in a cell are cell number and the assigned gainCorr. The yellow filled circle (black open circle for yellow-colored cells) means the cell is converged.

Day 87-88

Final results for day 87-88

- Dead + Bad: 31 + 27 (0.046)
- Total converged cells: 1087/1264 (0.8600)

detId 8: 350/394 (0.8883)

detId 9: 361/394 (0.9162)

detId 10: 180/238 (0.7563)

detId 11: 196/238 (0.8235)

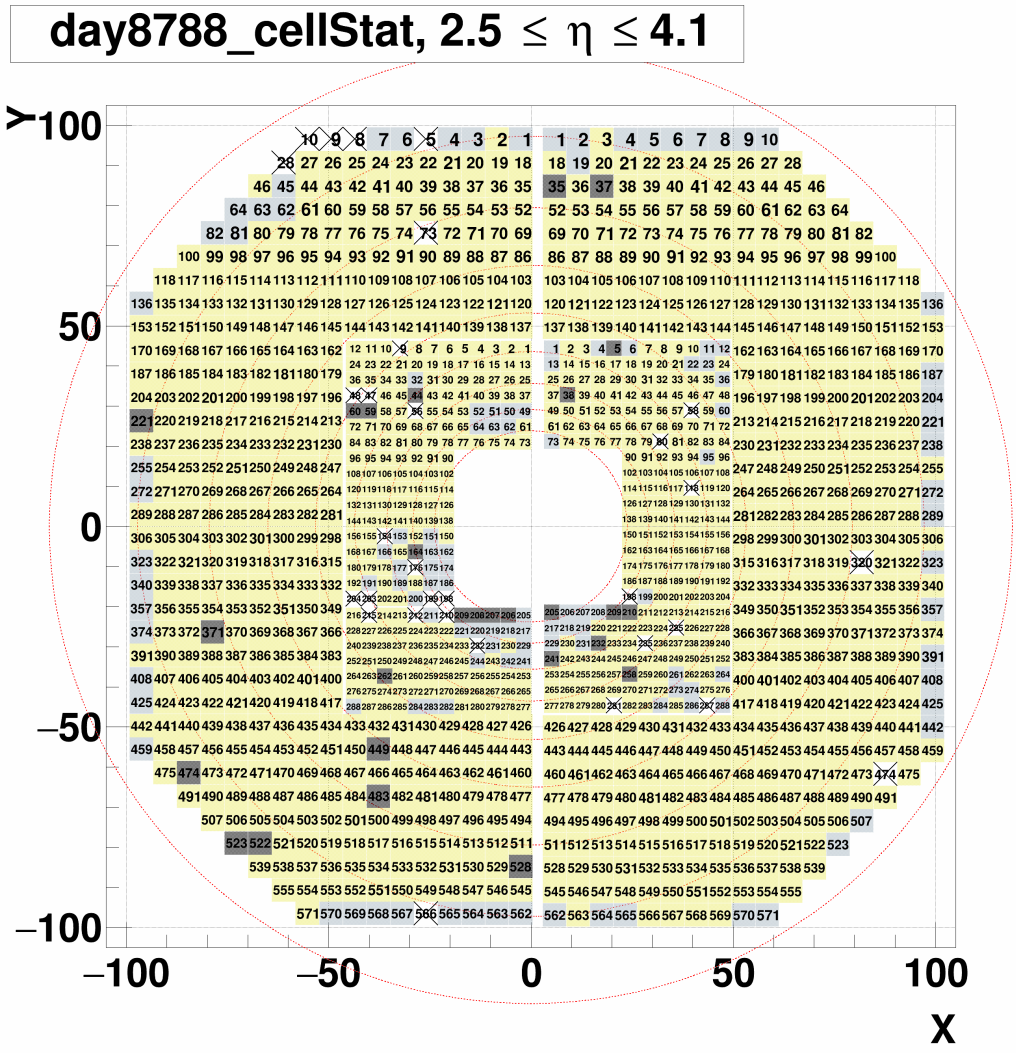

Figure 3.13: Final map of cell status for day 87-88. Each color corresponds to: good but not converged yet (light blue), bad (black), dead (white with crossing), and converged (yellow), respectively.

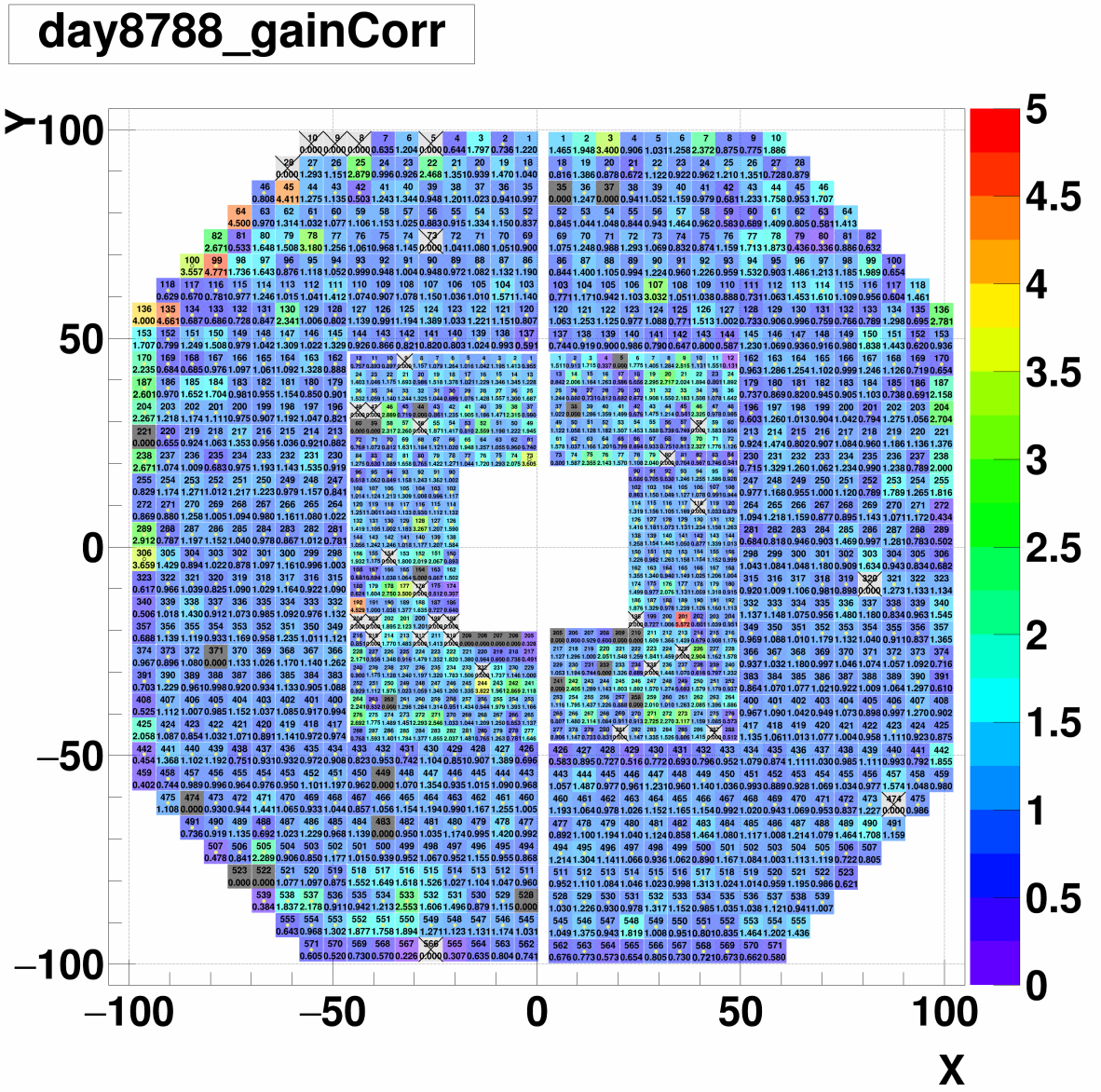

Figure 3.14: Final map of gainCorr for day 87-88. The numbers in a cell are cell number and the assigned gainCorr. The yellow filled circle (black open circle for yellow-colored cells) means the cell is converged.

Day 89-90

Final results for day 89-90

- Dead + Bad: 31 + 25 (0.044)
- Total converged cells: 1079/1264 (0.8536)

detId 8: 352/394 (0.8934)

detId 9: 359/394 (0.9112)

detId 10: 174/238 (0.7311)

detId 11: 194/238 (0.8151)

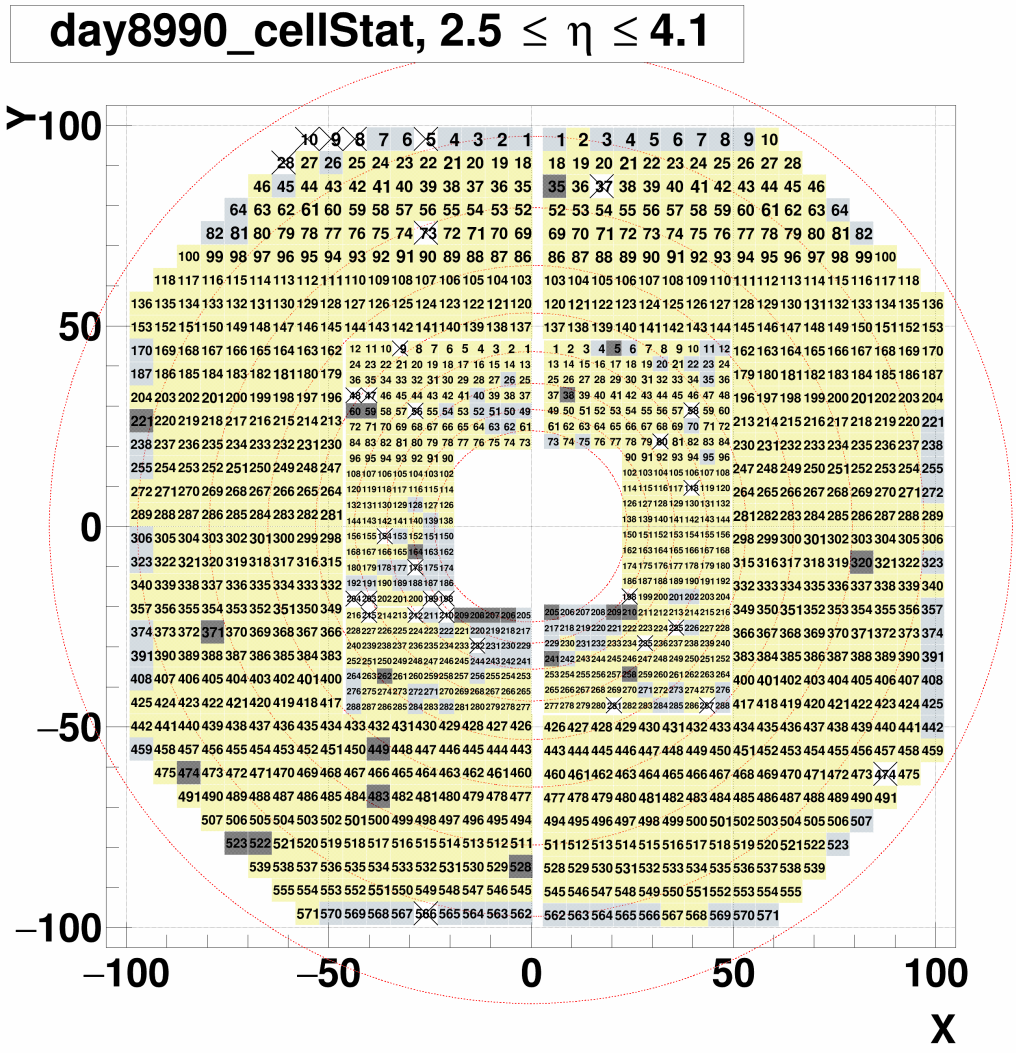

Figure 3.15: Final map of cell status for day 89-90. Each color corresponds to: good but not converged yet (light blue), bad (black), dead (white with crossing), and converged (yellow), respectively.

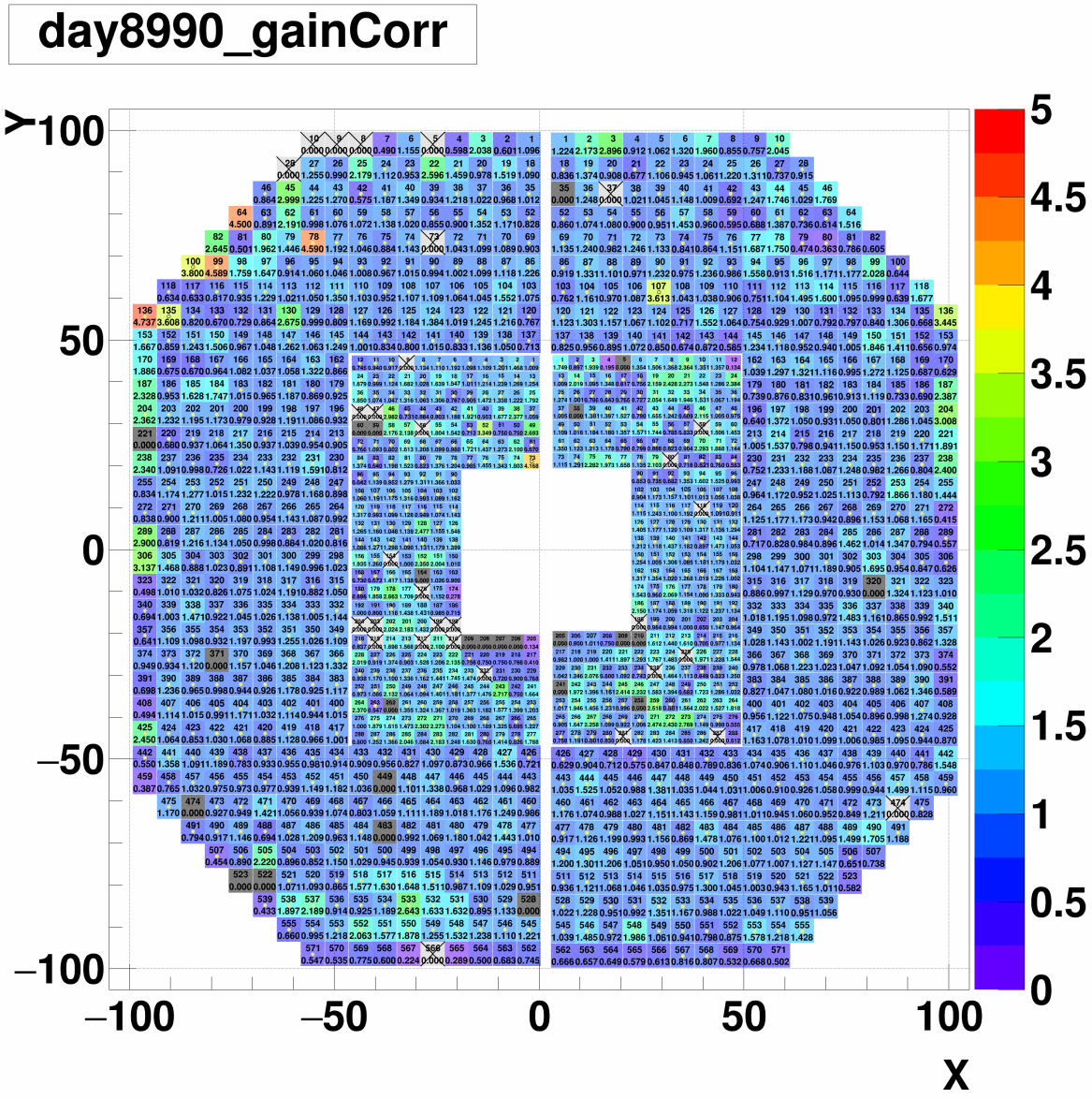

Figure 3.16: Final map of gainCorr for day 89-90. The numbers in a cell are cell number and the assigned gainCorr. The yellow filled circle (black open circle for yellow-colored cells) means the cell is converged.

Day 91-93

Final results for day 91-93

- Dead + Bad: 30 + 25 (0.044)
- Total converged cells: 1038/1264 (0.8212)

  detId 8: 347/394 (0.8807)

  detId 9: 358/394 (0.9086)

  detId 10: 160/238 (0.6723)

  detId 11: 173/238 (0.7269)

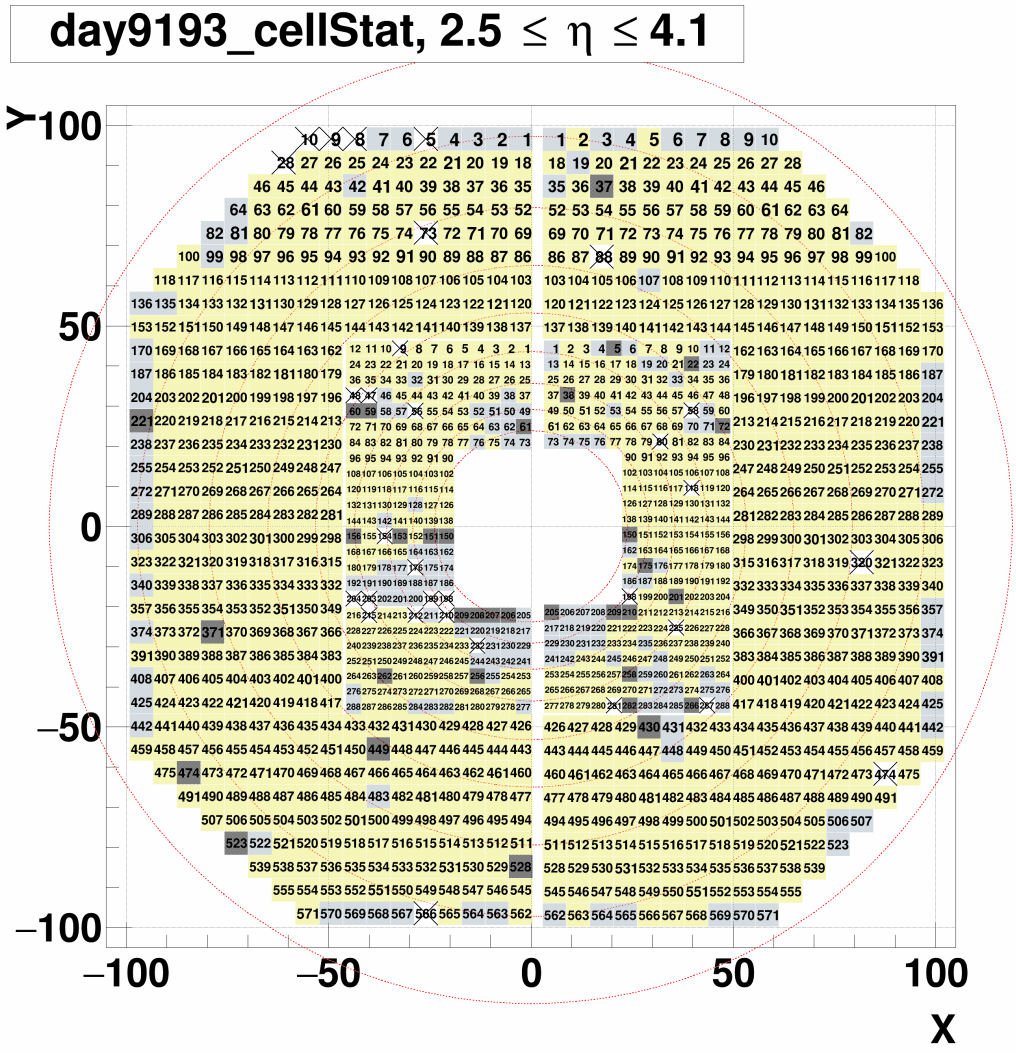

Figure 3.17: Final map of cell status for day 91-93. Each color corresponds to: good but not converged yet (light blue), bad (black), dead (white with crossing), and converged (yellow), respectively.

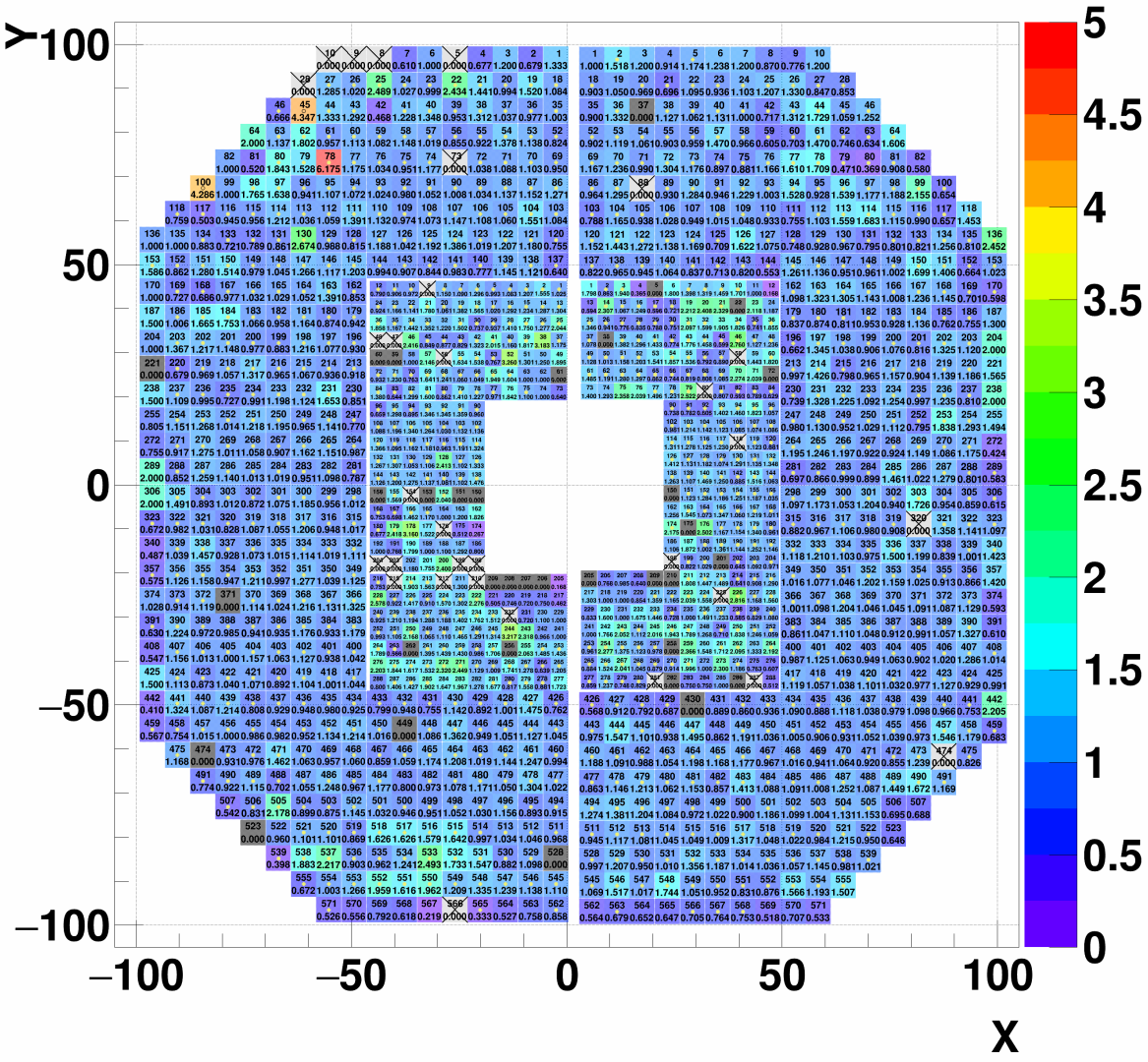

Figure 3.18: Final map of gainCorr for day 91-93. The numbers in a cell are cell number and the assigned gainCorr. The yellow filled circle (black open circle for yellow-colored cells) means the cell is converged.

Appendix A

Additional QA plots for RUN15pptrans

A.1 Bad/Dead/Hot channels QA

This section shows list of all bad/dead/hot channels masked out in the calibration. The QA criteria can be found in section 2.3.1, and the conditions used for period separation can be found in section 3.1. Note that the ADC distributions shown in this appendix are all bad or hot channels.

Summary of number of dead/bad channels by period

1. day 66-69: 10/40 (dead/bad)
2. day 69-73: 11/46
3. day 77-79: 28/26
4. day 80-81: 30/21
5. day 82-84: 30/25
6. day 85-86: 29/31
7. day 87-88: 31/27
8. day 89-90: 31/25
9. day 91-93: 30/25

Day 66-69

QA results for RUN15pp200trans day 66-69 are as follows.

Dead channels (total 10)

- detId 8: 5, 8, 9, 10, 28
- detId 9: None
- detId 10: 215
- detId 11: 58, 225, 235, 258

Bad channels (total 40)

- detId 8: 221, 371, 449, 474, 483, 522, 528, 566
- detId 9: 35, 220, 320, 474
- detId 10: 9, 47, 48, 151, 154, 176, 177, 199, 203, 205, 206, 207, 208, 209, 210, 212, 218, 262, 263
- detId 11: 9, 10, 80, 118, 198, 205, 241, 278, 287

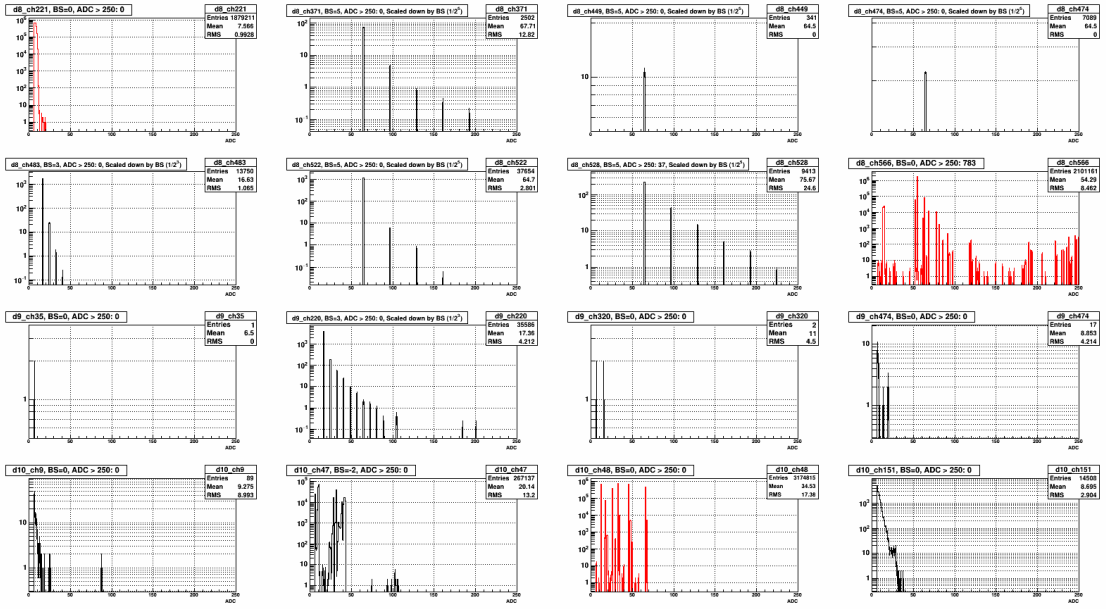

Figure A.1: Bad channels' ADC distribution, RUN15pp200trans, day 66-69, 1/2

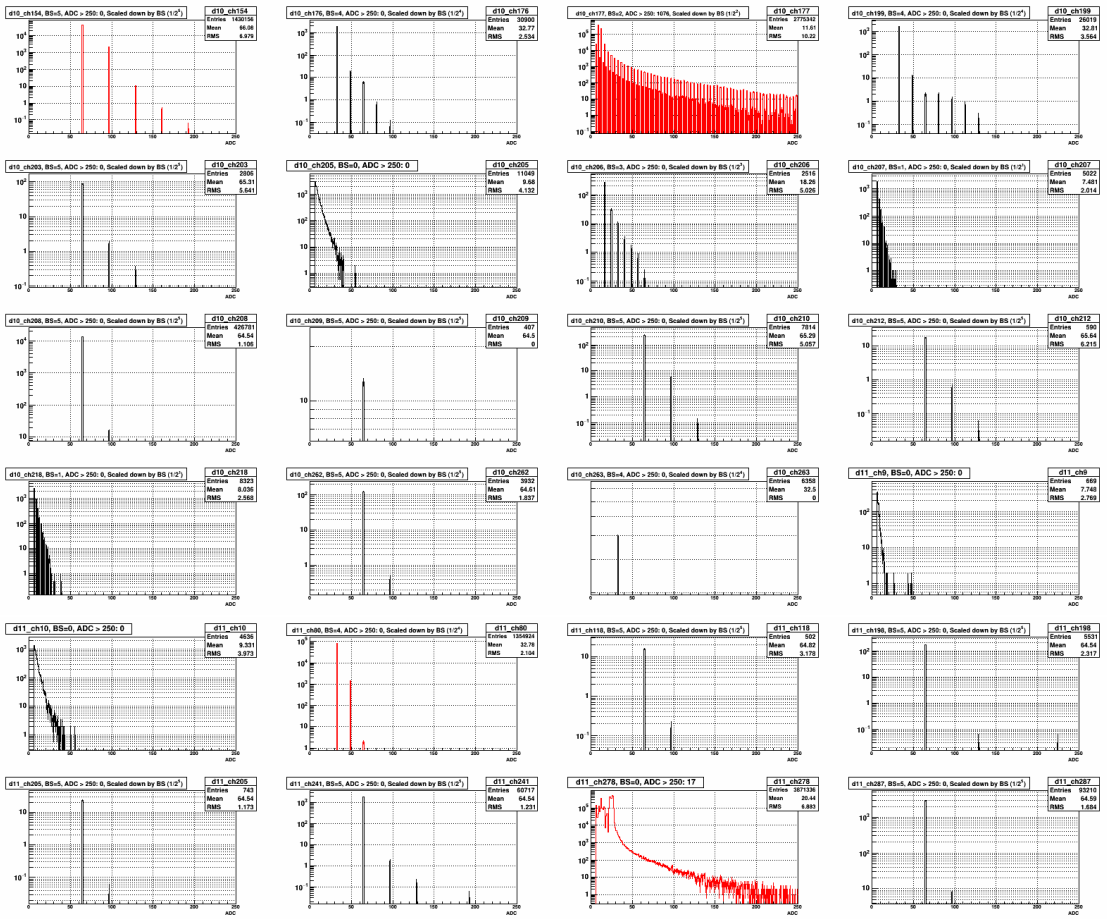

Figure A.2: Bad channels' ADC distribution, RUN15pp200trans, day 66-69, 2/2

Day 69-73

QA results for RUN15pp200trans day 69-73 are as follows.

Dead channels (total 11)

- detId 8: 8, 9, 10, 28,
- detId 9: 35, 320
- detId 10: 48, 215
- detId 11: 58, 225, 258

Bad channels (total 46)

- detId 8: 5, 135, 221, 371, 449, 474, 483, 566
- detId 9: 220, 474
- detId 10: 9, 47, 59, 60, 153, 154, 176, 198, 199, 203, 206, 207, 208, 209, 210, 212, 262, 263, 283
- detId 11: 9, 10, 12, 61, 80, 118, 198, 200, 205, 209, 210, 219, 235, 241, 278, 286, 287

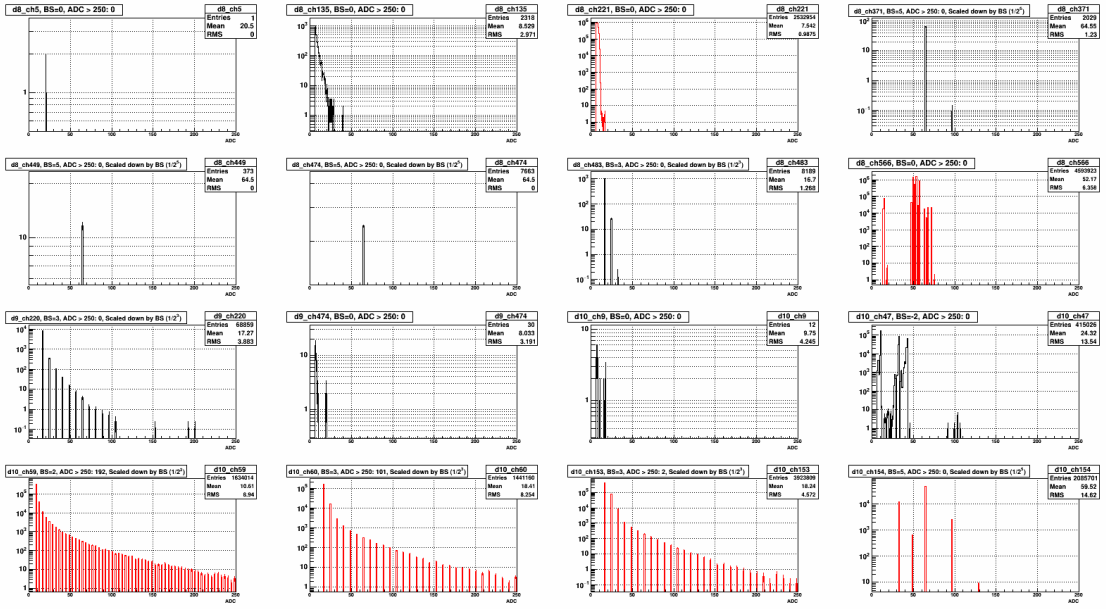

Figure A.3: Bad channels' ADC distribution, RUN15pp200trans, day 69-73, 1/2

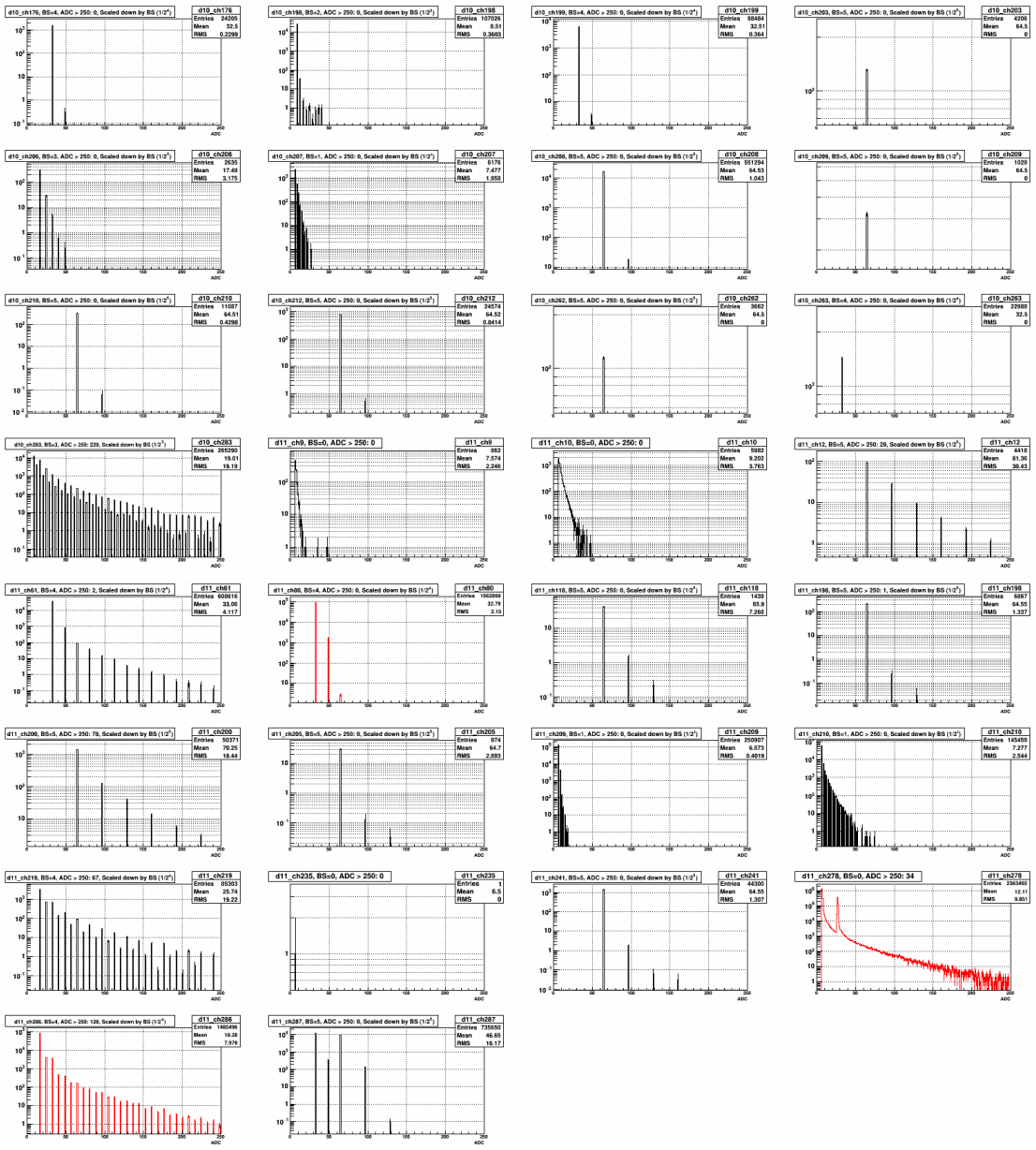

Figure A.4: Bad channels' ADC distribution, RUN15pp200trans, day 69-73, 2/2

Day 77-79

QA results for RUN15pp200trans day 77-79 are as follows.

Dead channels (total 28)

- detId 8: 5, 8, 9, 10, 28, 73
- detId 9: 474
- detId 10: 9, 47, 48, 154, 176, 198, 199, 203, 204, 210, 212, 215, 232
- detId 11: 58, 80, 118, 198, 225, 235, 281, 287

Bad channels (total 26)

- detId 8: 221, 371, 449, 474, 483, 522, 523, 528, 566
- detId 9: 35, 220, 320
- detId 10: 44, 153, 206, 207, 208, 209, 262
- detId 11: 38, 61, 205, 209, 210, 241, 258

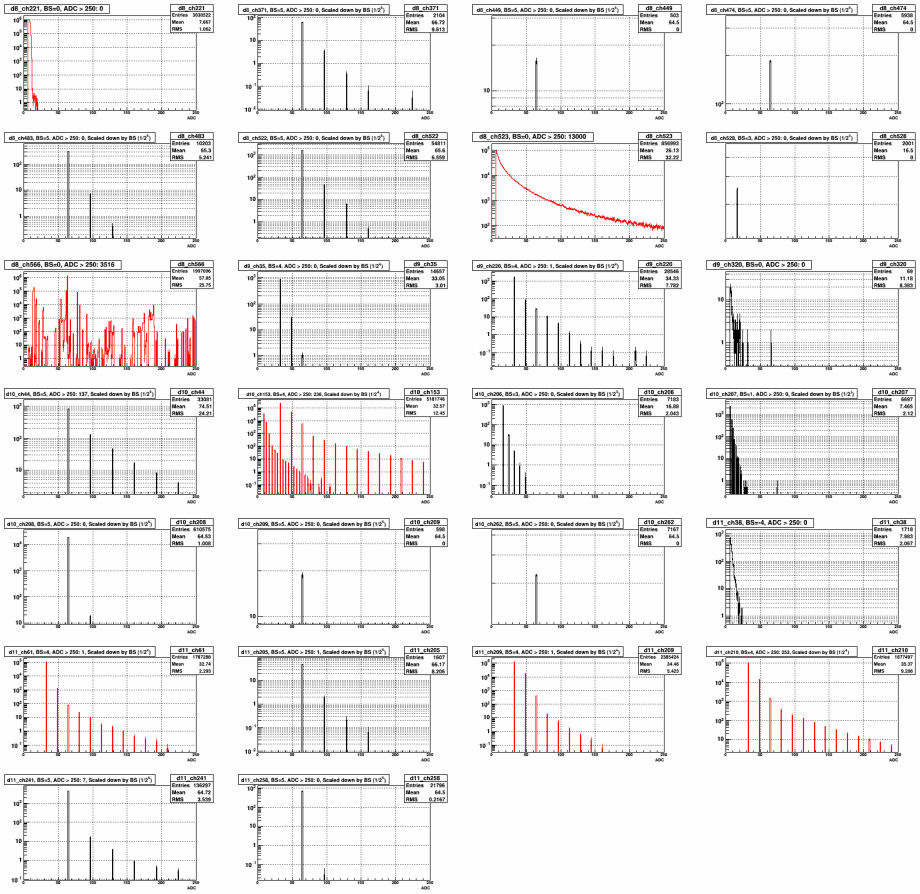

Figure A.5: Bad channels' ADC distribution, RUN15pp200trans, day 77-79

Day 80-81

QA results for RUN15pp200trans day 80-81 are as follows.

Dead channels (total 30)

- detId 8: 5, 8, 9, 10, 28, 73
- detId 9: 320, 474
- detId 10: 9, 47, 48, 56, 154, 176, 198, 199, 203, 204, 210, 212, 215, 232
- detId 11: 58, 80, 118, 198, 225, 235, 281, 287

Bad channels (total 21)

- detId 8: 221, 449, 474, 528, 566
- detId 9: 37
- detId 10: 191, 206, 207, 208, 209, 262, 288
- detId 11: 5, 38, 205, 206, 209, 210, 241, 258

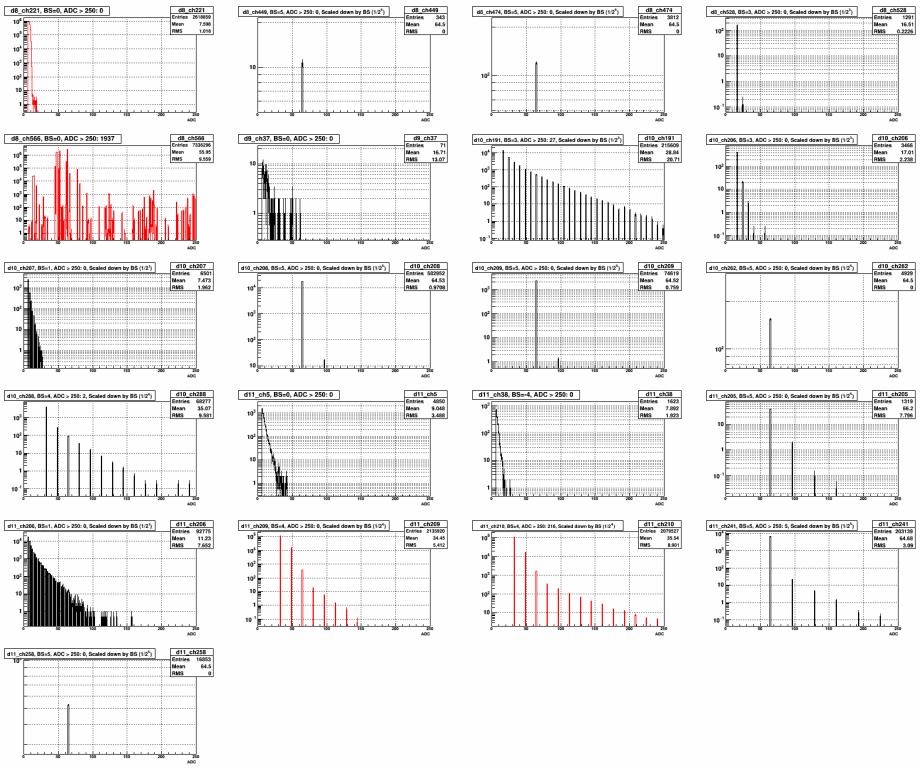

Figure A.6: Bad channels' ADC distribution, RUN15pp200trans, day 80-81

Day 82-84

QA results for RUN15pp200trans day 82-84 are as follows.

Dead channels (total 30)

- detId 8: 5, 8, 9, 10, 28, 73,
- detId 9: 320, 474
- detId 10: 9, 47, 48, 56, 154, 176, 198, 199, 203, 204, 210, 212, 215, 232
- detId 11: 58, 80, 118, 198, 225, 235, 281, 287

Bad channels (total 25)

- detId 8: 221, 371, 449, 474, 483, 522, 523, 528, 566
- detId 9: 35
- detId 10: 59, 60, 164, 206, 207, 208, 209, 262
- detId 11: 38, 205, 209, 210, 232, 241, 258

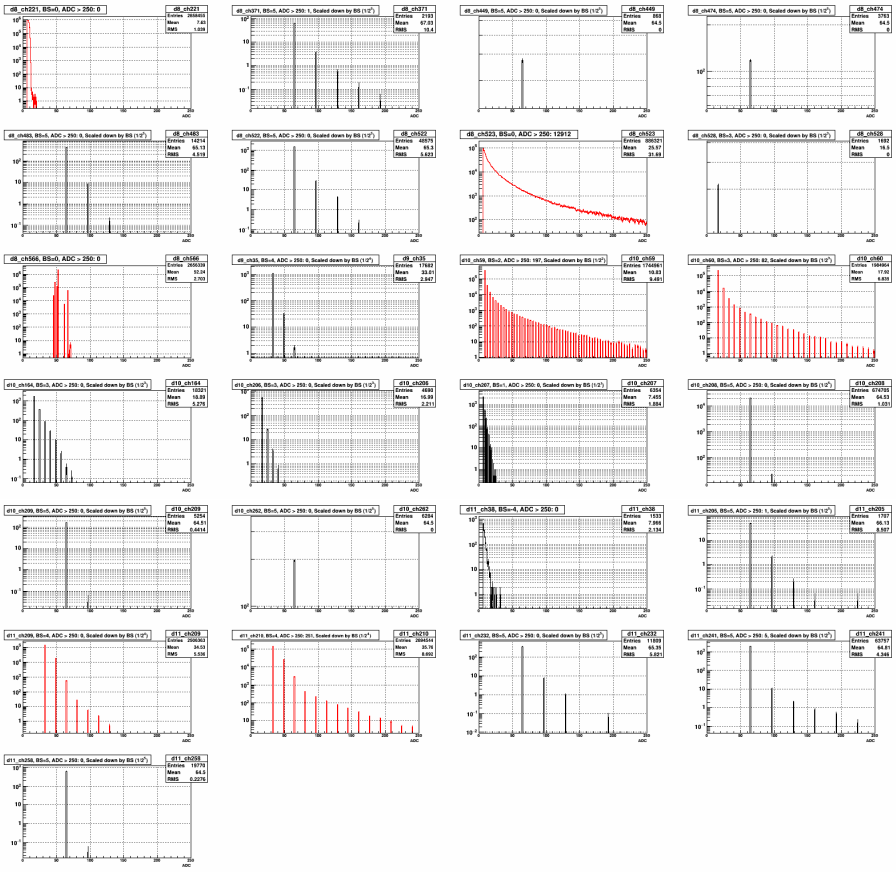

Figure A.7: Bad channels' ADC distribution, RUN15pp200trans, day 82-84

Day 85-86

QA results for RUN15pp200trans day 85-86 are as follows.

Dead channels (total 29)

- detId 8: 5, 8, 9, 10, 28, 73, 566
- detId 9: 474
- detId 10: 9, 47, 48, 56, 154, 176, 198, 199, 203, 204, 210, 212, 215, 232
- detId 11: 58, 80, 118, 198, 225, 281, 287

Bad channels (total 31)

- detId 8: 221, 371, 449, 474, 483, 522, 523, 528
- detId 9: 35, 220, 320
- detId 10: 44, 164, 206, 207, 208, 209, 246, 256, 262
- detId 11: 5, 38, 61, 205, 209, 210, 232, 235, 241, 258, 278

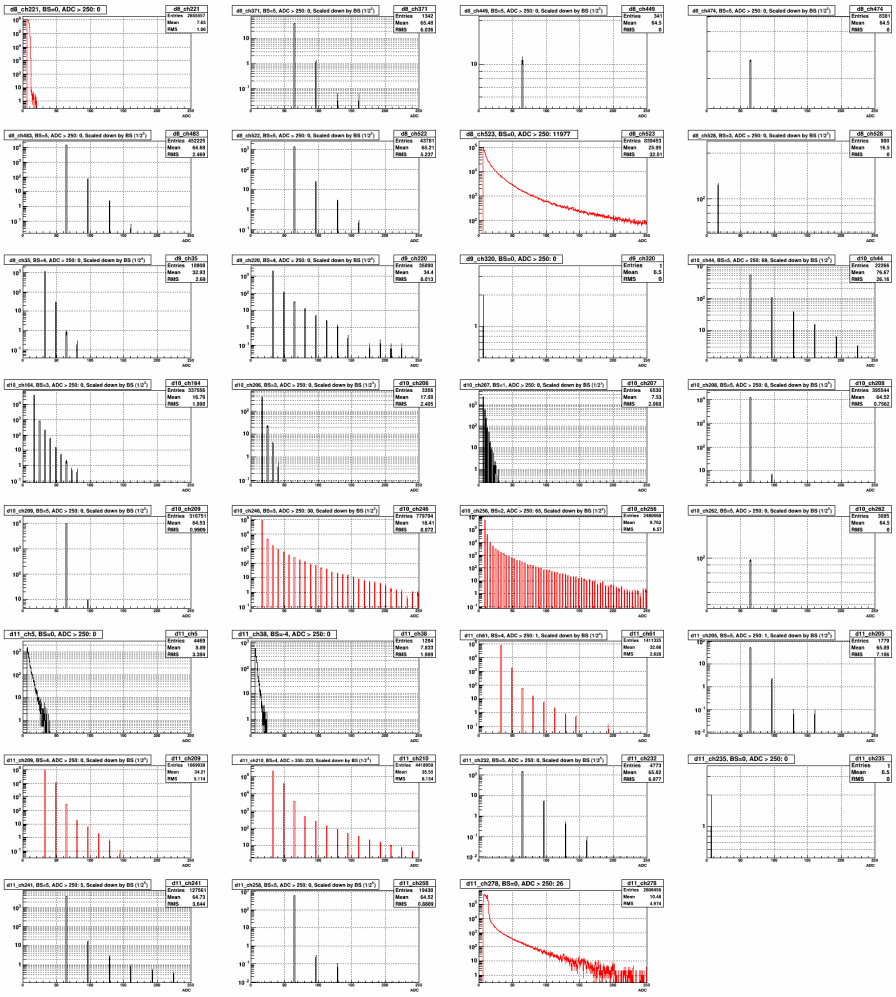

Figure A.8: Bad channels' ADC distribution, RUN15pp200trans, day 85-86

Day 87-88

QA results for RUN15pp200trans day 87-88 are as follows.

Dead channels (total 31)

- detId 8: 5, 8, 9, 10, 28, 73, 566
- detId 9: 320, 474
- detId 10: 9, 47, 48, 56, 154, 176, 198, 199, 203, 204, 210, 212, 215, 232
- detId 11: 58, 80, 118, 198, 225, 235, 281, 287

Bad channels (total 27)

- detId 8: 221, 371, 449, 474, 483, 522, 523, 528
- detId 9: 35, 37
- detId 10: 44, 59, 60, 164, 206, 207, 208, 209, 262
- detId 11: 5, 38, 205, 209, 210, 232, 241, 258

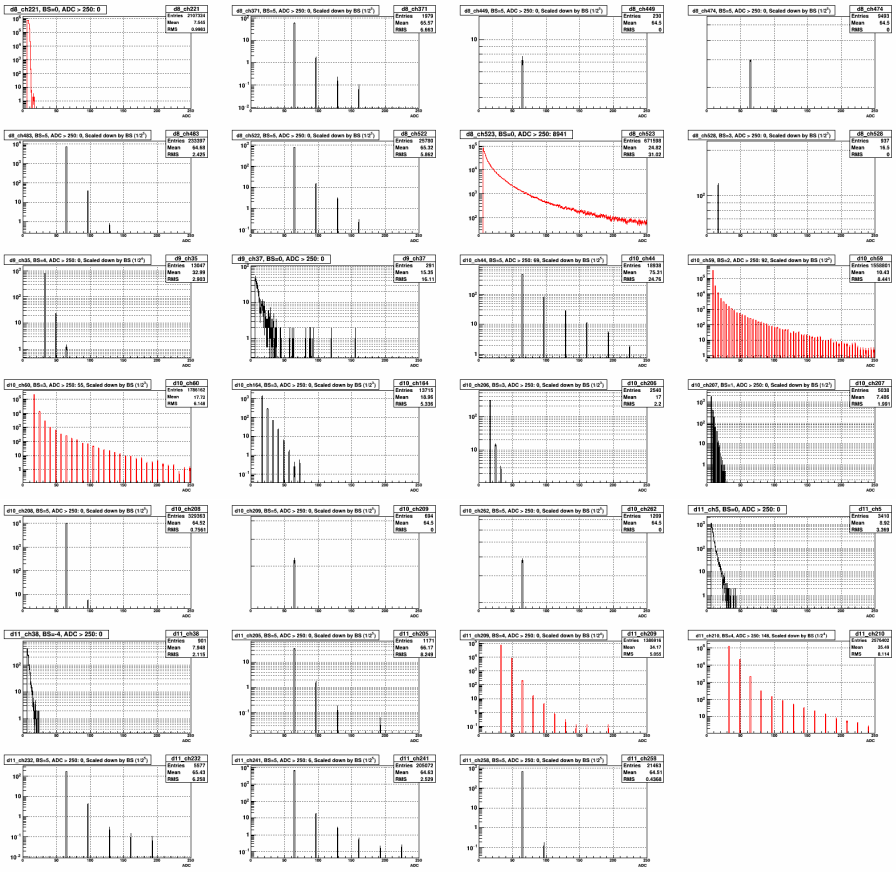

Figure A.9: Bad channels' ADC distribution, RUN15pp200trans, day 87-88

Day 89-90

QA results for RUN15pp200trans day 89-90 are as follows.

Dead channels (total 31)

- detId 8: 5, 8, 9, 10, 28, 73, 566
- detId 9: 37, 474
- detId 10: 9, 47, 48, 56, 154, 176, 198, 199, 203, 204, 210, 212, 215, 232
- detId 11: 58, 80, 118, 198, 225, 235, 281, 287

Bad channels (total 25)

- detId 8: 221, 371, 449, 474, 483, 522, 523, 528
- detId 9: 35, 320
- detId 10: 59, 60, 164, 206, 207, 208, 209, 262
- detId 11: 5, 38, 205, 209, 210, 241, 258

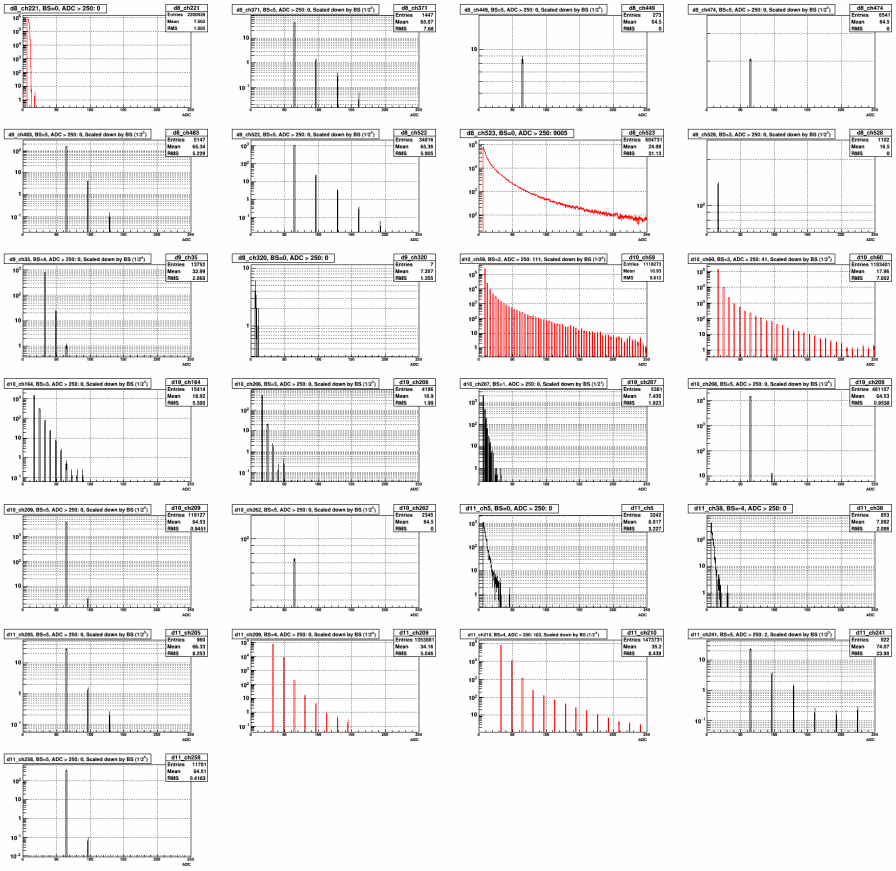

Figure A.10: Bad channels' ADC distribution, RUN15pp200trans, day 89-90

Day 91-93

QA results for RUN15pp200trans day 91-93 are as follows.

Dead channels (total 30)

- detId 8: 5, 8, 9, 10, 28, 73, 566
- detId 9: 474
- detId 10: 9, 47, 48, 56, 154, 176, 198, 199, 203, 204, 210, 212, 215, 232
- detId 11: 58, 80, 118, 198, 225, 235, 281, 287

Bad channels (total 25)

- detId 8: 221, 371, 449, 474, 483, 522, 528
- detId 9: 35, 37, 88, 320
- detId 10: 164, 206, 207, 208, 209, 262
- detId 11: 5, 38, 201, 205, 209, 210, 241, 258

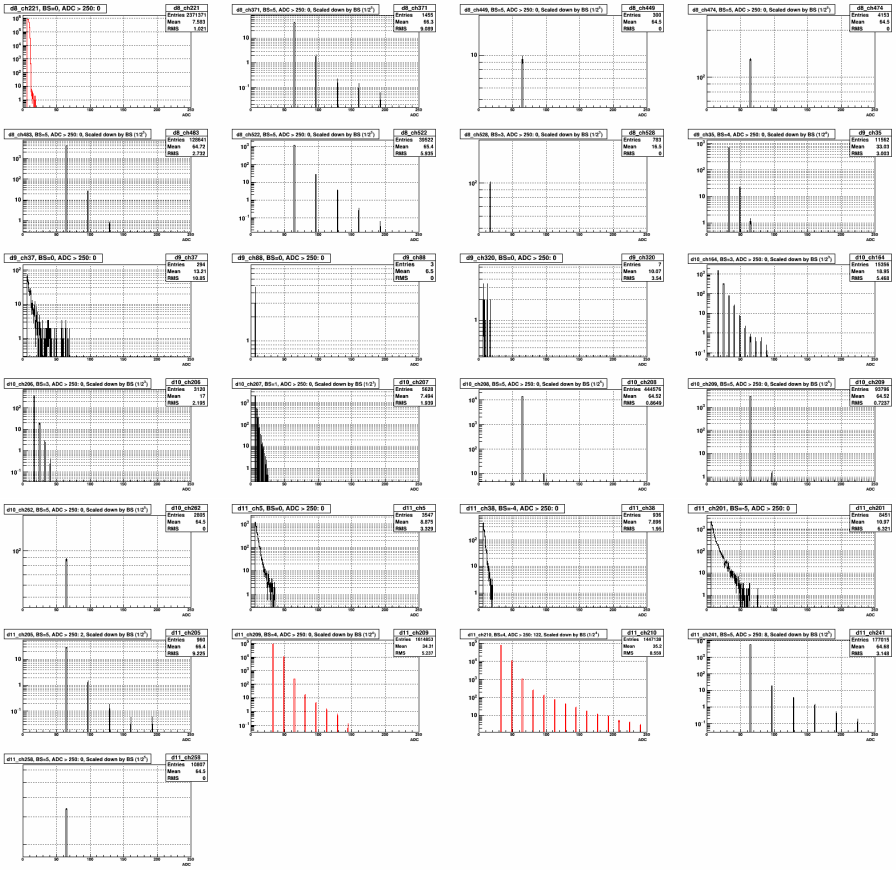

Figure A.11: Bad channels' ADC distribution, RUN15pp200trans, day 91-93

A.2 Mass vs. pairE, mass vs. Zgg, and Points' XY

Day 66-69

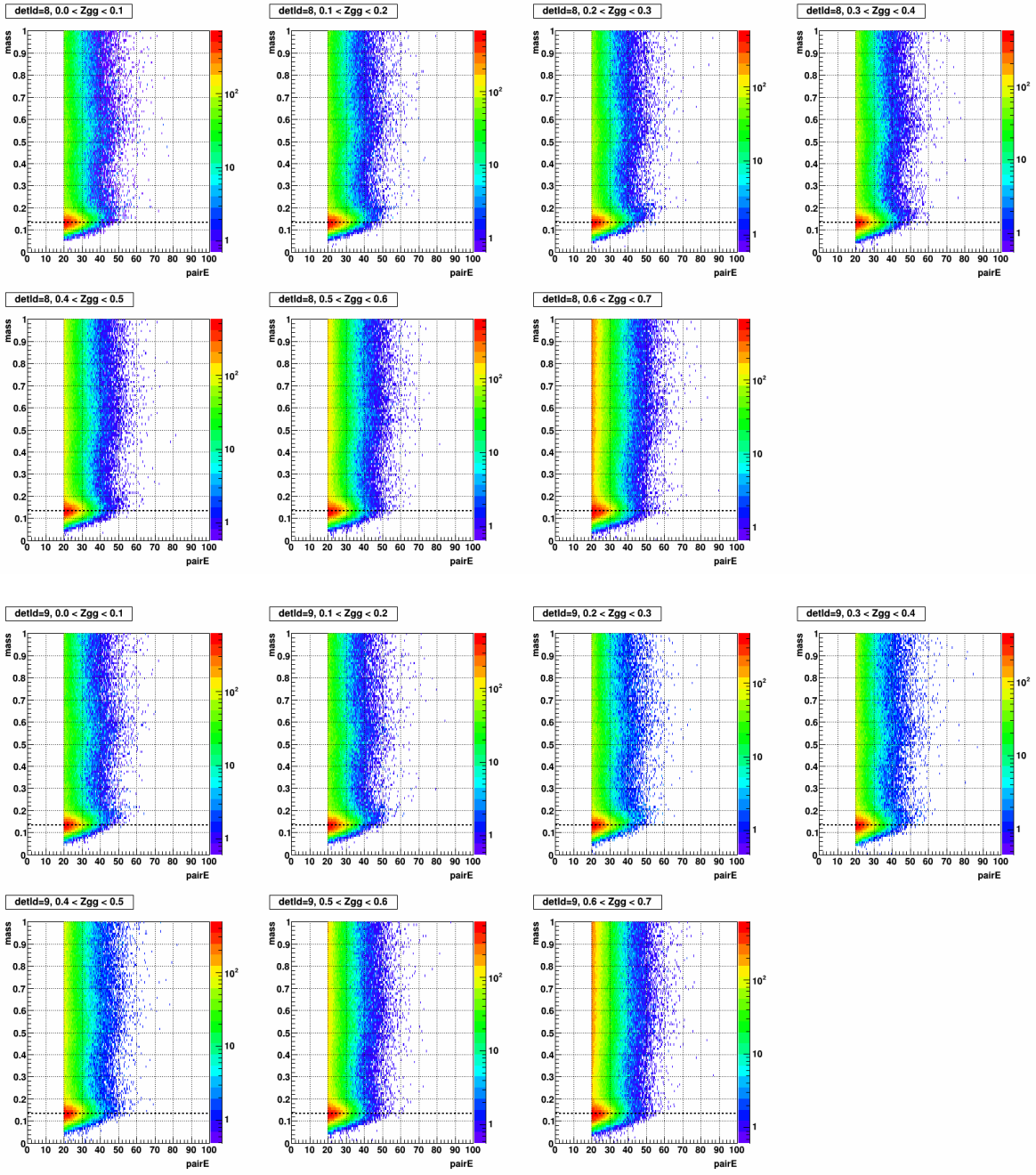

Figure A.12: Mass vs. pairE, separated by Zgg in the stepwidth of 0.1, for detId 8 (top 7) and detId 9 (bottom 7), day 66-69. All plots were obtained with calibration condition in section 2.2.3.

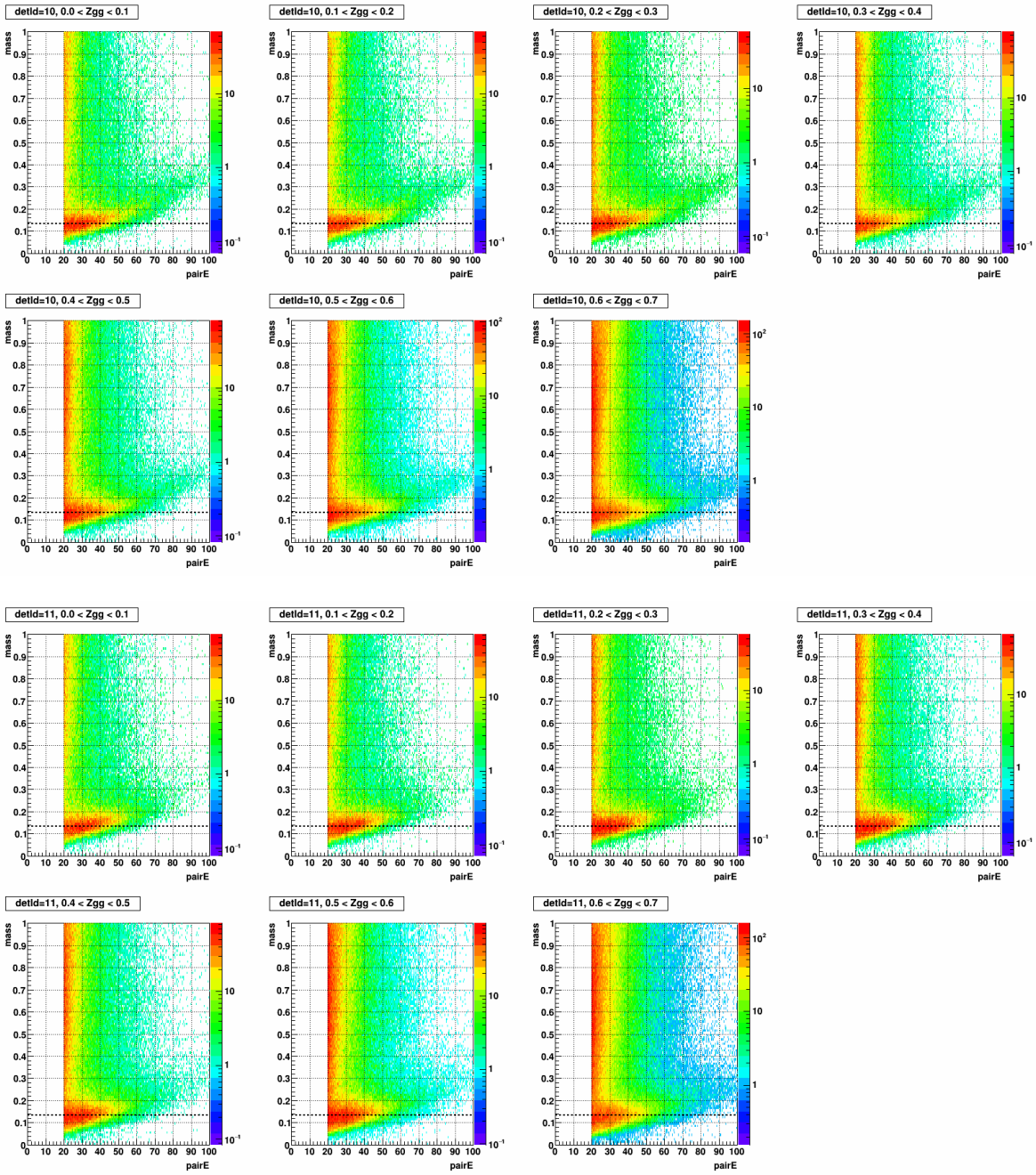

Figure A.13: Mass vs. pairE, separated by Zgg in the stepwidth of 0.1, for detId 10 (top 7) and detId 11 (bottom 7) day 66-69

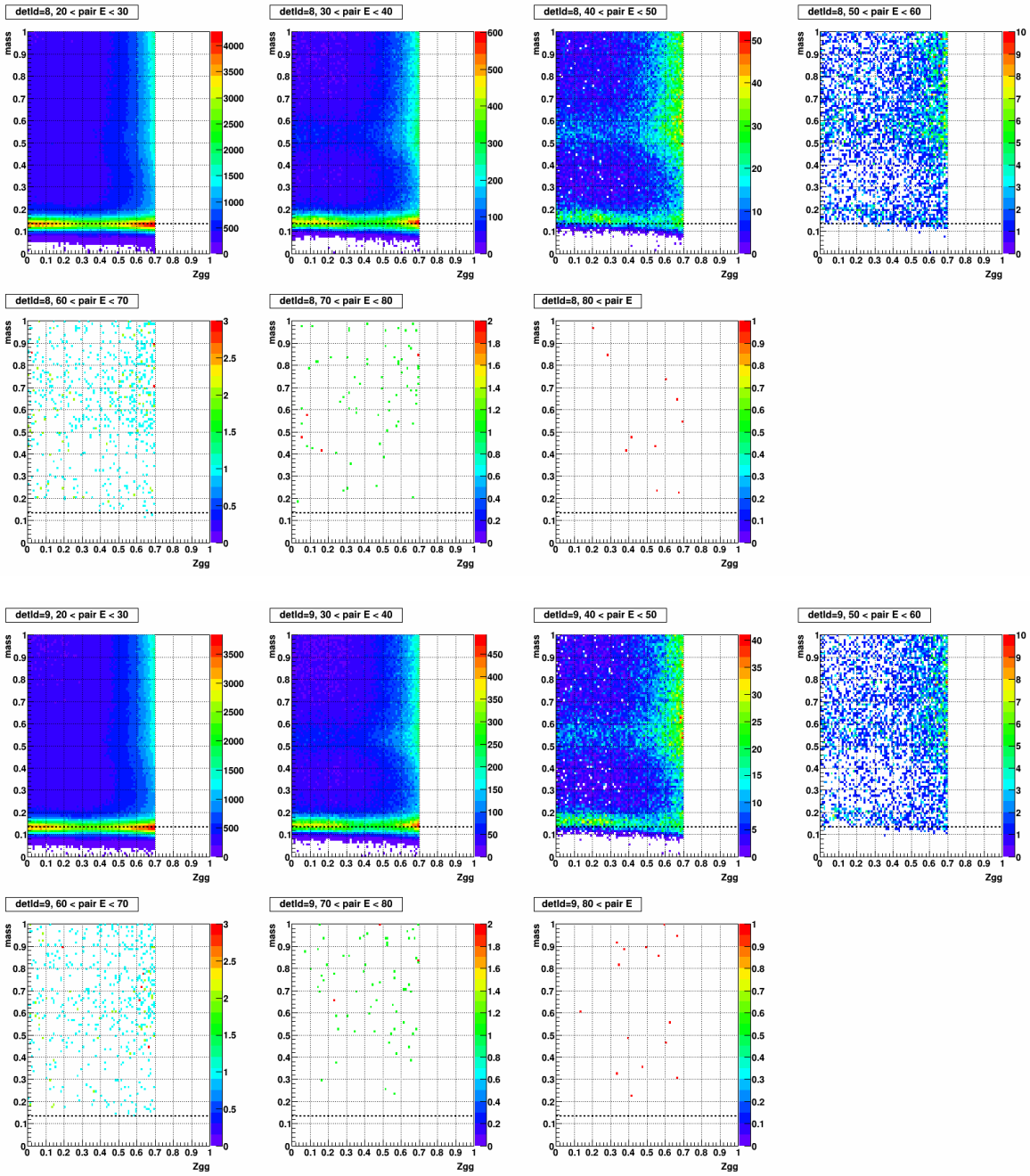

Figure A.14: Mass vs. Zgg, separated by pairE in the stepwidth of 10 (GeV), for detId 8 (top 7) and detId 9 (bottom 7), day 66-69

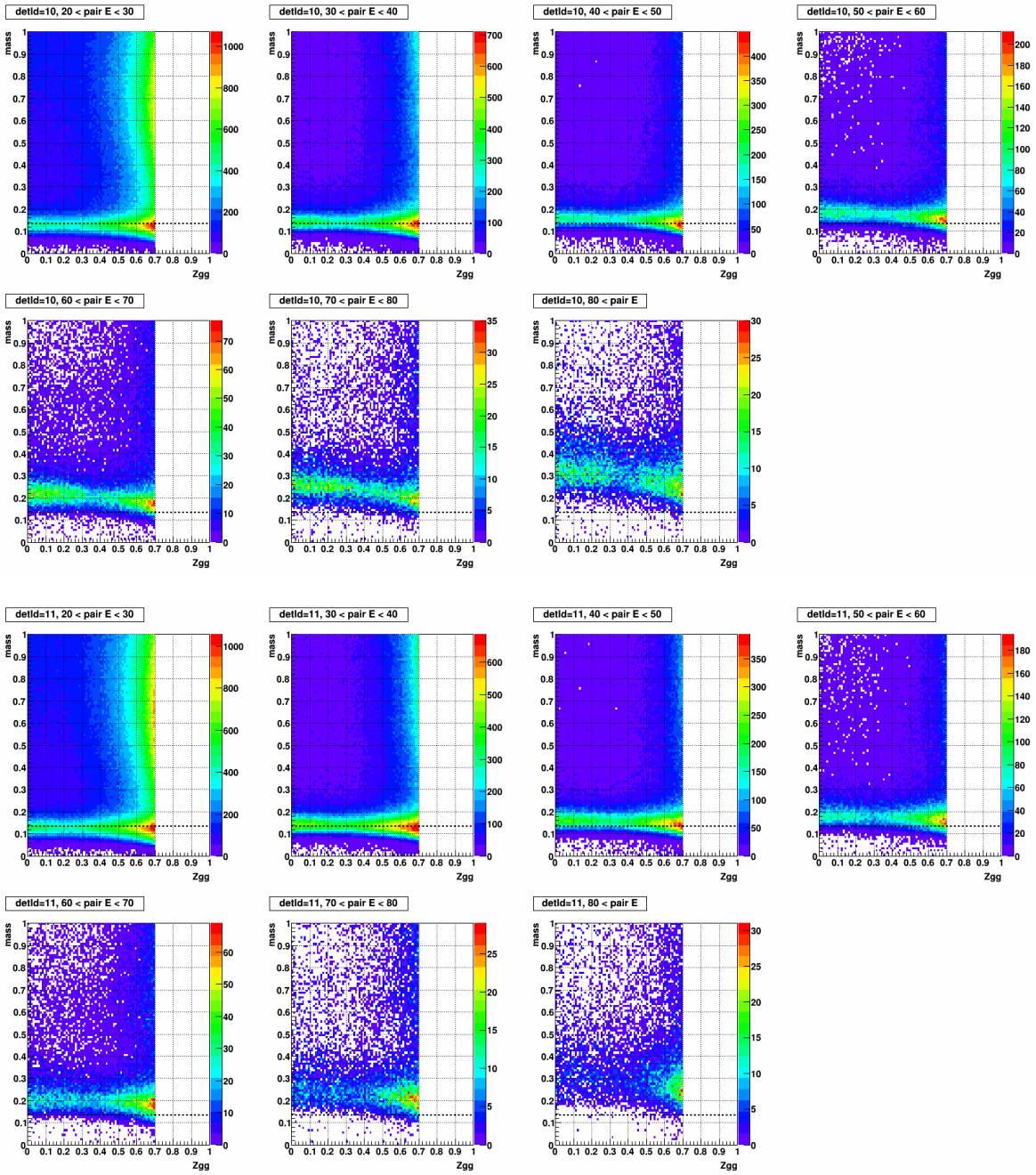

Figure A.15: Mass vs. Zgg, separated by pairE in the stepwidth of 10 (GeV), for detId 10 (top 7) and detId 11 (bottom 7), day 66-69

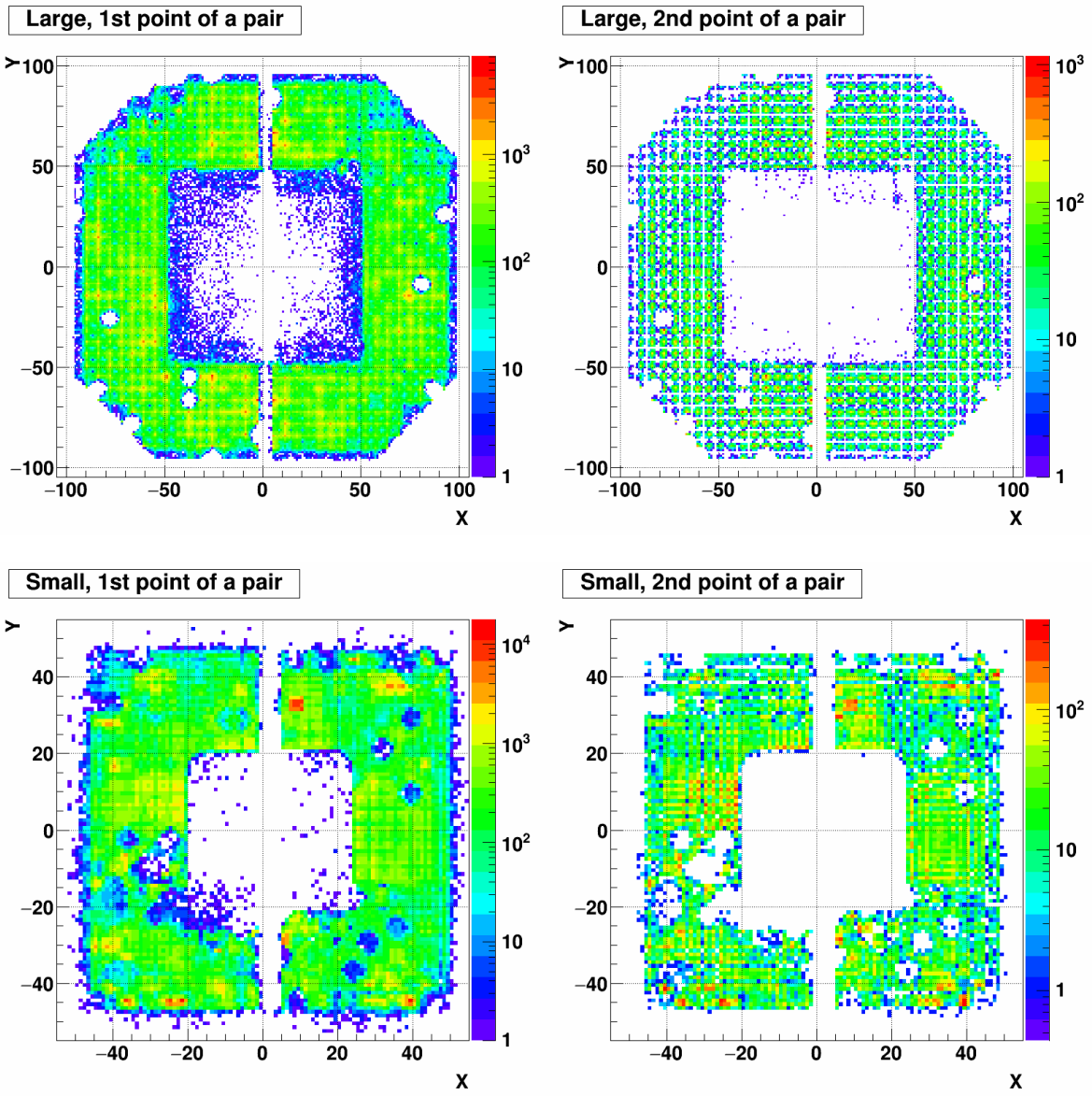

Figure A.16: XY distribution of 1st (left) and 2nd (right) point of a pair. Top row shows the large cells and Bottom row shows the small cells. The period is day 66-69.

Day 69-73

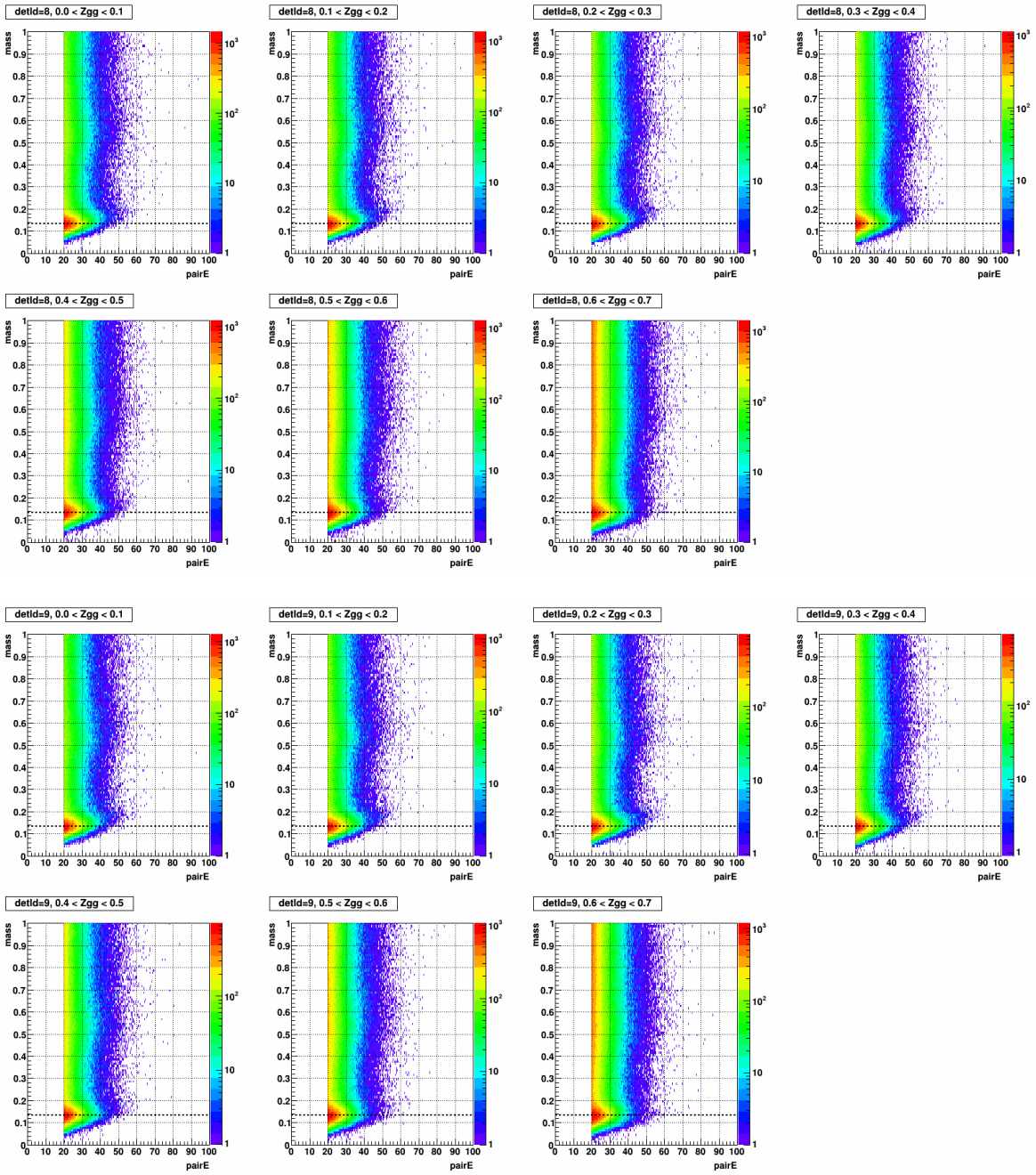

Figure A.17: Mass vs. pairE, separated by Zgg in the stepwidth of 0.1, for detId 8 (top 7) and detId 9 (bottom 7), day 69-73

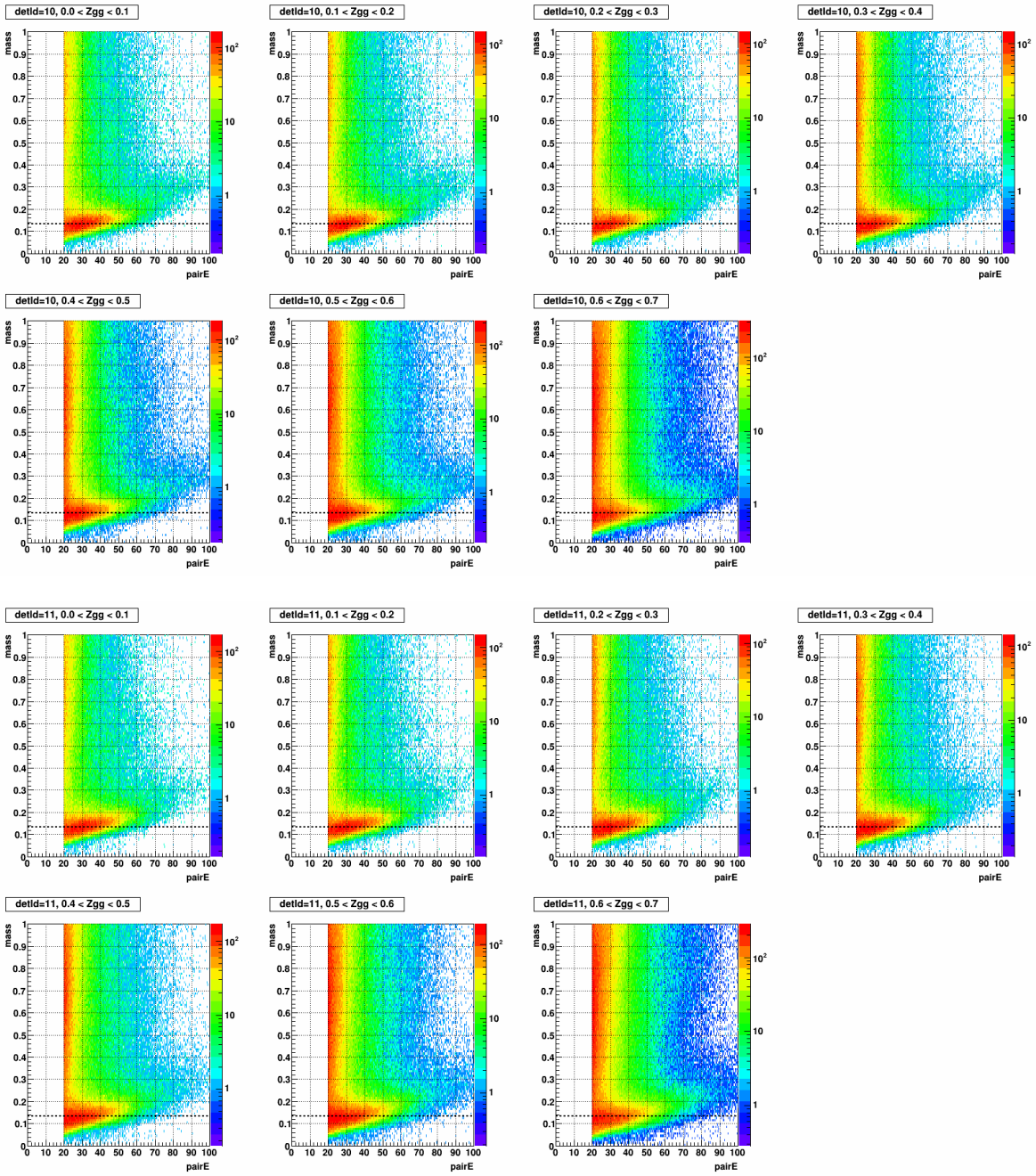

Figure A.18: Mass vs. pairE, separated by Zgg in the stepwidth of 0.1, for detId 10 (top 7) and detId 11 (bottom 7) day 69-73

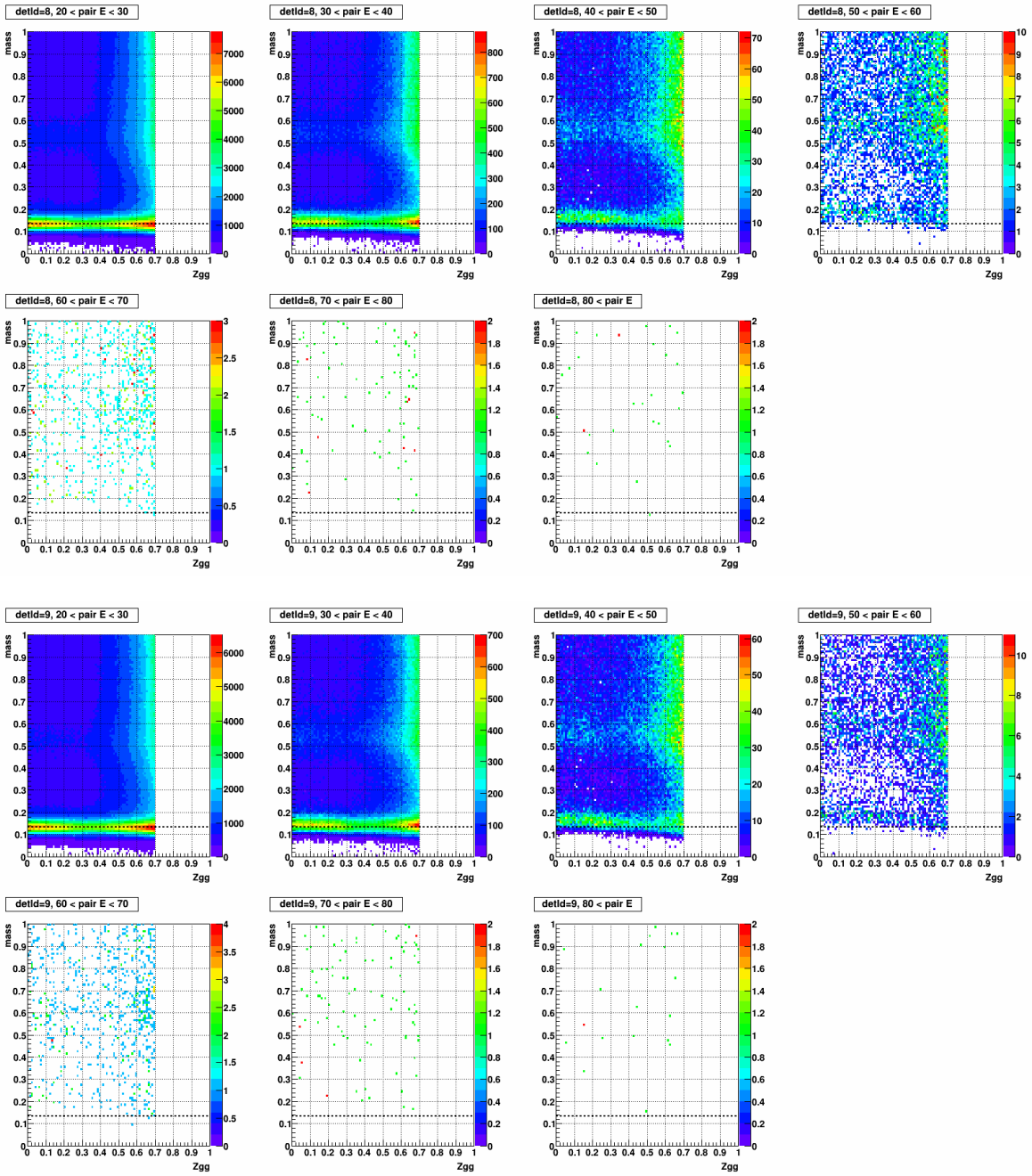

Figure A.19: Mass vs. Zgg, separated by pairE in the stepwidth of 10 (GeV), for detId 8 (top 7) and detId 9 (bottom 7), day 69-73

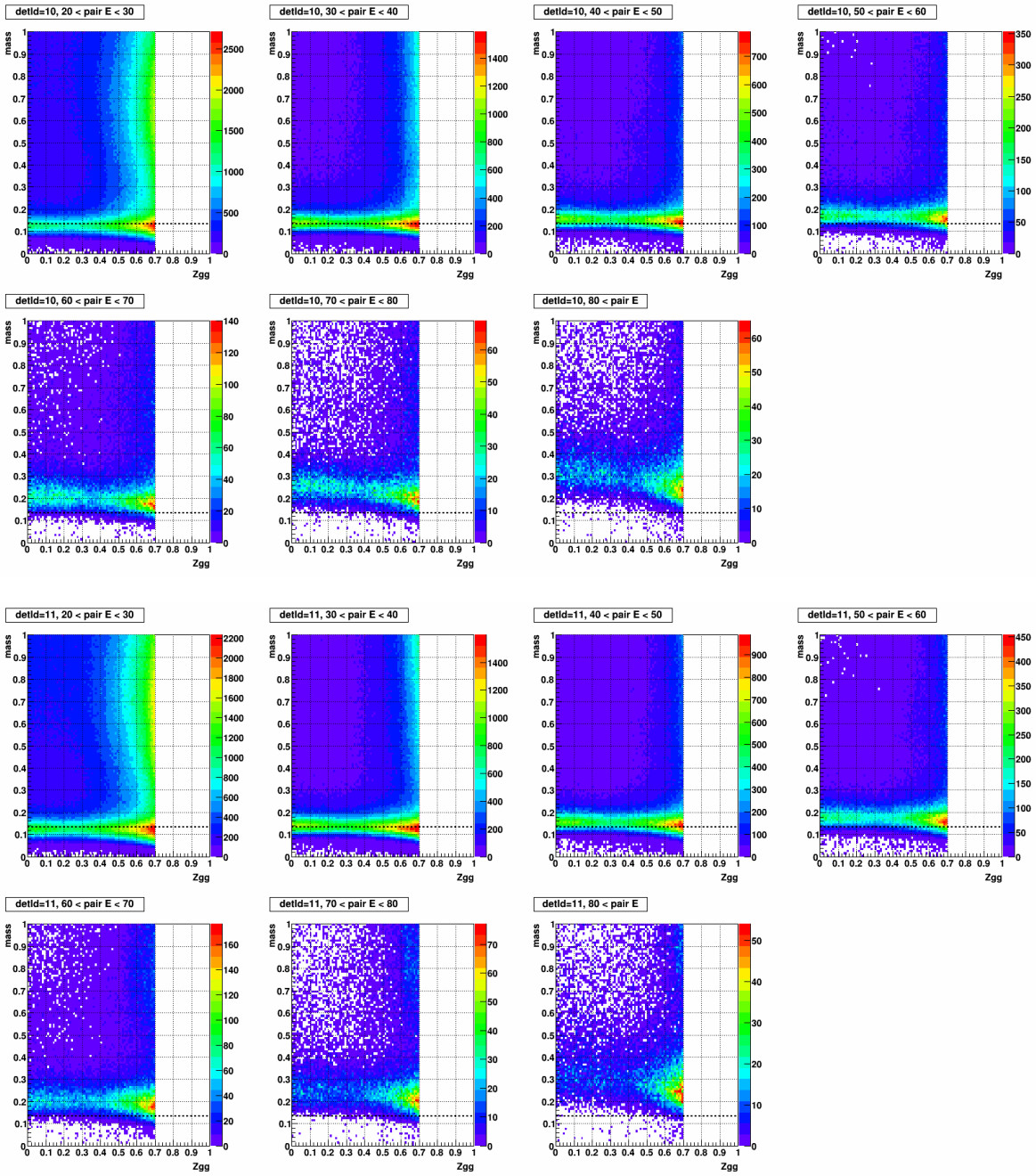

Figure A.20: Mass vs. Zgg, separated by pairE in the stepwidth of 10 (GeV), for detId 10 (top 7) and detId 11 (bottom 7), day 69-73

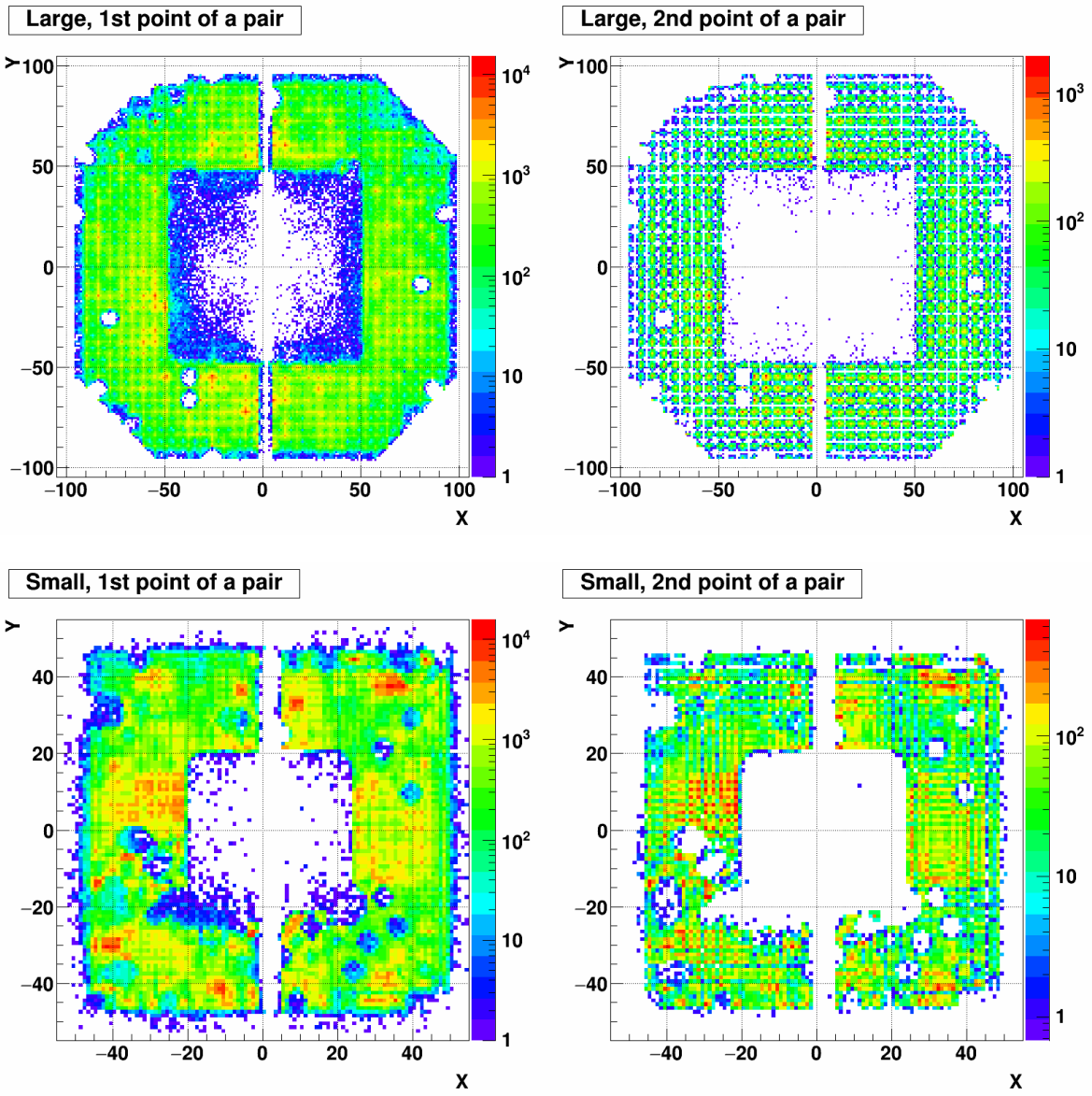

Figure A.21: XY distribution of 1st (left) and 2nd (right) point of a pair. Top row shows the large cells and Bottom row shows the small cells. The period is day 69-73.

Day 77-79

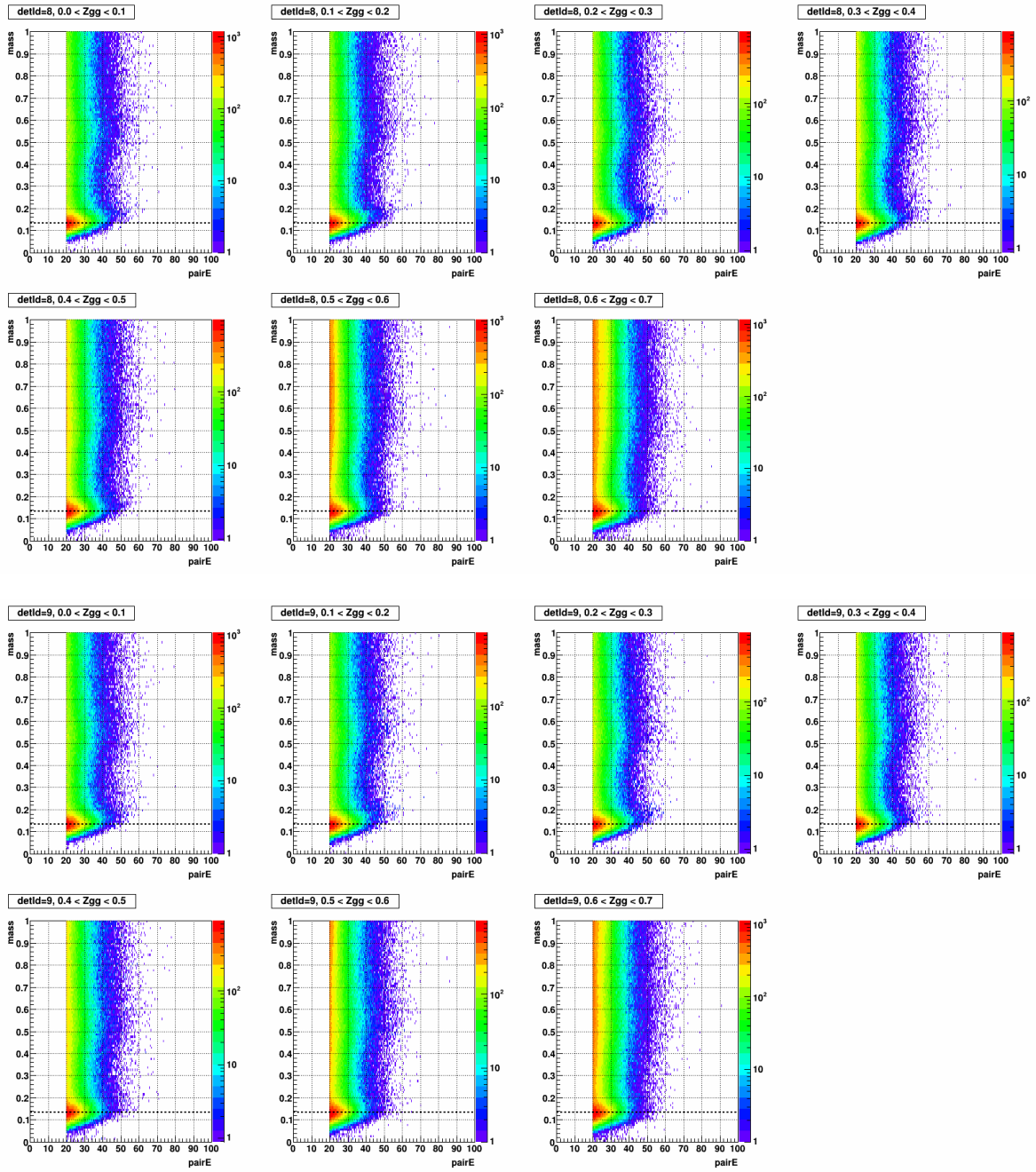

Figure A.22: Mass vs. pairE, separated by Zgg in the stepwidth of 0.1, for detId 8 (top 7) and detId 9 (bottom 7), day 77-79

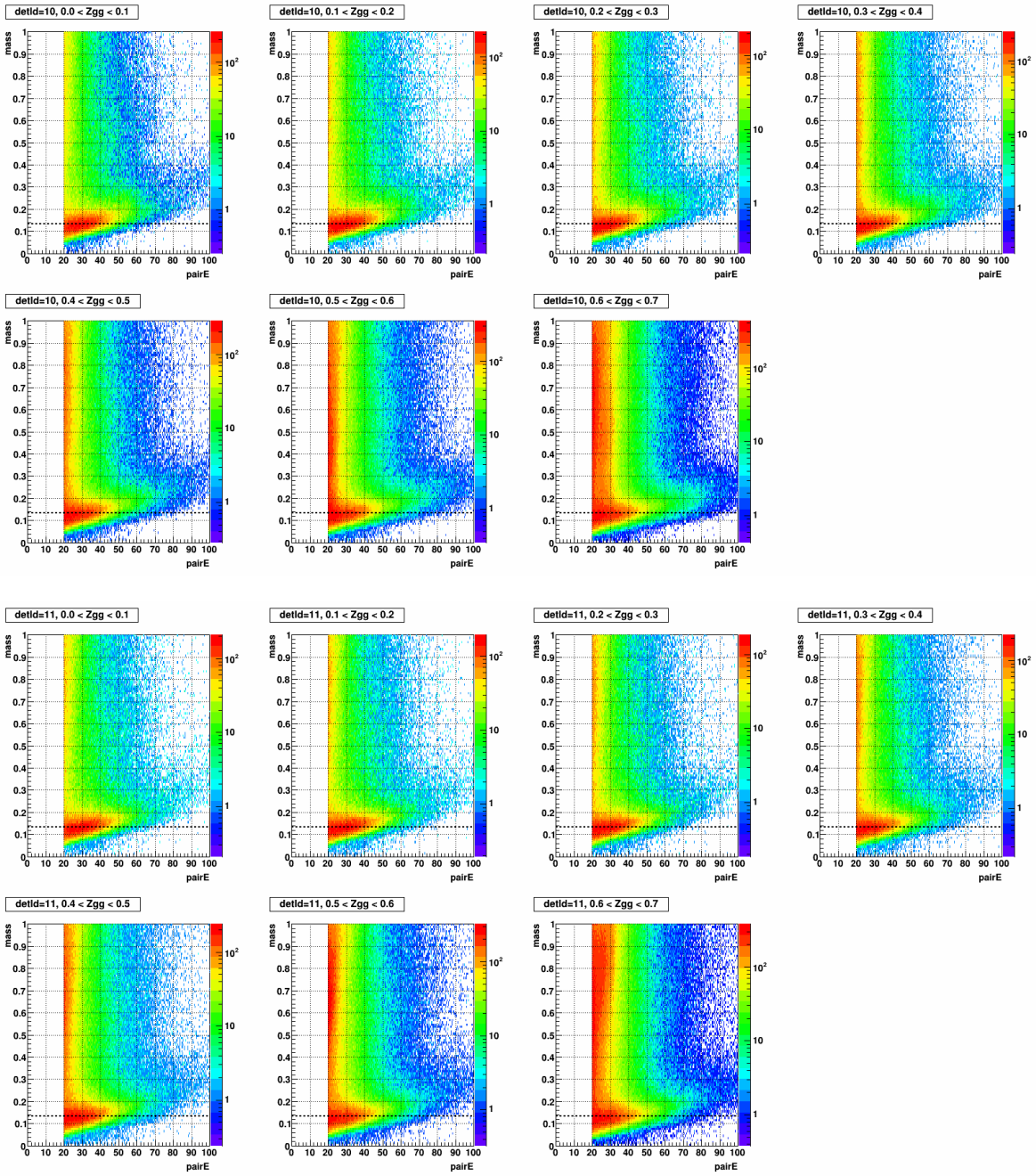

Figure A.23: Mass vs. pairE, separated by Zgg in the stepwidth of 0.1, for detId 10 (top 7) and detId 11 (bottom 7) day 77-79

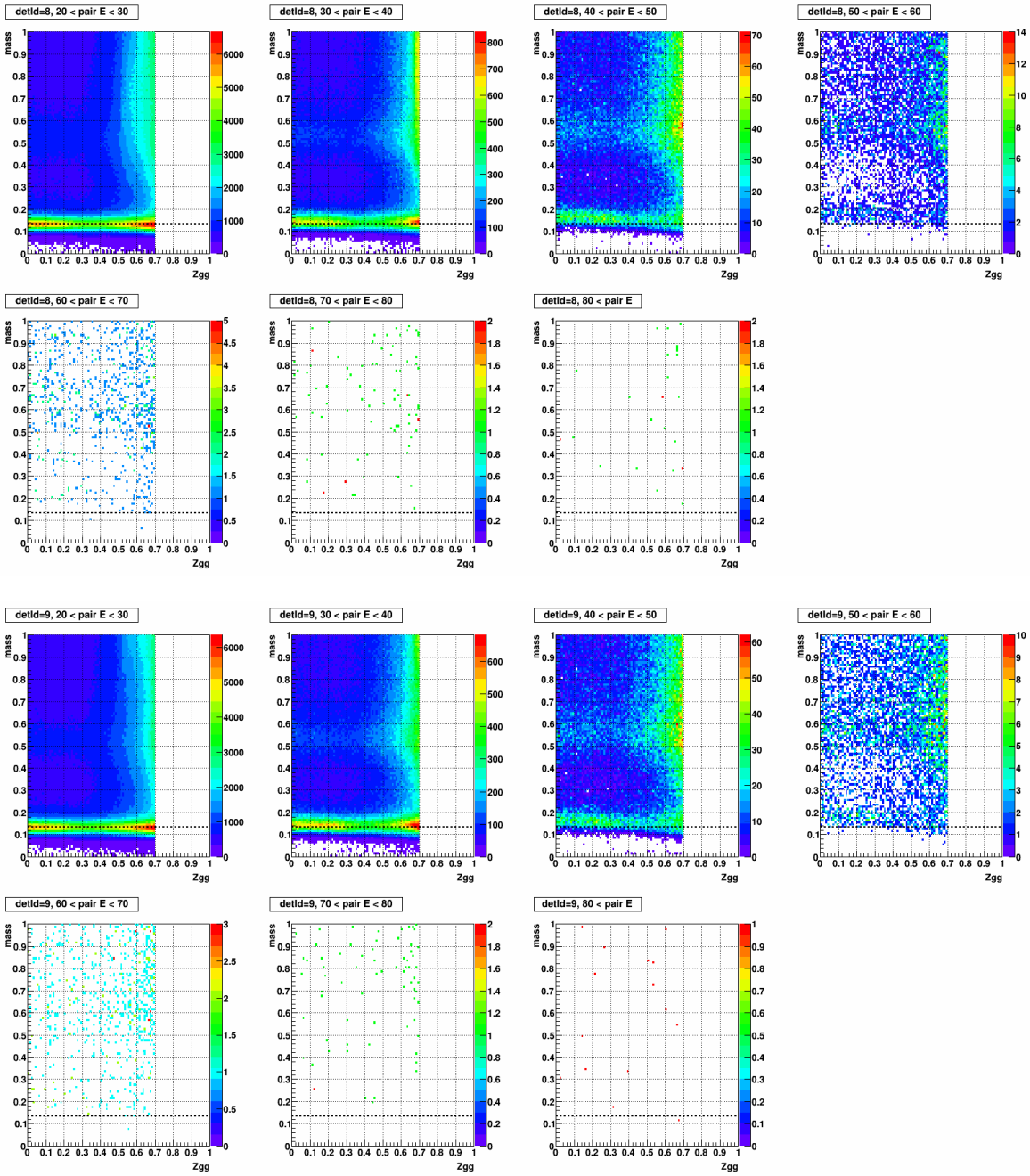

Figure A.24: Mass vs. Zgg, separated by pairE in the stepwidth of 10 (GeV), for detId 8 (top 7) and detId 9 (bottom 7), day 77-79

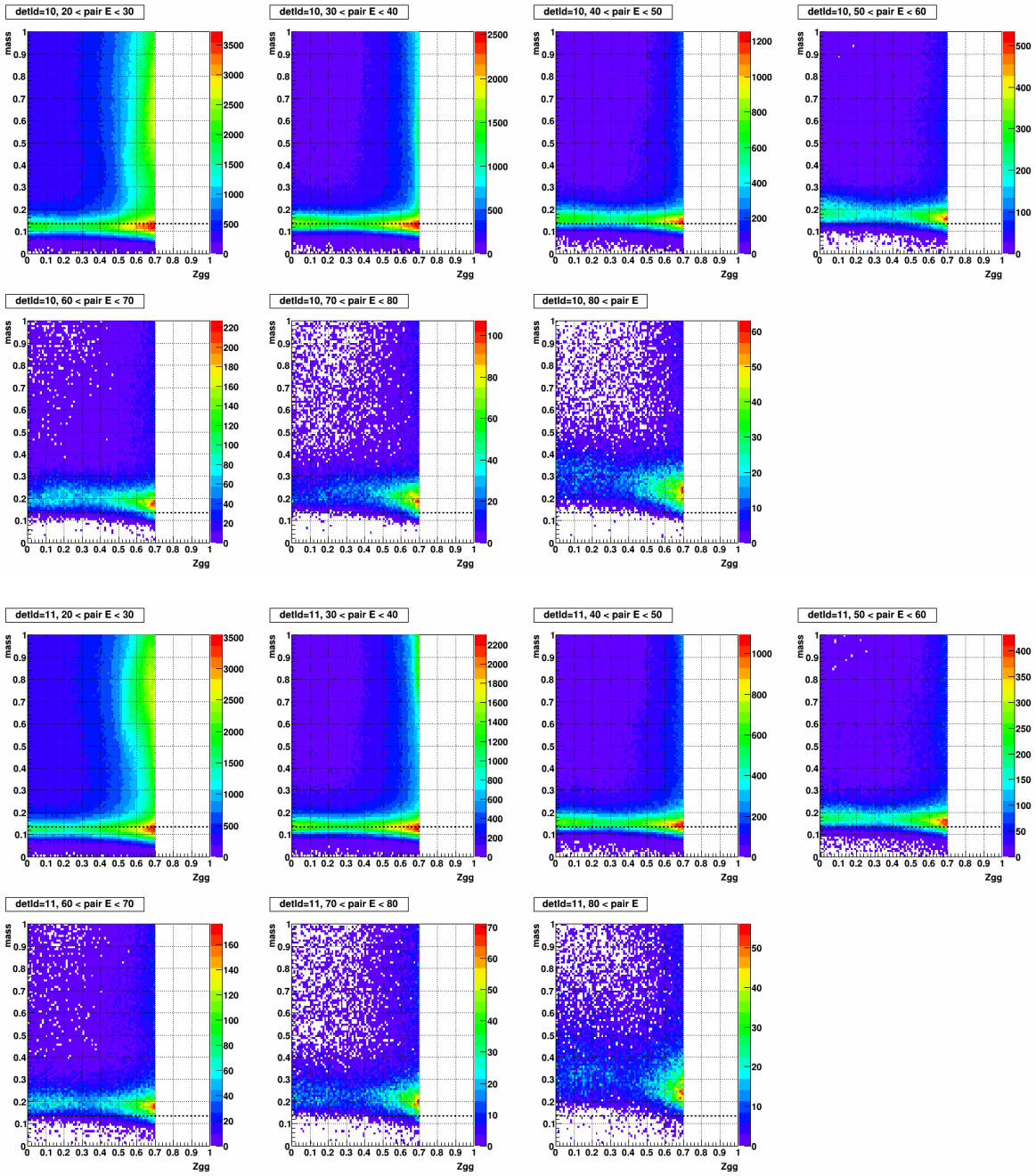

Figure A.25: Mass vs. Zgg, separated by pairE in the stepwidth of 10 (GeV), for detId 10 (top 7) and detId 11 (bottom 7), day 77-79

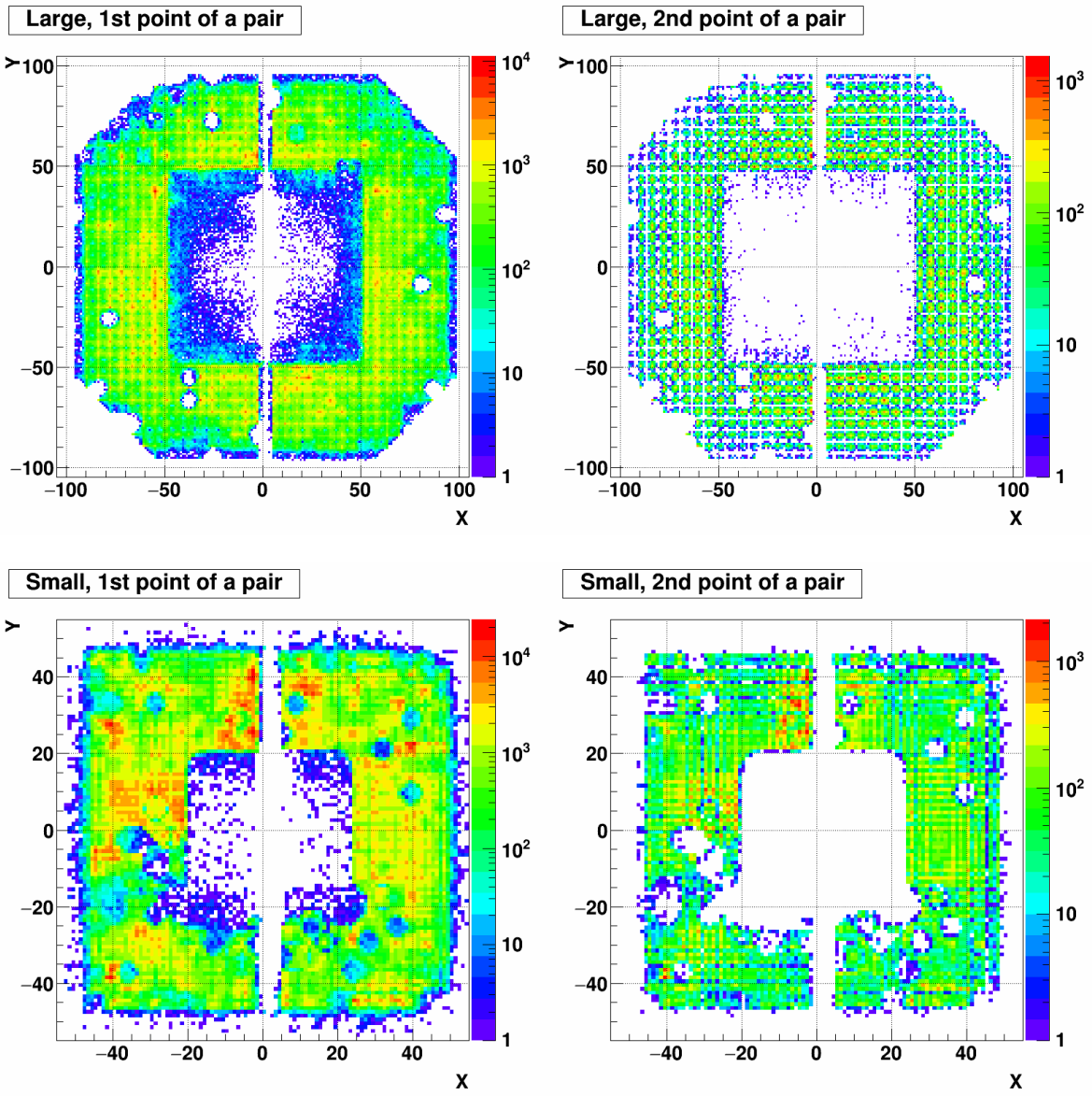

Figure A.26: XY distribution of 1st (left) and 2nd (right) point of a pair. Top row shows the large cells and Bottom row shows the small cells. The period is day 77-79.

Day 80-81

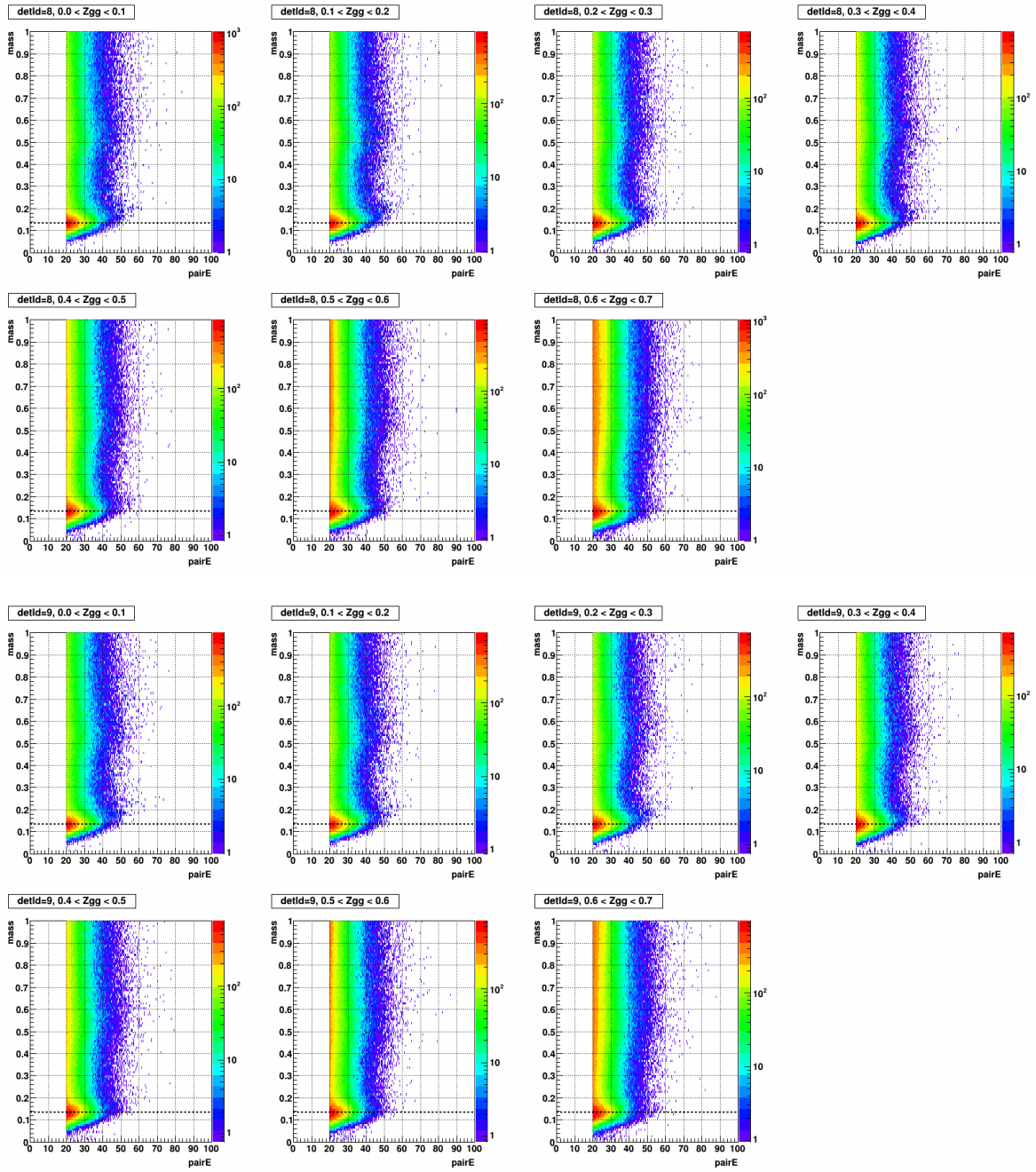

Figure A.27: Mass vs. pairE, separated by Zgg in the stepwidth of 0.1, for detId 8 (top 7) and detId 9 (bottom 7), day 80-81

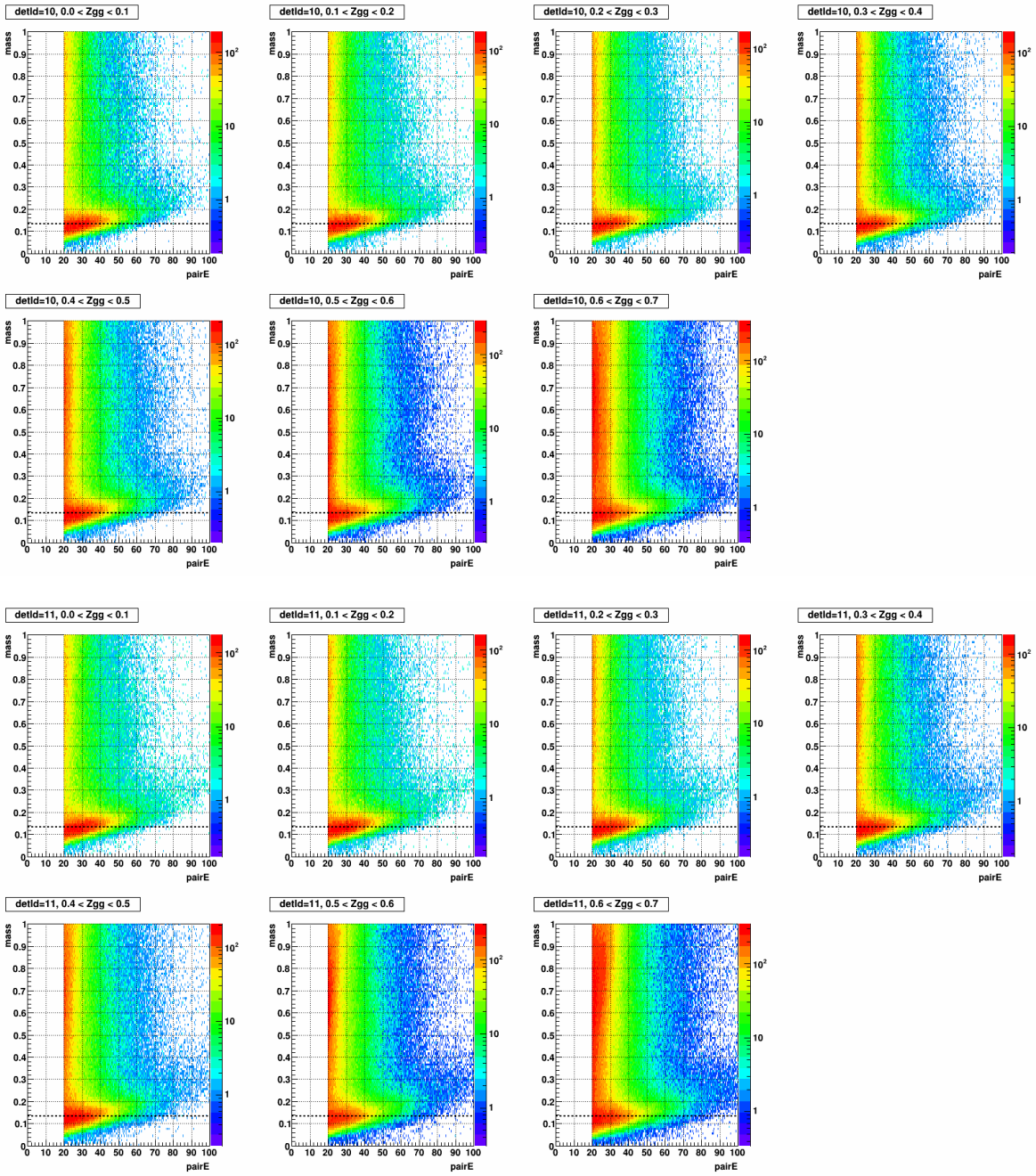

Figure A.28: Mass vs. pairE, separated by Zgg in the stepwidth of 0.1, for detId 10 (top 7) and detId 11 (bottom 7) day 80-81

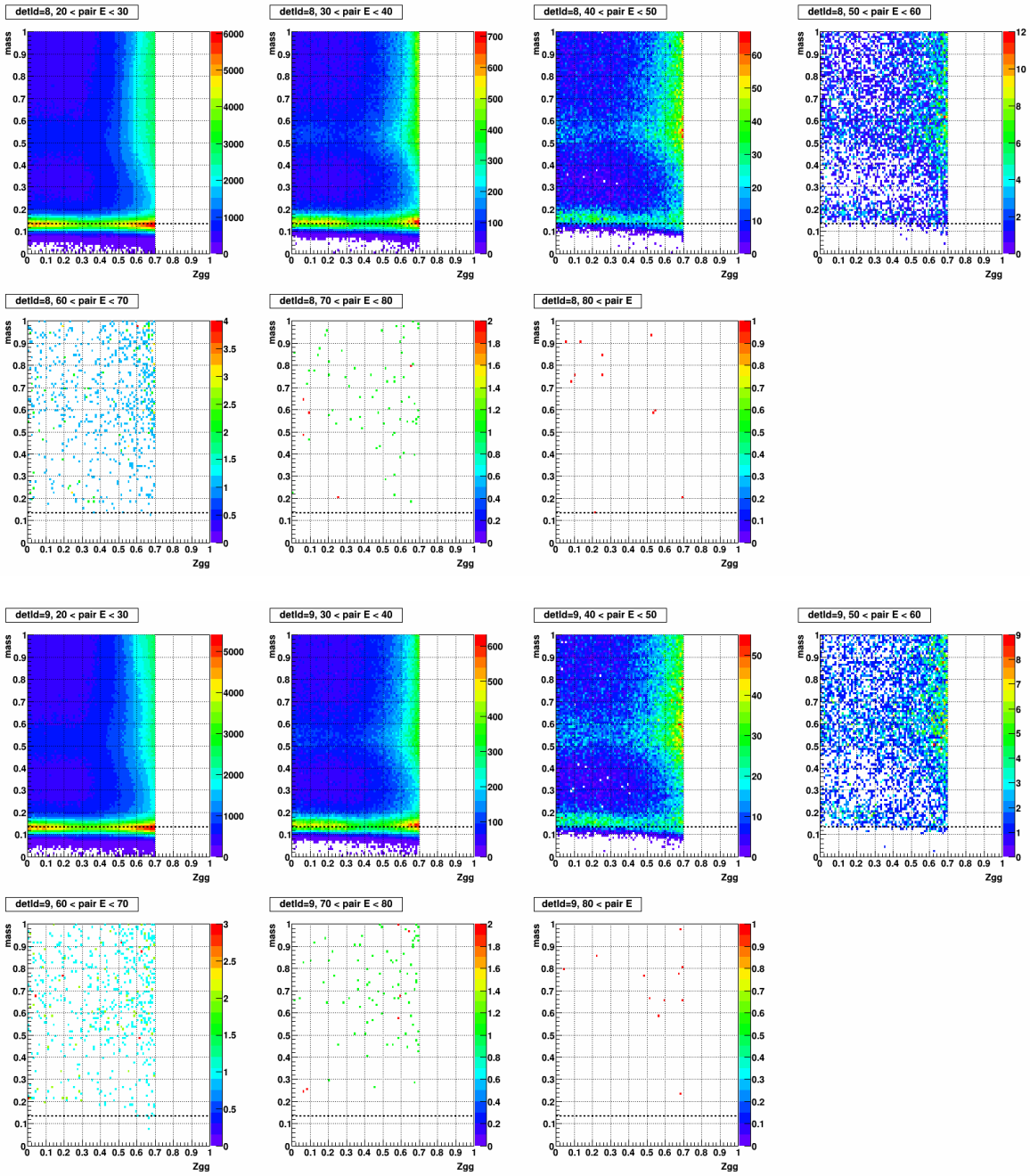

Figure A.29: Mass vs. Zgg, separated by pairE in the stepwidth of 10 (GeV), for detId 8 (top 7) and detId 9 (bottom 7), day 80-81

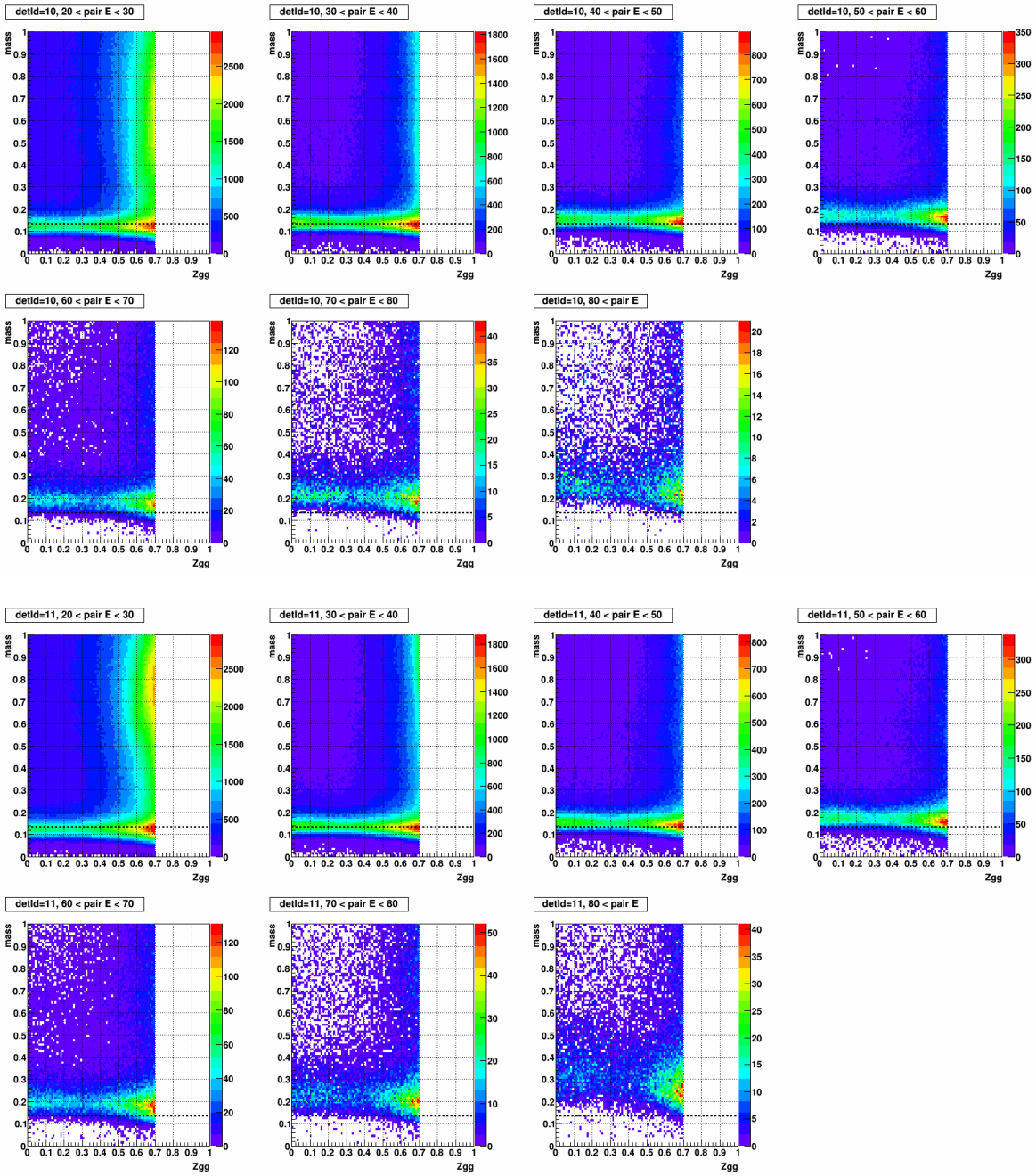

Figure A.30: Mass vs. Zgg, separated by pairE in the stepwidth of 10 (GeV), for detId 10 (top 7) and detId 11 (bottom 7), day 80-81

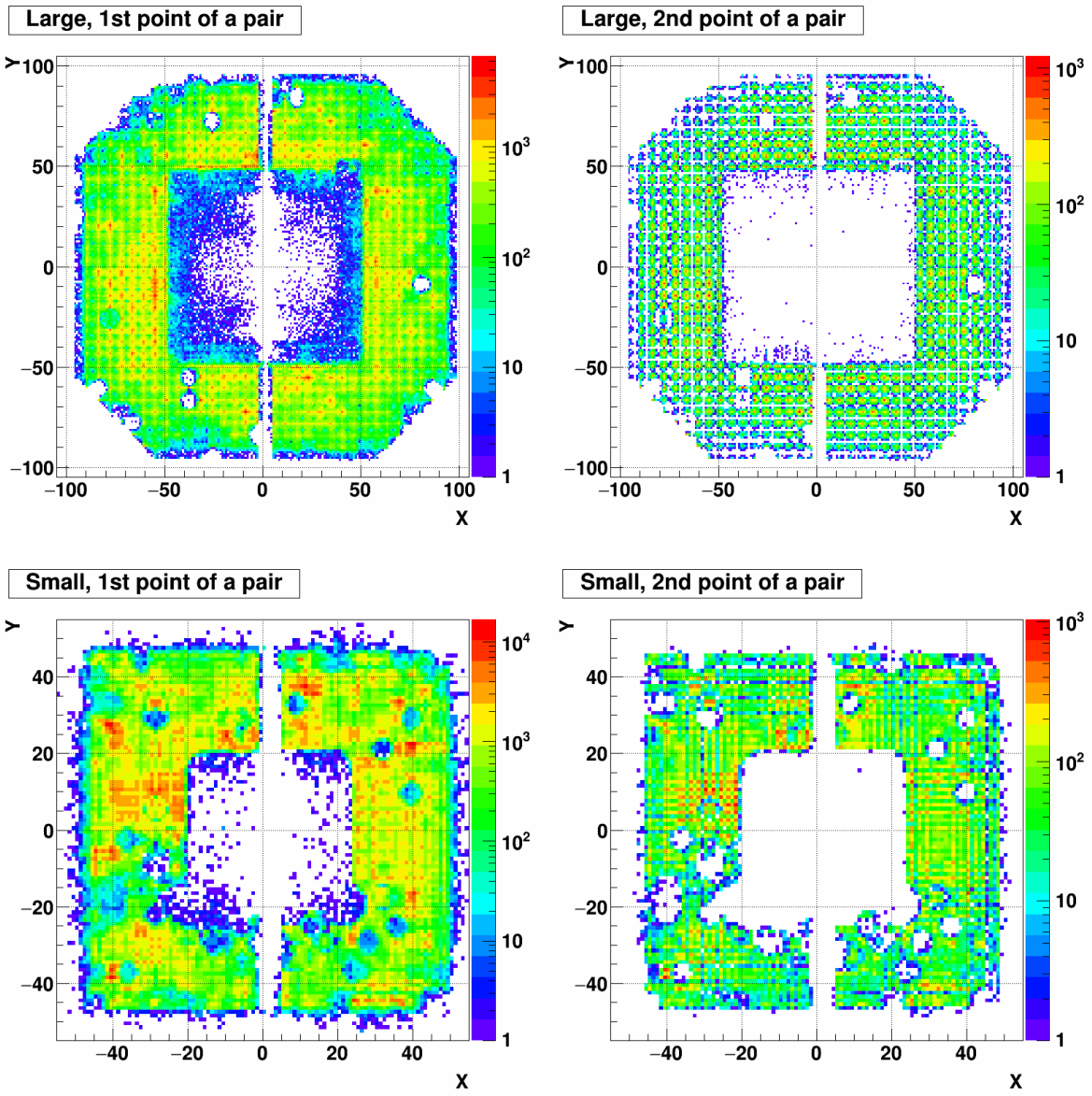

Figure A.31: XY distribution of 1st (left) and 2nd (right) point of a pair. Top row shows the large cells and Bottom row shows the small cells. The period is day 80-81.

Day 82-84

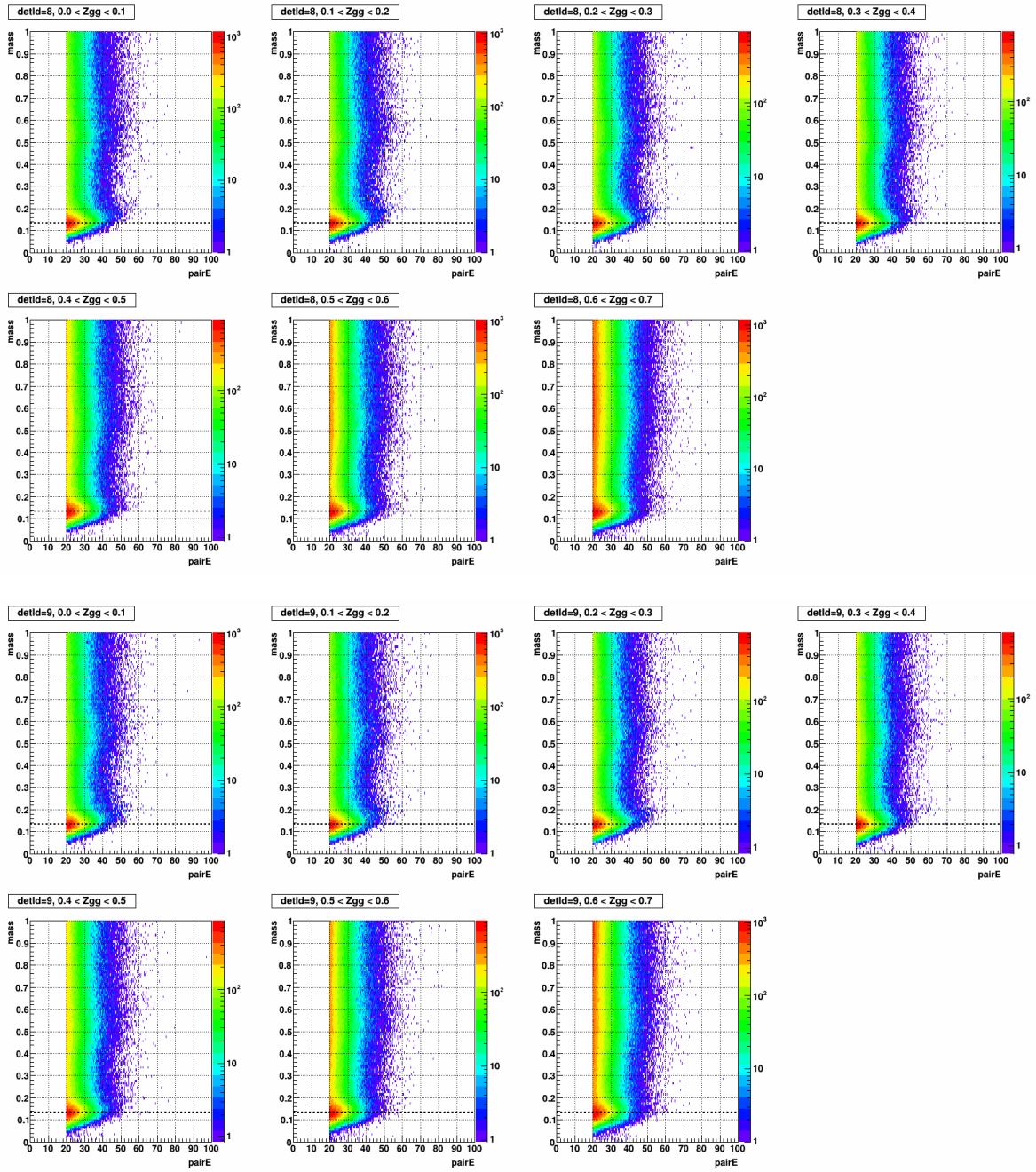

Figure A.32: Mass vs. pairE, separated by Zgg in the stepwidth of 0.1, for detId 8 (top 7) and detId 9 (bottom 7), day 82-84

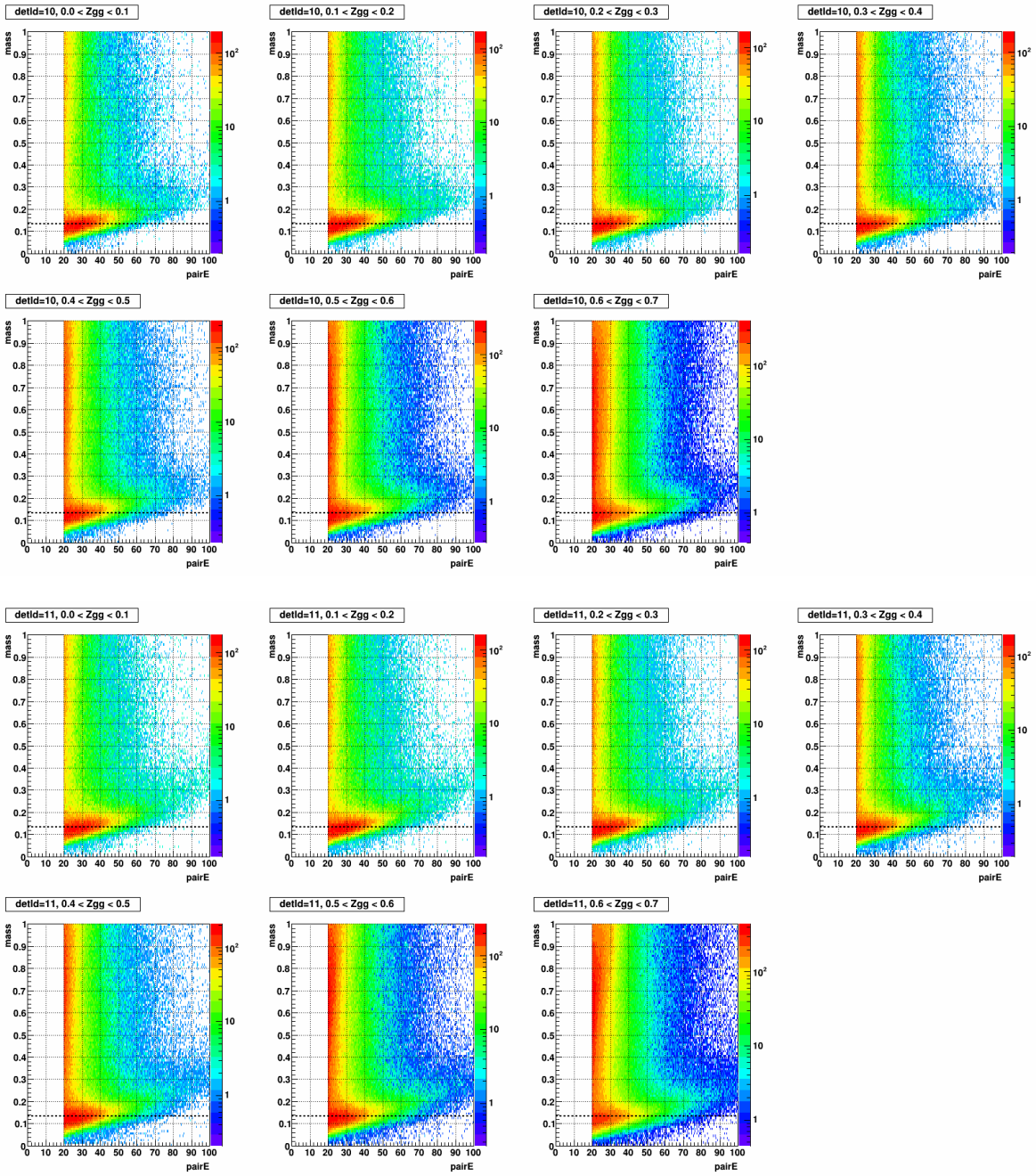

Figure A.33: Mass vs. pairE, separated by Zgg in the stepwidth of 0.1, for detId 10 (top 7) and detId 11 (bottom 7) day 82-84

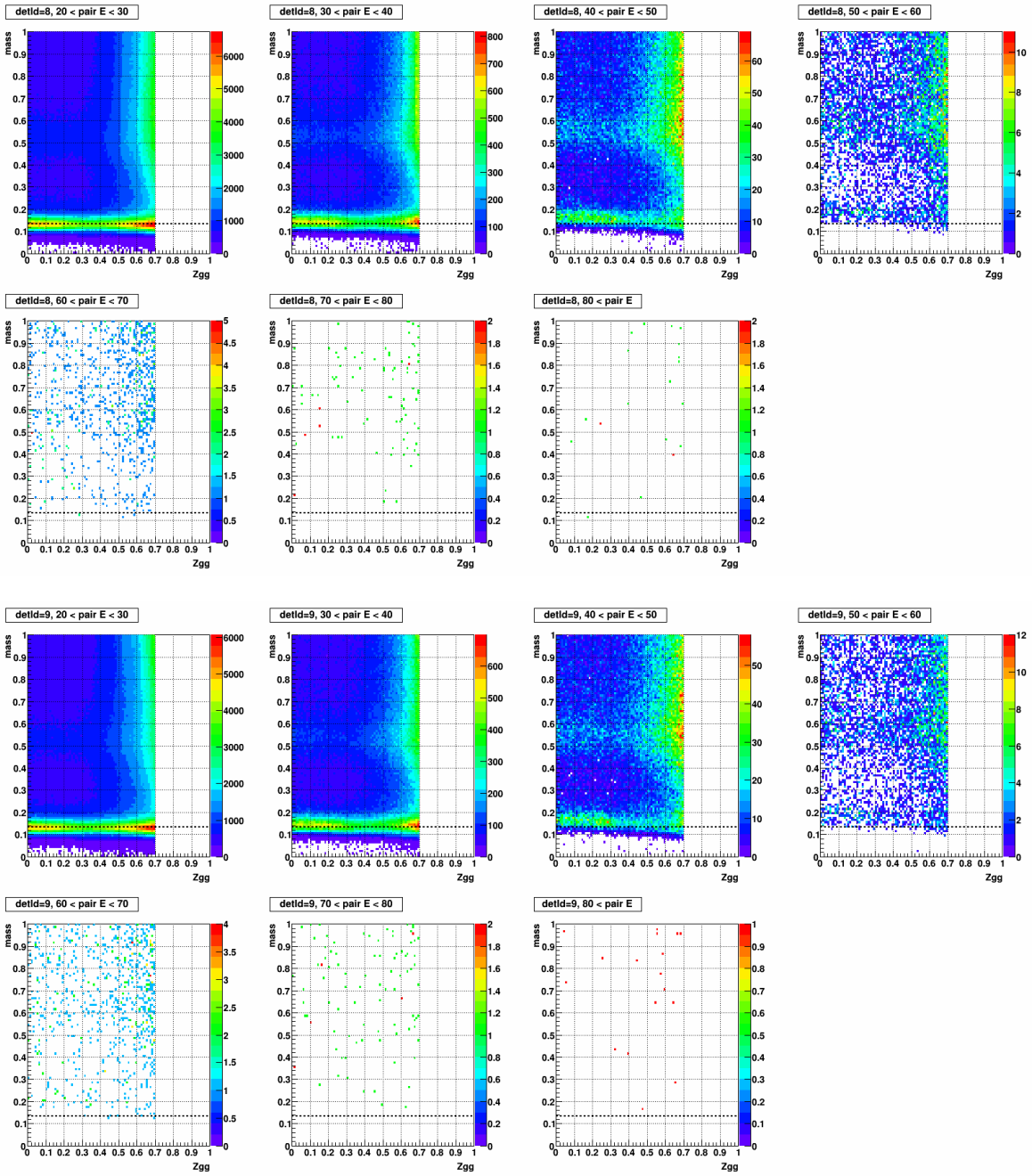

Figure A.34: Mass vs. Zgg, separated by pairE in the stepwidth of 10 (GeV), for detId 8 (top 7) and detId 9 (bottom 7), day 82-84

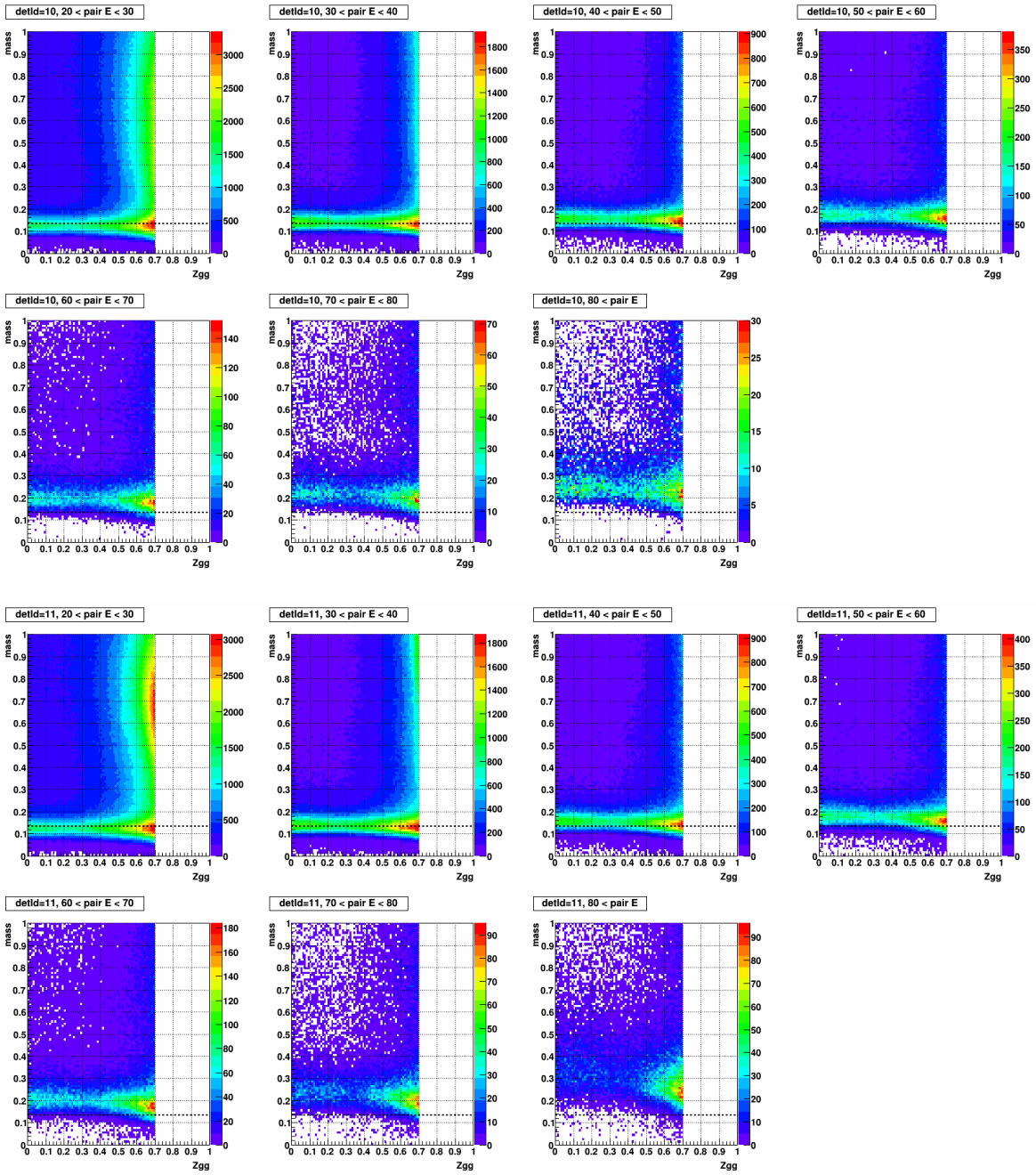

Figure A.35: Mass vs. Zgg, separated by pairE in the stepwidth of 10 (GeV), for detId 10 (top 7) and detId 11 (bottom 7), day 82-84

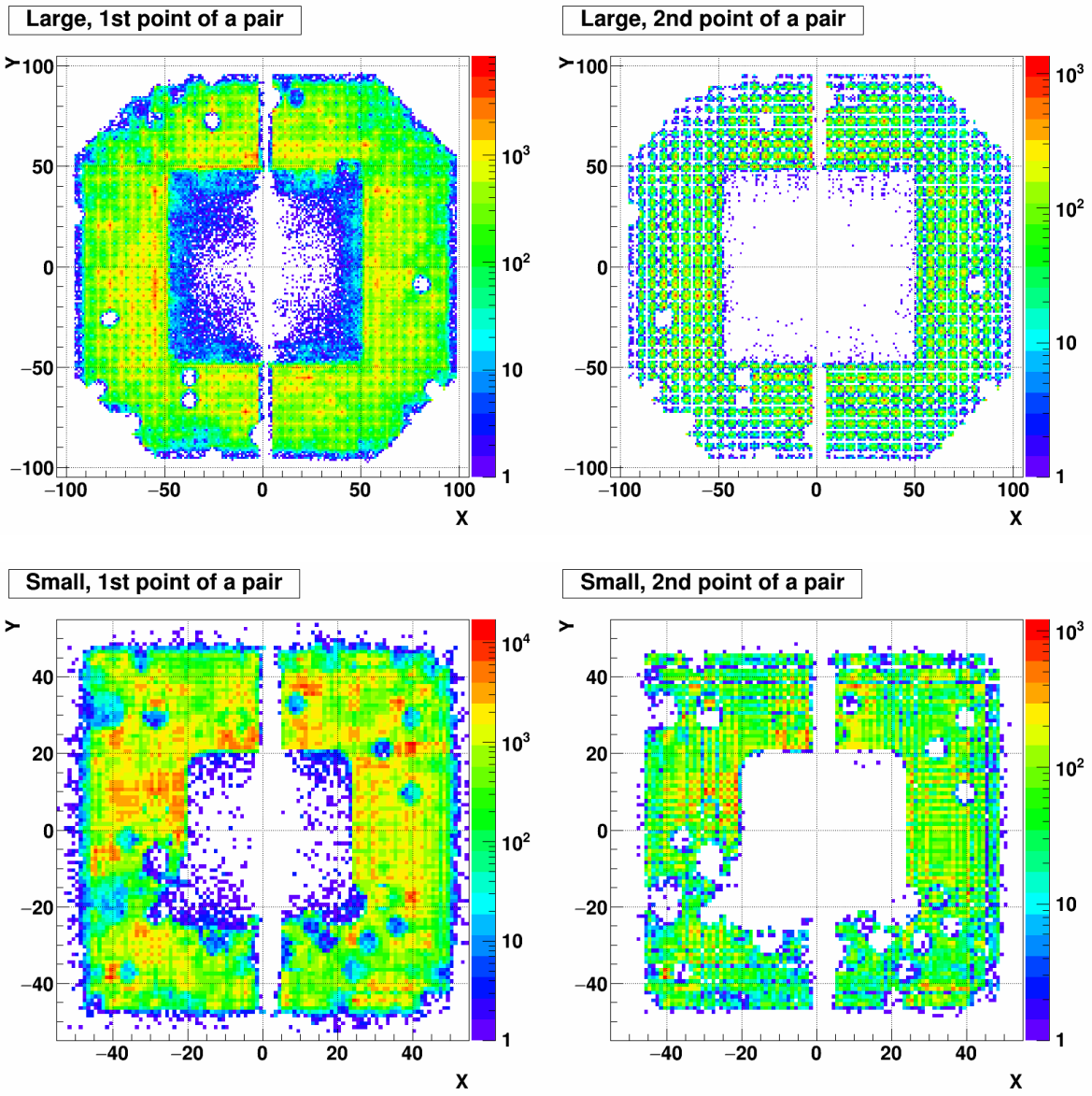

Figure A.36: XY distribution of 1st (left) and 2nd (right) point of a pair. Top row shows the large cells and Bottom row shows the small cells. The period is day 82-84.

Day 85-86

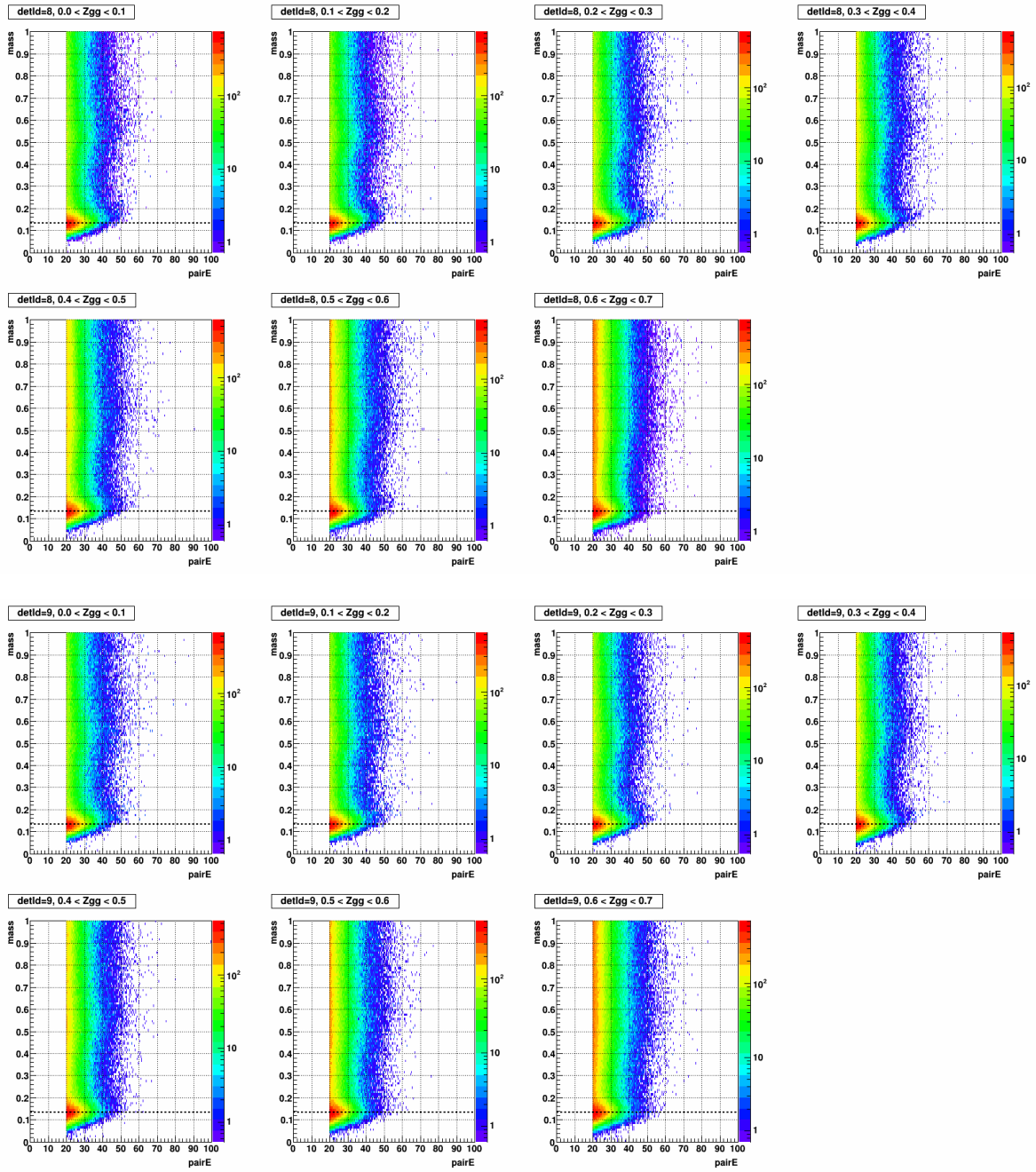

Figure A.37: Mass vs. pairE, separated by Zgg in the stepwidth of 0.1, for detId 8 (top 7) and detId 9 (bottom 7), day 85-86

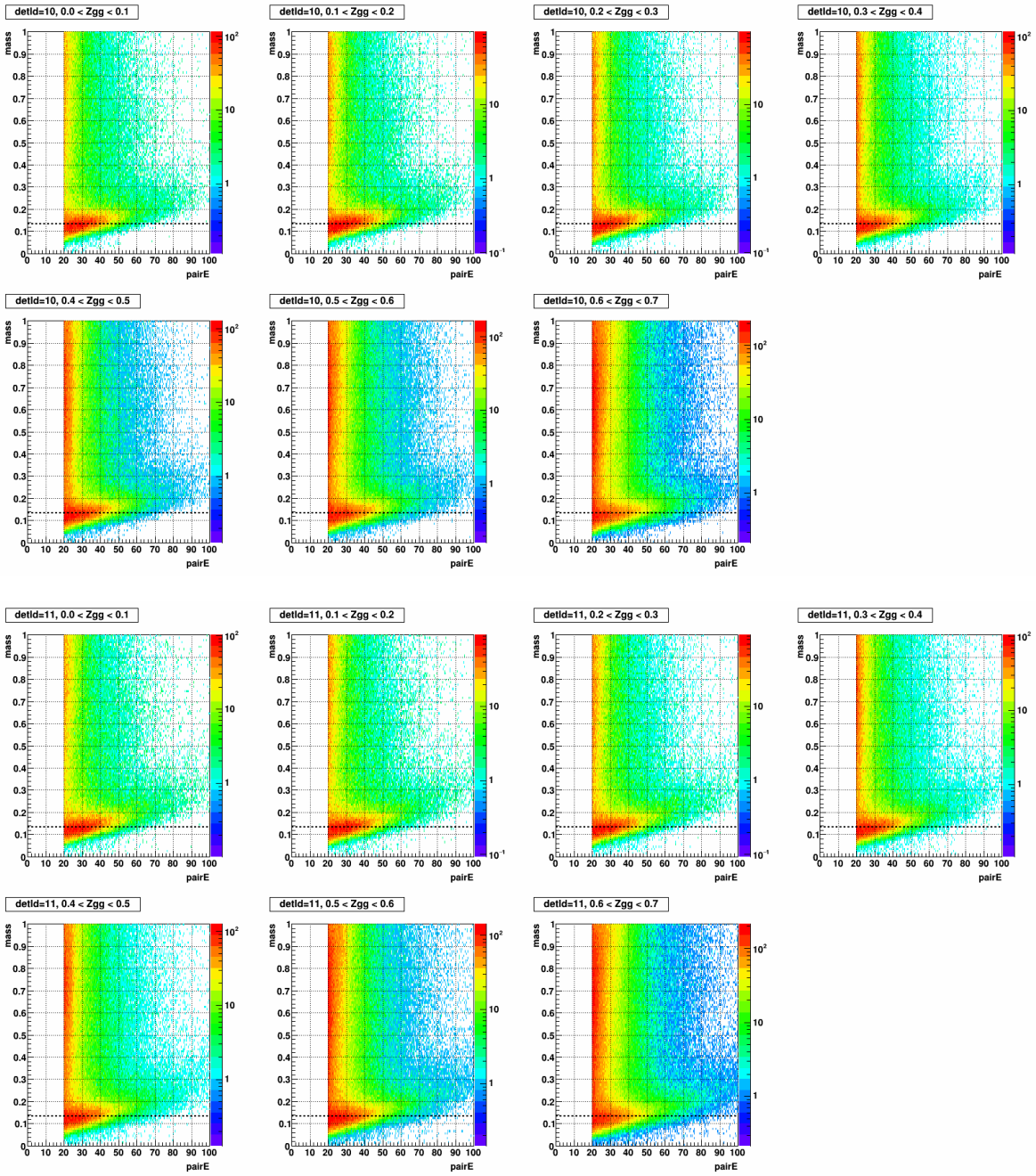

Figure A.38: Mass vs. pairE, separated by Zgg in the stepwidth of 0.1, for detId 10 (top 7) and detId 11 (bottom 7) day 85-86

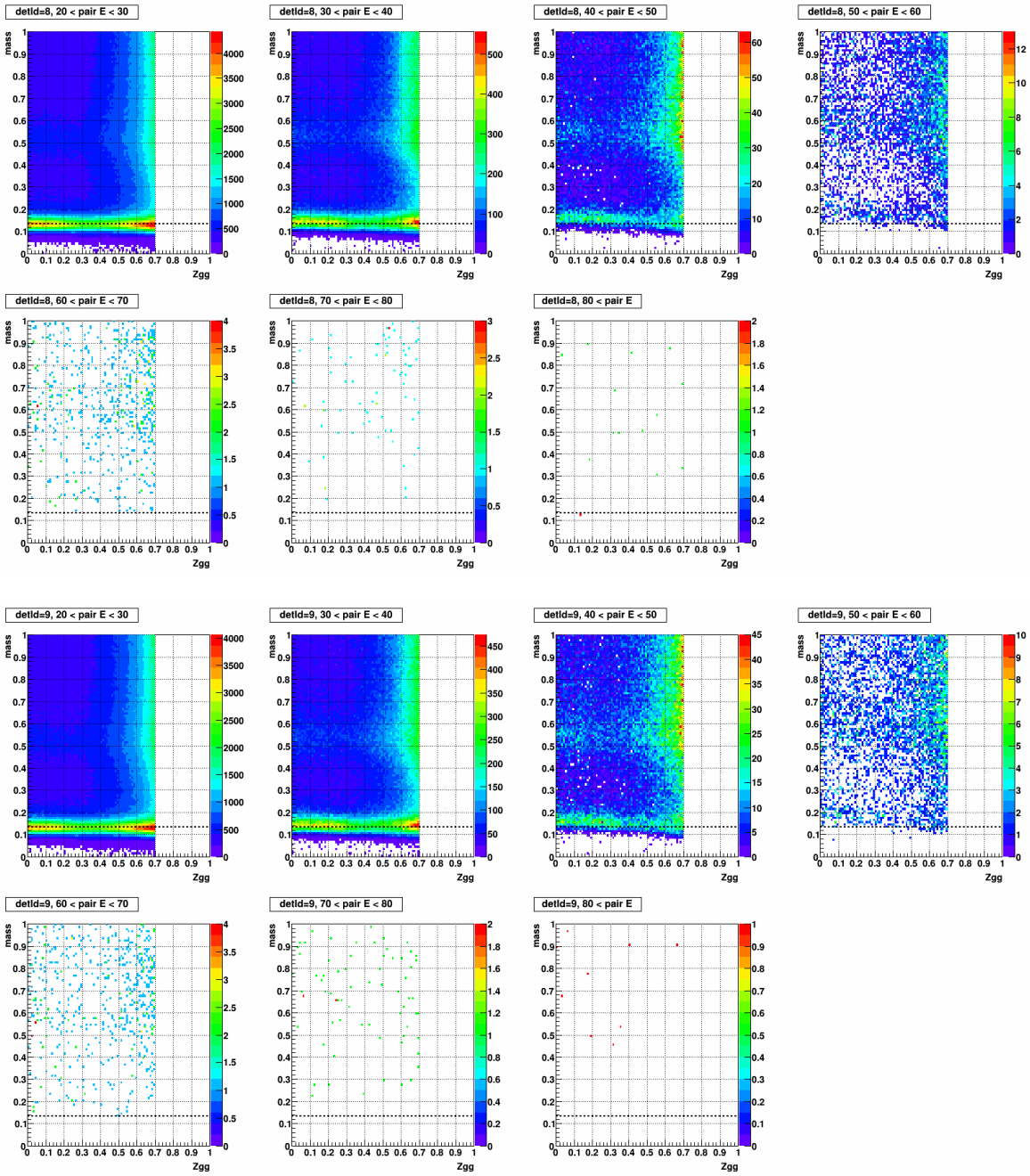

Figure A.39: Mass vs. Zgg, separated by pairE in the stepwidth of 10 (GeV), for detId 8 (top 7) and detId 9 (bottom 7), day 85-86

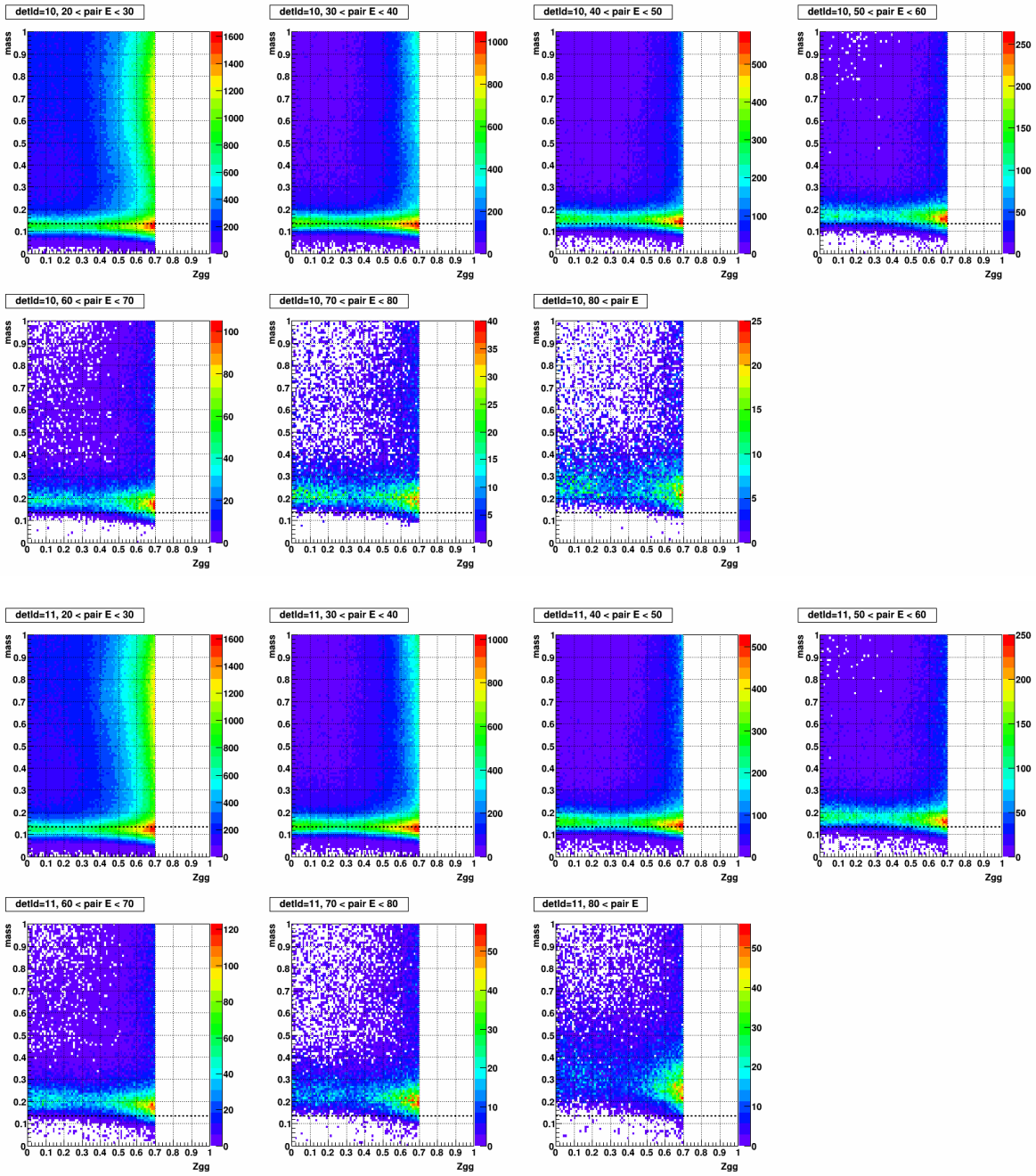

Figure A.40: Mass vs. Zgg, separated by pairE in the stepwidth of 10 (GeV), for detId 10 (top 7) and detId 11 (bottom 7), day 85-86

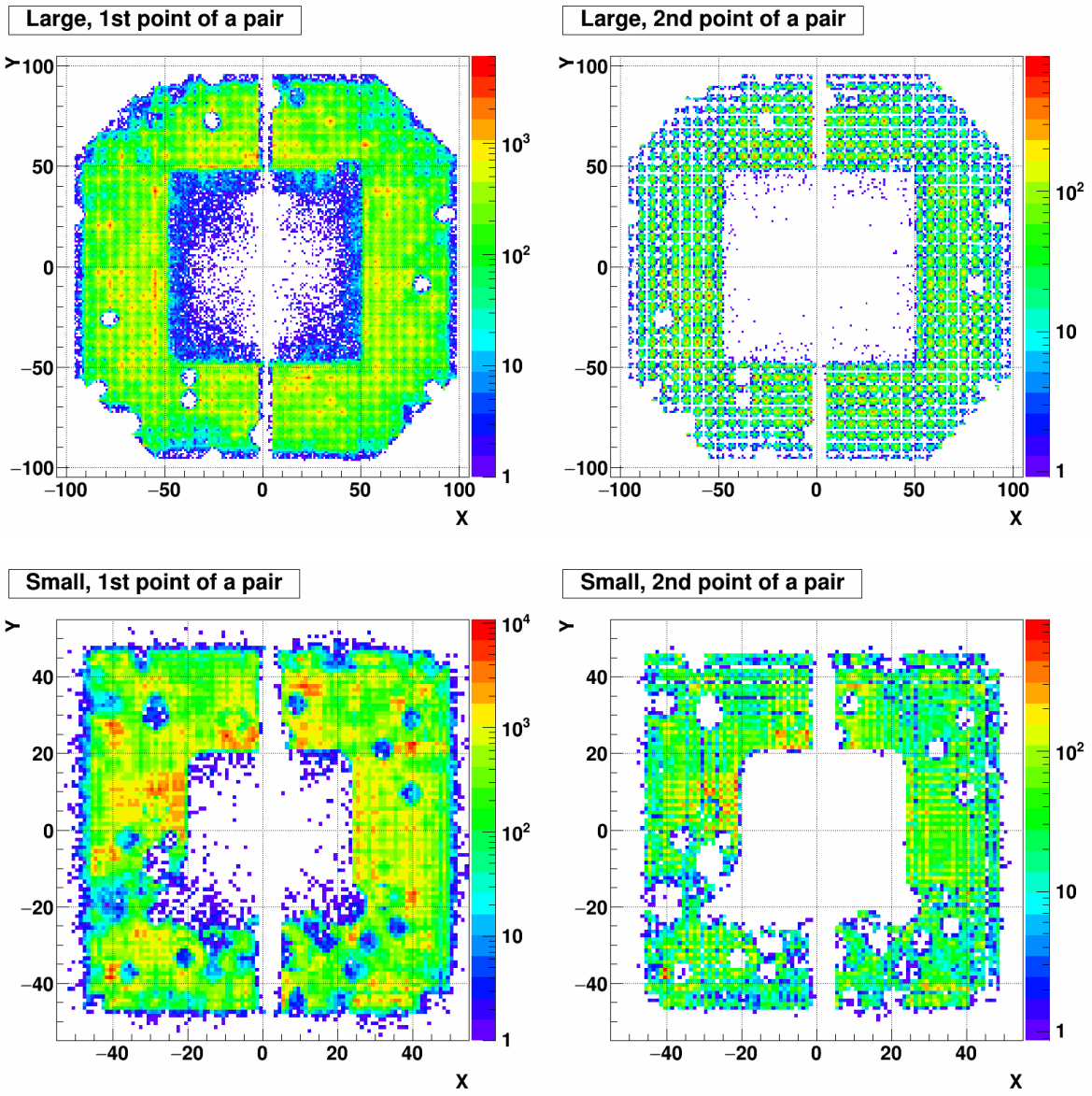

Figure A.41: XY distribution of 1st (left) and 2nd (right) point of a pair. Top row shows the large cells and Bottom row shows the small cells. The period is day 85-86.

Day 87-88

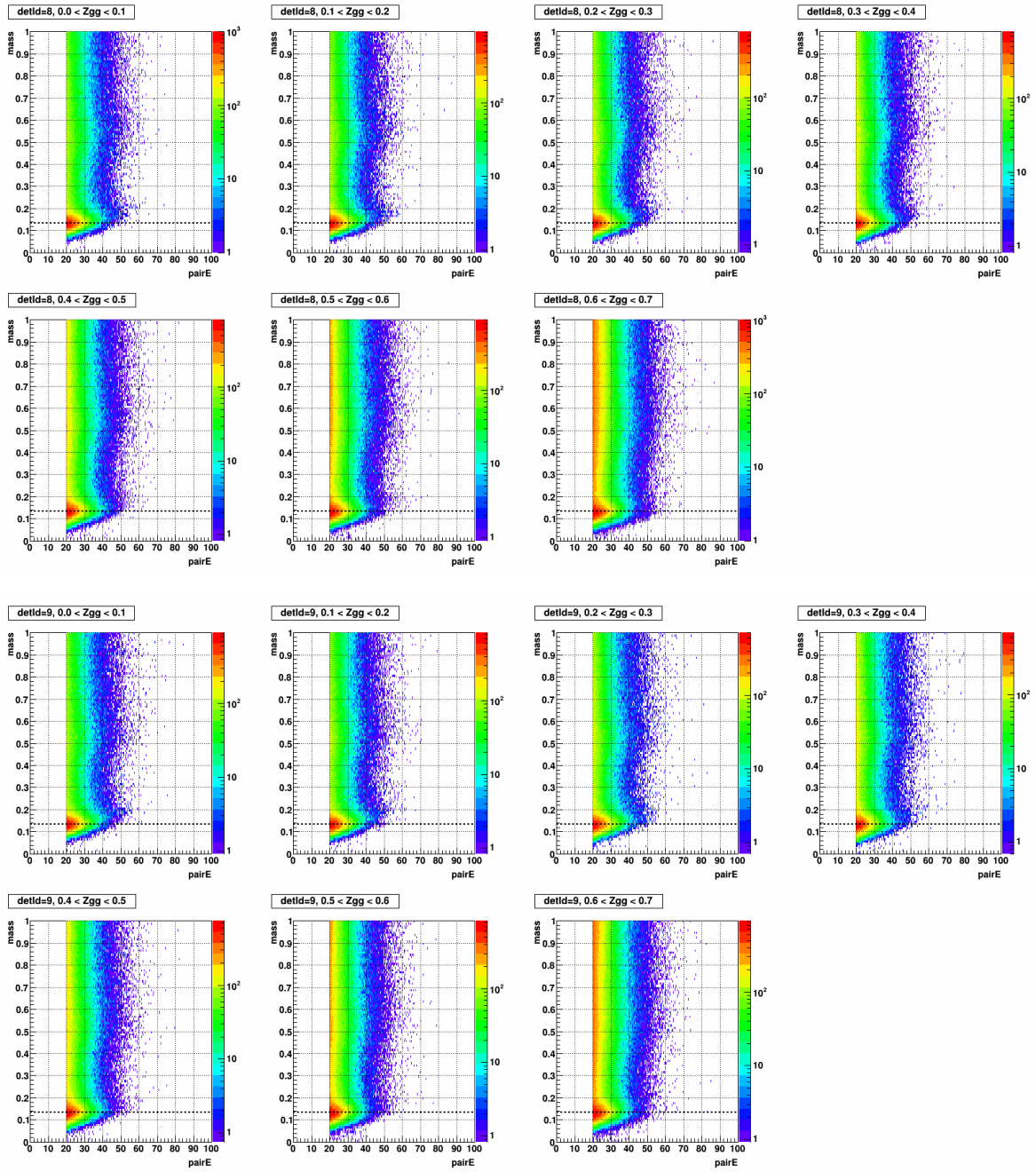

Figure A.42: Mass vs. pairE, separated by Zgg in the stepwidth of 0.1, for detId 8 (top 7) and detId 9 (bottom 7), day 87-88

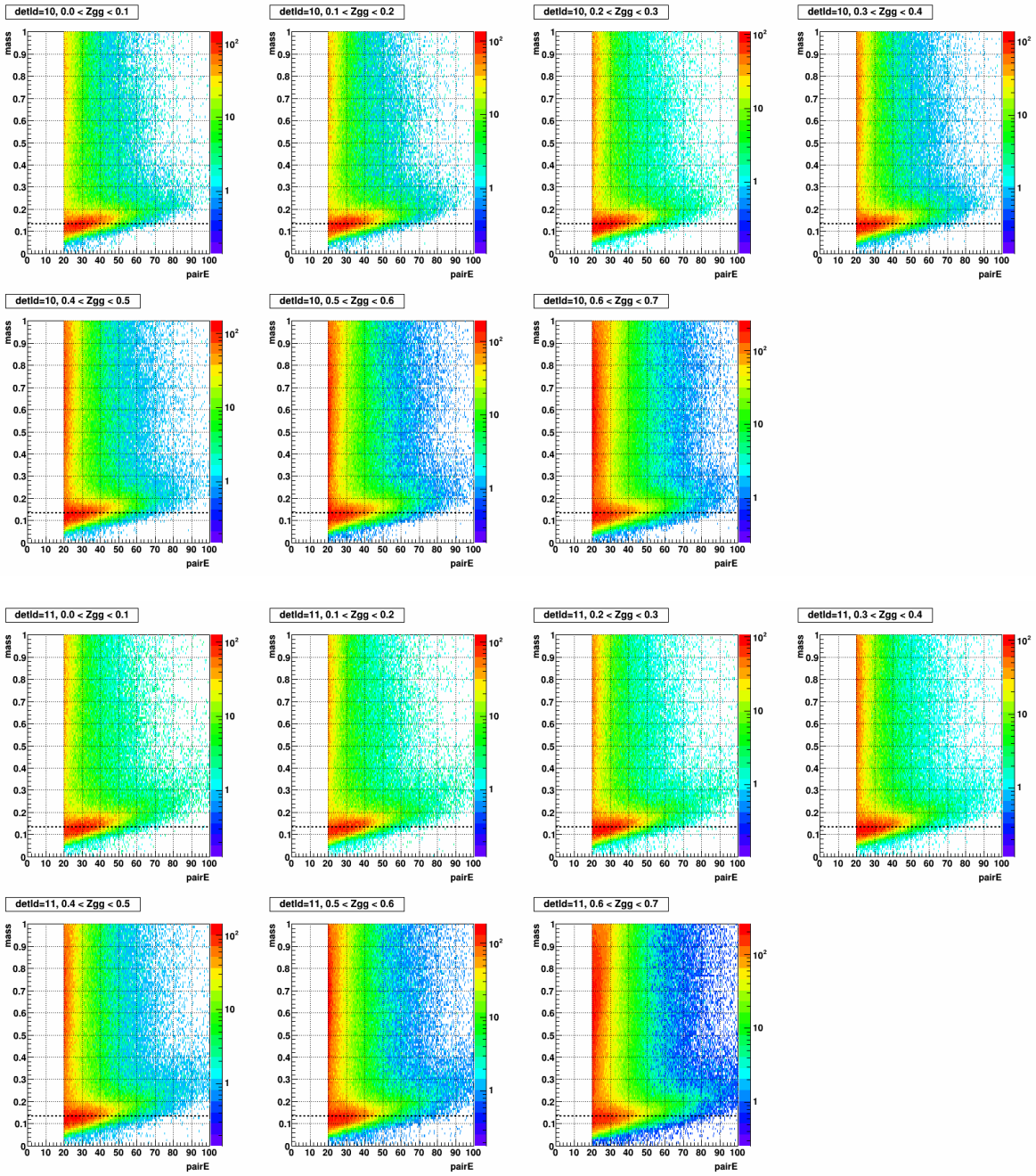

Figure A.43: Mass vs. pairE, separated by Zgg in the stepwidth of 0.1, for detId 10 (top 7) and detId 11 (bottom 7) day 87-88

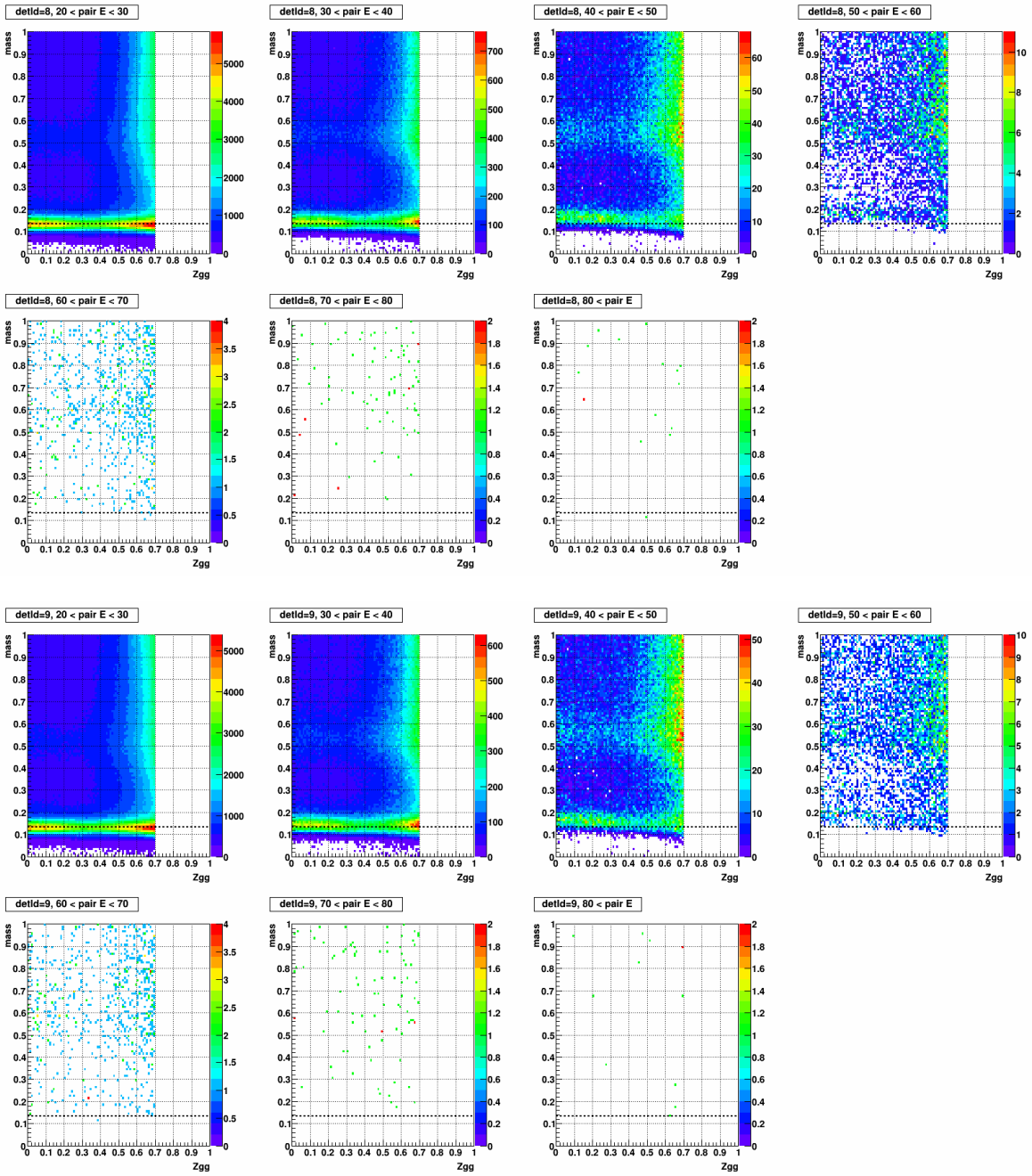

Figure A.44: Mass vs. Zgg, separated by pairE in the stepwidth of 10 (GeV), for detId 8 (top 7) and detId 9 (bottom 7), day 87-88

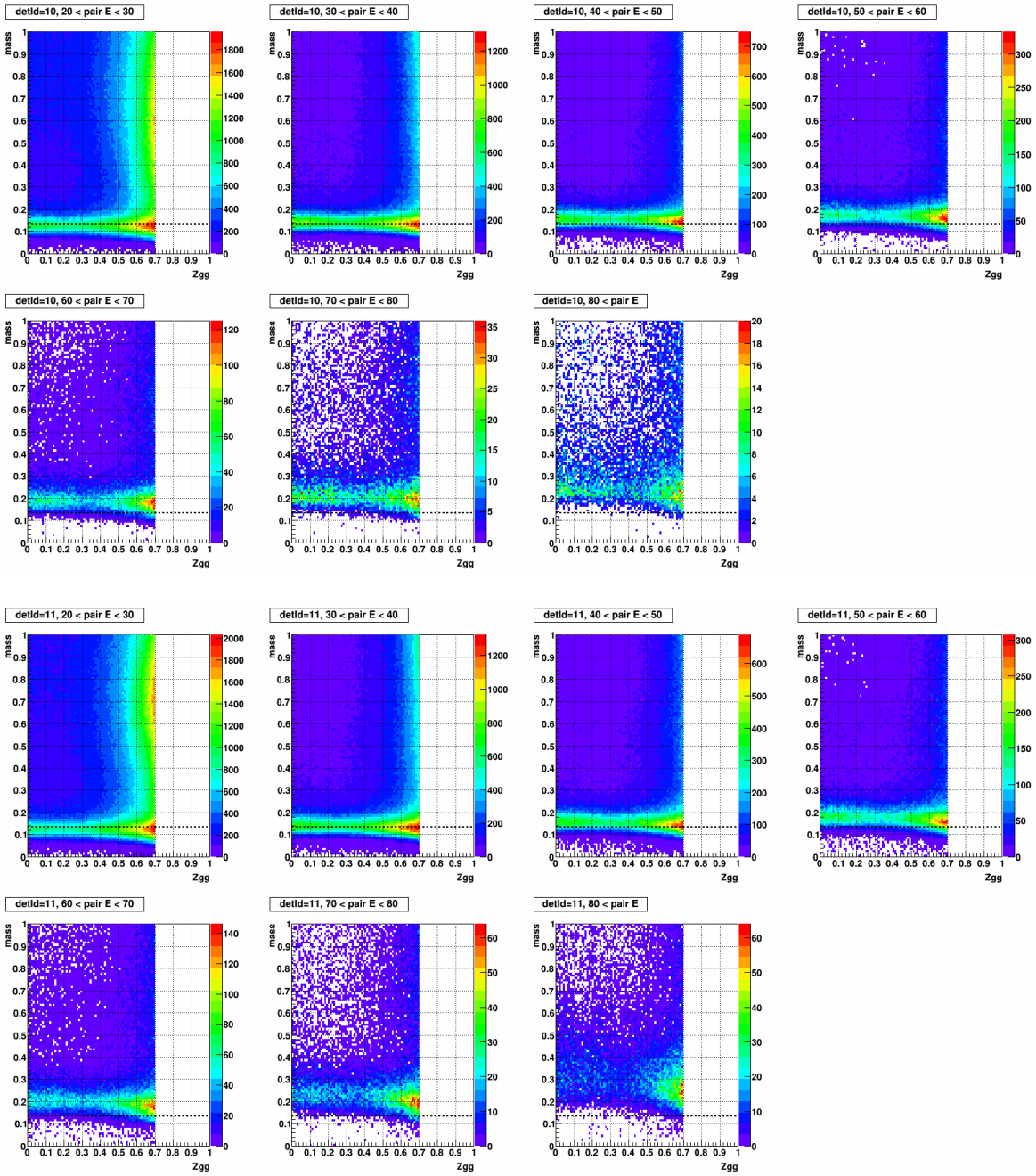

Figure A.45: Mass vs. Zgg, separated by pairE in the stepwidth of 10 (GeV), for detId 10 (top 7) and detId 11 (bottom 7), day 87-88

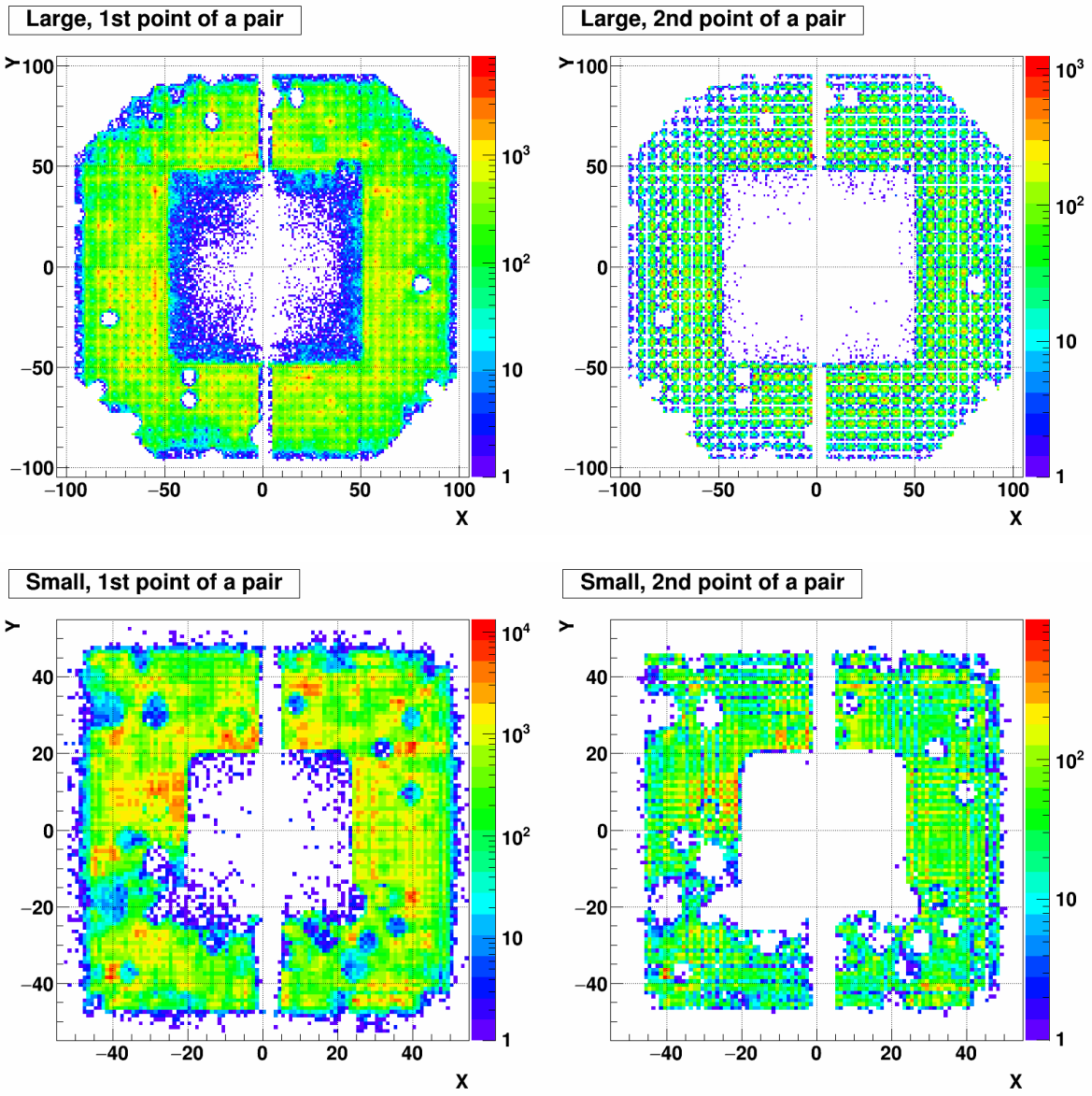

Figure A.46: XY distribution of 1st (left) and 2nd (right) point of a pair. Top row shows the large cells and Bottom row shows the small cells. The period is day 87-88.

Day 89-90

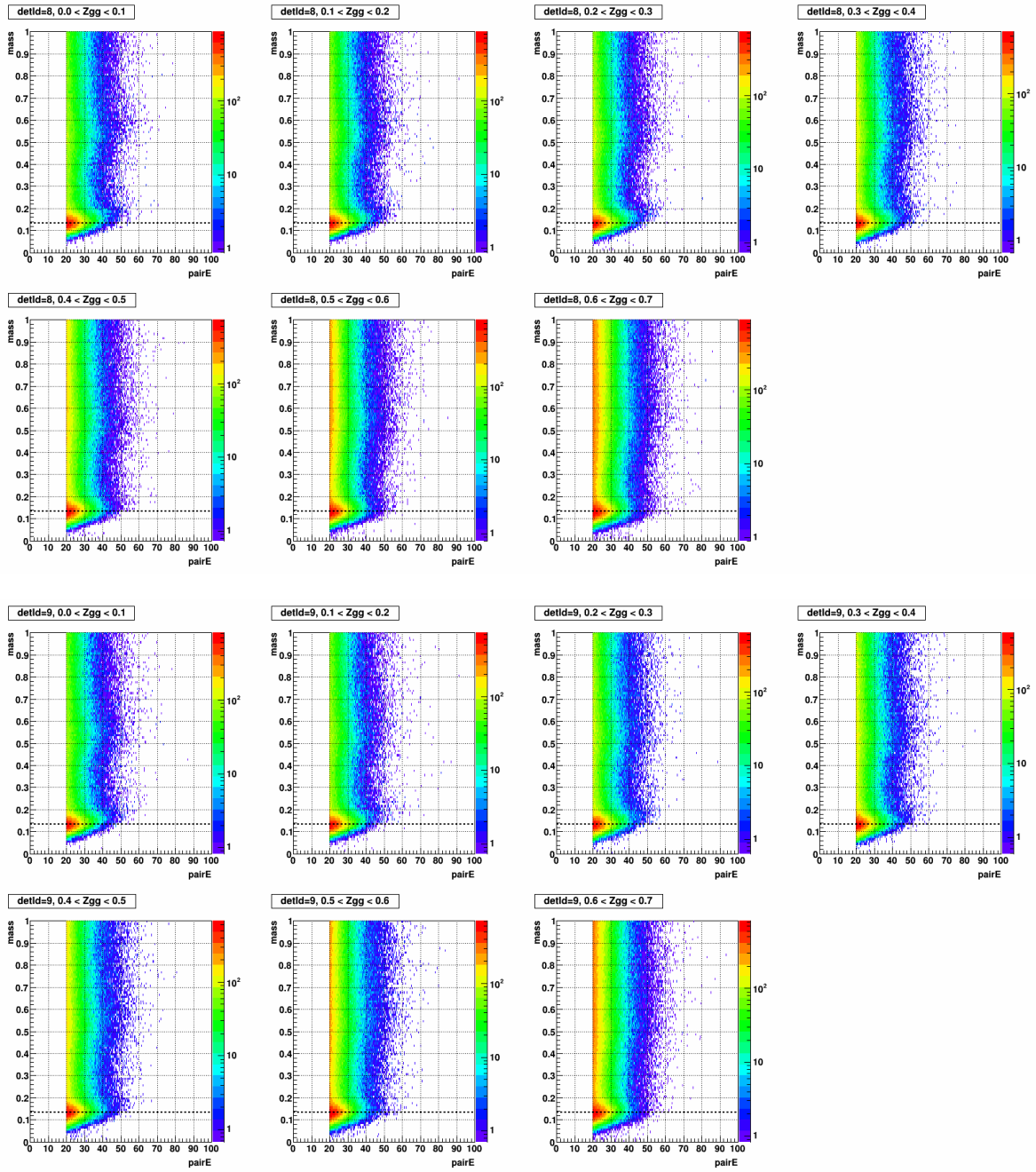

Figure A.47: Mass vs. pairE, separated by Zgg in the stepwidth of 0.1, for detId 8 (top 7) and detId 9 (bottom 7), day 89-90

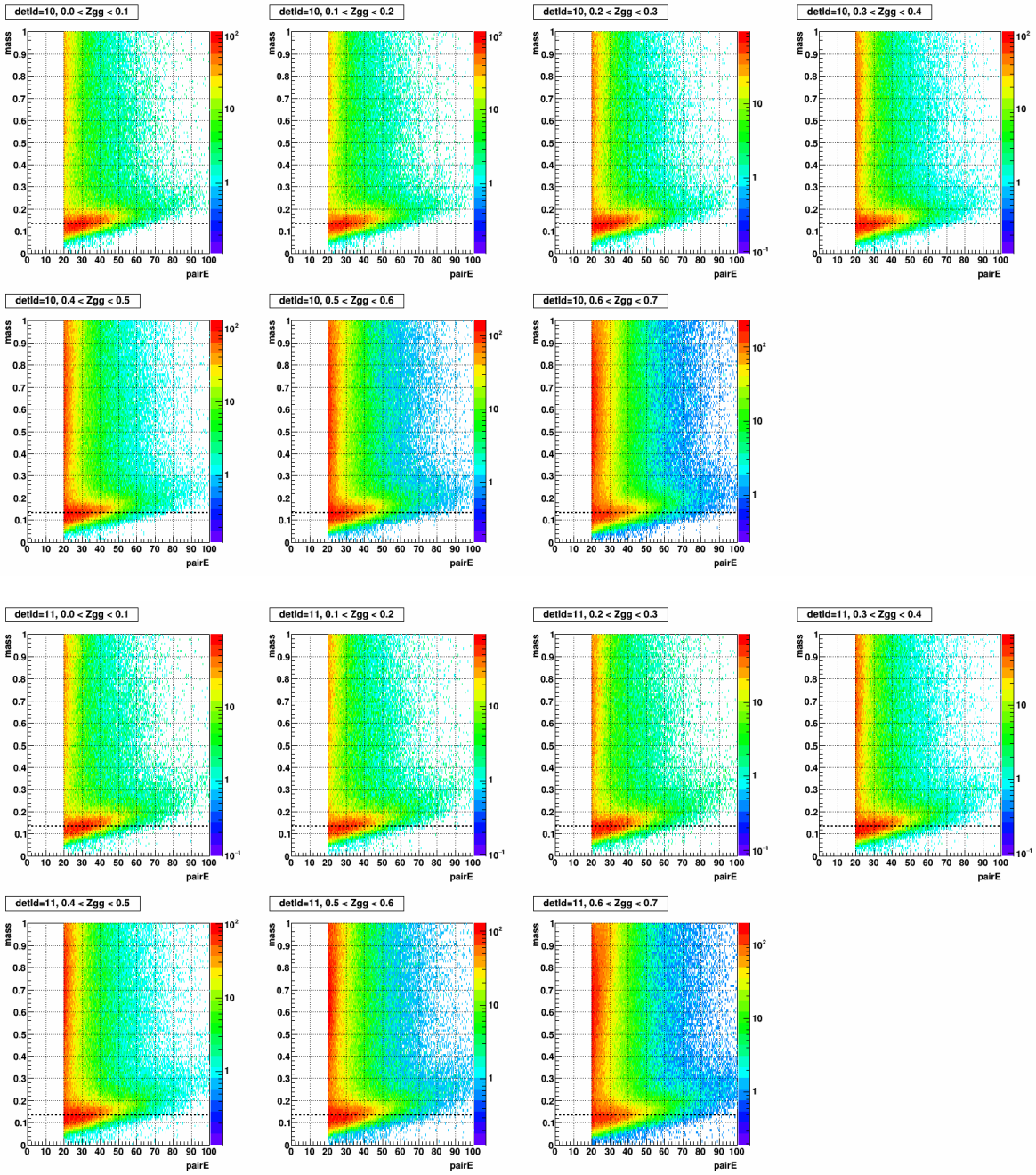

Figure A.48: Mass vs. pairE, separated by Zgg in the stepwidth of 0.1, for detId 10 (top 7) and detId 11 (bottom 7) day 89-90

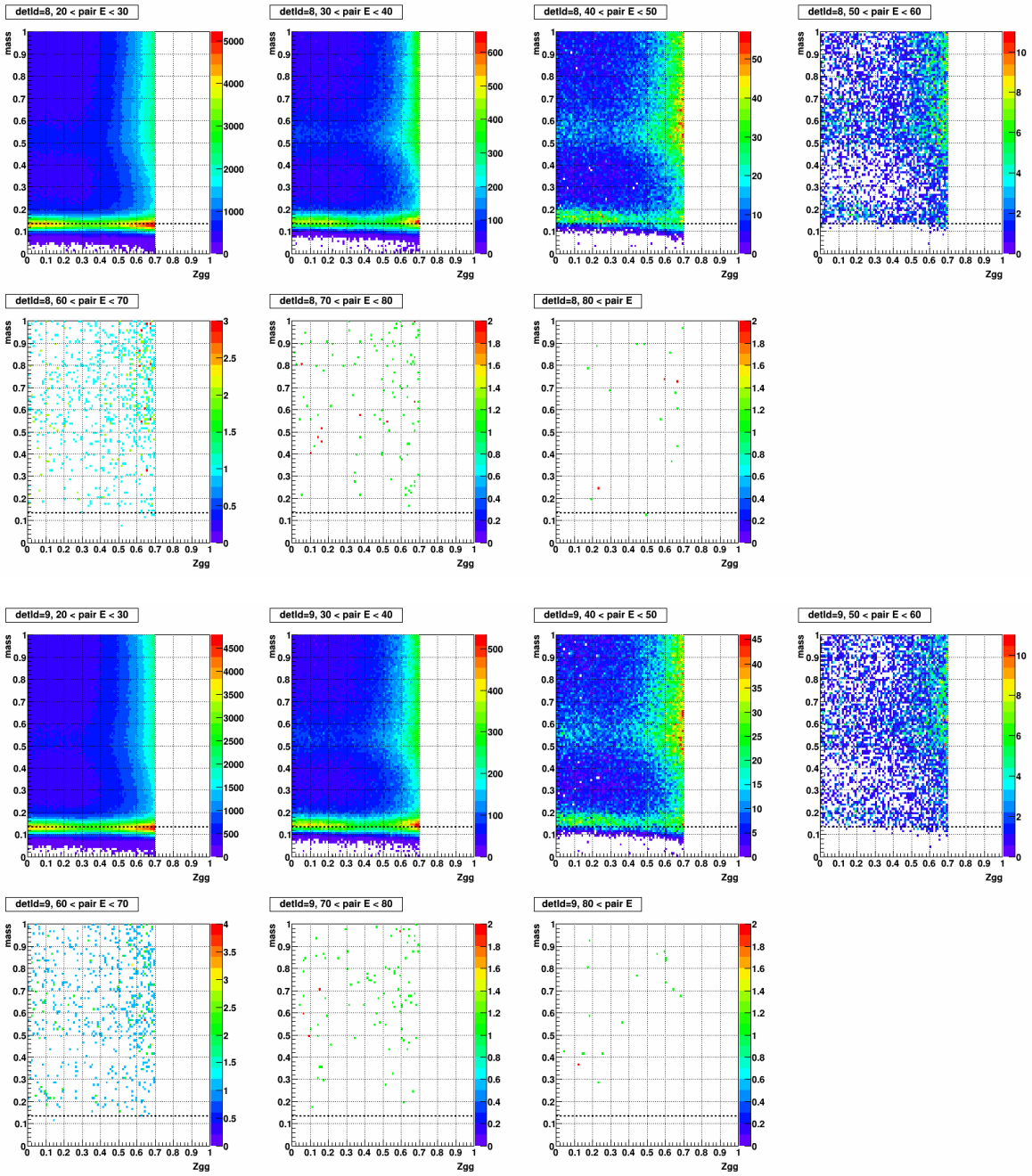

Figure A.49: Mass vs. Zgg, separated by pairE in the stepwidth of 10 (GeV), for detId 8 (top 7) and detId 9 (bottom 7), day 89-90

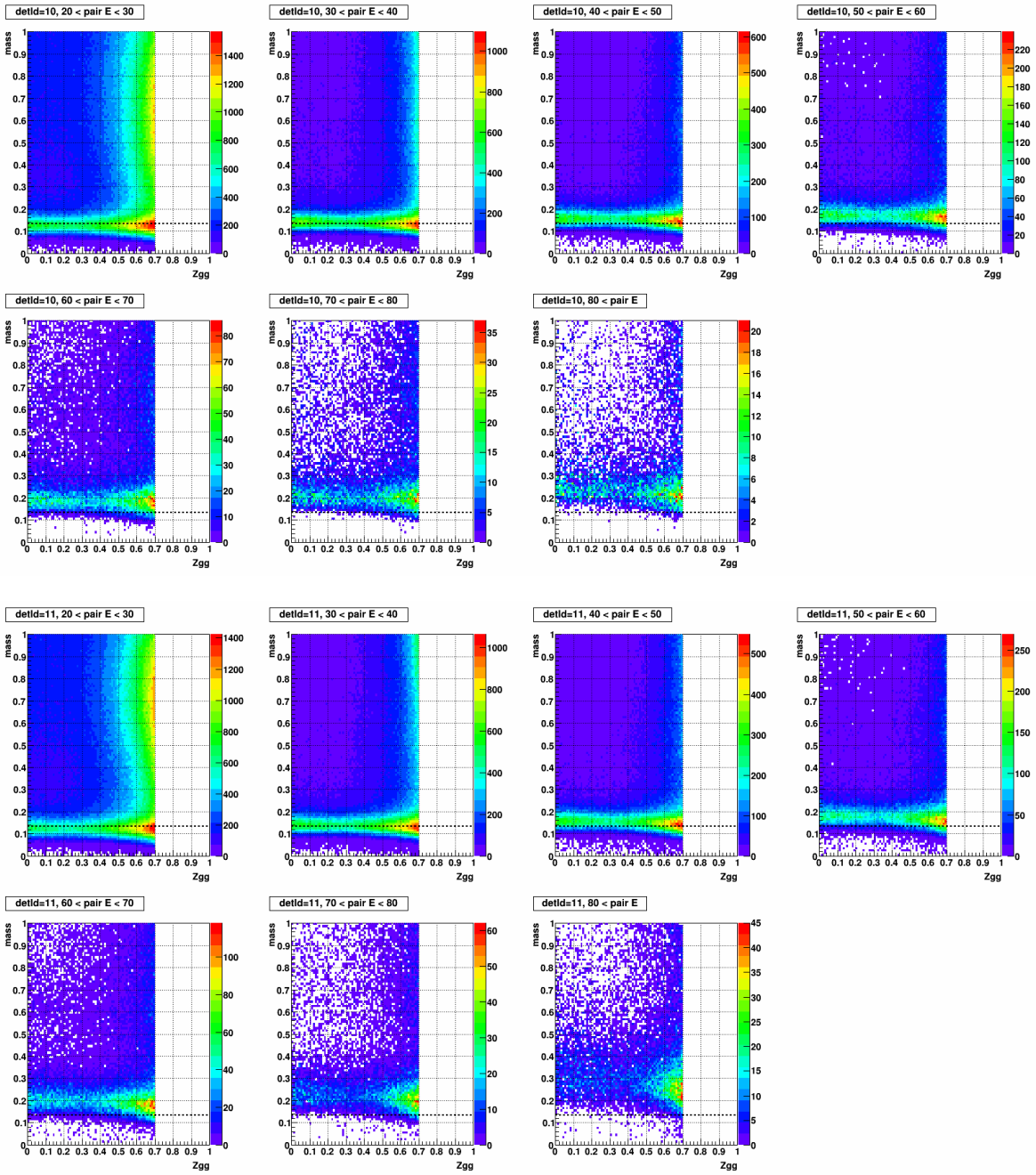

Figure A.50: Mass vs. Zgg, separated by pairE in the stepwidth of 10 (GeV), for detId 10 (top 7) and detId 11 (bottom 7), day 89-90

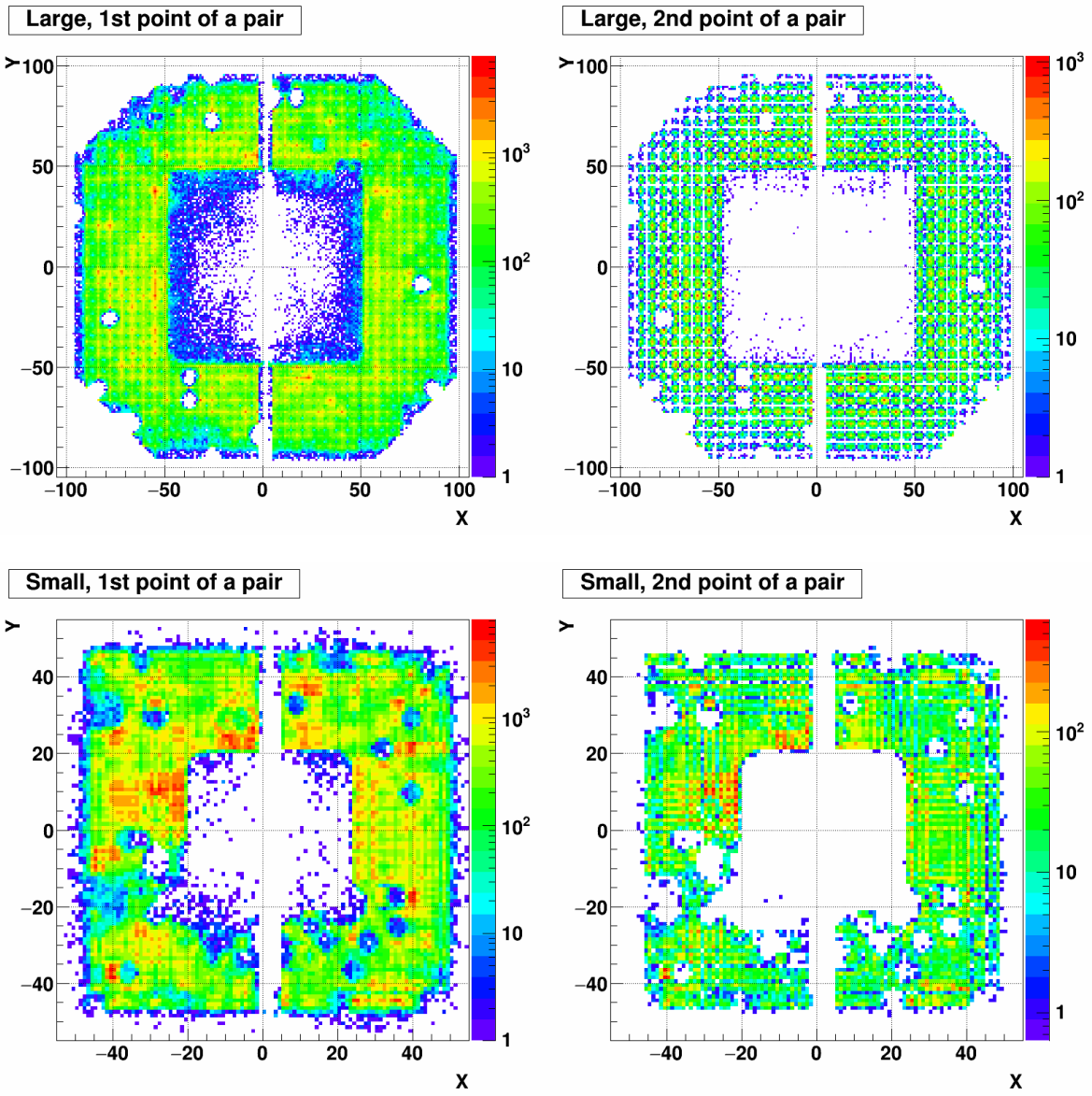

Figure A.51: XY distribution of 1st (left) and 2nd (right) point of a pair. Top row shows the large cells and Bottom row shows the small cells. The period is day 89-90.

Day 91-93

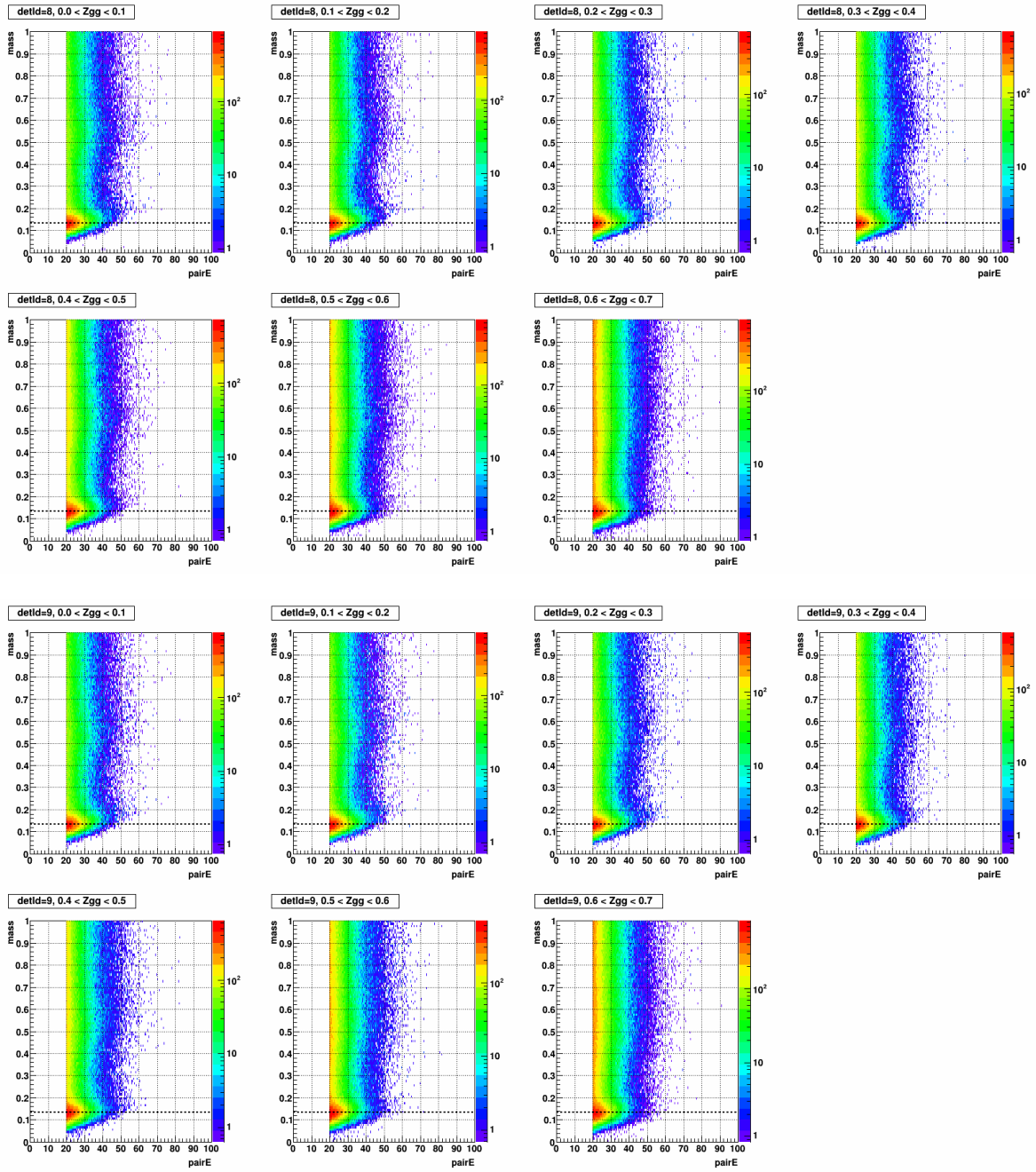

Figure A.52: Mass vs. pairE, separated by Zgg in the stepwidth of 0.1, for detId 8 (top 7) and detId 9 (bottom 7), day 91-93

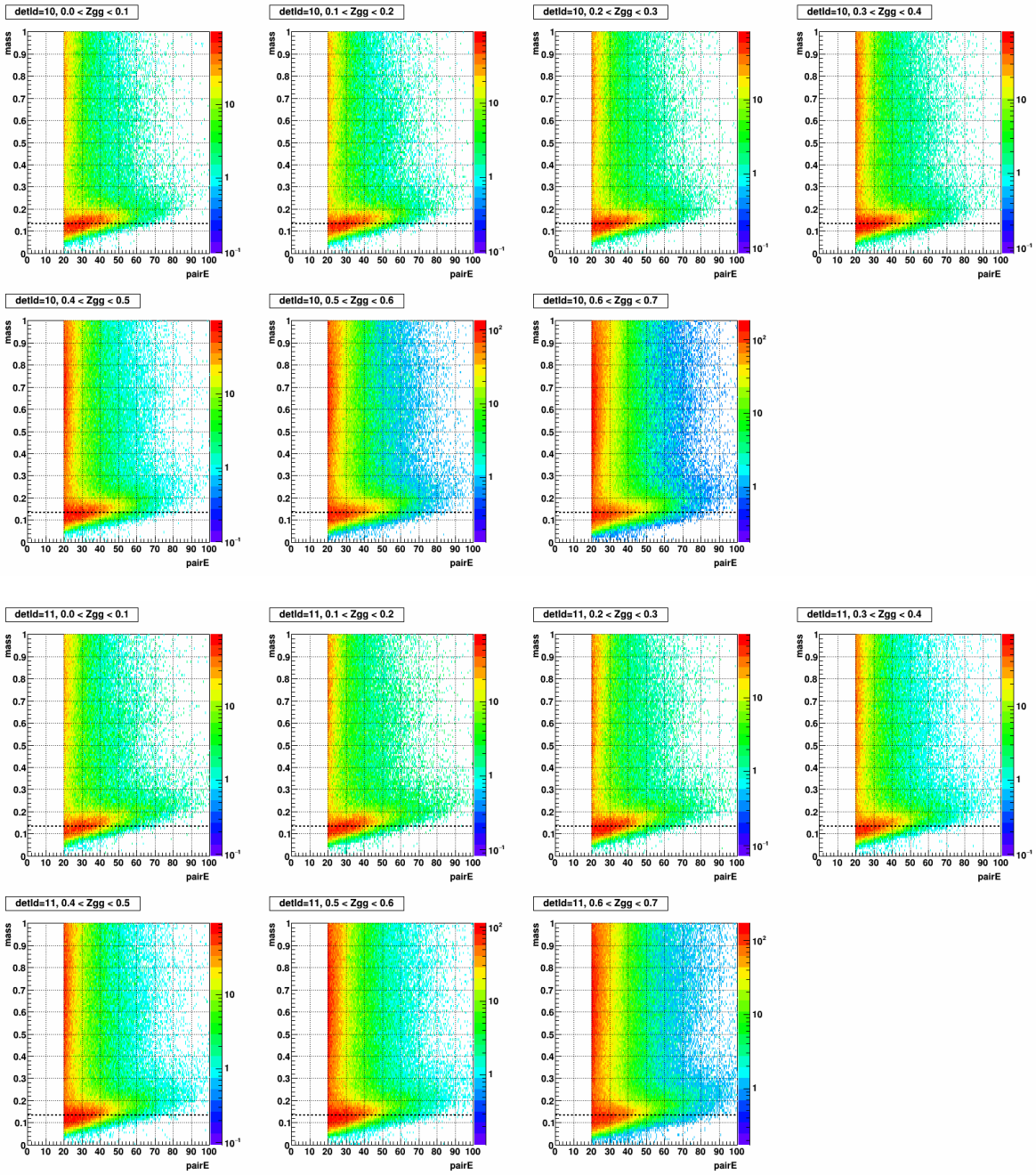

Figure A.53: Mass vs. pairE, separated by Zgg in the stepwidth of 0.1, for detId 10 (top 7) and detId 11 (bottom 7) day 91-93

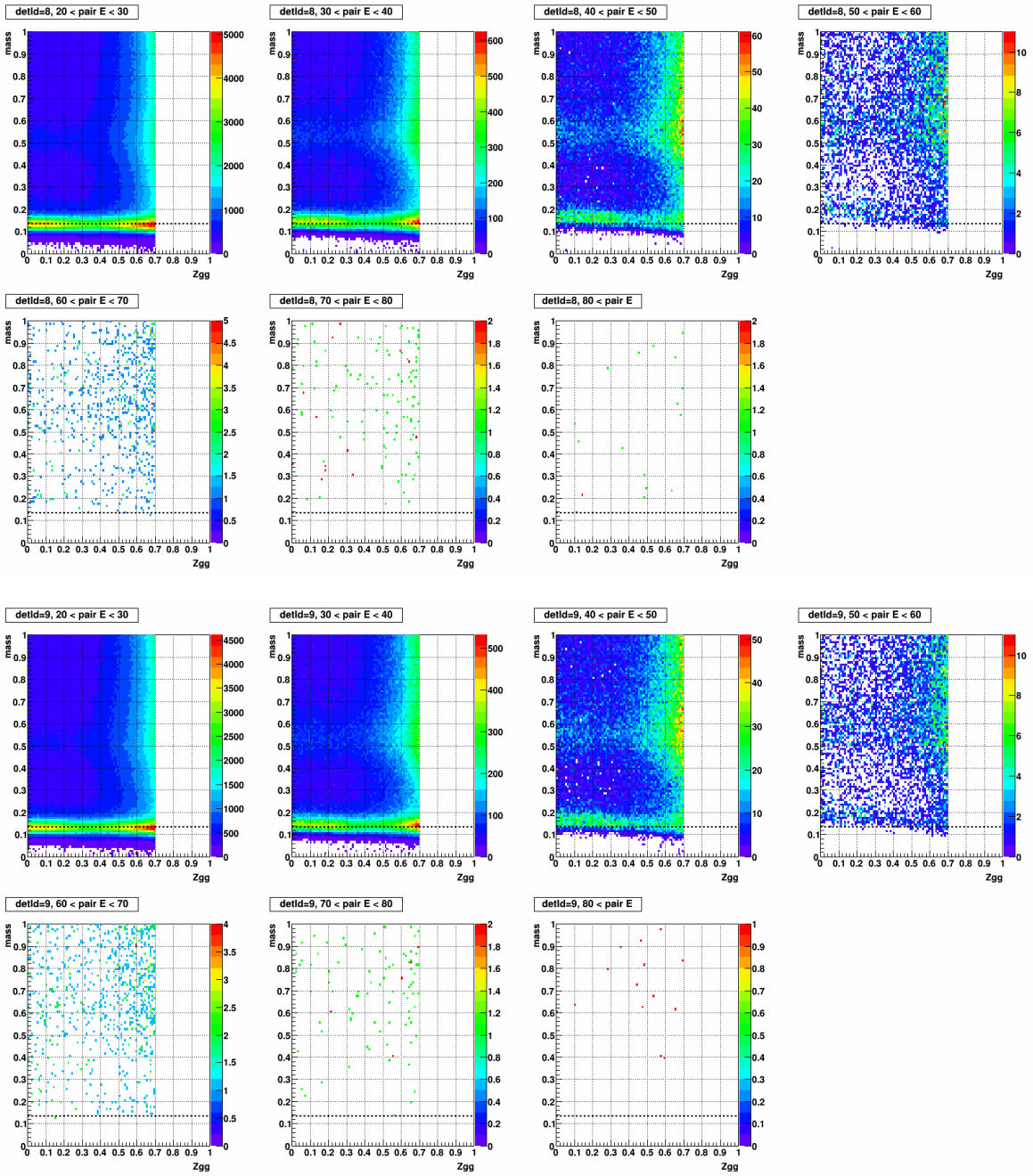

Figure A.54: Mass vs. Zgg, separated by pairE in the stepwidth of 10 (GeV), for detId 8 (top 7) and detId 9 (bottom 7), day 91-93

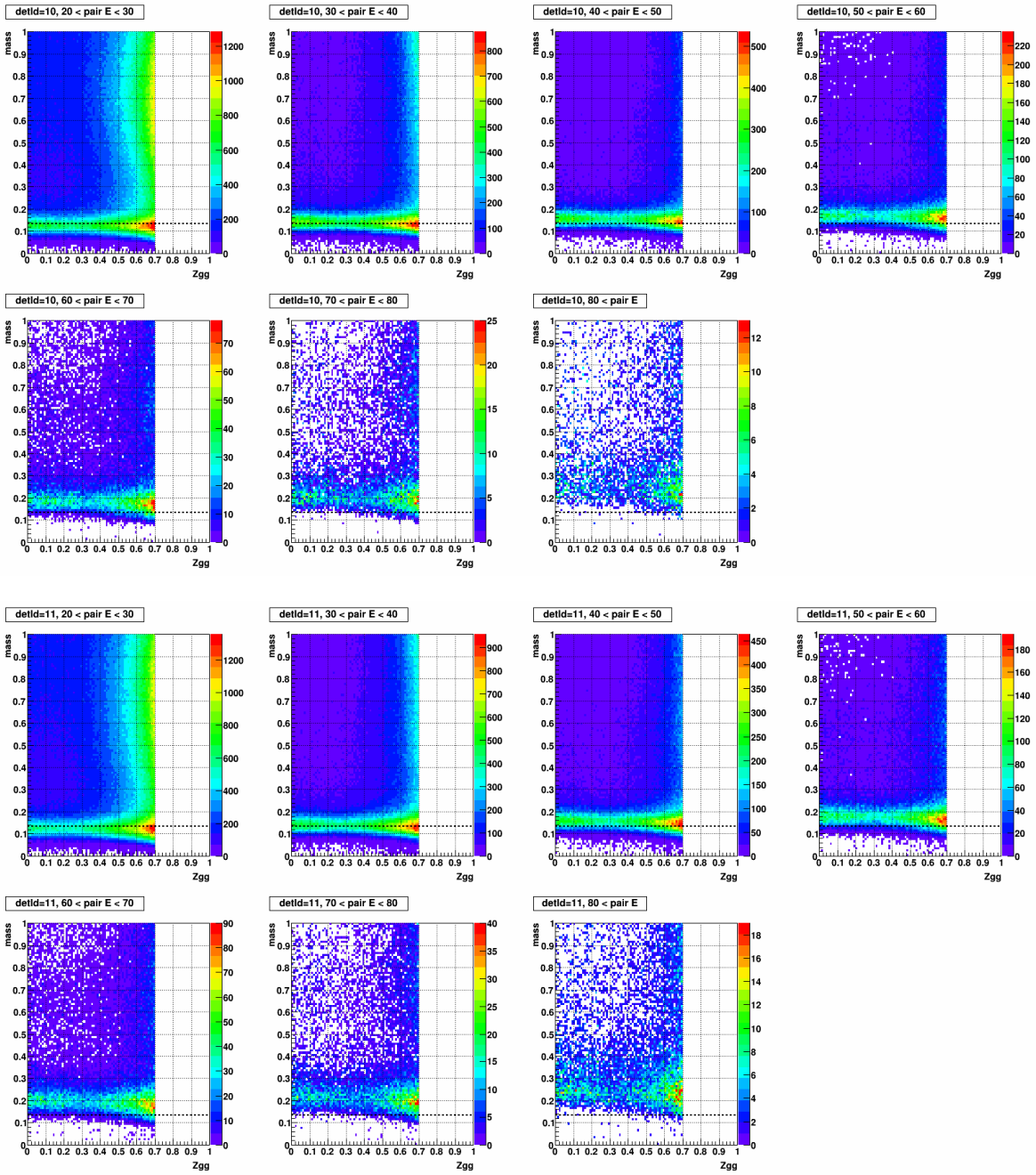

Figure A.55: Mass vs. Zgg, separated by pairE in the stepwidth of 10 (GeV), for detId 10 (top 7) and detId 11 (bottom 7), day 91-93

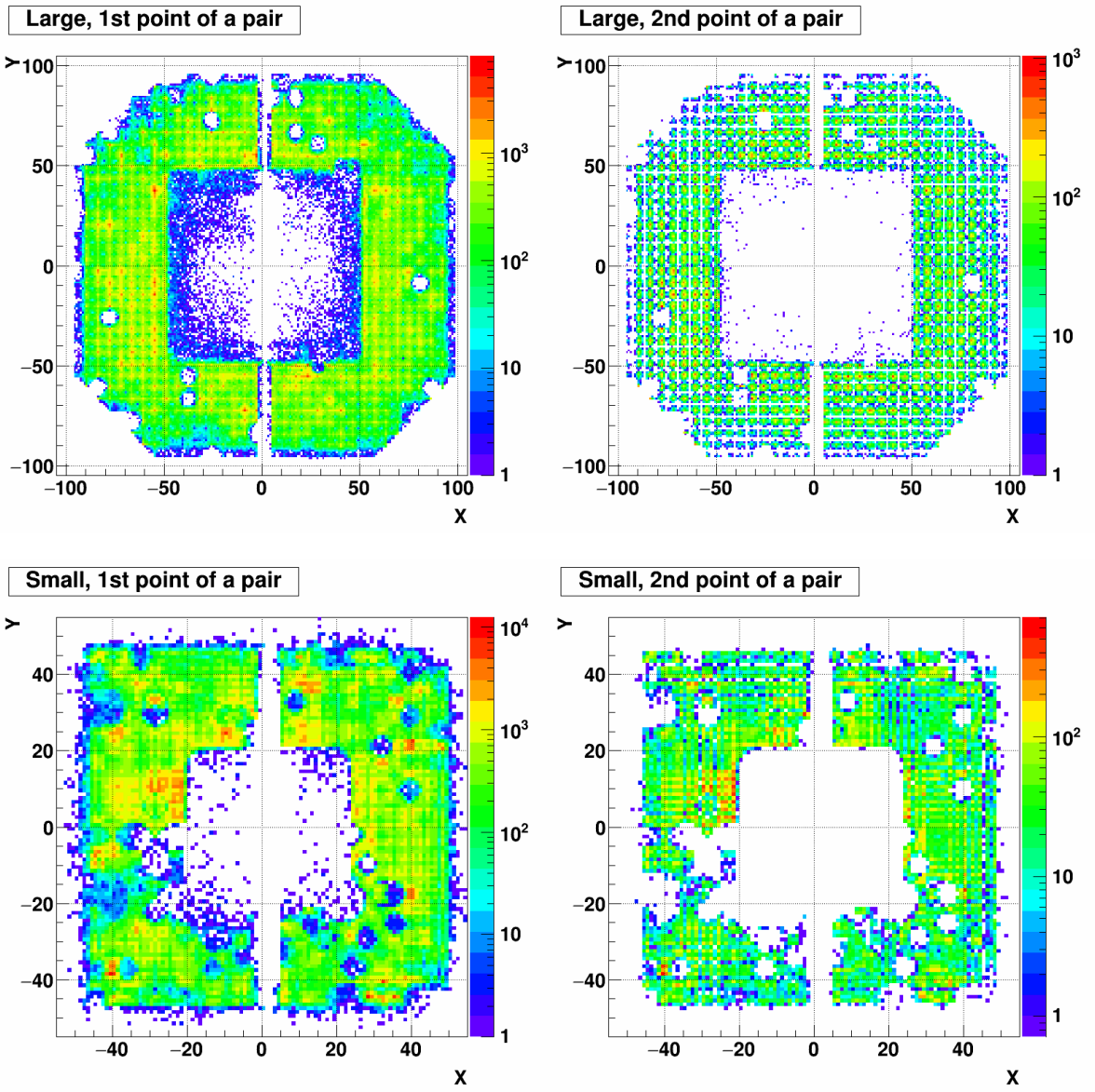

Figure A.56: XY distribution of 1st (left) and 2nd (right) point of a pair. Top row shows the large cells and Bottom row shows the small cells. The period is day 91-93.

List of Figures

1.1 An example of an in-situ QA map. The red-colored cells indicate they're cold. The other colors' meanings are as follows: bad (black), dead (white with crossing), calibration is underway (blue), and calibration is finished (yellow). 7

2.1 Incidence of a particle into FMS. Plot generated by David Kapukchyan 8
2.2 Passage of a particle into a typical large cell (top, red) and a typical small cell (bottom, green). In small cells, the majority of passage length contained in a cell. Plots generated by David Kapukchyan. 9
2.3 Summary of the overall calibration process 11
2.4 A sample of mass vs. channels histogram by StFmsCalibMaker (left) and a channel's mass distribution obtained by projecting an x bin (right). 13
2.5 Display of FmsMapBase.txt (left) and FmsMapBitShift.txt (right) obtained by function *GetMap*. From left each value means: detId, channel, gain, column, row, x, y, detId, channel, and bit shift, respectively. 14
2.6 A diagram shows the development of an EM shower across small and large cells (side view). Yellow-colored cells indicate they're fired by the shower. 16
2.7 One quadrant (top half of detId 8 and 10) of FMS (top left), red-marked cells' y/z position and distance to the vertex (top right), and schematic diagram of a pair of red marked cells in top view (bottom). A pair of red marked cells indicate closest cells from the beam pipe by its type (large or small) [a], which expected to suffer merging effect most seriously. In the bottom plot, ∼30 (cm) indicates a typical zVtx shift in RUN15, z indicates the distance between the vertex to shower max (15 cm from cell surface), and Δd indicates the distance between two showers which can be distinguished by reconstruction algorithm, respectively. 17

2.8 FMS cluster categorization by σ_{max}. Each plot indicates σ_{max} vs. energy. Each row indicates large (Top) or small (Bottom) cells. Each column indicates different types of samples: single photon MC (left), π^0 MC (middle), and RUN15 data (right), respectively. Each line (either red or black) on top of each plot indicates σ_{max} cut determines the number of photons in this cluster. Finally, the area marked as "Amb" between red and black lines indicates ambiguous. The study and plot generation was done by Akio Ogawa. [11] 19
2.9 A π^0 event with one distinct leading energy cell (left) or A π^0 event with its energy distributed over multiple cells (right). The value inside a cell denotes the ratio of the cell's energy to the π^0's energy. 20
2.10 Ratio (percentage) of each hit's energy to the pair (π^0 candidate) energy separated by detId. Black line indicates all hit and Red filled histogram indicates leading energy hit. The blue vertical line on top of each histogram indicates the final cut (30 %). Top four distributions were obtained from day 82-84 and Bottom for distributions were obtained from day 89-90 in RUN15pptrans. As two different periods show the ratio distribution does not vary over time. 21
2.11 Example of fit on reconstructed mass distribution for a large cell (left) or a small cell (right). Dashed lines on top of mass distribution indicates combined fit (red), combined fit's signal part (blue), combined fit's background part (green), and true π^0 mass (magenta) respectively. 22
2.12 Flow of overall fit process for a cell including a preliminary fit. Starting from top left and in the counterclockwise direction, each plot indicates: raw reconstructed mass distribution (top left), signal part with preliminary fit (bottom left), BG part with preliminary fit (bottom right), and raw distribution with final combined fit (top right), respectively. In top-left plot, magenta line indicates true π^0 mass (0.135 GeV) and blue lines indicate the range of signal part defined by 0.135 ± 0.06. 23
2.13 Example of suspicious case caught by fit quality criteria and retry attempts followed by. The fit succeeded in 2nd attempt and escaped the loop. 24
2.14 FMS cells' fit χ^2/NDF distribution after a full iteration. Each row shows the results of each detId and each column shows a different range ([0, 25] for left and [0, 5] for right). For each plot, black filled histograms indicate all cells and red line histograms indicate converged cells. The large spike at $\chi^2/\mathrm{NDF} = 0$ in right column indicates cells with too small statistics (fit process returns 0 if the fit is not performed at all). Note that bad or dead cells are excluded beforehand. Finally, this distribution is obtained from day 91-93 in RUN15pptrans. 26

2.15 A couple of examples for convergence over iterations. For the left column, from top to bottom each row indicates: fit $\chi 2^2$/NDF, mass$_{fit}$, width of the mass, and gainCorr, respectively. Each mass distribution in the right column corresponds to each iteration index in the left plot. Both examples show mass$_{fit}$ and gainCorr gradually approach to certain value as iteration goes on. 28
2.16 Zgg distribution of a few channels in detId 11. Black (Red) distribution indicates FMS (Physics) stream, and Line (Filled) distribution indicates its point pair energy requirements is 20 < E (GeV) < 40 (35 < E < 40). 29
2.17 Concentration in point energy (left) and a hot channel responsible to (right) 30
2.18 Examples of a dead cell (top left) and three bad cells (top right and bottom). 31
2.19 Cell vs. run for detId 8 (left) and its Y projection with normalization by # of runs (right). For the left plot, each bin content corresponds to a cell's # of entries normalized by # of triggers. Also note that both axes are indices, instead of actual cell or run number to remove dummy numbers. For the right plot red vertical line indicates a rough hot channel threshold defined by its own mean and RMS. Lastly, these plots were obtained from Day 80-81 in RUN15pp200trans. 32
2.20 ADC distributions of detId 11, channels 421-428. No corrections were applied. 33
2.21 ADC distributions of detId 11, channels 421-428. Channels with positive bit shift (426 and 428) were normalized by $1/2^{\mathrm{BS}}$ for proper comparison. 33
2.22 ADC distributions, Hit energy distributions (Blue), and Reconstructed mass distributions (Magenta) of detId 11, channels 421-428. Note that arbitrary value (10) was multiplied for each hit energy to draw it on top of the ADC distribution. Also Mass distribution's x is independent of drawn x-axis: its range is always [0, 0.5 (GeV)] and the vertical dashed line indicates position of the π^0 mass (0.135 GeV). 34
2.23 Examples of typical skewed mass for two different channels in different periods. The top plot was obtained from day 77-79 and The bottom plot was obtained from day 69-73. 35
2.24 Hypothesis for how the skewed mass distribution happens. Left 3 diagrams show how the skewed cell being formed in 1D: middle shows the raw ADC, top shows the successful reconstruction by proper calibration (light green bars on top of the ADC means hit energy and an arrow means reconstructed point), and bottom shows the cluster split into two by poor calibration which ends up as skewed cell, respectively. Right 3 diagrams' format is similar to the left 3, but it shows the explanation in 2D. 36

2.25 A crosscheck performed for the hypothesis. By choosing one skewed cell and one specific event, two different gainCorr was tested: in one case the cell was skewed (left) and in the other case it wasn't (right), respectively. Then the event's hit (each colored cell), clusters (colored boundary around connected cells), and reconstructed points (star) are checked. A single point in the right plot (in red dashed circle) splits into two in the left plot. 37
2.26 An example of cluster quality study on a typical skewed cell. Each color in all plots are corresponds to the mass separation in top left plot (mass < 0.1, $0.1 <$ mass < 0.2, and mass > 0.2). The top left plot shows mass distribution before and after the cut in its title. The top right plot shows the number of participating cells per cluster [a]. 2nd and 3rd rows show σ_{max} (left column) and σ_{min} (right column) of a cluster, but the values smaller than 0.01 are not included in the 2nd row. 38
2.27 Surviving statistics for each QA item. Each bin was normalized by 1st bin's entries. Each column corresponds to each detId and Each row corresponds to the top half and bottom half of FMS. 41
2.28 Slewing corrected BBC zVtx [9] distribution for day 80-81 (leff) and day 91-93 (right). 41
2.29 Schematic diagrams of effect of zVtx shift to the π^0 opening angle (left) and components for opening angle correction (right). 735 cm is a typical distance between zero point and the shower maximum position in the FMS cell. 42
2.30 Difference between the values before and after the zVtx correction, for reconstructed mass (left) and for opening angle (right) 42
2.31 Effect of zVtx application on the π^0 mass, obtained from day 80-81. Each plot corresponds to each detId. Black (Red) lines indicate the mass without (with) zVtx correction. The bottom four plots are exactly the same plots to the top four but normalized by its own maximum to check the shift more clearly. Note that the calibration applied in these plots are the one before zVtx correction is officially introduced: thus the calibration is optimized to the case without zVtx correction (black lines). Lastly, the conditions applied for these plots are not exactly the same as the QA items explained earlier in this section. The closest item is the QA6. . . . 43
2.32 Mass distributions for QA6 (Zgg $< 0.7 +$ zVtx + Single point cluster + *Cluster quality cut*), separated by pair energy in the stepwidth of 10 GeV. Each plot corresponds to a detId's top half or bottom half. 44
2.33 Mass vs. pair energy (top 8 plots) and Mass vs. Zgg (bottom 8 plots) in the condition of QA1 (Zgg $< 0.7 +$ zVtx). Each column corresponds to each detId and Each row corresponds to either the top half or bottom half of the FMS. 46
2.34 Mass vs. pair energy and Mass vs. Zgg for QA2 (Zgg $< 0.7 +$ zVtx + Single point cluster). 47

2.35 Mass vs. pair energy and Mass vs. Zgg for QA3 (Zgg < 0.7 + zVtx + Two points from same cluster). 48
2.36 Mass vs. pair energy and Mass vs. Zgg for QA4 (Zgg < 0.7 + zVtx + Else condition of QA2 and QA3). 49
2.37 Mass vs. pair energy and Mass vs. Zgg for QA5 (Zgg < 0.7 + zVtx + *Cluster quality cut*). 50
2.38 Mass vs. pair energy and Mass vs. Zgg for QA6 (Zgg < 0.7 + zVtx + Single point cluster + *Cluster quality cut*). This is the closest condition to the calibration. 51
2.39 1D mass distribution for each QA items. The top four plots are large cells and Bottom four plots are small cells. Each row corresponds to either the top half or bottom half of the FMS. 52
2.40 Examples of poor statistics case (top 9) and dirty distribution case (bottom 9). . . . 54
2.41 Results of radiation damage study by using FMS LED, by Stephen Trentalange (2016). 55
2.42 The groups separated by cell type (large or small) and the cell's η. Each group was determined to have a similar number of cells (250 ± 30). The red dashed rings indicate η in the range of $2.5 < \eta < 4.1$ with stepwidth of 0.2 57
2.43 Results of degradation study by final gainCorr values in day 77-93. Each plot corresponds to the group in Fig. 2.42. Each x bin indicates the difference between the later period and the earliest period (ex. day 8081 - day7779). Y-axis indicates gainCorr difference of the same cell in two different periods (ΔGC), normalized by the earliest period's gainCorr (GC_0) 57
2.44 Invariant mass for multiple periods in day 77 - 93, obtained with similar condition to the calibration (QA6 in section 2.3.3). Each distribution was normalized by the number of events. Each column corresponds to the different detId and Each row corresponds to the top half or bottom half of the FMS. The clear degradation effect can be seen in small cells. 58

3.1 Final map of cell status for day 66-69. Each color corresponds to: good but not converged yet (light blue), bad (black), dead (white with crossing), and converged (yellow), respectively. 60
3.2 Final map of gainCorr for day 66-69. The numbers in a cell are cell number and the assigned gainCorr. The yellow filled circle (black open circle for yellow-colored cells) means the cell is converged. 61
3.3 Final map of cell status for day 69-73. Each color corresponds to: good but not converged yet (light blue), bad (black), dead (white with crossing), and converged (yellow), respectively. 62

3.4 Final map of gainCorr for day 69-73. The numbers in a cell are cell number and the assigned gainCorr. The yellow filled circle (black open circle for yellow-colored cells) means the cell is converged. 63
3.5 Final map of cell status for day 77-79. Each color corresponds to: good but not converged yet (light blue), bad (black), dead (white with crossing), and converged (yellow), respectively. 64
3.6 Final map of gainCorr for day 77-79. The numbers in a cell are cell number and the assigned gainCorr. The yellow filled circle (black open circle for yellow-colored cells) means the cell is converged. 65
3.7 Final map of cell status for day 80-81. Each color corresponds to: good but not converged yet (light blue), bad (black), dead (white with crossing), and converged (yellow), respectively. 66
3.8 Final map of gainCorr for day 80-81. The numbers in a cell are cell number and the assigned gainCorr. The yellow filled circle (black open circle for yellow-colored cells) means the cell is converged. 67
3.9 Final map of cell status for day 82-84. Each color corresponds to: good but not converged yet (light blue), bad (black), dead (white with crossing), and converged (yellow), respectively. 68
3.10 Final map of gainCorr for day 82-84. The numbers in a cell are cell number and the assigned gainCorr. The yellow filled circle (black open circle for yellow-colored cells) means the cell is converged. 69
3.11 Final map of cell status for day 85-86. Each color corresponds to: good but not converged yet (light blue), bad (black), dead (white with crossing), and converged (yellow), respectively. 70
3.12 Final map of gainCorr for day 85-86. The numbers in a cell are cell number and the assigned gainCorr. The yellow filled circle (black open circle for yellow-colored cells) means the cell is converged. 71
3.13 Final map of cell status for day 87-88. Each color corresponds to: good but not converged yet (light blue), bad (black), dead (white with crossing), and converged (yellow), respectively. 72
3.14 Final map of gainCorr for day 87-88. The numbers in a cell are cell number and the assigned gainCorr. The yellow filled circle (black open circle for yellow-colored cells) means the cell is converged. 73
3.15 Final map of cell status for day 89-90. Each color corresponds to: good but not converged yet (light blue), bad (black), dead (white with crossing), and converged (yellow), respectively. 74

3.16 Final map of gainCorr for day 89-90. The numbers in a cell are cell number and the assigned gainCorr. The yellow filled circle (black open circle for yellow-colored cells) means the cell is converged. 75
3.17 Final map of cell status for day 91-93. Each color corresponds to: good but not converged yet (light blue), bad (black), dead (white with crossing), and converged (yellow), respectively. 76
3.18 Final map of gainCorr for day 91-93. The numbers in a cell are cell number and the assigned gainCorr. The yellow filled circle (black open circle for yellow-colored cells) means the cell is converged. 77

A.1 Bad channels' ADC distribution, RUN15pp200trans, day 66-69, 1/2 79
A.2 Bad channels' ADC distribution, RUN15pp200trans, day 66-69, 2/2 80
A.3 Bad channels' ADC distribution, RUN15pp200trans, day 69-73, 1/2 81
A.4 Bad channels' ADC distribution, RUN15pp200trans, day 69-73, 2/2 82
A.5 Bad channels' ADC distribution, RUN15pp200trans, day 77-79 83
A.6 Bad channels' ADC distribution, RUN15pp200trans, day 80-81 84
A.7 Bad channels' ADC distribution, RUN15pp200trans, day 82-84 85
A.8 Bad channels' ADC distribution, RUN15pp200trans, day 85-86 86
A.9 Bad channels' ADC distribution, RUN15pp200trans, day 87-88 87
A.10 Bad channels' ADC distribution, RUN15pp200trans, day 89-90 88
A.11 Bad channels' ADC distribution, RUN15pp200trans, day 91-93 89
A.12 Mass vs. pairE, separated by Zgg in the stepwidth of 0.1, for detId 8 (top 7) and detId 9 (bottom 7), day 66-69. All plots were obtained with calibration condition in section 2.2.3. 90
A.13 Mass vs. pairE, separated by Zgg in the stepwidth of 0.1, for detId 10 (top 7) and detId 11 (bottom 7) day 66-69 91
A.14 Mass vs. Zgg, separated by pairE in the stepwidth of 10 (GeV), for detId 8 (top 7) and detId 9 (bottom 7), day 66-69 92
A.15 Mass vs. Zgg, separated by pairE in the stepwidth of 10 (GeV), for detId 10 (top 7) and detId 11 (bottom 7), day 66-69 93
A.16 XY distribution of 1st (left) and 2nd (right) point of a pair. Top row shows the large cells and Bottom row shows the small cells. The period is day 66-69. 94
A.17 Mass vs. pairE, separated by Zgg in the stepwidth of 0.1, for detId 8 (top 7) and detId 9 (bottom 7), day 69-73 95
A.18 Mass vs. pairE, separated by Zgg in the stepwidth of 0.1, for detId 10 (top 7) and detId 11 (bottom 7) day 69-73 96
A.19 Mass vs. Zgg, separated by pairE in the stepwidth of 10 (GeV), for detId 8 (top 7) and detId 9 (bottom 7), day 69-73 97

A.20 Mass vs. Zgg, separated by pairE in the stepwidth of 10 (GeV), for detId 10 (top 7) and detId 11 (bottom 7), day 69-73 98
A.21 XY distribution of 1st (left) and 2nd (right) point of a pair. Top row shows the large cells and Bottom row shows the small cells. The period is day 69-73. 99
A.22 Mass vs. pairE, separated by Zgg in the stepwidth of 0.1, for detId 8 (top 7) and detId 9 (bottom 7), day 77-79 100
A.23 Mass vs. pairE, separated by Zgg in the stepwidth of 0.1, for detId 10 (top 7) and detId 11 (bottom 7) day 77-79 101
A.24 Mass vs. Zgg, separated by pairE in the stepwidth of 10 (GeV), for detId 8 (top 7) and detId 9 (bottom 7), day 77-79 102
A.25 Mass vs. Zgg, separated by pairE in the stepwidth of 10 (GeV), for detId 10 (top 7) and detId 11 (bottom 7), day 77-79 103
A.26 XY distribution of 1st (left) and 2nd (right) point of a pair. Top row shows the large cells and Bottom row shows the small cells. The period is day 77-79. 104
A.27 Mass vs. pairE, separated by Zgg in the stepwidth of 0.1, for detId 8 (top 7) and detId 9 (bottom 7), day 80-81 105
A.28 Mass vs. pairE, separated by Zgg in the stepwidth of 0.1, for detId 10 (top 7) and detId 11 (bottom 7) day 80-81 106
A.29 Mass vs. Zgg, separated by pairE in the stepwidth of 10 (GeV), for detId 8 (top 7) and detId 9 (bottom 7), day 80-81 107
A.30 Mass vs. Zgg, separated by pairE in the stepwidth of 10 (GeV), for detId 10 (top 7) and detId 11 (bottom 7), day 80-81 108
A.31 XY distribution of 1st (left) and 2nd (right) point of a pair. Top row shows the large cells and Bottom row shows the small cells. The period is day 80-81. 109
A.32 Mass vs. pairE, separated by Zgg in the stepwidth of 0.1, for detId 8 (top 7) and detId 9 (bottom 7), day 82-84 110
A.33 Mass vs. pairE, separated by Zgg in the stepwidth of 0.1, for detId 10 (top 7) and detId 11 (bottom 7) day 82-84 111
A.34 Mass vs. Zgg, separated by pairE in the stepwidth of 10 (GeV), for detId 8 (top 7) and detId 9 (bottom 7), day 82-84 112
A.35 Mass vs. Zgg, separated by pairE in the stepwidth of 10 (GeV), for detId 10 (top 7) and detId 11 (bottom 7), day 82-84 113
A.36 XY distribution of 1st (left) and 2nd (right) point of a pair. Top row shows the large cells and Bottom row shows the small cells. The period is day 82-84. 114
A.37 Mass vs. pairE, separated by Zgg in the stepwidth of 0.1, for detId 8 (top 7) and detId 9 (bottom 7), day 85-86 115
A.38 Mass vs. pairE, separated by Zgg in the stepwidth of 0.1, for detId 10 (top 7) and detId 11 (bottom 7) day 85-86 116

A.39 Mass vs. Zgg, separated by pairE in the stepwidth of 10 (GeV), for detId 8 (top 7) and detId 9 (bottom 7), day 85-86 117
A.40 Mass vs. Zgg, separated by pairE in the stepwidth of 10 (GeV), for detId 10 (top 7) and detId 11 (bottom 7), day 85-86 118
A.41 XY distribution of 1st (left) and 2nd (right) point of a pair. Top row shows the large cells and Bottom row shows the small cells. The period is day 85-86. 119
A.42 Mass vs. pairE, separated by Zgg in the stepwidth of 0.1, for detId 8 (top 7) and detId 9 (bottom 7), day 87-88 120
A.43 Mass vs. pairE, separated by Zgg in the stepwidth of 0.1, for detId 10 (top 7) and detId 11 (bottom 7) day 87-88 121
A.44 Mass vs. Zgg, separated by pairE in the stepwidth of 10 (GeV), for detId 8 (top 7) and detId 9 (bottom 7), day 87-88 122
A.45 Mass vs. Zgg, separated by pairE in the stepwidth of 10 (GeV), for detId 10 (top 7) and detId 11 (bottom 7), day 87-88 123
A.46 XY distribution of 1st (left) and 2nd (right) point of a pair. Top row shows the large cells and Bottom row shows the small cells. The period is day 87-88. 124
A.47 Mass vs. pairE, separated by Zgg in the stepwidth of 0.1, for detId 8 (top 7) and detId 9 (bottom 7), day 89-90 125
A.48 Mass vs. pairE, separated by Zgg in the stepwidth of 0.1, for detId 10 (top 7) and detId 11 (bottom 7) day 89-90 126
A.49 Mass vs. Zgg, separated by pairE in the stepwidth of 10 (GeV), for detId 8 (top 7) and detId 9 (bottom 7), day 89-90 127
A.50 Mass vs. Zgg, separated by pairE in the stepwidth of 10 (GeV), for detId 10 (top 7) and detId 11 (bottom 7), day 89-90 128
A.51 XY distribution of 1st (left) and 2nd (right) point of a pair. Top row shows the large cells and Bottom row shows the small cells. The period is day 89-90. 129
A.52 Mass vs. pairE, separated by Zgg in the stepwidth of 0.1, for detId 8 (top 7) and detId 9 (bottom 7), day 91-93 130
A.53 Mass vs. pairE, separated by Zgg in the stepwidth of 0.1, for detId 10 (top 7) and detId 11 (bottom 7) day 91-93 131
A.54 Mass vs. Zgg, separated by pairE in the stepwidth of 10 (GeV), for detId 8 (top 7) and detId 9 (bottom 7), day 91-93 132
A.55 Mass vs. Zgg, separated by pairE in the stepwidth of 10 (GeV), for detId 10 (top 7) and detId 11 (bottom 7), day 91-93 133
A.56 XY distribution of 1st (left) and 2nd (right) point of a pair. Top row shows the large cells and Bottom row shows the small cells. The period is day 91-93. 134

List of Tables

2.1 Notable differences between new and conventional framework 10
2.2 Data stream and Trigger condition by purpose 12
2.3 Calculation of shower merging start π^0 energy 18

Bibliography

[1] Chong Kim. Run15 fms calibration reports. https://drupal.star.bnl.gov/STAR/blog/ckimstar/run15-fms-calibration-report-spin-pwg-0.

[2] Particle Data Group. Light unflavored mseons summary tables. http://pdg.lbl.gov/2015/tables/rpp2015-sum-mesons.pdf, 2015.

[3] Akio Ogawa. Fms stable running periods (run15). https://www.star.bnl.gov/protected/spin/akio/fms2015/epoch.html.

[4] Christopher Dilks. Fms operation timeline for run15 - run17. https://drupal.star.bnl.gov/STAR/system/files/TIMELINE.txt.

[5] STAR Collaboration. Star run log. https://online.star.bnl.gov/RunLog/.

[6] Chong Kim. Fms bit shift qa. https://drupal.star.bnl.gov/STAR/system/files/note_9.pdf, Nov 2017.

[7] Akio Ogawa. Modified code to cluster and fit large and small cells together. https://www.star.bnl.gov/protected/spin/akio/fms2015/closegap.html.

[8] Zhanwen Zhu. Improvement of π^0 reconstruction algorithm. Sep 2018.

[9] Oleg Eyser. Bbc slewing correction study. https://drupal.star.bnl.gov/STAR/blog/oleg/bbc-timing-calibration-slewing-correction-run-15.

[10] Chong Kim. Fms point's z position in run15. https://drupal.star.bnl.gov/STAR/blog/ckimstar/fms-points-z-comments-meeting-aug-7.

[11] Akio Ogawa. Fms cluster categorization by sigma max. https://www.star.bnl.gov/protected/spin/akio/fms2015/sigmax.html.

[12] Chong Kim. Fms zgg bump study report. https://drupal.star.bnl.gov/STAR/system/files/CKim_FMS_180802.pdf.

[13] Chong Kim. Cluster quality qa report. https://drupal.star.bnl.gov/STAR/system/files/CKim_FMSCalib_181022.pdf.

[14] Chong Kim. Run15pp200trans final qa with low energy part. https://drupal.star.bnl.gov/STAR/blog/ckimstar/run15-pptrans-calibration-final-qa-1.

[15] Stephen Trentalange. Estimates for the uv curing system for the fms. https://www.star.bnl.gov/protected/spin/trent/damage_control/damage.html.

[16] Stephen Heppelmann. Led on coldplates. https://drupal.star.bnl.gov/STAR/blog/heppel/led-coldplates.